COO-4501-4

SOURCES OF OZONE AND SULFATES IN NORTHEASTERN UNITED STATES

Annual Progress Report

to the

United States Department of Energy

Contract No. DE-AC02-77EV04501

by the New York State Department of Health 464 5000

and Health Research, Inc. — 950 0522

Albany, New York 12201

June 30, 1980

DISCLAIMER

Sources of Ozone and Sulfate in Northeastern United States

Annual Progress Report
to the
United States Department of Energy
Contract No. DE-AC02-77EV04501.A000
June 30, 1980

Liaquat Husain, Principal Investigator
Research Scientist VII and
Director, Chemical Sciences Laboratory

Vincent Dutkiewicz, Co-Investigator
Pravin Parekh, Co-Investigator
Chemical Sciences Laboratory
Environmental Health Institute
Division of Laboratories and Research
New York State Department of Health
Albany, New York 12201

and

Health Research, Inc.
Empire State Plaza - Tower Bldg.
Albany, New York 12237

✓ Submitted By

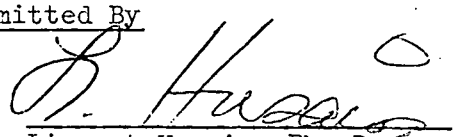

Liaquat Husain, Ph. D.
Principal Investigator

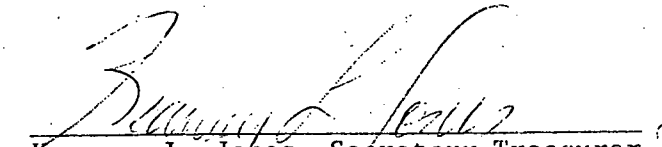

Kearney L. Jones, Secretary-Treasurer
Health Research, Inc.
Empire State Plaza - Tower Bldg.
Albany, NY 12237

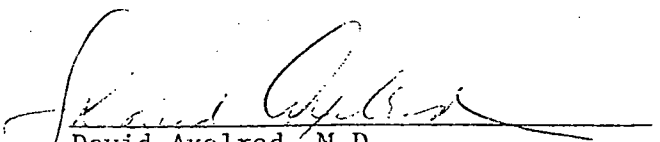

David Axelrod, M.D.
Commissioner
New York State Department of Health
Empire State Plaza - Tower Bldg.
Albany, New York 12237

TABLE OF CONTENTS

TABLE OF CONTENTS
(continued)

1. SUMMARY

1.1 Objectives

Ozone observed at Whiteface Mountain, N.Y., may be derived from (1) the stratosphere, (2) photochemical production from pollutant NO_x and hydrocarbons emitted in urban/industrial areas, with subsequent transport of O_3 to Whiteface Mountain, and (3) photochemical production from NO_x and hydrocarbons including terpenes, etc. emitted from vegetation in the vicinity of Whiteface Mountain. At the beginning of this study it had been established that high ^7Be concentrations were often associated with high O_3. No attempts had been made to quantify stratospheric O_3 from ^7Be measurements. To accomplish this, the following information is required: relationship between ^7Be and O_3 at the source (stratosphere), ^7Be produced in the troposphere, and removal of ^7Be and O_3 during transport from tropopause to ground level.

The principal objective of this work was to assess ^7Be and ^{32}P as stratospheric tracers and, if possible, use them to quantify stratospheric O_3. Other objectives of this program were: to study the relationship between O_3 and SO_4^{2-}, use SO_4^{2-} as an indicator of (2) above, to study the long-range transport of pollutants and try to identify emission sources and establish daily, monthly and seasonal variations of SO_4^{2-} and trace elements thus generating a data base to study long-term trends.

1.2 Accomplishments

The salient features of this study were the first determinations of $^7Be/O_3$ ratios in the lower stratosphere and upper troposphere and gathering continuous data of radionuclides ^7Be, ^{32}P and ^{33}P along with O_3, SO_4^{2-} and several trace elements from June 1978 to December 1979. Although some of the conclusions and interpretations are tentative and will undoubtedly

be refined as this work proceeds, at this time the significant accomplishments of this study are: (a) a quantitative relationship between ^{7}Be and O_3 in the stratosphere was established and it is applied to estimate stratospheric O_3 on a global and episodic basis, (b) global ^{7}Be measurements suggests that the stratospheric influx in the northern hemisphere is twice that in the southern, (c) the $^{7}Be/^{32}P$ ratios yield an average transport time of $\sim$ 7 days during spring and summer for stratospheric air from tropopause to Whiteface Mountain, supporting tropopause folding as the predominant mechanism of stratospheric-tropospheric exchange during spring and summer, (d) daily measurements yield an empirical observation that $\geq$ 10 μg SO_4^{2-}/m^3 is associated with O_3 in excess of 50 ppbv, suggesting SO_4^{2-} as a potential tracer for transported tropospheric O_3, (e) statistical treatment of data and air trajectory analysis revealed four anthropogenic sources for SO_4^{2-} and trace elements analyzed, and (f) monthly and seasonal profiles for SO_4^{2-} and several trace metals at Whiteface Mountain during 1979 have been determined. Also, in the course of this study an elegant and sensitive microanalytical method to measure total particulate sulfur in aerosols by pyrolysis microcoulometry has been developed. This method could be used for sulfur determination in high-volume air particulate samples collected for as short a time as half an hour.

One phase of our study calls for calculations of 400-1400 meters, 6-h surface trajectories using Heffter's model. This has been accomplished for part of 1979 and should be completed by the end of this year for remaining days in 1979. Comparison between 6-h trajectories and elemental concentrations for an entire year may provide statistically meaningful information regarding the region(s) where episodic high concentration originate.

The work discussed here was conducted during January 1, 1979 and June 30, 1980 with one-year funding provided by U.S. Department of Energy

for January to December 31, 1979 period. A six-month no-cost extension was granted so that the analyses of samples collected through December 31, 1979 could be completed. Two reprints and four preprints prepared from this work and discussed in this study are attached as appendices.

I. Determination of Stratospheric Ozone at Ground Level Using $^{7}Be/O_3$ Ratios, Dutkiewicz and Husain, Geophys. Res. Lett. 6, 171-174 (1979), a reprint of this paper is attached as Appendix I.

II. Long Range Transport of Trace Elements, Husain and Samson, J. Geophys. Res. 84, 1237-1240 (1979), a reprint of this paper is attached as Appendix II.

III. On the Origin of Tropospheric Ozone, Husain, Dutkiewicz and Rusheed, submitted to Nature, a preprint of this paper is attached as Appendix III.

IV. Transport Time of Stratospheric Air from Tropopause to Ground Level, Dutkiewicz, Rusheed and Husain, Submitted to J. Geophys. Res., a preprint of this paper is attached as Appendix IV.

V. Determination of Total Particulate Sulfur at Whiteface Mountain, N.Y. by Pyrolysis Microcoulometry, Canelli and Husain, submitted to Atmospheric Environment, a preprint of this paper is attached as Appendix V.

VI. Summertime Concentration of Trace Elements in Atmospheric Aerosols at Remote Sites in New York State, Parekh and Husain, submitted to Atmospheric Environment, a preprint of this paper is attached as Appendix VI.

2. EXPERIMENTAL

2.1 Particulate Sampling at Whiteface Mountain

At the 1.5 km summit of Whiteface Mountain, N.Y., 24-h suspended air particulate samples were collected using high-volume air samplers as described in an earlier report (Husain et al., 1978, henceforth identified as Report I). Daily particulate sampling for January 1 through December 31, 1979 period was carried out by the technical staff of the Atmospheric Sciences Research Center under a subcontract to the Research Foundation, State University of New York, Albany. The samples were collected from midnight to midnight during 1978 but noon to noon (EST) during 1979.

A constant air flow of 1.3 standard m^3/min was maintained with Sierra Model 310* mass flow controllers. The calibration of the controllers was checked periodically by measuring the pressure drop across a standard orifice and the manufacturer's supplied calibration data with corrections for ambient temperature and pressure. The controllers have performed well with less than a $\pm$ 5% change between calibrations.

2.2 Analyses

A variety of chemical and radiochemical analyses were performed on the particulates. These are summarized in Fig. 1. The radiochemical procedures are described below. Sulfate and trace element analytical methods are described in Appendices V and VI, and Section 11.

2.3 Radiochemical Analysis of Whiteface Mountain Samples

^{7}Be concentration was measured by whole-filter NaI(Tl) gamma-ray spectrometry (Report I). A least squares computer code was used to subtract the background and deconvolute the 478 keV gamma ray intensity. The uncertainty in ^{7}Be is primarily determined by the quality of the counting

---

*Mention of trade names or commercial products does not constitute endorsement or recommendation by New York State.

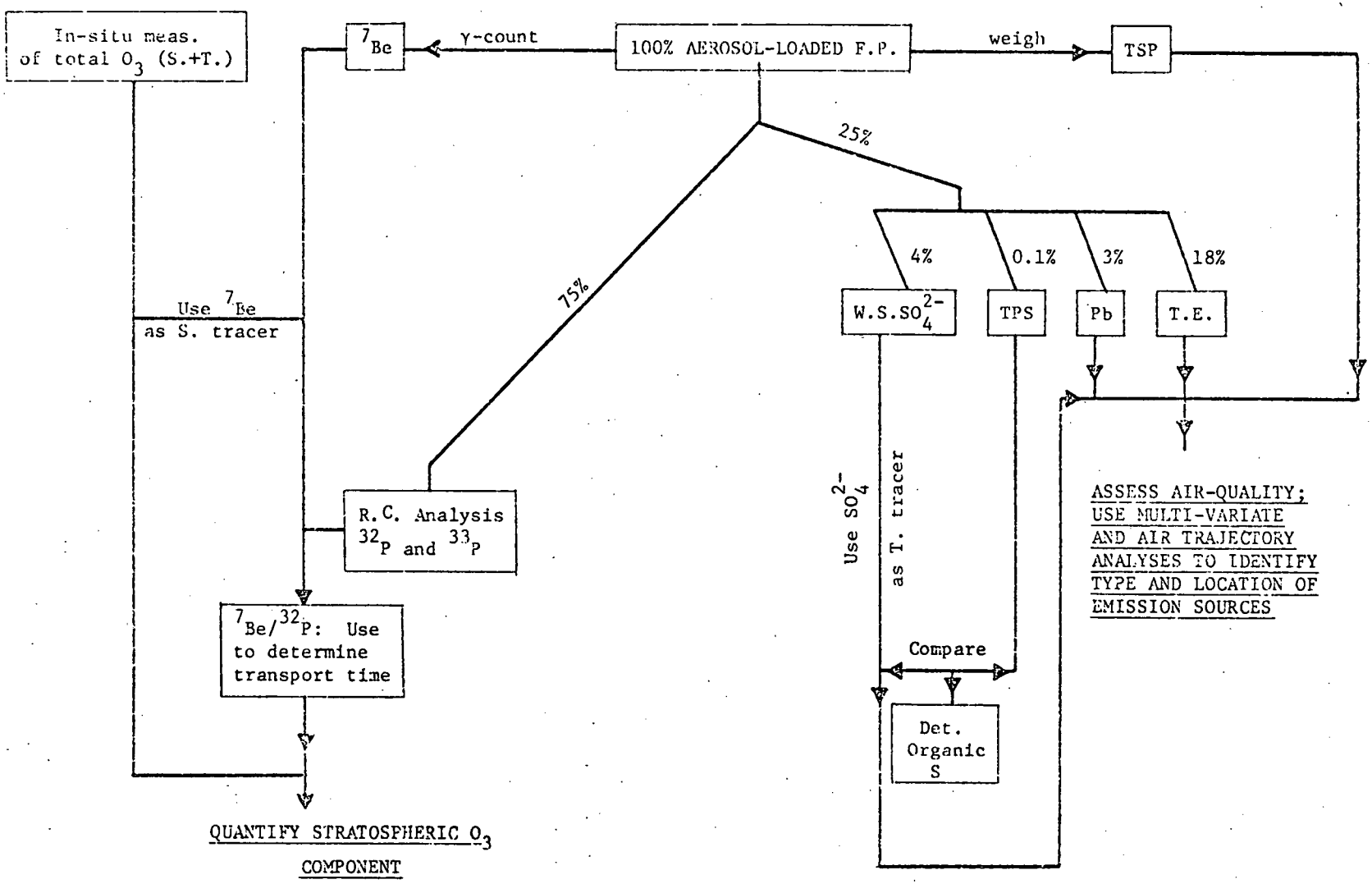

S.	Stratospheric	R.C.	Radiochemical	TSP	Total suspended particulates
T.	Tropospheric	T.E.	Trace Elements	TPS	Total particulate sulfur
F.P.	Filter paper (Whatman 41)			W.S.	Water soluble

Fig. 1. Flow chart showing the objectives and analyses scheme of filtered air particulate samples collected at Whiteface Mountain.

statistics although the quality of the computer fit is also a factor. The estimated uncertainties and detection limit for reported ^{7}Be activity in 24-h high-volume filters is shown in Fig. 2. Above 100 fCi/m^3 ($fCi = 10^{-15}$ Ci) the uncertainty approaches $\pm$ 5%.

The radiochemical procedure used to separate ^{32}P and ^{33}P from the filter particulates was described in Report I. To expedite counting the ^{32}P-^{33}P residues, 4 low-background gas-flow proportional counters described in section 2.3 of Report I were fabricated. These counters have a background count rate of 0.4 $\pm$ 0.03 cpm, where the error represents one sigma standard deviation in a series of 10 or more background counts. The procedure used to determine ^{32}P and ^{33}P requires counting each sample several times with and without a 29 mg/cm^2 Al absorber. This absorber thickness is sufficient to stop ^{33}P betas while still passing 66% of the higher energy ^{32}P beta particles. The additional counters improved accuracy by increasing the total number of times each sample could be counted. The ^{32}P activity was determined by fitting the net count rate in a series of absorber counts to a 14.3-d decay curve and comparing the net cpm at the time of sampling to that of ^{32}P standard counted under the same geometry. The ^{32}P decay curve was then used to subtract the ^{32}P count rate in the non-absorber counts, yielding the ^{33}P activity. The procedure was tested by assuring the residual cpm followed a 25-d decay. The quality of the data is demonstrated by the resultant decay curves from a representative sample shown in Fig. 3. The absorber and non-absorber counts follow 14.3- and 25-d decay, respectively, verifying both the purity of the sample and the quality of the counting data.

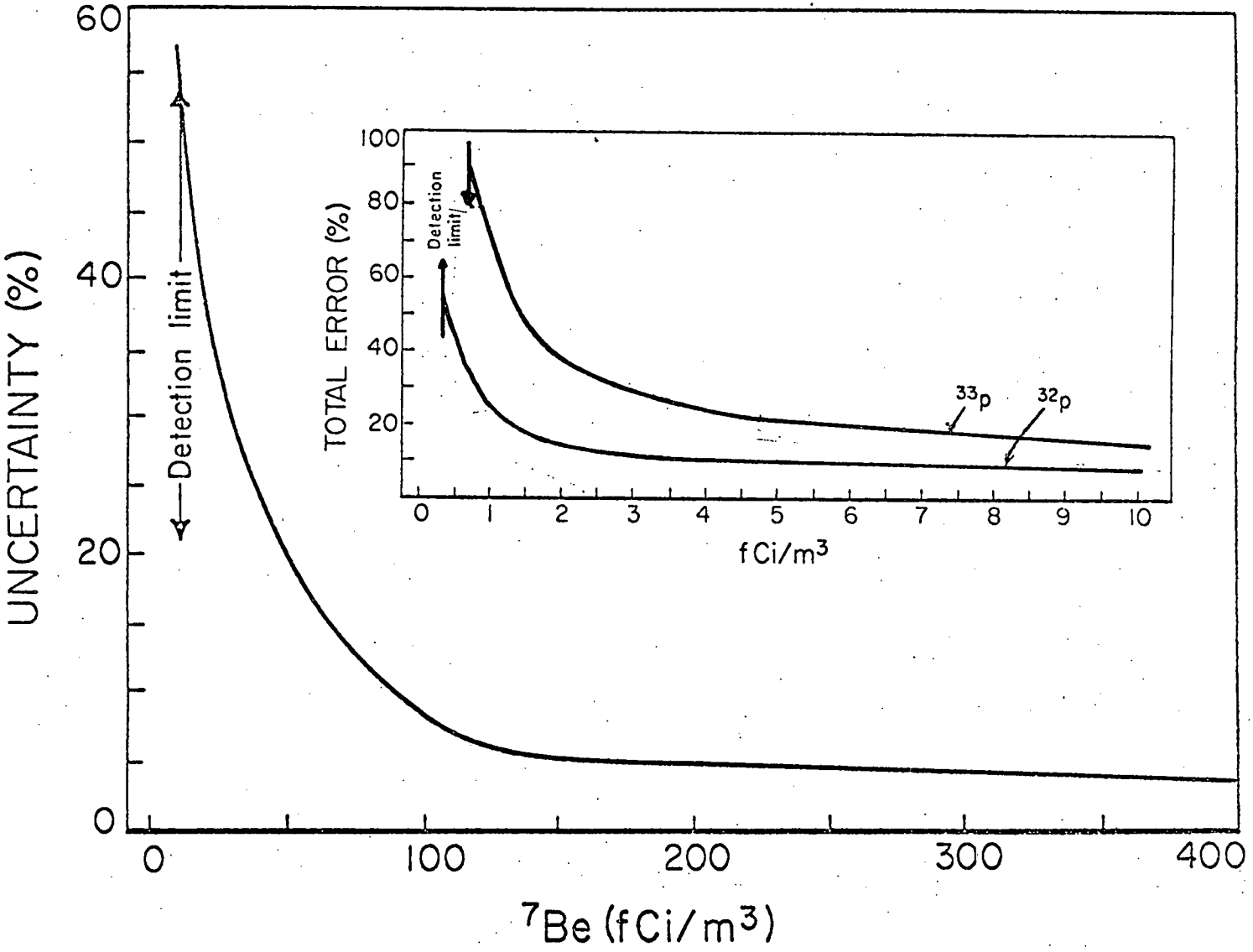

Fig. 2. Estimated uncertainties in ^{7}Be, ^{32}P and ^{33}P concentrations measured in 24-h high-volume air samples (Average total air volume sampled $\approx$ 1800 standard m^{3}).

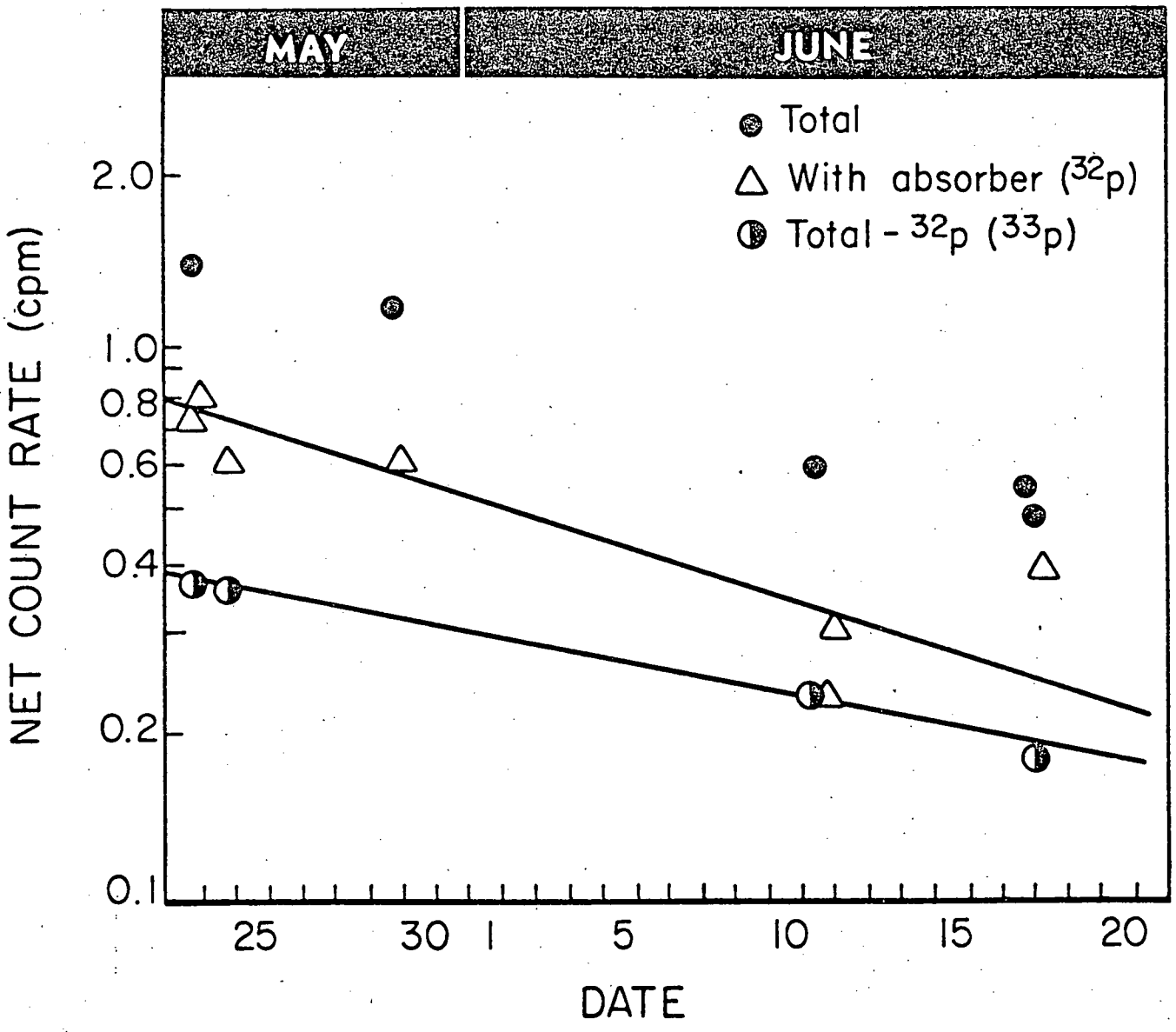

Fig. 3. Representative decay curve fits to ^{32}P and ^{33}P counting data from 24-h high-volume air samples. The upper and lower lines respectively correspond to 14.3- and 25-d decay.

The uncertainty in the concentration of radionuclides reported include errors in air volume, counting statistics, chemical yield, and counter efficiency. Statistical errors in counting contribute the largest uncertainty. The error in the counting rate was calculated by the following relationship:

$$\% \text{ error} = \frac{100}{C} \sqrt{\frac{s}{t_s} + \frac{b}{t_b}}$$

where s and b are, respectively, the total and background count rate (in cpm) and C is the net count rate (C = s-b). The quantity t_s and t_b are, respectively, the sample and background count times. In the case of ^{32}P, errors due to yield, counter efficiency, and air volume were 3%, 2%, and 5%, respectively. The squares of the individual errors were added to get the square of the total error. The lower curve in inset in Fig. 2 shows the estimated uncertainty versus concentration of ^{32}P in fCi/m^3. This was calculated considering that on the average 12 days elapsed between sample collection and the first count. It can be seen that for concentration > 3 fCi/m^3, the total error for ^{32}P is $\leq$ 10%.

The calculation of ^{33}P concentration is carried out by subtracting ^{32}P count rate from total β^- activity as described in previous section. Since the efficiency of counting ^{33}P β^- particles is much smaller than ^{32}P (7% compared to 35% for ^{32}P), its detection limit and uncertainties are much higher than for ^{32}P. Estimated ^{33}P uncertainties in Fig. 2 show that a ^{33}P concentration of 3 fCi/m^3, has a total uncertainty of 28% and for concentration $\geq$ 5 fCi/m^3 it is less than 20%.

2.4 High Altitude Sampling and Analysis

In Report I we described our initial measurements of $^{7}Be/O_3$ ratios at 9.8-12.2 km. Some of these results have already been published (Dutkiewicz and Husain, 1979; Appendix I), and some are in the process of publication (Husain et al., 1980; Appendix III). NASA's Global Atmospheric Sampling Program (GASP) was terminated in June, 1979. All of the samples collected during this program have been analyzed for both ^{7}Be and ^{90}Sr and the data reported here.

The particulate samples were collected on IPC 1478 filters using an automated sampling system mounted in the nose of two commercial B747 jetliners (Perkins and Gustafsson, 1976). O_3 was continuously measured with a UV absorption photometer, recently described by Tiefermann (1979). The samples were collected between 9.8 and 12.2 km altitude and 11^{o}-$56^{o}N$. Altitude and geographical location during sampling were recorded from the aircrafts' navigational system. The filters were analyzed for ^{7}Be using gamma-spectrometry with a 45-cc Ge(Li) detector connected to a 4096-channel pulse height analyzer. A partial γ-ray spectrum from a typical stratospheric sample is shown in Fig. 4. Significant peaks have been highlighted and in some cases radionuclides assigned. This particular sample is rich in fresh fission products, presumably from the September 1977 Chinese nuclear detonation. Even in this case, the 478 keV ^{7}Be γ-line is clearly resolved. Absolute ^{7}Be concentration was determined by comparing the area under the 478 keV peak in the sample with that of a ^{7}Be standard counted under the same geometry. Background subtraction and peak integration were performed with a least squares computer code. Statistical uncertainties in the absolute ^{7}Be concentration were generally $< \pm$ 10%.

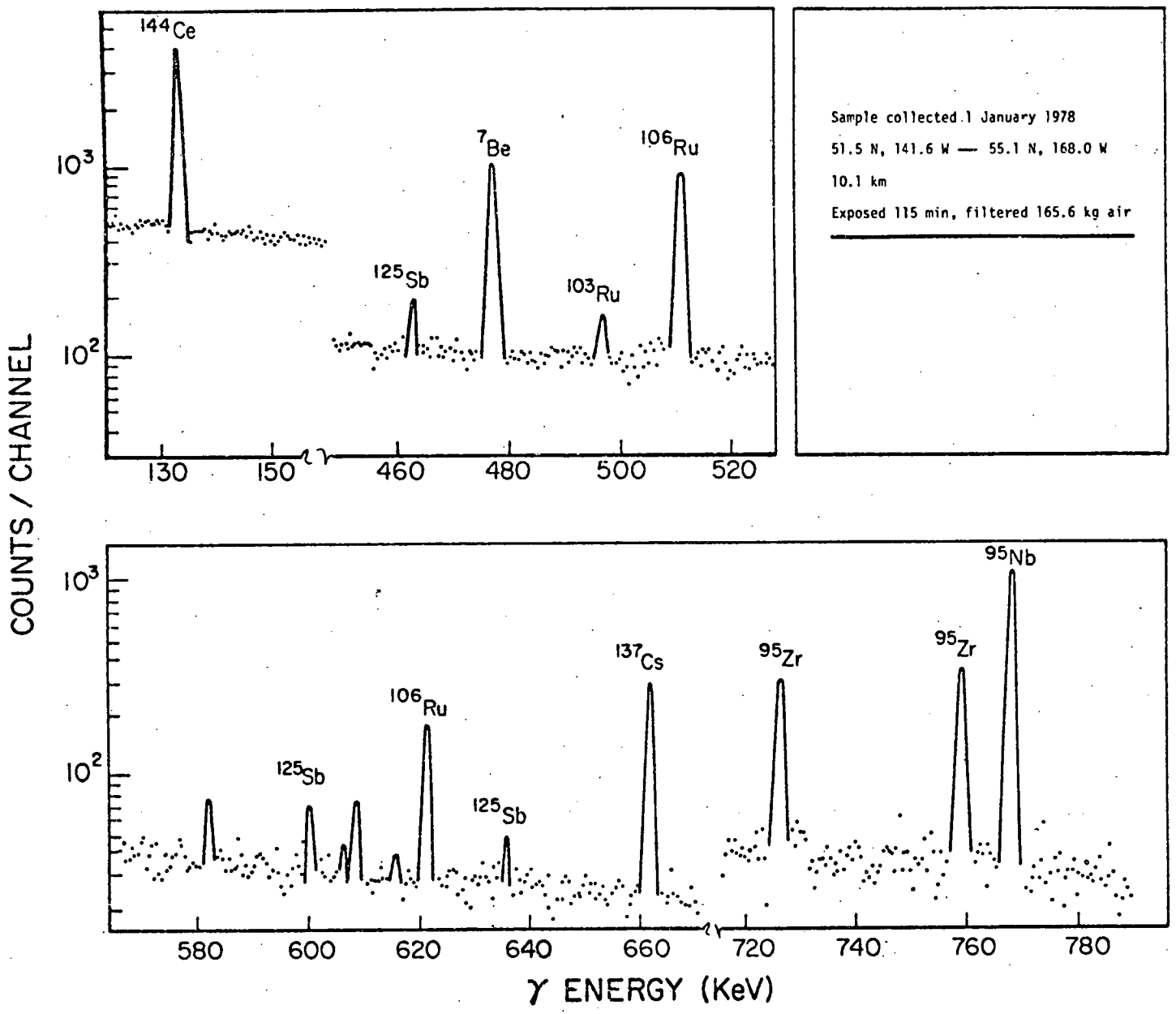

Fig. 4. Representative Ge(Li) γ spectrum of a stratospheric air sample collected by NASA's Global Atmospheric Sampling Program. Significant peak intensities are highlighted by solid curves, and radionuclides assigned.

The concentration of ^{90}Sr ($t_{1/2}$ = 29 y) in GASP samples was determined from one-quarter of each filter using standard radiochemical procedures. Briefly, strontium was radiochemically separated from the filters and the ^{90}Sr-daughter ^{90}Y ($t_{1/2}$ = 2.67 d) was removed. ^{90}Y was then allowed to ingrow for at least 2 weeks so equilibrium with the ^{90}Sr parent was attained. Then ^{90}Y was precipitated as yttrium oxalate, ignited to yttrium oxide, weighed, and mounted on Whatman 42 filters which had been precoated with asbestos slurry. The filters were sealed with mylar tape and β^- counted several times on the low background gas flow proportional counter. ^{90}Sr activity was determined by fitting the ^{90}Y counting data with a 2.67-d half-life. Corrections for chemical recovery and counting efficiency were applied.

2.5 Instrumentation

In addition to the two low background β-counting systems described in Report I, three more units have been built. Two of these have been used for ^{32}P and ^{33}P counting and the third system, which has a larger counting volume, was used for ^{90}Sr measurements in GASP samples. Electronics for these counters were purchased with USDOE funds.

Although GASP filter samples were γ-counted with a Ge(Li) detector, there was not sufficient time available to count all of the daily samples on the Ge(Li) detector. Hence, we have now ordered a large Ge(Li) detector with 24% efficiency relative to a 7.6 x 7.6 cm NaI(Tl) detector, resolution of 1.9 keV at 1332 keV, and a 4096-channel analyzer. This Ge(Li) detector will be used for γ-counting the daily samples.

3. STRATOSPHERIC TRACERS

3.1 ^{7}Be

The interaction of high energy cosmic ray protons and neutrons with O_2, N_2 and Ar in the atmosphere produces many short-lived radioisotopes, including ^{7}Be ($t_{1/2}$ = 53.3 d), which can be used to study atmospheric dynamics (Lal and Peters, 1967). The vertical profile of observed annual average ^{7}Be concentrations at $\sim 45^{o}$N is shown in Fig. 5. Measurements up to 3 km were made from ground-based sites but above 3 km aircrafts were used for sampling. The number of measurements averaged for each point is indicated by a numeral by the side of the point in Fig. 5. The large variability of concentrations in the 9 to 12 km range reflects the fact that at these altitudes both stratospheric and tropospheric air can be sampled. Thus, our measurements on GASP samples were separated according to <u>in-situ</u> ozone ($O_3 \geq 200$ ppbv, stratospheric; and $O_3 \leq 100$ ppbv, tropospheric). Likewise, the measurements of Young et al. (1970) at 9 and 12 km were divided into high and low concentration averages consistent with our GASP results. Two distinct ^{7}Be concentration ranges are evident, corresponding to stratospheric and tropospheric air. The dashed and solid lines have been drawn respectively through the presumed stratospheric and tropospheric ^{7}Be concentrations to help guide the eye.

Although the ^{7}Be concentration shows (Fig. 5) a 5-fold increase from surface to $\sim$ 10 km, the change in concentration is much more dramatic ($\sim$ 10-fold) between 10 to 12 km. Considering that the troposphere invariably contains stratospheric contributions, the ratio of ^{7}Be concentration in the stratosphere to that in the troposphere is probably much larger. Our measurements (to be discussed later in this report) on both sides of tropopause yield a ratio as high as $\sim$ 50 for stratospheric to tropospheric ^{7}Be. From

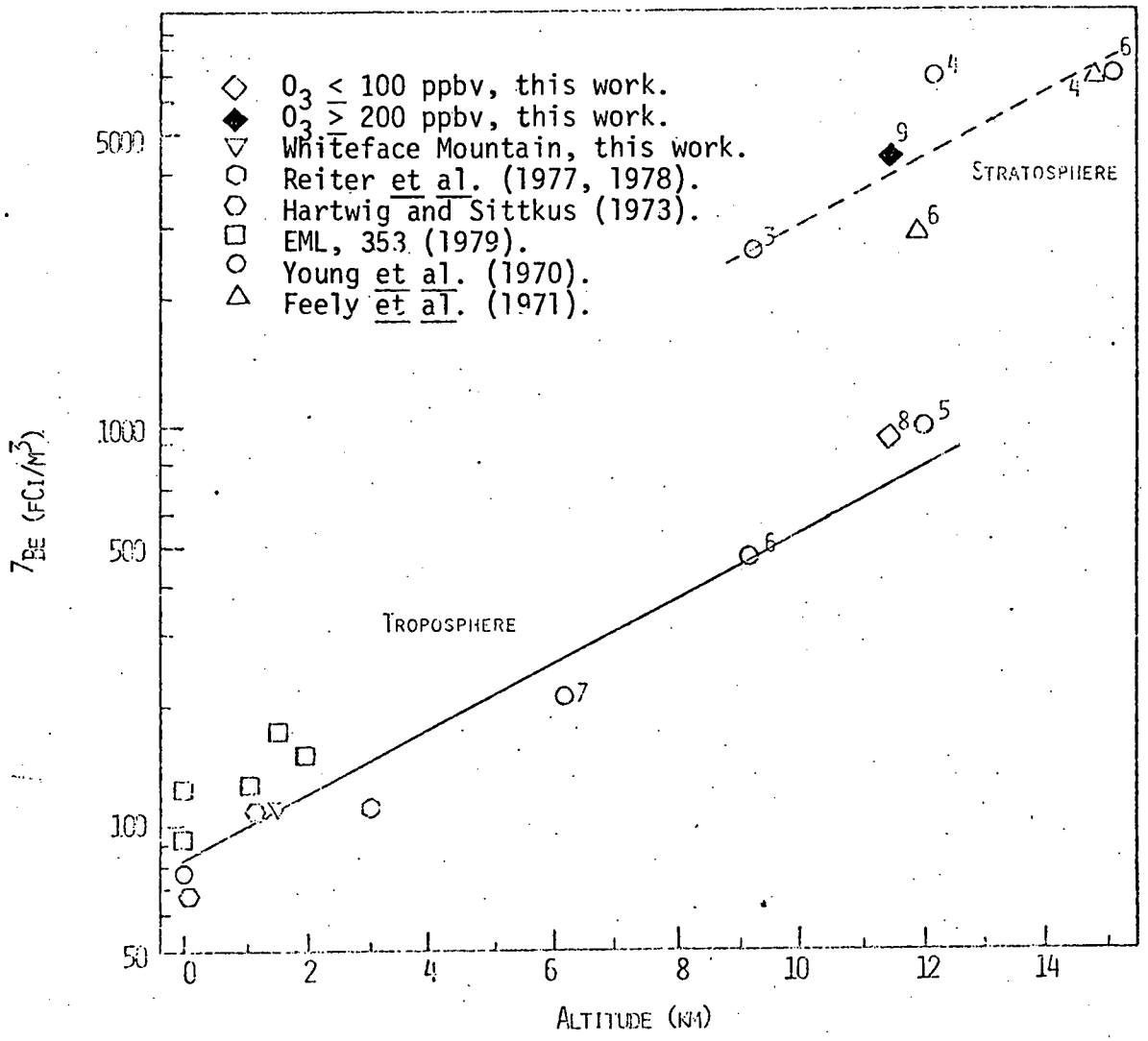

Fig. 5. Vertical ^{7}Be concentration profiles for $\sim 45^\circ$N. Points up to 3 km are annual averages of measurements at ground (or mountain) sites. Points at or above 6 km are averages of a series of aircraft measurements (the number of measurements averaged for each point is indicated by a digit near each symbol). Since the measurements at 9 to 12 km can be either tropospheric or stratospheric, separate averages, assumed to correspond to stratospheric and tropospheric air, are indicated. The dashed and solid lines are drawn respectively through the presumed stratospheric and tropospheric measurements to aid the eye.

Fig. 5 a ratio of ∿ 70 is obtained for ^{7}Be concentration at 15 km to that at ground level. In addition to this highly favorable ^{7}Be concentration gradient, it is expected that the relatively small variation in cosmic ray particle flux and slow mixing in the stratosphere minimize variation in the ^{7}Be concentration in the stratosphere. These arguments combined with the convenience of ^{7}Be measurements and a half-life comparable to the time-scale of the dynamic processes studied, has resulted in many attempts to use ^{7}Be as a stratospheric tracer in surface air (Husain et al., 1977, 1979; Dutkiewicz and Husain, 1979; Ludwick et al., 1975; E. Reiter et al., 1977; Singh et al., 1979; Wolff et al., 1979 A). These studies used the ground level ^{7}Be concentration measurements to deduce information relating to stratospheric intrusions and associated transfer of ozone into the troposphere assuming all of the observed ^{7}Be originated in the stratosphere. Although the average ^{7}Be concentration in the lower stratosphere is many times that in surface air, the magnitude of the stratospheric ^{7}Be present in the troposphere depends upon the intensity of stratospheric-tropospheric exchange, transport process and the mean residence time. Therefore, it is important to subtract the ^{7}Be produced in the troposphere (hereafter referred to as tropospheric ^{7}Be) before using the observed ^{7}Be values to deduce information regarding stratospheric inputs. Fortunately, this correction is relatively simple to make if applied to the observed ^{7}Be data on a long-term basis, e.g., monthly or annual averages. On a daily basis, however, the tropospheric ^{7}Be can vary several fold. To use ^{7}Be as a stratospheric tracer on a daily or episodic basis, it is important to know the intensity of the stratospheric contribution. This can be partially achieved if two radioisotopes with considerably different half-lives are used. The discussion below shows that $^{7}Be/^{32}P$ ratio could be used as a stratospheric tracer on a daily or episodic basis.

3.2 $^{7}Be/^{32}P$

Because of the limitations of using ^{7}Be concentration alone as a stratospheric tracer discussed above, we have also utilized $^{7}Be/^{32}P$ ratios as indicators of stratospheric air. A paper summarizing our studies on $^{7}Be/^{32}P$ ratios has been submitted to J. Geophys. Res. A preprint is attached as Appendix IV. Briefly, the average of 90 measurements in the lower stratosphere yields a $^{7}Be/^{32}P$ ratio of 80 (Feely et al., 1971) in reasonable agreement with the theoretical equilibrium ratio of 100±20 (Lal and Peters, 1967). Due to relatively short irradiation times (or residence times) of aerosols in the troposphere (e.g., Machta et al., 1970; Martell and Moore, 1975; Reiter, 1975 and ref. therein), the $^{7}Be/^{32}P$ ratio does not reach equilibrium and hence the value for this ratio is expected to be much smaller in the troposphere. The ^{7}Be and ^{32}P production rates yield a minimum $^{7}Be/^{32}P$ ratio of 22, which can be observed only in a freshly cleansed air mass. Using a mean residence time of 30 days, however, and equilibrium value 80 (i.e., the stratospheric value) we obtain a $^{7}Be/^{32}P$ ratio of 38 for purely tropospheric air. When tropospheric air mixes with stratospheric air $^{7}Be/^{32}P$ ratio between 38 and 80 would result depending upon the relative proportions of the stratospheric and tropospheric component as shown in Fig. 6. The decay of the stratospheric ^{7}Be and ^{32}P concentrations have not been included. If a stratospheric air mass remains relatively intact in the troposphere for a significant length of time, the $^{7}Be/^{32}P$ ratios will be > 80 due to the more rapid decay of ^{32}P ($t_{1/2}$ = 14.3 d) compared to ^{7}Be ($t_{1/2}$ = 53.3 d). Therefore, $^{7}Be/^{32}P$ ratio could provide significant information about the origin of an air mass. For example, if the observed $^{7}Be/^{32}P$ ratio is between 22 and 38 but the ^{7}Be concentration is high, it may be inferred that the air mass

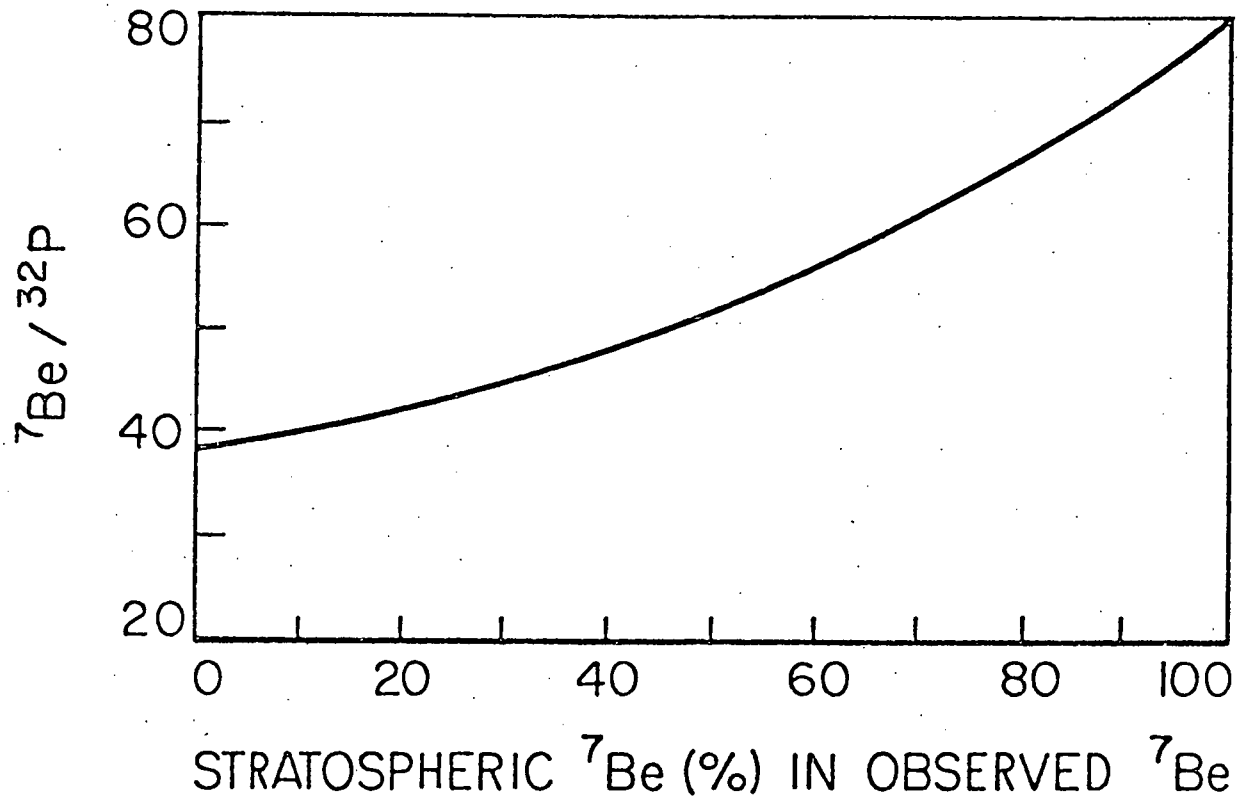

Fig. 6. $^{7}Be/^{32}P$ activity ratio for mixed stratospheric ($^{7}Be/^{32}P$ = 80) and tropospheric ($^{7}Be/^{32}P$ = 38) air masses as a function of the % of the resultant ^{7}Be concentration originating in the stratosphere.

is of tropospheric origin and that high ^{7}Be concentration suggests the air mass originating in the upper troposphere.

A high $^{7}Be/^{32}P$ ratio, say > 60, even if the ^{7}Be concentration is low suggests a substantial stratospheric contribution. The low ^{7}Be concentration may be due to atmospheric cleansing processes. We can think of exceptions to the above generalizations, e.g., in isolated cases tropospheric irradiation time could be very long so that $^{7}Be/^{32}P$ ratio of a tropospheric air mass could be > 38. However, an irradiation time of 75 days is required to produce a $^{7}Be/^{32}P$ ratio of 50. This is an unusually long time for a dynamic troposphere. But to be on the conservative side, we have used $^{7}Be/^{32}P$ ratio as a tracer only on those days when $^{7}Be/^{32}P \geq 60$.

4. TROPOSPHERIC TRACER

4.1 Sulfate

Since at times transported photochemically produced O_3 can be present in large amounts at Whiteface Mountain, it is highly desirable to develop a tropospheric tracer to assist the resolution of sources of O_3. As discussed in Section 10 sulfate concentrations can be used as an indicator of transported pollutants at Whiteface Mountain. Our daily measurements of sulfate are discussed in Section 11. To search for some clear relationship between transported O_3 and sulfate we compared daily O_3 concentrations with sulfate concentrations on days when the latter exceeded a value of 10 $\mu g/m^3$. Fig. 7 shows our daily data obtained during June-August, 1977 and June, 1978-December, 1979. It is distinctly clear from Fig. 7 that an O_3 concentration in excess of 50 ppbv is observed when the sulfate concentration exceeds 10 $\mu g/m^3$. This empirical observation strongly suggests the possibility of using sulfate as a tracer of the transported photochemical O_3 component.

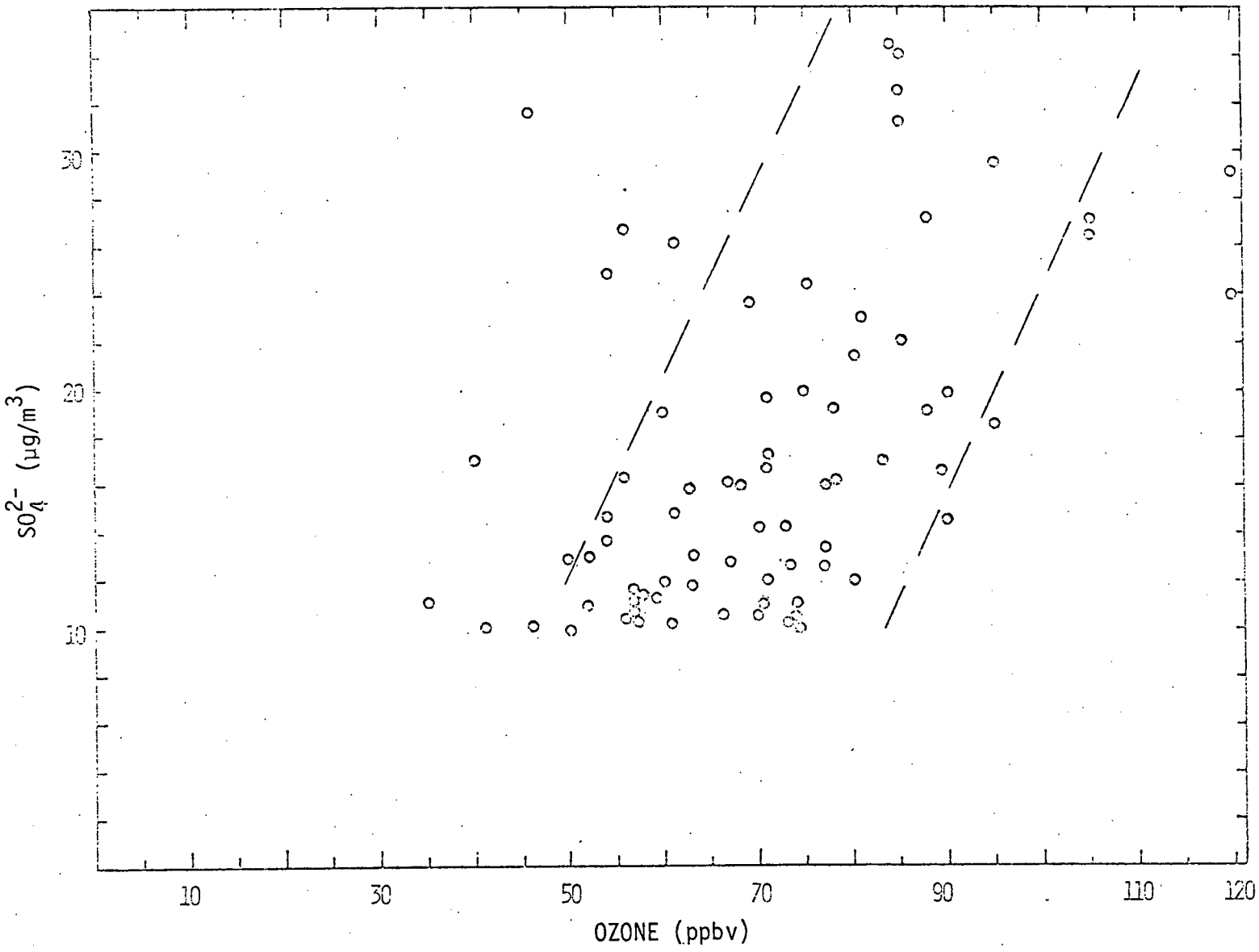

Fig. 7. Relationship between O_3 concentration in ambient air versus SO_4^{2-} concentration in air particulates at Whiteface Mountain showing that for SO_4^{2-} concentration $\geq$ 10 $\mu g/m^3$, O_3 concentration exceeds 50 ppbv. The dashed lines are drawn parallel to the best least squares fit for the points encompassed in the field.

To further investigate the relationship between sulfate and O_3 we have plotted in Fig. 8 our measurements of O_3, sulfate and ^7Be concentrations carried out on 6-h samples collected during June 13 to 25, 1979. In the 6-h data it is observed that when SO_4^{2-} concentration $\geq$ 10 $\mu g/m^3$, O_3 exceeds 70 ppbv. A comparison between ^7Be, O_3 and sulfate is a little more revealing. On June 13 and 14, SO_4^{2-} concentration is < 0.5 $\mu g/m^3$; ^7Be, 170-260 fCi/m^3 and O_3, 35-45 ppbv. In the morning of June 15, the sulfate and O_3 concentrations suddenly increase, but ^7Be remains $\sim$ 200 fCi/m^3. Although not quantitative, sulfate and O_3 concentrations vary in similar fashion during June 15 and 18. There was precipitation on June 18 which lowered the concentrations for all three species. On June 19, ^7Be increased to $\sim$ 250 fCi/m^3 but sulfate concentration remained < 0.5 $\mu g/m^3$. During this period O_3 followed ^7Be. Between June 19 and 22 the ^7Be and O_3 concentrations were high and appear fairly well related. The sulfate concentration remained < 0.5 $\mu g/m^3$ until June 21 and began to increase slowly. ^7Be and O_3 peaked at 0-600 hours on June 22 and then began to decline. On the other hand, sulfate increased to 14 $\mu g/m^3$ at 1200-1800 hours on June 22.

Further support of sulfate as a tropospheric tracer is found in surface trajectories (Heffter, 1980), which illustrate the directional origin of the air masses. The 6-h trajectories arriving at Whiteface Mountain on June 14 and 15 are shown in Fig. 9. It is observed that on June 14, the trajectories are from the northwest, when ^7Be concentration was high but sulfate < 0.5 $\mu g/m^3$. On June 15 the direction of trajectories changed to southwest, and sulfate concentrations suddenly increased. Husain and Samson (1979) and Galvin et al. (1978) have shown that high concentrations of trace elements, particulates and sulfates often originates in the midwest (southwest of Whiteface Mountain).

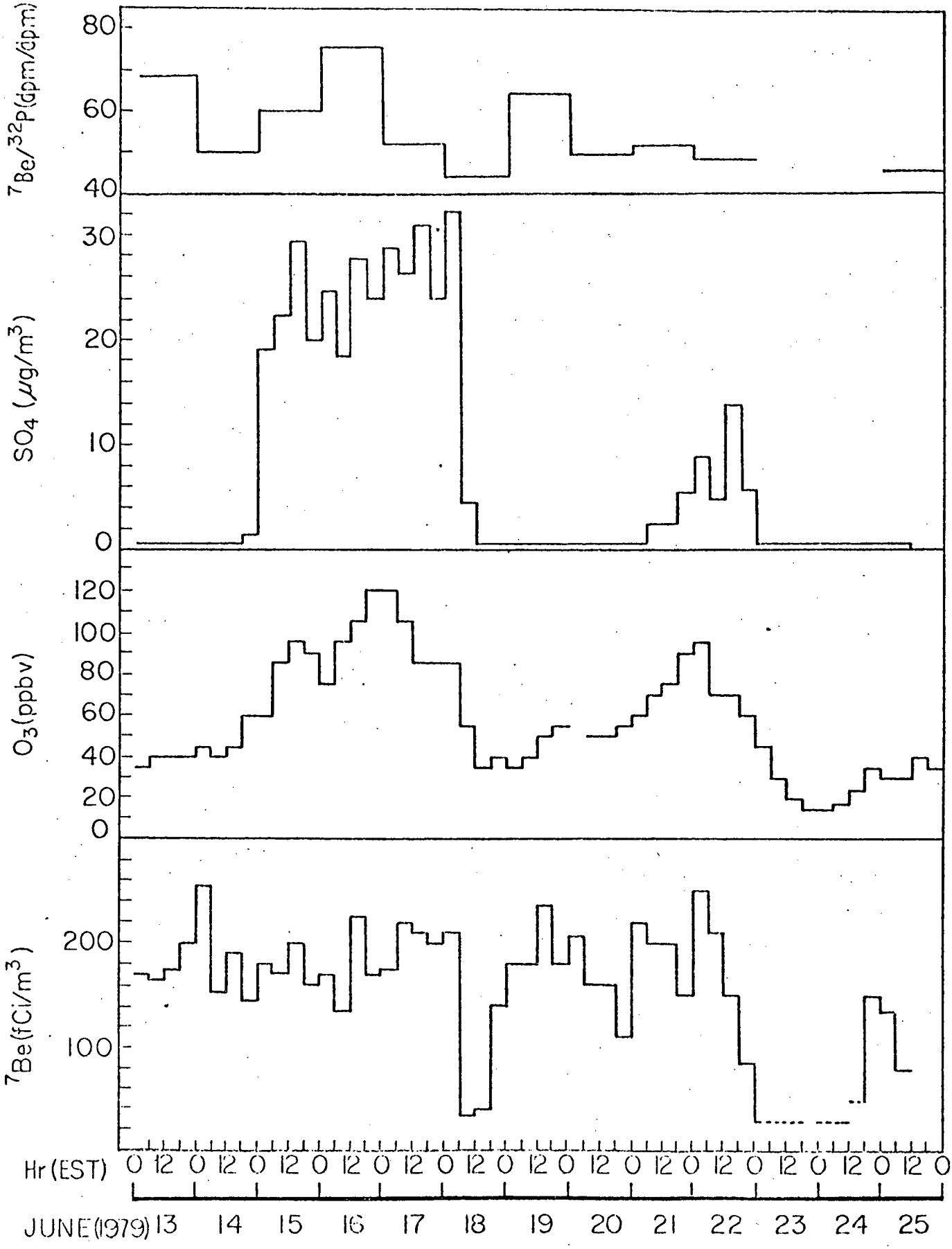

Fig. 8. 6-h ^{7}Be, O_3 and SO_4^{2-} concentration and 24-h $^{7}Be/^{32}P$ ratios measured at Whiteface Mountain between June 13 and 25, 1979.

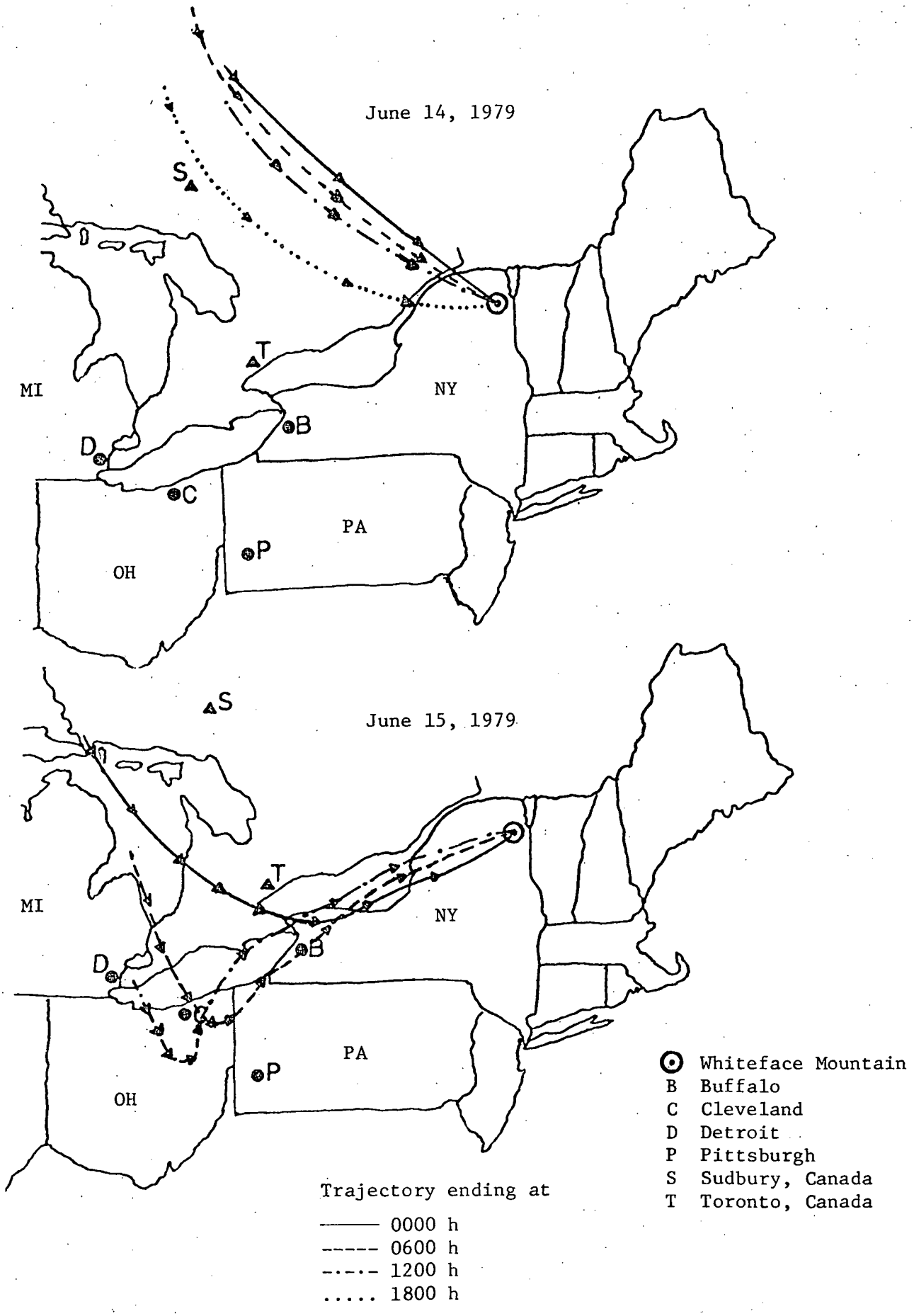

Fig. 9. Backward surface (0.4-1.4 km) trajectories for air arriving at Whiteface Mountain on June 14 and 15, 1979. Each arrow head represents a 6-h interval.

The above examples were intended to illustrate that both ^{7}Be and sulfate can be utilized to gain insight into the sources of O_3. It may be possible to quantify the transported photochemically produced O_3 using sulfate concentration measured over a very short time span. At the very least the simultaneous sulfate measurements will assist in the interpretation of ^{7}Be and O_3 data.

5. TEMPORAL SYSTEMATICS OF ^{7}Be, O_3 AND $^{7}Be/^{32}P$ AT WHITEFACE MOUNTAIN

5.1 Monthly Correlations of ^{7}Be and O_3

Daily ^{7}Be, ^{32}P, ^{33}P and O_3 concentrations determined since June, 1978 at Whiteface Mountain are listed in Table 1. Uncertainties for ^{7}Be, ^{32}P and ^{33}P can be inferred from Fig. 2. The ^{33}P results are given for completeness, however, because of the large uncertainties these results are not discussed.

The importance of the stratosphere as a source of surface O_3 can be inferred from a comparison of monthly average ^{7}Be and O_3 (Fig. 10). The general features of the ^{7}Be and O_3 profiles are similar. Both have maximum concentrations in June and July and minima in December and January. Also, both concentrations increase in November, 1978 and rise sharply in February. However, ^{7}Be concentration during June and July decrease steadily from 1977 through 1979, while O_3 increased slightly.

It must be kept in mind that while ^{7}Be primarily originates in the stratosphere and upper troposphere, O_3 also has significant ground level sources (i.e., transported urban-industrial pollution). Thus, any direct correlation of ^{7}Be and O_3 may be masked. This will become more evident as the time scale of measured ^{7}Be and O_3 is decreased.

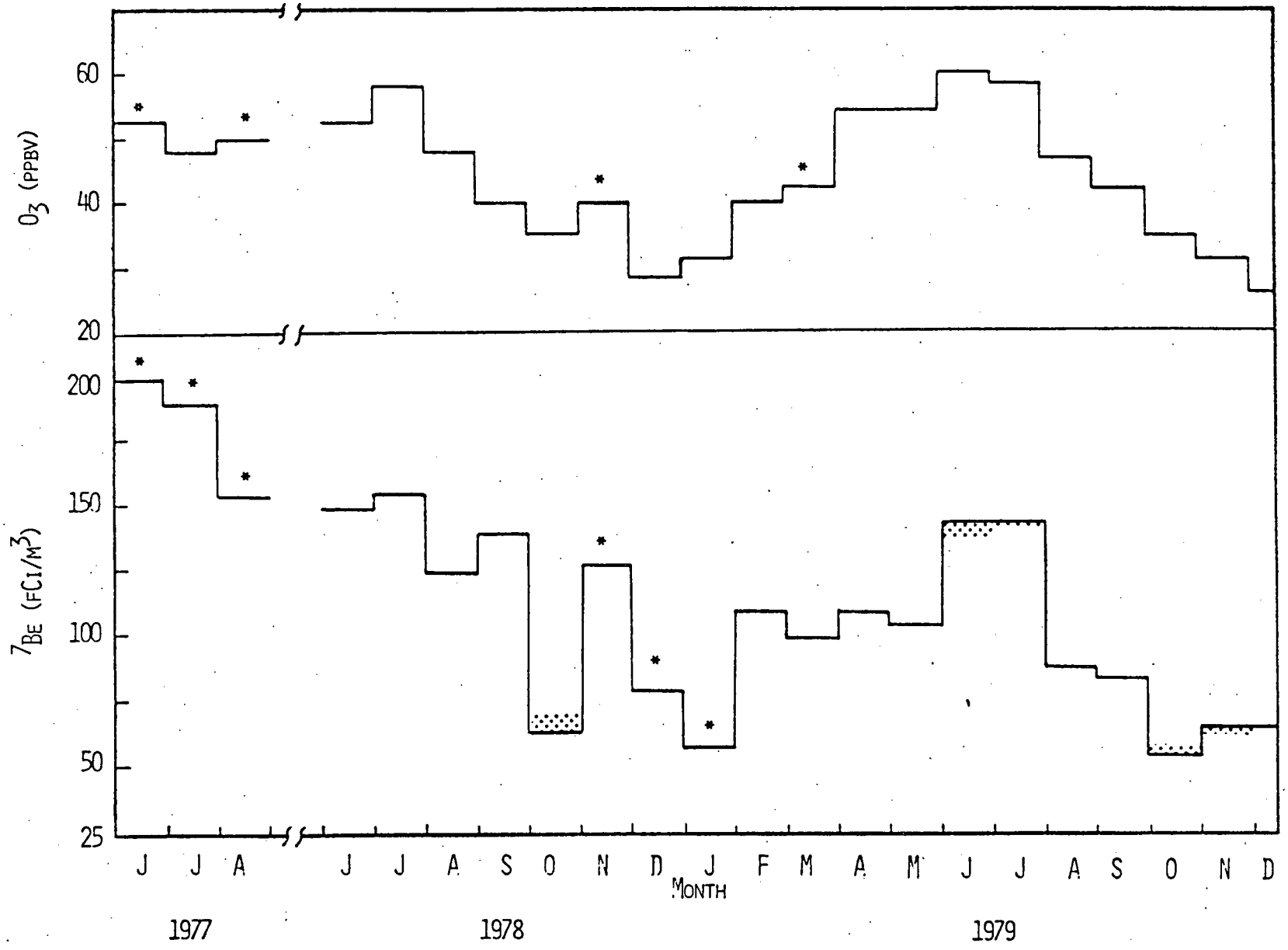

Fig. 10. Monthly average ^{7}Be and ozone concentrations measured at Whiteface Mountain. Shaded areas represent the uncertainties in the monthly averages due to upper limit measurement. Months where < 25 days of daily measurements were averaged are indicated by asterisks (*).

5.2 Correlation Between Bi-Weekly ^{7}Be and O_3

To examine more closely whether there is a quantitative relationship between ^{7}Be and O_3 at Whiteface Mountain, a scatter plot of bi-weekly averages is shown in Fig. 11A. ^{7}Be and O_3 clearly increase together, although considerable fluctuations are evident. Since transported ozone to this site can be large and variable (Coffey and Stasiuk, 1974), some scattering of the data is not surprising. Excluding the three points indicated in Fig. 11A, a linear regression fit of this data is shown by the solid line. This line yields a correlation coefficient, $r = 0.78$. For 35 data pairs there is $< 0.1\%$ probability of obtaining this value of r from random uncorrelated data. However, the regression line does not pass through the origin, rather it intersects the O_3 axis at 18 ppbv. The inverse of the slope of this line corresponds to a $^{7}Be/O_3$ ratio of 4.2 $fCi/m^3/ppbv$, which is a factor of 2.6 lower than the average ratio observed in the lower stratosphere (Appendices I and III), although, it's comparable to the upper tropospheric ratio of 5.4 $fCi/m^3/ppbv$ deduced for spring and summer months in Section 6.2.

Fig. 11B is a scatter plot of bi-weekly ^{7}Be and O_3 data from Zugspitze, Germany (R. Reiter et al., 1977 and 1978). Although the data generally follow the same trend as Fig. 11A, linear regression analysis yields $r = 0.66$ which is somewhat lower than 0.78 value obtained for Whiteface Mountain data. However, this value of r is still significantly high for the number of data pairs compared, and supports the correlation of ^{7}Be and O_3. The slope of the regression line is different at Zugspitze compared to Whiteface Mountain. The resultant $^{7}Be/O_3$ ratio is 7.6 $fCi/m^3/ppbv$, which falls in between the upper tropospheric and stratospheric ratios. The difference in the slope of the regression lines in Fig. 11 may be related

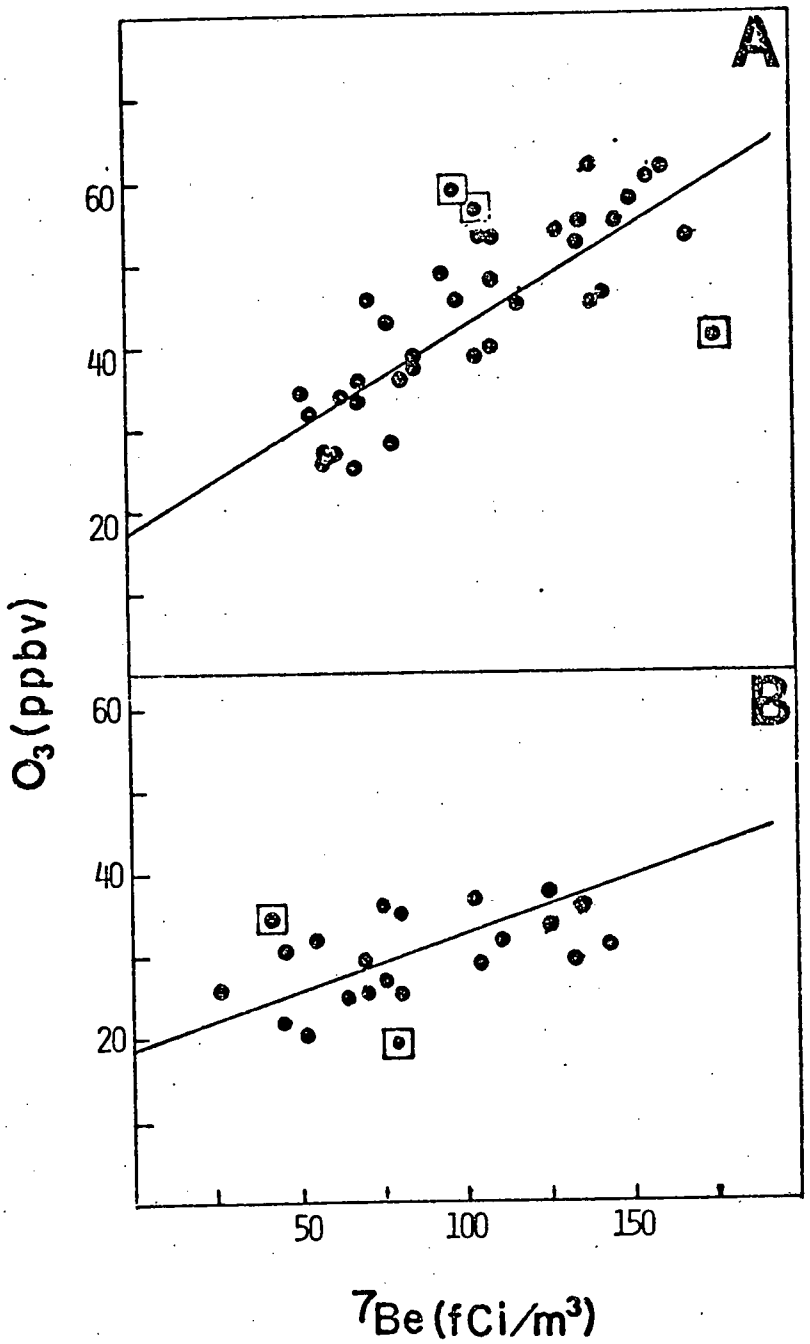

Fig. 11. Scatter plot of bi-weekly average ^{7}Be and ozone concentrations measured at (A) Whiteface Mountain, N.Y. and (B) Zugspitze, Germany (R. Reiter et al., 1977 and 1978). Solid lines are linear regression fits to the data.

to different effects of the transported O_3 components at the two sites. For example, if the largest effect of transported O_3 at Whiteface Mountain also corresponds to summer months when ^7Be concentration is highest (SO_4^{2-} also maximum, Section 11), this could increase the slope in Fig. 11A (or decrease the implied $^7Be/O_3$ ratio). More detailed study of the data at the two sites is needed.

5.3 Correlation of Daily ^7Be, $^7Be/^{32}P$ and O_3

On a daily basis the comparison of ^7Be and O_3 is even more complex. In Figs. 12-14 daily ^7Be, O_3 and $^7Be/^{32}P$ data are shown. To facilitate comparison between the ^7Be and O_3, values higher than the monthly averages have been shaded. In general, the shaded periods occur at the same time for both ^7Be and O_3. However, a simple quantitative relationship between ^7Be and O_3 is not clearly evident. Several examples will illustrate this point.

There are four periods in April (Fig. 12) when ^7Be concentration exceeded 115 fCi/m^3 (the monthly average), April 8, 17-21, 24-25 and 30. On April 8, ^7Be concentration increased from 25 fCi/m^3 on April 7 to 215 fCi/m^3 (+190 fCi/m^3), while O_3 increased from 42 to 55 ppbv (+13 ppbv). The ratio of ^7Be increment to the O_3 increment is 14.6 fCi/m^3/ppbv, which is in fair agreement with the measured lower stratospheric ratio of 10.9 in spring (Dutkiewicz and Husain, 1979). On April 17, ^7Be increased by 155 fCi/m^3 from the previous day whereas O_3 increased by 11 ppbv yielding the incremental ratio of 14.1, again in fair agreement with the stratospheric value. Note the $^7Be/^{32}P$ ratio is 60 on April 17, supporting a large stratospheric component. However, this simple relationship is not always the case. For example, an incremental ratio of 4.2 fCi/m^3/ppbv

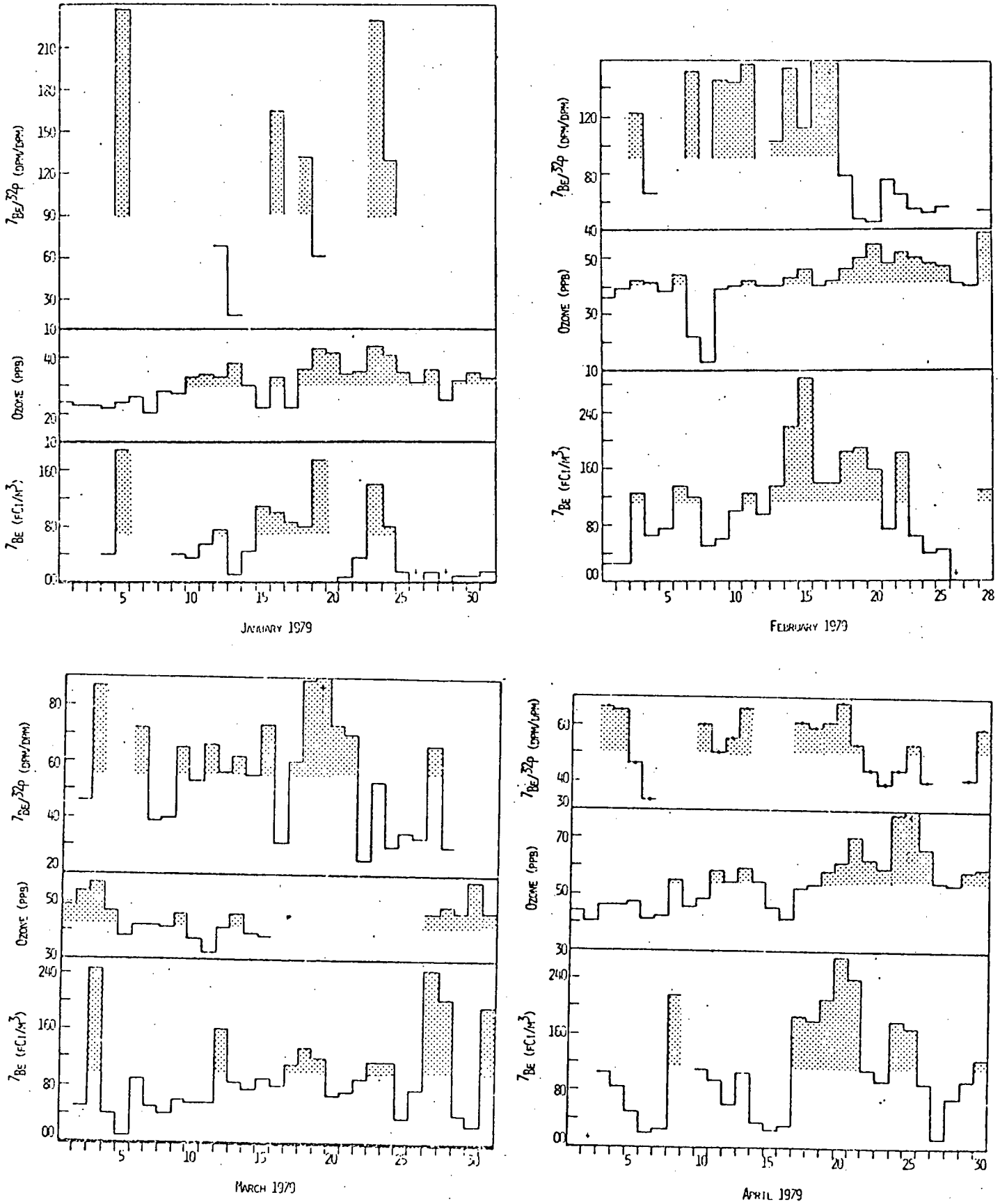

Fig. 12. Daily concentrations of ^{7}Be and ozone and $^{7}Be/^{32}P$ ratios measured at Whiteface Mountain, N.Y., January through April, 1979. To facilitate comparison larger than the monthly average have been shaded.

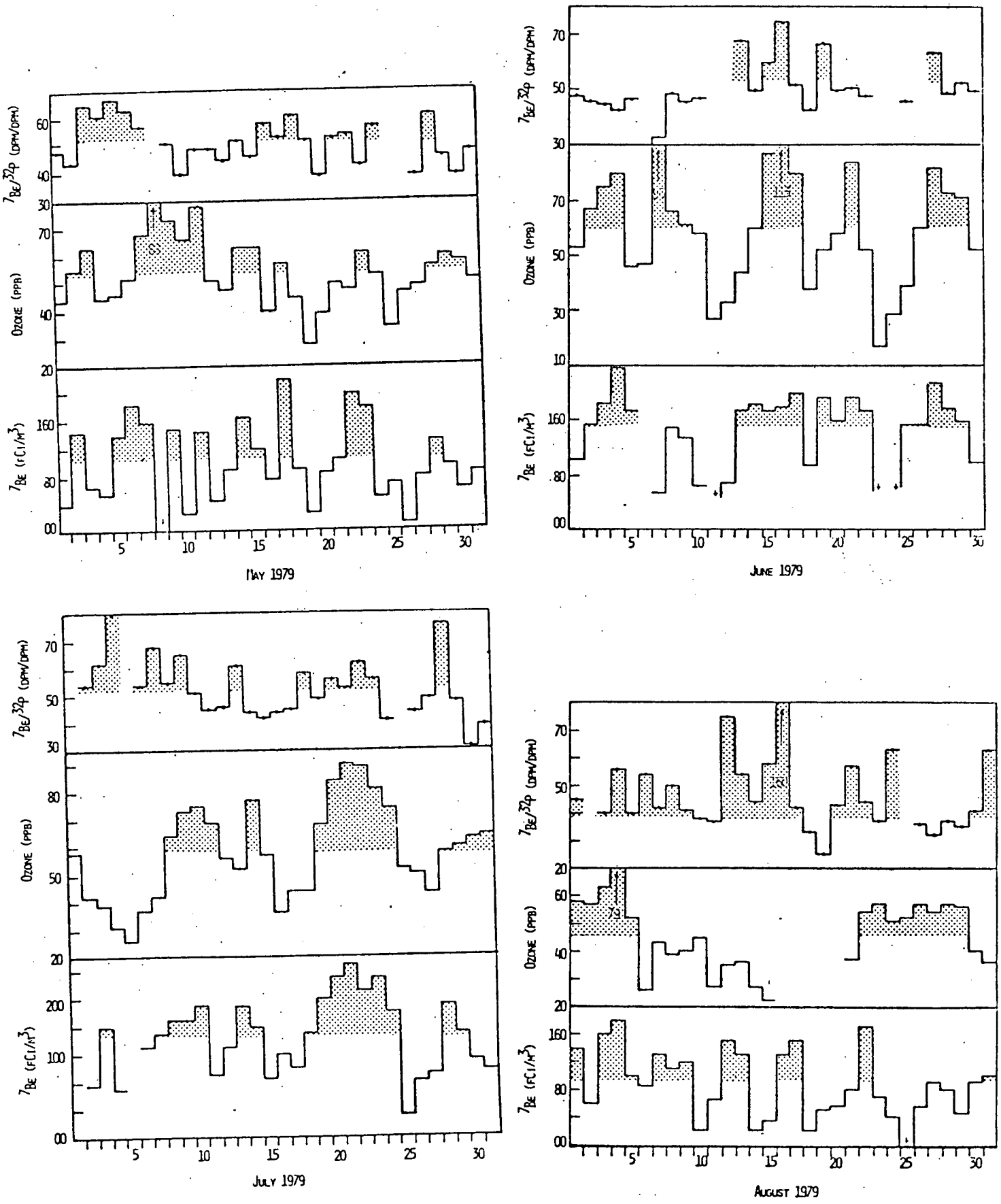

Fig. 13. Same as Fig. 12 except for May through August, 1979.

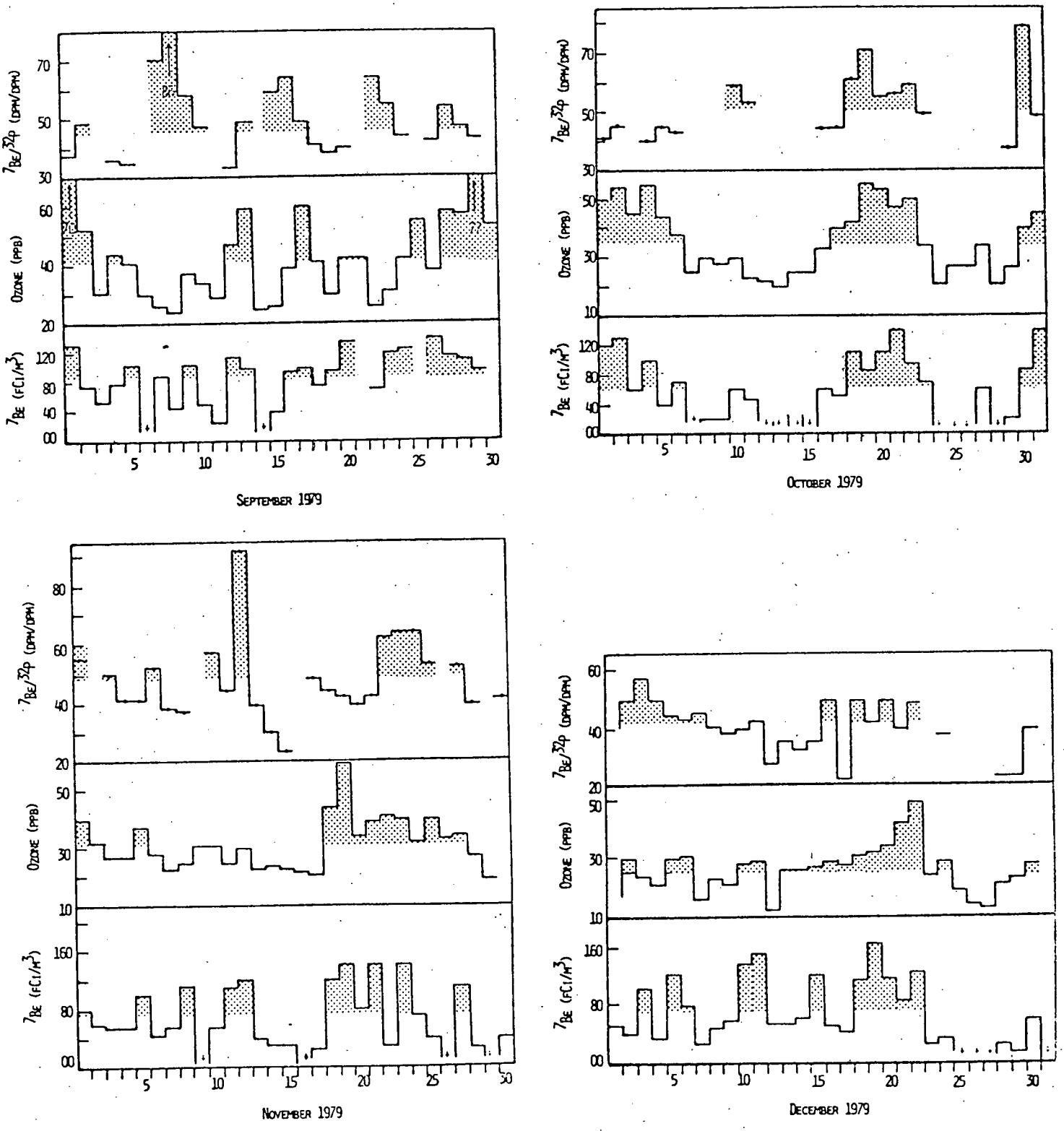

Fig. 14. Same as Fig. 12 except for September through December, 1979.

is observed on April 24. This suggests an additional O_3 source on this day. The sulfate concentration can be enlightening here. For example, we measured 1.1 and 1.8 μg SO_4^{2-}/m^3 on April 8 and 17 but 8.3 $\mu g/m^3$ on April 24. Since SO_4^{2-} is pollution derived it suggests transported photochemical O_3 on April 24. Hence, the lower $^7Be/O_3$ ratio of 4.2 fCi/m^3/ppbv is understandable. Also, the $^7Be/^{32}P$ ratio is only 44 on April 24, indicating mixed tropospheric and stratospheric air.

Similarly in July, Fig. 13 there are five episodes of above average ^7Be (July 3, 8-10, 13, 14, 19-24 and 28). The most pronounced peak is on July 19-24. The incremental ratio for July 18-19 is $\sim$ 4, far lower than the stratospheric value. However, a large tropospheric O_3 component is indicated by a SO_4^{2-} concentration of 6.2 and 34.5 $\mu g/m^3$, respectively on July 19 and 20, and $^7Be/^{32}P$ ratios of 49 and 56 respectively. Clearly, both stratospheric and ground level O_3 sources influence this site, and their delineation on a daily basis is far from trivial. Possibly the most practical approach, with our present knowledge of atmospheric transport, is to quantify the stratospheric component on an average monthly basis. The quantification of episodic stratospheric O_3 will be discussed further in Section 7.2.

6. DETERMINATION OF STRATOSPHERIC O_3 FROM ^7Be MEASUREMENTS

6.1 General Technique

Stratospheric O_3 contributions in surface air can be determined from ground level ^7Be measuremens if, (1) $^7Be/O_3$ ratio in the stratosphere, (2) ^7Be component from tropospheric production, and (3) removal rates of ^7Be and O_3 during transport are known. We describe below our recent work on the determination of $^7Be/O_3$ ratios and tropospheric ^7Be component.

6.2 Determination of $^{7}Be/O_3$ Ratios in the Lower Stratosphere and the Upper Troposphere

Our measurements of $^{7}Be/O_3$ ratios in the stratosphere for 35^{o}-$42^{o}N$ for January-June, 1978, and 20^{o}-$50^{o}N$ for October, 1977-March, 1979 have been published elsewhere (Dutkiewicz and Husain, 1979, Appendix I; Husain et al., 1980, Appendix III). These papers did not include all of our data. Therefore, we present briefly all of our $^{7}Be/O_3$ ratio measurements here. In addition to $^{7}Be/O_3$, ^{90}Sr concentrations were also measured in each sample. The discussion of ^{90}Sr data will be deferred to a latter section in this report.

Concentrations of ^{7}Be, ^{90}Sr and O_3 at 9.8-12.2 km and 11^{o}-$56^{o}N$ for October, 1977 through June, 1979 are given in Table 2. There is a preponderance of data in 30^{o}-$40^{o}N$ and paucity of data above $45^{o}N$ and below $20^{o}N$. Tropopause data for our samples are still being analyzed by NASA. Therefore, as discussed earlier (Dutkiewicz and Husain, 1979) we have tentatively analyzed assigned samples as stratospheric and tropospheric on the basis of observed O_3 concentrations as follows: $O_3 > 200$ ppbv, stratosphere, and $O_3 < 100$ ppbv, troposphere. Following this criterion, it is observed that ^{7}Be measurements in the stratosphere have relatively lower uncertainties. Also in many of the upper tropospheric samples only an upper limit for the ^{7}Be concentration could be determined. ^{7}Be concentration vary from 150 (which is similar to ground level values) to 7,300 fCi/m^3 whereas O_3 vary from 30 to 670 ppbv. Clearly, these samples represent both the stratosphere and troposphere. At the altitude of these studies, O_3 produced from pollutant NO_x and hydrocarbons must be minimal. It is, therefore, interesting to study the correlation between ^{7}Be and O_3.

The ^{7}Be and O_3 data from Table 2 is plotted in Fig. 15. Uncertainties in O_3 and ^{7}Be concentrations are shown respectively by vertical and horizontal bars. The solid line represents a linear regression fit to the data and has a slope of 0.072 ppbv/fCi/m^3. The linear correlation coefficient (r) for this line is 0.89, which, for a data set of this size corresponds to 99% probability that ^{7}Be and O_3 are linearly correlated. In light of experimental uncertainties, the small non-zero intercept may be neglected. The solid line then corresponds to a constant $^{7}Be/O_3$ ratio of 14 fCi/m^3/ppbv. In Fig. 1 of Appendix III, we observe that there is a small but noticeable seasonal variation in the stratospheric $^{7}Be/O_3$ ratio, with higher values observed during fall and winter, when the largest proportion of the samples were collected. Thus, the $^{7}Be/O_3$ ratio determined from the solid line fit to the data in Fig. 15, may be biased on the high side. In Appendix III, we determined a more representative annual average $^{7}Be/O_3$ ratio of 11 fCi/m^3/ppbv from stratospheric data. This corresponds to the dashed line in Fig. 15. In view of the experimental uncertainties, the dashed line is probably a better representation of the complete data set. However, tropospheric $^{7}Be/O_3$ ratios (O_3 < 100 pbbv) generally fall above this line. As discussed above, only the upper limit of the ^{7}Be concentration could be measured in many upper tropospheric samples. Hence, we have taken a different approach to obtain $^{7}Be/O_3$ ratio in the upper troposphere based on all of our measurements. In Fig. 16 we show the tropospheric $^{7}Be/O_3$ ratio distributions for March through August and September through February periods 30^{o}-60^{o}N. In obtaining these distributions we have included the upper limit measurements by assuming that there is an equal probability that the real value lies in any 2 fCi/m^3/ppbv interval below the upper limit. The

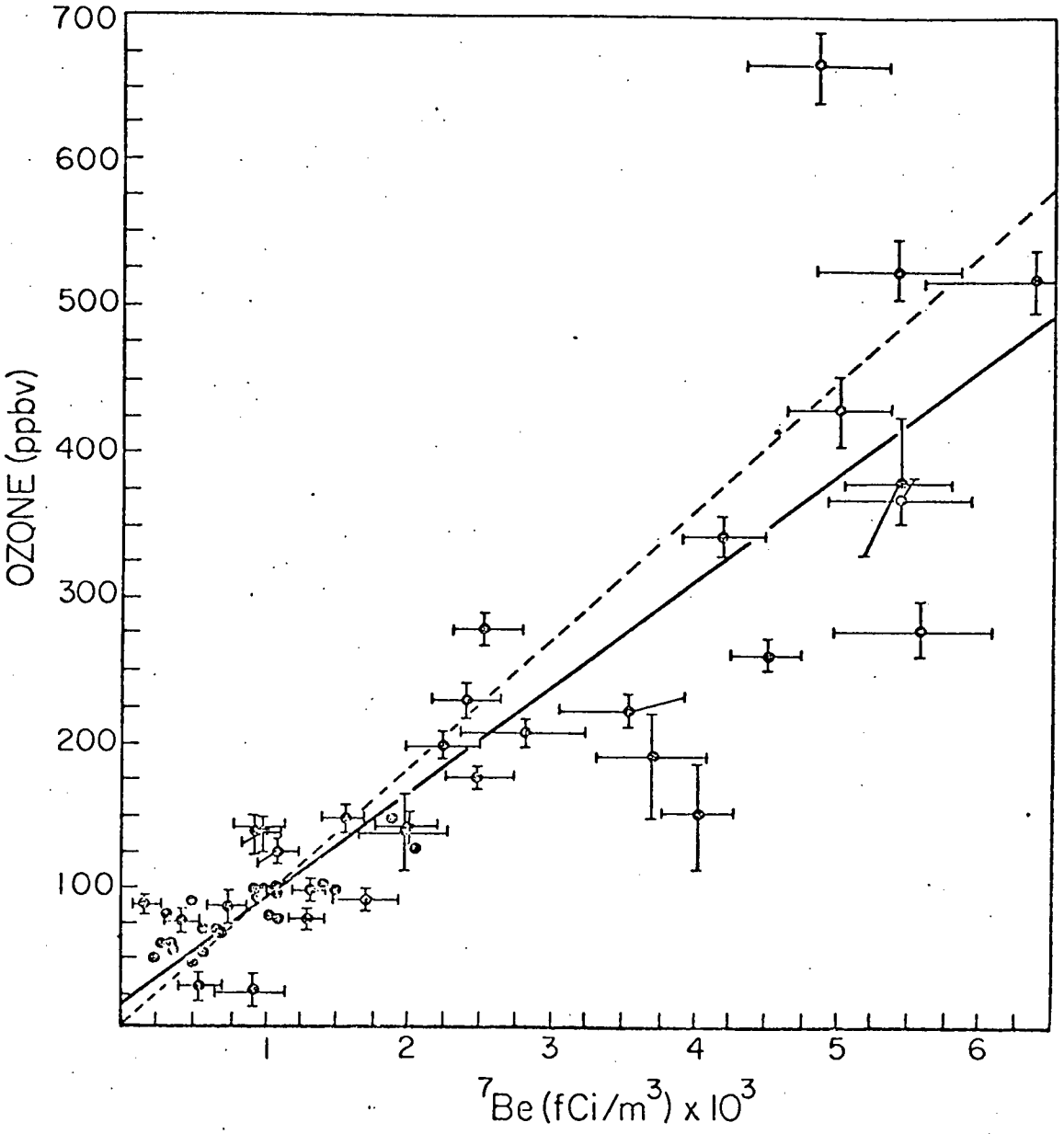

Fig. 15. Scatter plot of ^{7}Be and ozone measured at 9.8 to 12 km, 30°-60°N. Vertical and horizontal bars, respectively, correspond to uncertainties in ozone and ^{7}Be where space permits. The solid line is a linear regression fit to the data (r = .89). The dashed line corresponds to a constant ^{7}Be/ozone ratio of 11 fCi/m^{3}/ppbV determined from only stratospheric measurements as explained in the text.

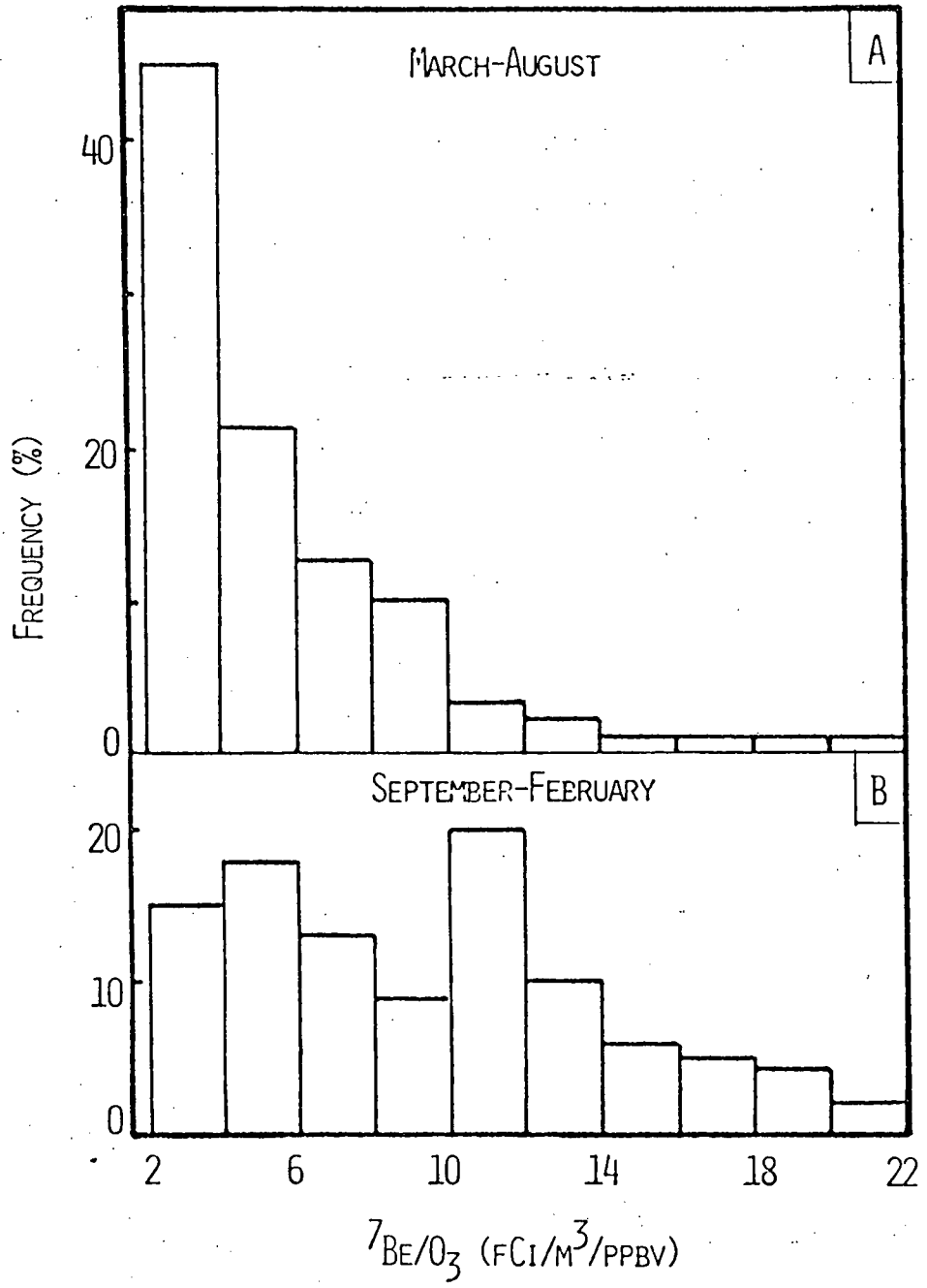

Fig. 16. Distribution of $^7Be/O_3$ ratios measured in tropospheric air ($O_3 \lesssim 100$ pbbV) at 9.8-12 km, 30°-60°N. Upper limit ratios have also been included as discussed in the text.

distribution for March-August is strongly peaked at low $^{7}Be/O_3$ ratios (Fig. 16). An average ratio of 5.4 fCi/m^3/ppbv is obtained. For September-February, the distribution is broad and no meaningful average $^{7}Be/O_3$ ratio can be obtained.

We note in passing that $^{7}Be/O_3$ ratio just below the tropopause are approximately one-half of those observed just above the tropopause. For dilution of the stratospheric air by the upper tropospheric air to account for the ratio change a relatively higher O_3 concentration in the upper troposphere is needed. Alternately, a more rapid removal of ^{7}Be aerosols will also result in lowering of the stratospheric $^{7}Be/O_3$ ratio. In the upper troposphere there is expected to be relatively higher production of ^{7}Be than O_3 as the concentration of anthropogenic NO_x and hydrocarbons decreases. However, Liu et al. (1980) have recently proposed that O_3 may be produced in the upper troposphere from odd nitrogen species transported from the stratosphere. This mechanism could explain our results.

6.3 Tropospheric ^{7}Be

Within the lower 5 km of the atmosphere the production rate of cosmogenic radionuclides is relatively small (Lal and Peters, 1967). Rapid circulation and precipitation scavenging in the lower atmosphere results in aerosol lifetimes on the order of only a few days (Machta et al., 1970; Martell and Moore, 1974; Reiter, 1975 and references therein). These factors all limit ^{7}Be production, so that the net ^{7}Be concentration produced in the lower 5 km is expected to be negligible. Therefore, the observed ^{7}Be concentration primarily originates aloft (upper troposphere and primarily lower stratosphere). In order to use ^{7}Be to quantify stratospheric ozone, the tropospheric component which is mixed in during transport should be

subtracted. This is particularly important on a daily or episodic basis since rapid mixing can at times bring down upper tropospheric air which can have a relatively high ^{7}Be concentration (Fig. 5). To determine the tropospheric component it is necessary to consider regions or times when the stratospheric influence is known to be minimal, since a small contribution from the stratosphere is sufficient to significantly effect surface ^{7}Be concentrations. Also, in order to quantify stratospheric ozone on a daily basis, the tropospheric component should also be known on a daily basis, or at least the range of most probable variation must be considered.

In Appendix III global ^{7}Be data was used to estimate the tropospheric component. The theoretical latitudinal profile of tropospheric production (Lal and Peters, 1967) was normalized to global ^{7}Be concentrations at the equator and $60^{o}N$ and $60^{o}S$ (regions of apparent small stratospheric influence). An average background ^{7}Be concentration of 50 fCi/m^{3} was obtained for mid latitudes, with slightly lower values at the poles and equator. Since this estimate is based on global data which in many cases has been averaged over several years, we have adopted 50 fCi/m^{3} as the average tropospheric contributions. ^{7}Be data from Whiteface Mountain supports this value for the tropospheric component. During October through January, when the stratospheric component from tropopause folding is expected to be minimum (Danielsen and Mohnen, 1977), the distribution of ^{7}Be concentration peaks below 75 fCi/m^{3} (Fig. 17).. Also, with the exception of November, 1978, monthly averages during this period fall between 55 and 75 fCi/m^{3}. Since a small stratospheric contribution is possible at this time, these results are consistent with 50 fCi/m^{3} as the average background ^{7}Be produced in the troposphere.

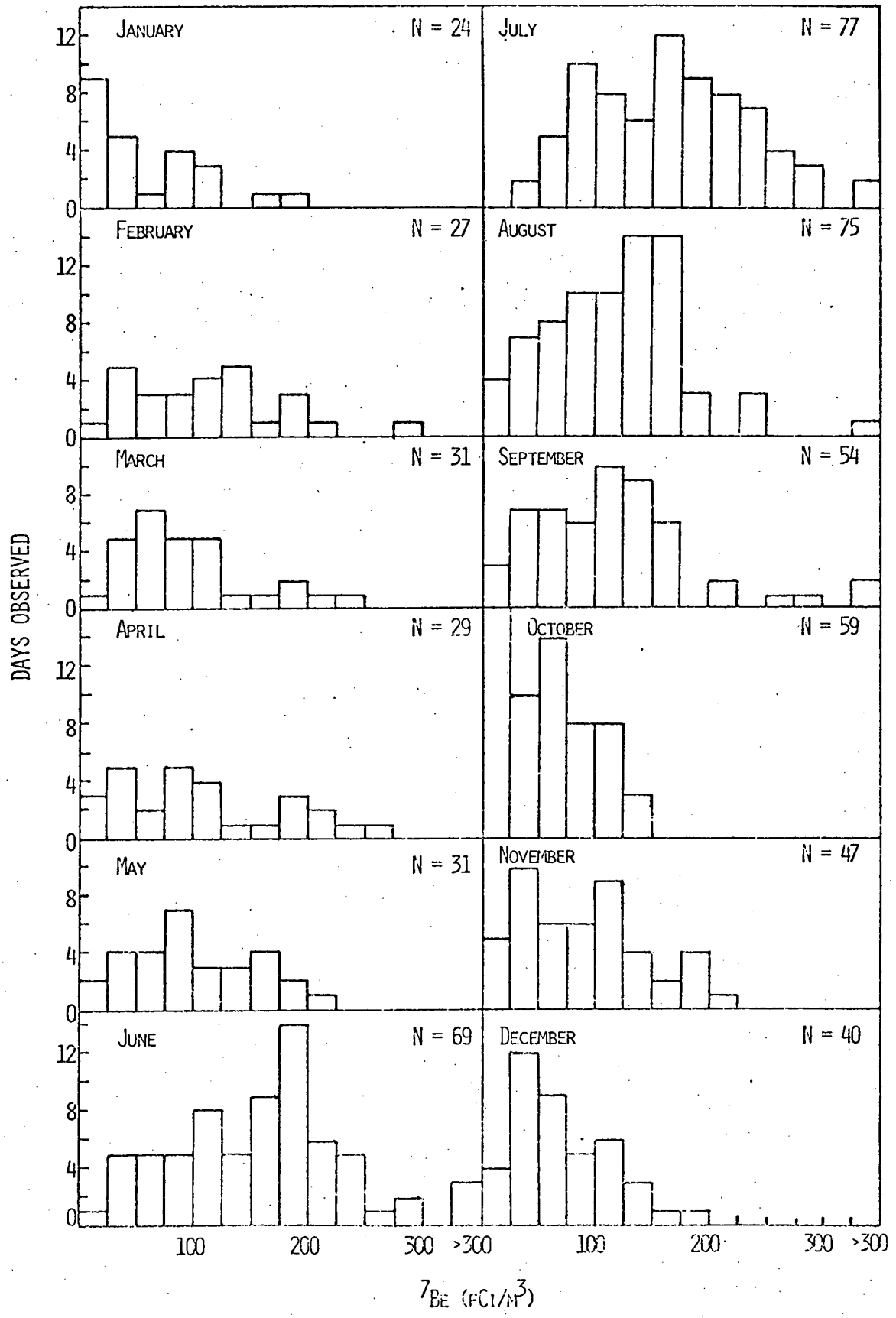

Fig. 17. Monthly distributions of 24-h ^{7}Be concentrations measured at Whiteface Mountain, N.Y., between 1977 and 1979.

It is also possible to deduce tropospheric ^{7}Be component from $^{7}Be/^{32}P$ data. In section 3.2 we have argued that for tropospheric air the $^{7}Be/^{32}P$ ratio is between 22 and 38. Thus, the average ^{7}Be concentration on these days should represent tropospheric production. This criteria and the data in Table 1 yields a value of 74 ± 44 fCi/m^3, where the uncertainty is the 1 σ deviation. Except for 1979, the data in Table 1 was preferentially obtained during summer months, a time of high stratospheric-tropospheric exchange. Using only 1979 data lowers the average tropospheric ^{7}Be component to 65 ± 40 fCi/m^3. Including the days when ^{32}P was below the detection limit (hence $^{7}Be/^{32}P$ could not be determined) further lowers the tropospheric ^{7}Be component to 45 ± 40 fCi/m^3. In summary, therefore, our tropospheric ^{7}Be component as 50 fCi/m^3 appears well established.

6.4 Mean Residence Times of ^{7}Be and O_3

Please see Appendix III for the discussion of the mean residence times of ^{7}Be and O_3.

7. ESTIMATES OF STRATOSPHERIC O_3 IN SURFACE AIR

7.1 Global

A paper entitled, "On the Origin of Tropospheric Ozone" has been submitted to Nature. A preprint is attached to this report as Appendix III. In this paper the impact of stratospheric-tropospheric exchange on the tropospheric O_3 budget is assessed using ^{7}Be as a tracer. A comprehensive global ^{7}Be latitudinal profile is presented from available data in the literature. This profile demonstrates that stratospheric-tropospheric exchange is approximately two times greater in the northern compared to southern hemisphere, in agreement with recent General Circulation Model

calculations (Mahlman et al., 1980 and Gidel and Shapiro, 1980). Also, ^{7}Be is observed to be strongly peaked in surface air between 20° and 45°N and 15° and 40°S. It cannot be inferred from this data whether this is caused by a greater exchange flux in these latitude bands or whether tropospheric mixing patterns preferentially transport stratospheric air to the surface in these regions.

Using equation 3 and values of k_1 and k_2 discussed in Appendix III, the component of tropospheric O_3 originating from the stratosphere is calculated. The results show that at least half of the annual average surface O_3 at 20°-50°N and essentially all the O_3 at 60°-90°N originates from the stratosphere. Calculations in the southern hemisphere is hampered by the lack of directly measured $^{7}Be/O_3$ ratios in the stratosphere as well as less abundant surface ^{7}Be measurements, especially 60°-90°S. For 10°-40°S, our calculations suggest at least half of the observed O_3 originates from the stratosphere.

7.2 Episodic

The problems involved in calculating the stratospheric component in episodic high ozone periods have been discussed. However, it is possible to estimate the average impact of stratospheric O_3 due to the rapid subsidence of stratospheric air. We assume days with peak ^{7}Be concentration > 175 fCi/m^3 corresponds to rapid stratospheric subsidence. This value is 3.5 times the estimated tropospheric background concentration (Section 5.2) and 4% of the observed concentration in the lower stratosphere (Appendix I and Fig. 5). Although this value for the ^{7}Be concentration may appear low for rapid transport, many of the cases included have ^{7}Be concentration > 250 fCi/m^3. Support for this assumption can be inferred from Fig. 17.

With the exception of June and July, ^{7}Be concentration is only infrequently greater than this concentration. Thus, it is reasonable to assume that rapid stratospheric subsidence is respondible for most of the observed ^{7}Be concentration on these days. At times the ^{7}Be concentration does remain above this level for several consecutive days, particularly in summer (Fig. 12-14). In these cases the day with the highest ^{7}Be concentration is assumed to correspond to rapid transport.

^{7}Be and O_3 concentrations and $^{7}Be/^{32}P$ ratios were averaged for 33 such peak days and 5 days prior to and after the peak. SO_4^{2-} concentration was also averaged for 25 cases where sufficient data was available. The results are shown in Fig. 18. The average ^{7}Be concentration on the peak days (day 0) sharply increase from 160 to 250 fCi/m^3. The $^{7}Be/^{32}P$ ratio and O_3 also peak on this day. In fact, the average $^{7}Be/^{32}P$ ratio (65) is approaching the measured ratios in the lower stratosphere (Feely et al., 1971), supporting our assumption that the ^{7}Be concentration observed on these peak days is of recent stratospheric origin. On the day after the peak (day + 1), ^{7}Be and $^{7}Be/^{32}P$ ratio show a dramatic decrease, while only a modest decrease in O_3 is observed. However, SO_4^{2-} concentration is low on day 0 but shows a dramatic increase on day + 1 suggesting increased impact from distant polluted areas.

Assumed baseline values for ^{7}Be, and O_3 are shown as dashed lines in Fig. 18. We assume that only the ^{7}Be concentration above the dashed line for days -1 to 1 corresponds to the component rapidly transported. Using the stratospheric $^{7}Be/O_3$ ratio of 11 $fCi/m^3/ppbv$, and assuming no fractionation of ^{7}Be and O_3 during transport, the estimated O_3 associated with rapidly

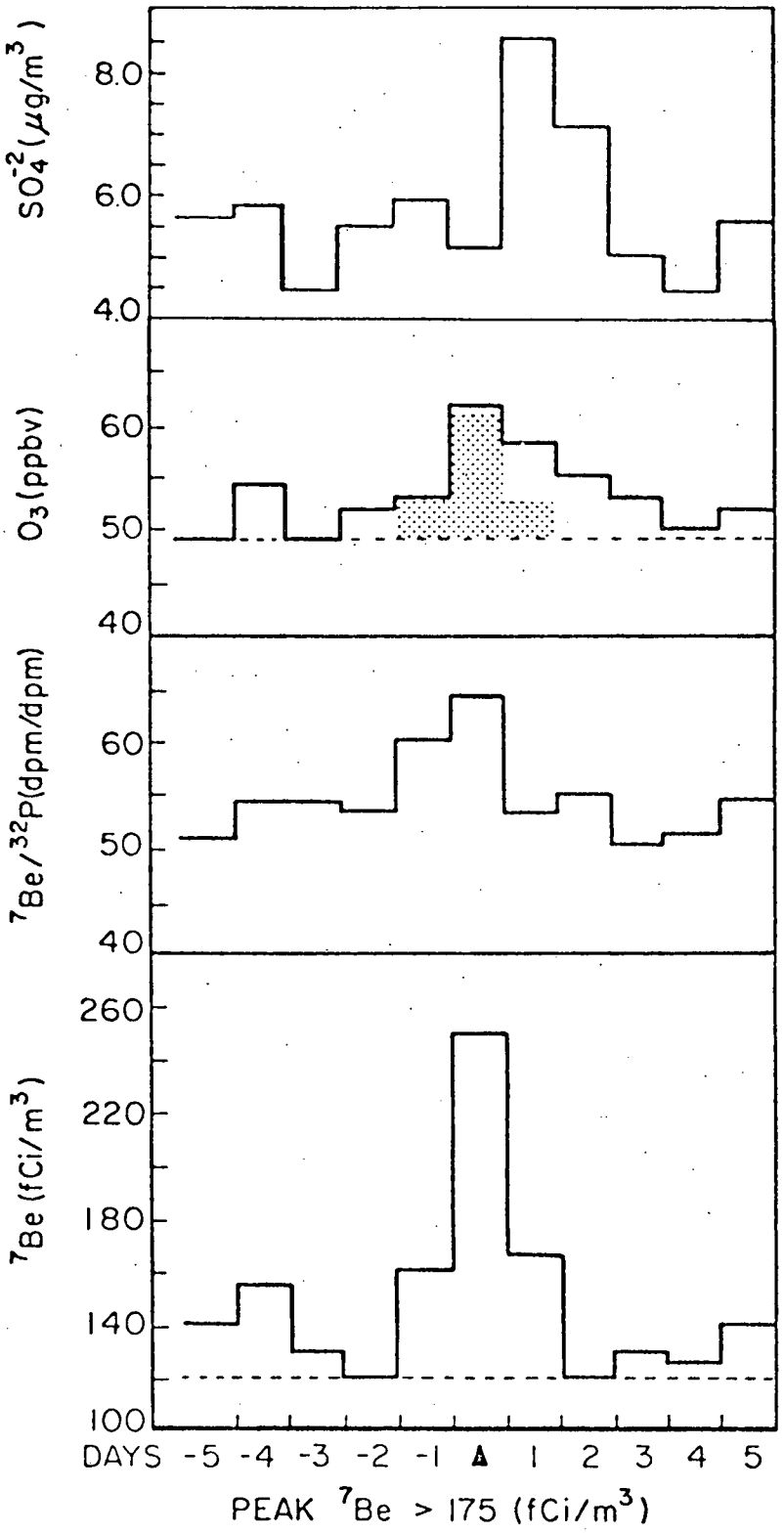

Fig. 18. Average ^7Be, ozone and SO_4^{2-} concentrations and $^7Be/^{32}P$ ratios for days when the peak ^7Be concentration > 175 fCi/m^3, and the 5 days prior to and after the peak day. The dashed lines correspond to assumed baseline ozone and ^7Be concentrations and the shaded ozone is the estimated stratospheric ozone associated with the ^7Be concentration greater than the baseline value as explained in the text.

transported stratospheric air is shown shaded. For day 0 and day -1, essentially all of the increased O_3 is accounted for. However, the O_3 estimated for the day + 1 is too small to account for the observed concentration. In fact, the O_3 does not return to baseline values for 4 days, while ^7Be returns to baseline concentration on day + 2. As mentioned above the high SO_4^{2-} concentrations on day + 1 and + 2 strongly suggests that the backside of the weather system causing the rapid stratospheric subsidence, also favors transport from distant ground level O_3 sources, as proposed by Husain et al., (1977) to explain the fact that at times O_3 was observed to peak a day after ^7Be.

Although the average increased O_3 during the time of peak ^7Be in Fig. 18 can be accounted for using stratospheric $^7Be/O_3$ ratios, the increased concentration is only 12 ppbv. As the baseline O_3 for these 33 cases is 48 ppbv, this amounts to only a 25% increase. However, assumed baseline O_3 (i.e., 48 ppbv) is not necessarily from tropospheric sources. The high baseline O_3 and ^7Be can in part be explained by the fact that most of the cases averaged occurred in spring and summer months when the average ^7Be is highest and stratospheric impact is the greatest. The baseline $^7Be/^{32}P$ ratios (50) and ^7Be concentration (120 fCi/m^3) are both higher than expected for purely tropospheric air, and support a stratospheric component for the baseline O_3 indicated in Fig. 18. However, the magnitude of this component is difficult to estimate. The point to be made here is that rapid subsidence of stratospheric air can increase surface O_3, although on the average, the increase is only approximately 25% of the observed O_3. The other significant point is the fact that the peak SO_4^{2-} concentration generally

occurs the day after peak ^{7}Be, and therefore is likely to be associated with the backside of the same weather system. Thus, stratospheric subsidence may intensify the impact of photochemical pollution episodes.

As we have already mentioned, applying the $^{7}Be/O_3$ technique on an individual daily basis cannot yet be done with confidence. The fate of stratospheric air parcells in the troposphere must be understood more fully (i.e., mixing and transport mechanisms) so that any fractionation of ^{7}Be and O_3 during transport can be accounted for.

8. STRATOSPHERIC MEAN RESIDENCE TIMES

Our high altitude measurements began in October 1977, shortly after Chinese nuclear detonation in the previous month. Our ^{90}Sr data provides an excellent opportunity to determine the lower stratospheric aerosol mean residence times. Using $O_3 > 200$ ppbv, for stratospheric samples, we have plotted in Fig. 19 only the stratospheric ratios of $^{7}Be/O_3$, $^{90}Sr/O_3$, and $^{90}Sr/^{7}Be$ measured at 35^{o}-$55^{o}N$. Uncertainties are shown by vertical bars. During 1979 the sampling times were reduced from 2 to 1 h, thus reducing by half the air volumes filtered. Furthermore, ^{90}Sr concentrations in 1979 were much lower than those in 1978. The decreased specific activity increased the experimental uncertainties (Fig. 19). Therefore, for mean residence time determination we have restricted ourselves to 1978 data. It is evident both from $^{90}Sr/O_3$ and $^{90}Sr/^{7}Be$ ratios in Fig. 19 that ^{90}Sr is decreasing exponentially, although the slopes of $^{90}Sr/O_3$ and $^{90}Sr/^{7}Be$ regression lines are different. On the other hand, $^{7}Be/O_3$ ratios show relatively small variations, which could be seasonal (Appendix III). This suggestion is supported by the fact that the $^{7}Be/O_3$ ratios in 1979 are about the same as those in 1978, contrary to $^{90}Sr/O_3$ and $^{90}Sr/^{7}Be$ values.

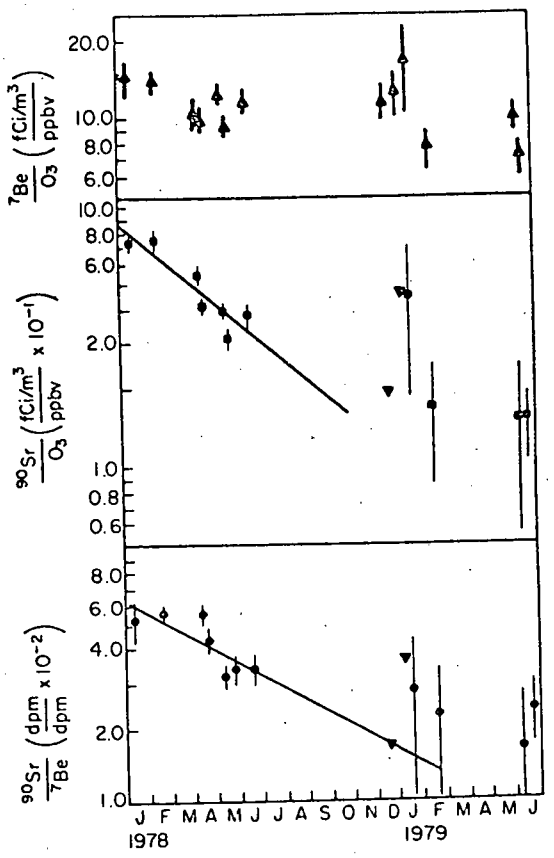

Fig. 19. $^{7}Be/O_3$, $^{90}Sr/O_3$ and $^{90}Sr/^{7}Be$ ratios measured in stratospheric samples (O_3 > 200 ppbv) collected at 10 to 12 km. Estimated uncertainties are indicated by vertical bars. Solid lines are regression fits to exponential decay curves for the 1978 measurements as explained in the text.

Both $^{90}Sr/O_3$ and $^{90}Sr/^{7}Be$ ratios could be used to determine aerosol mean residence time in the lower stratosphere. A mean residence time of 270 days is obtained from $^{90}Sr/^{7}Be$ data whereas $^{90}Sr/O_3$ ratio yield a value of 180 days. The variation in $^{7}Be/O_3$ ratio is reflected in the two values for the mean residence time. Both values are lower than $\sim$ 1 year mean residence time determined by other workers (Reiter, 1975 and ref. therein). However, mean residence time depends on the altitude of fission product injection and the latitude of measurements. Higher $^{90}Sr/O_3$ and $^{90}Sr/^{7}Be$ ratios in 1979 than expected from the solid lines in Fig. 19 may suggest descending fresh upper stratospheric air during winter months, possibly from the polar stratosphere as suggested by earlier tracer experiments (e.g., Martell, 1970; Feely et al., 1971).

9. TRANSPORT TIMES OF STRATOSPHERIC AIR TO WHITEFACE MOUNTAIN

The transport time of stratospheric air reaching Whiteface Mountain, New York was studied using the activity ratios of cosmic ray-produced $^{7}Be/^{32}P$. The observed ratios can be expressed as a function of the fraction of observed ^{7}Be which originated in the stratosphere and the time spent by the stratospheric air parcel in the troposphere prior to sampling. Thus, for cases where the stratospheric and tropospheric ^{7}Be components can be inferred and the stratospheric component dominates, the transport time can be determined from $^{7}Be/^{32}P$ activity ratios. For the summers of 1977 and 1978 and the spring and the summer of 1979, 44 occasions when stratospheric air reached this site were studied. The mean transport time was 7 days, but on most occasions the time was $\leq$ 5 days. For the fall of 1978 and the winter and fall of 1979, 12 cases were studied. The mean transport time was 16 days, but many occasions suggesting longer transport times were not included due to large

uncertainties in the $^{7}Be/^{32}P$ ratios. The transport times determined in this work are much shorter than those estimated for stratospheric-tropospheric exchange occurring via mean meridional circulation but comparable to travel times associated with tropopause folding events. These results provide compelling evidence in support of tropopause folding as the predominant mechanisms for stratospheric-tropospheric exchange.

A paper on this subject has been submitted to J. Geophys. Res. A preprint is attached as Appendix IV.

10. SOURCES OF SULFATE AND TRACE ELEMENTS IN SUMMER AEROSOLS

Trace elements in summer aerosols collected during 3 consecutive summers of 1975 through 1977 at Whiteface Mountain and 4 other sites were analyzed by instrumental neutron activation analysis. Sulfate in these aerosols was determined by colorimetric method (Appendix VI). Of the 94 samples analyzed, 18 of them showed high concentrations of SO_4^{2-} and several trace elements. Surface wind trajectories showed these high concentrations are transported by stagnant air masses from distant sources lying south and southwest of the site. Relative to their crustal abundances Cr, Zn, As, Se, Br, Sb and SO_4^{2-} were found to be highly enriched in these aerosols with enrichment factors ranging from 15 for Cr to 12,000 for Se. To investigate sources of such high atmospheric enrichments we considered cases with high episodic concentrations of SO_4^{2-} ($\geq$ 10 $\mu g/m^3$). Such episodic events with SO_4^{2-} concentrations $\geq$ 10 $\mu g/m^3$ have also been suggested in Section 4 of this report as tracer for tropospheric O_3.

Statistical data reduction showed that these episodic cases seemed to retain the identity of the distant sources. Multivariate analysis on the 18 recorded episodic events revealed 4 different anthropogenic sources: (1) fossil fuel (SO_4^{2-}, As, Se), (2) Municipal refuse incinerators (Zn, Sb), (3) iron and steel works (Cr and possibly Fe, Mn) and (4) automobile exhaust (Br). Details on these aspects of the study may be found in a reprint of the paper entitled, "Long Range Transport of Trace Elements" and preprint on "Summertime Concentration of Trace Elements in Atmospheric Aerosols at Remote Sites in New York State" (submitted to Atmospheric Environment). These have been attached as Appendices II and VI respectively.

11. DISTRIBUTION PATTERNS OF SULFATE, TOTAL SUSPENDED PARTICULATES, AND TRACE METAL CONCENTRATIONS IN AIR PARTICULATES

From the above studies (Appendices II and VI) we observed that at remote Whiteface Mountain average trace element and SO_4^{2-} concentrations in summer aerosols is more typical of urban rather than remote regions. A legitimate question is whether these elevated urban-like concentrations prevail during the rest of the year. To address this question we undertook a year-round investigation on trace elements and SO_4^{2-} contents in aerosols collected daily during 1979 at the site. As far as we are aware, no such daily studies at remote areas have been attempted in an uninterrupted manner for a whole year. In addition, the study generates a data base for airborne SO_4^{2-} and trace metals essential to check the effectiveness of future measures to control SO_4^{2-} and other pollutants at the emission sources. The data base should prove particularly useful in view of the bilateral agreement between the U.S. and Canada to tackle the problem of acid rain (Ember, 1979). Because of its geographic position, Whiteface Mountain

as an elegant 'window' to study long-range transport of sulfate into the northeastern United States from the industrial Midwest and/or the world's largest Cu-Ni smelter at Sudbury, Ontario.

11.1 Experimental

Details on sample collection were discussed in Section 2.1, those on total suspended particulate (TSP) and water-soluble SO_4^{2-} determinations have been discussed in our previous articles (Appendices II and VI).

11.1.1 Determination of trace elements by atomic absorption spectrometry

Including the 6-h air samples collected during the period of June 11 through June 25 (4 per day), about 400 air filters were collected during 1979. Although instrumental neutron activation analysis (INAA) was successfully used in our previous study (Appendices II and VI), the method was impractical for such a large number of samples especially without a nearby neutron-irradiation facility. Therefore, our existing analytical facilities in Atomic Absorption Spectrophotometer (AAS) Instrumentation Lab. Model IL-35 and Varian Model AA5 (flame) and Perkin Elmer Model HGA2100 (flameless) were used for multi-element analysis of the air filters. Because of lack of sensitivity and/or practical difficulties in AAS we were not able to determine Cr, Mn, As, Se, Br, and Sb analyzed in our previous study (Appendices II and VI). On the other hand, additional elements Mg, Al, Ca, and Pb could be determined by AAS. The first 3 elements were of particular interest since these were also included in the precipitation chemistry network

(Benkovitz, 1980) besides the annual total deposition of Mg, K, Ca by rain plays an important role in the nutrient cycle of certain ecosystems (Allen et al., 1968).

Since volatilization-deposition (condensation) is the accepted process for the presence of several trace elements from anthropogenic sources in the atmospheric aerosols, it is logical to consider losses by volatilization in the recovery of these elements from filter paper in the lab for subsequent analysis. Ashing the filter paper in a muffle furnace at 550°C entails losses of ∿ 40-60% for elements like Zn, Cd, Sb, Pb (Thompson et al., 1970). Because of relatively reduced losses (4-5%), low-temperature ashing using oxygen plasma is recommended (Harrison, 1977). Wet digestion of the aerosol-loaded filter paper with 3M HNO_3 has been recommended by EPA (Long et al., 1979) for the determination of Pb. In preliminary runs, both low-temperature ashing using oxygen plasma and wet nitric acid digestion, were tested for the preparation of sample solution for analysis by AAS.

11.1.2 Low temperature ashing (LTA)

The Lab for Electronics (LFE) Corporation Low Temperature Asher Model 302 in which 2 samples can be ashed simultaneously, was used in this work. About 50 cm^2 of the filter paper was ashed in a silica boat in an oxygen plasma, with standard operating conditions of: RF power 100 watts; O_2 flow rate 200 cc/min; plasma chamber pressure 0.5-1 mm and ashing time 30-40 min. Completion of ashing was indicated by a change in the color of the O_2 plasma glow from an initial blue-grey to a clear purple red.

After ashing, the residue was quantitatively transferred to a clean platinum dish with 1 ml conc. HNO_3 (J.T. Baker's ULTREX HNO_3) and 2-3 ml double-distilled water. About 2-3 drops of HF (48% v/v) was added to the dish and the solution was gently evaporated to dryness at 80°-90°C. The residue was dissolved in 1 ml conc. HNO_3, warmed, diluted to about 5 ml, quantitatively transferred to a 50-ml volumetric flask and made up to the mark with double-distilled water. The elements Na, Mg, Al, K, Ca, Fe and Zn were determined by AAS.

11.1.3 Wet nitric-acid digestion (WND)

Filter paper of known area was immersed in 3M HNO_3 solution in a test-tube having a plastic screw-cap. The tube was placed in a steam bath, heated for 30 min and then placed in an ultrasonic vibrator for 10 min. After agitation, it was placed back in a steam bath and again heated for 15 min. Pb content in the sample solution was determined by AAS (flame or graphite furnace).

Reagent and filter paper/reagent blanks were also prepared with each batch of sample solution prepared.

11.1.4 Comparison of results by LTA and WND

To check the reliability of the above methods, 5 air filters previously analyzed by INAA (Appendix VI) were analyzed using WND and LTA methods.

Results in Table 3 show that K concentrations determined by the 3 methods are in good agreement. In contrast, the Na values show large variations. Considering that in the wet nitric-acid digestion procedure Na and K should behave alike, the disagreement in Na data by the two methods (samples 2 and 5) as well as with INAA results (samples 1 and 4),

suggest that the high scatter could either be due to different degrees of external contamination and/or heterogeneous distribution of Na in Whatman 41 filter paper. The filter paper blanks analyzed by INAA and AAS gave highly scattered values of Na ranging from below detection limit of $\sim$ 80 ng/cm^2 to 560 ng/cm^2. Na concentration determined by INAA in two splits of samples collected at High Point, N.J. on July 17 and 21, 1976 only agreed within 25-50% which is rather poor for Na (expected precision for Na analysis $\pm$ 10% or better) (Appendix VI). These results suggest that Whatman 41 filter paper is heterogeneously distributed with respect to Na. Thus, Na values in aerosol studies using Whatman 41 filter paper may be unreliable. The inconclusive factor analysis for Na in our previous work (Appendix VI) may be attributable to the above problems in Na determination.

Fe and Zn results by LTA and INAA are in reasonable agreement except for Fe value of sample 1. The consistently low values of Fe by WND presumably arise from partial adsorption of Fe^{3+} ions on filter paper pulp which is inevitable in wet acid digestion and/or incapability of nitric acid to open the silicate component of the aerosol in the absence of HF. This is also reflected in the low values of Al by WND relative to that determined by LTA. In contradistinction, relatively high Zn values by WND suggest contamination. The contamination was traced in the screw-cap lining of the test tube used in the WND. Analytical results for Pb by LTA are inconsistent with those obtained by WND, recommended by EPA (Long et al., 1979). The reason for low Pb by LTA is not clear. Pb, therefore, was determined via WND. Except for Pb, however, low-temperature ashing yielded reliable results and was adopted in this work.

11.1.5 System blank

Periodically during the course of sample collection filter papers were placed in the sampling chamber for 3 days without filtering air through them. These filters were analyzed for trace elements and treated as system blanks (SB). The results on 23 SB are given in Table 4. In calculating the mean suspect values (question marked) are omitted. Included in this table are the concentrations on fresh Whatman 41 filter paper determined by Dams et al. (1972) using INAA. The concentrations of Na, Al, K and Fe are systematically higher in SB compared to fresh filter paper suggesting that SB were perhaps slightly 'soiled' during the 3-d exposure to the turbulent air in the sampling chamber.

11.2 Daily, monthly and seasonal variations of sulfate, TSP and trace metal concentrations

The daily concentrations of TSP, Na, Mg, Al, K, Ca, Fe, Zn, Pb and SO_4^{2-} ions for the entire year of 1979 (after blank correction) are presented in Table 5. On thirteen days no sample could be collected. This is quite satisfactory in view of the severe weather conditions at Whiteface Mountain. Starting with the winter aerosols of January and February, analysis of Na, Mg, K, Ca and Zn were not done under optimum conditions. Hence poorer detection limits have been assigned to these elements for the 2 winter months.

Table 6 includes the monthly averages for the above 10 parameters, the associated standard errors, number of samples (n) analyzed and number of episodic (nEp) cases recorded per month. Since cases with SO_4^{2-} concentration > 10 $\mu g/m^3$ were not observed for January through March, November and December, cases with $\sim$ 5 $\mu g/m^3$ and greater were arbitrarily chosen as episodic. This value is considered adequate for the present discussion of

seasonal trends. The monthly averages are plotted in Fig. 20. The vertical bars correspond to one σ deviation of the means. Table 7 gives seasonal and annual averages of the 10 measured parameters. These values are plotted in Fig. 21. Seasonal averages are shown by data points while annual averages are indicated by broken lines. The 4 seasonal divisions of the year started with December (and not January). This was done because the monthly averages in Fig. 20 and Table 6 suggested that the seasonal changes could be brought out more conspicuously by such a division.

Figures 20 and 21 show that, with the exception of Na, the seasonal changes in the distribution patterns of the remaining 9 parameters are strikingly similar. All of them exhibit peak concentration during summer months. The deviation of Na may be ascribed to blank correction errors (filter inhomogeneity) discussed earlier. This element was therefore excluded in the discussion below.

From the value of R, the ratio of seasonal mean to annual mean, given in Table 7, it can be seen that the concentration levels of TSP, Al, K, Ca, Fe, Zn, Pb and SO_4^{2-} are lowest in winter (0.3-0.6 times the annual average) intermediate in spring and autumn (0.8-1.0 times the annual average) and highest in summer (1.3-1.9 times the annual average).

Fig. 22 is a plot of frequency of occurrence of episodic events (nEp) for respective months. The pattern more or less resembles those in Fig. 20 and thus substantiates our earlier conclusions (Appendix VI) that episodic events play a dominant role in the overall trace element distribution patterns in aerosols at Whiteface Mountain.

In view of the higher energy consumption of fossil fuel in winter months for heating purposes, the concentration levels and the frequency of

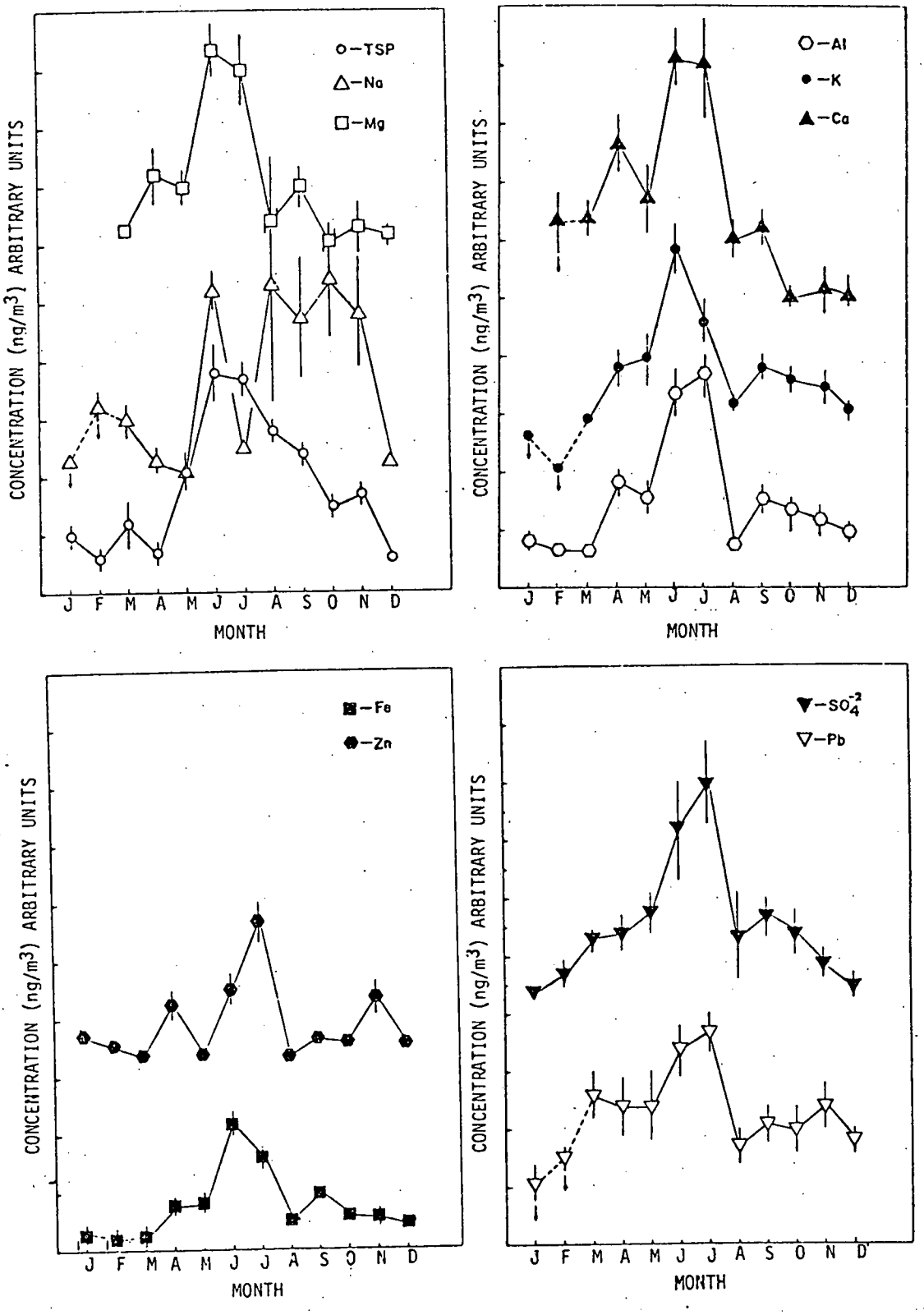

Fig. 20. Distribution patterns of TSP, Na, Mg, Al, K, Ca, Fe, Zn, Pb and SO_4^{2-} in air particulates at Whiteface Mountain, N.Y. (1979).

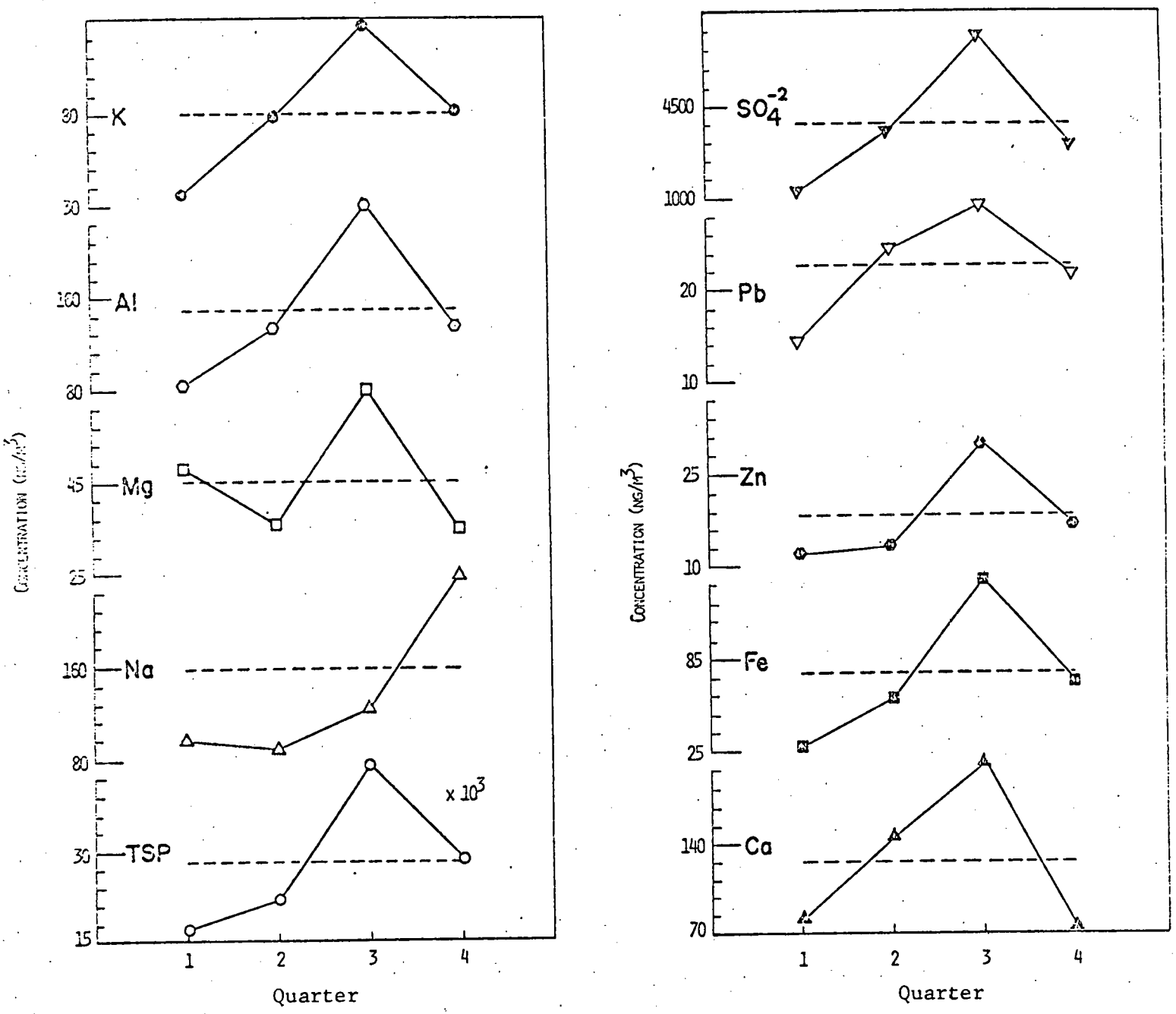

Fig. 21. Quarterly variation in elemental concentration in atmospheric aerosols. 1. Dec.-Feb., 2. Mar.-May, 3. Jun.-Aug., 4. Sep.-Nov. Annual average indicated by broken line.

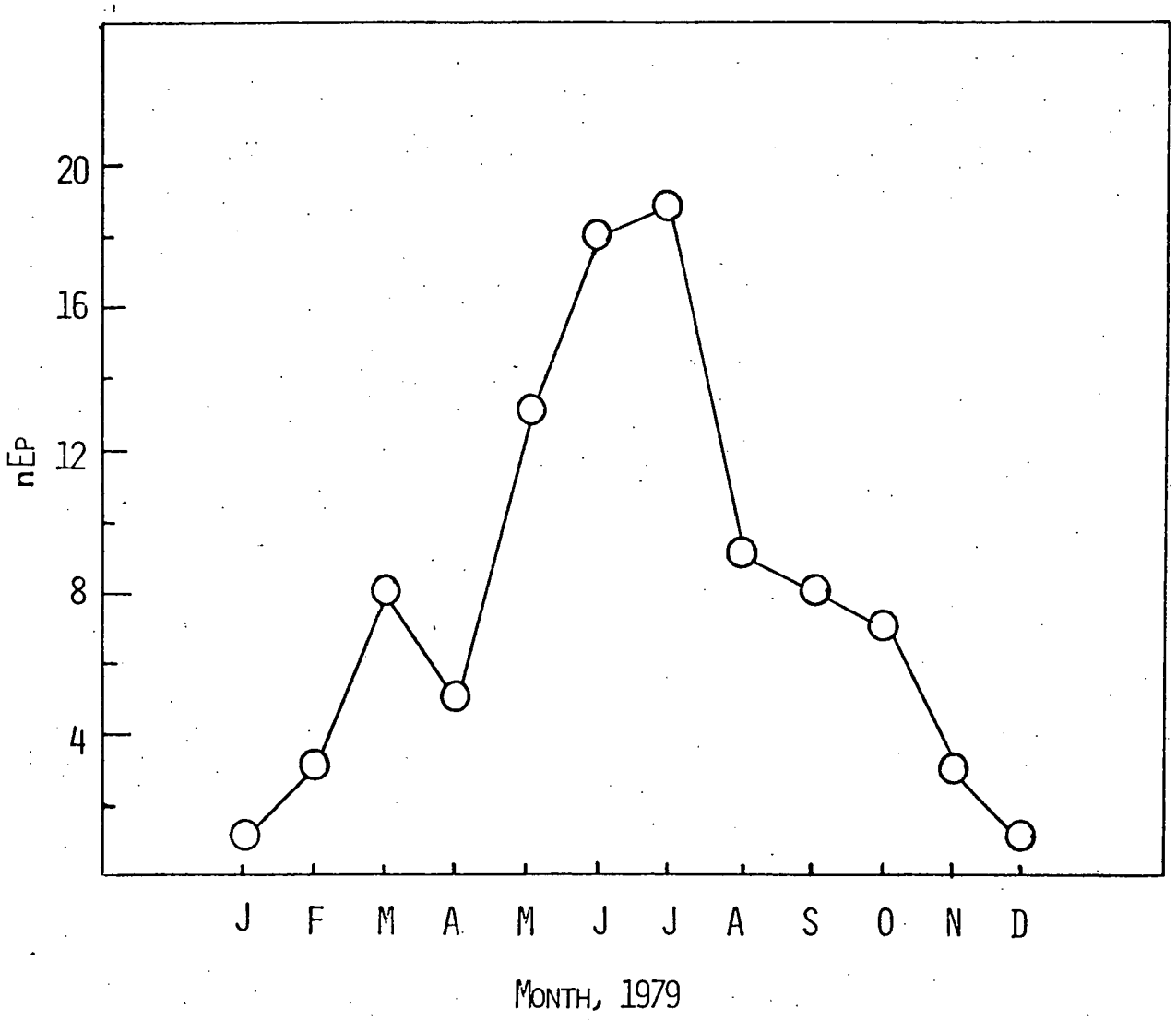

Fig. 22. Frequency (nEp) of monthly occurrences of episodic cases with SO_4^{2-} concentrations $\sim$ 5 $\mu g/m^3$ and greater.

occurrences of episodic concentrations ($\geq$ 5 μg SO_4^{2-}/m^3) of this energy-related SO_4^{2-} pollutant is expected to be high in winter months. The relatively low concentration of SO_4^{2-} and infrequent episodic events in winter months thus seem surprising. Kleinman et al. (1973) also observed summer maxima in the airborne trace metals and TSP measured in New York City and attribute the seasonal changes to changes in dispersion factor; low in summer and high in spring. The dispersion factor (DF) is the product of morning mixing height and surface wind speed. Since we are dealing with distant sources (see Appendices II and VI) two other factors should be considered: a) change in wind direction from the industrial midwest in summer to the north-northwestern regions of Canada in winter and b) more effective scavenging at the source and/or sink (sampling site); the midwinter snow cover precludes the reentrainment of the trace elements.

The observed seasonal profile for trace elements and SO_4^{2-} ions may therefore be a net result of the changes in DF, transport patterns and precipitation deposition. It should, therefore, be interesting to study the distribution of elements and ions in precipitation and dry deposition. In this context we have made an interesting comparison on the SO_4^{2-} ion concentration in aerosols and precipitation which is presented in Section 12 of this report.

11.3 Sulfate as a Tracer for Local Aerosols

Before trace elements/ions concentration levels can be used to check the effectiveness of control measures for pollutants in air, it is necessary to determine background (local) levels. Trace elements in tropospheric aerosols are derived from crustal materials (land and sea), natural processes like volcanic activities and man's industrial activities.

Our earlier attempt (Appendix VI) to determine background concentrations in summer aerosols was unsuccessful due to the high frequency of episodic events at Whiteface Mountain.

That being the case, how does one recognize the background aerosols? In our earlier study (Appendix VI), cases in which the recorded daily concentrations of SO_4^{2-} were $\geq$ 10 $\mu g/m^3$ were considered episodic. The high SO_4^{2-} concentrations were generally accompanied by high concentrations of several trace elements. As a matter of fact using the above SO_4^{2-} concentration level(s) as an index for the out-of-state input into the background aerosols at Whiteface Mountain, it was possible to identify 4 different man-made sources for trace elements in air at the site. Likewise in conjunction with ^7Be, SO_4^{2-} has been suggested as a tropospheric tracer for studying anthropogenic and stratospheric components of observed O_3 concentration in the troposphere (Section 4).

Since SO_4^{2-} in the troposphere results from the gas phase S transformation viz $S \rightarrow SO_2 \rightarrow SO_3 \rightarrow SO_4^{2-}$; be it natural (volcanic activity) or anthropogenic (coal/oil burning) it is expected to be uniformly distributed and may thus have a background concentration in aerosols. The reported background SO_4^{2-} concentration in ambient air over the central United States is 0.2-0.4 $\mu g/m^3$ (Kellogg et al., 1972). As a first approximation, we assume this to be the background concentration range of SO_4^{2-} at Whiteface Mountain and utilize it to recognize background aerosols.

In Table 8 and Fig. 23 the mean concentrations of trace elements on days with SO_4^{2-} concentration < 0.4 $\mu g/m^3$ are compared with literature values for background aerosols compiled by Cawse (1974). Column 6 of this table gives the minimum concentration of elements empirically determined from their respective enrichment-factor diagrams constructed by Rahn (1976).

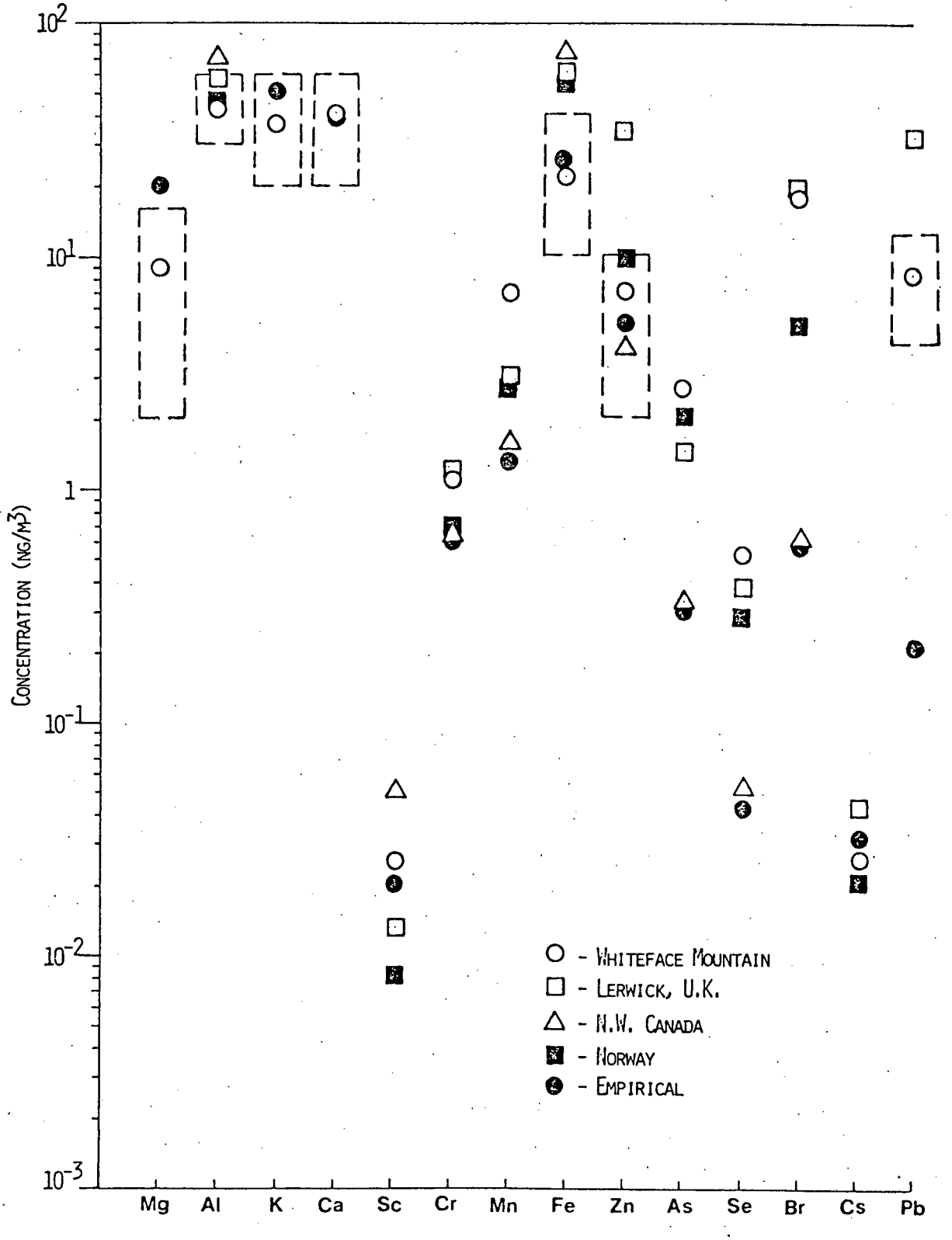

Fig. 23. Comparison of elemental concentration levels in background aerosols at Whiteface Mountain. (This work, 3 remote sites (Cawse, 1974) and empirical background aerosols (Rahn, 1976)).

In this empirical determination only continental aerosols were considered. Since the values were read out from Rahn's (1976) enrichment factor diagrams only approximate values could be derived. In the case of Sc, Cr, Mn, As, Se, Br and Cs (which were not determined in the present work) the mean of 2 measurements on July 5, 1975 and July 27, 1977 in which the SO_4^{2-} concentrations was $\sim$ 0.4 $\mu g/m^3$ are shown (Appendix VI).

The elemental background concentration levels calculated for Whiteface Mountain are in reasonable agreement with those listed by Cawse (1974) for background aerosols for three different regions of the world (Table 8 and Fig. 23). However, the background Pb concentrations at Whiteface Mountain are about 4 times lower than those observed at Lerwick. It should be interesting to note that Br also shows wide variability at different sites. The levels of these two elements in ambient air are appreciably influenced by highly localized factor in automotive exhaust (Appendix VI; King et al., 1976).

If one compares the values in column 2 with the empirically determined minimum concentration levels in column 6 (Table 8), one finds that the concentration levels of non-enriched elements like Mg, K, Ca, Sc, Fe and Cs (which are mostly present in the crustal derived component of the aerosols) match well. However, the enriched elements Cr, Zn, As, and Se are higher in the background aerosols at Whiteface Mountain. The close agreement in the background concentration levels of Cr, Zn, As, Se and Br in aerosols from N.W. Canada with the empirical background levels is not surprising because the lowest values in the enrichment factor diagrams of Rahn (1976) for these elements happen to be for these very regions (Ft. Smith, N.W. Territories, Jasper (Alberta, (Saskatchewan) and Prince Albert

National Park Canada). The high levels for the enriched elements perhaps reflect on the regional effects. In relation to man's industrial activity, Whiteface Mountain is certainly not as remote as the N.W. Territories and Saskatchewan. Thus, although there is a general chemical uniformity in the elemental distribution in background aerosols of the different regions of the globe, subtle differences especially with respect to the enriched elements are not surprising.

In column 7, Table 8 and Fig. 23 we show probable ranges of seven trace element concentrations in background aerosols at Whiteface Mountain. These are the elements for which a statistically significant number of data points are available for calculation of their background concentration levels.

12. COMPARISON OF SULFATE IN AEROSOLS AND SULFATE IN PRECIPITATION

The acid rain problem in northeastern United States has led to extensive investigation of SO_4^{2-} in the environment (Altshuller, 1973, 1976; Hornbeck et al., 1977; Pack, 1978, 1980; Izard and Jacobson, 1979; Likens et al., 1979). It has been suggested that high concentrations of SO_4^{2-} in the atmosphere are from out-of-state, being transported over long distances by high pressure systems; the emission sources lie S-SW (Ohio Valley regions) of NY State (Galvin et al., 1978; Samson, 1978). The acid precipitation affecting the NE region is chemically and meteorologically related to accumulation and scavenging precipitation of these pollutants (Wolff et al., 1979B).

No quantitative description of a source-to-sink model for anthropogenic S has yet been developed. Such quantification is essential to building up proper air pollution control strategy for sulfur. The Multi-State Atmospheric

Power Production Pollution Study (MAP3S) and Electric Power Research Institute (EPRI) programs have established trends of spatial and temporal distribution of several energy related pollutants including SO_4^{2-} (Pack, 1978, 1980; Dana, 1979). However, although airborne SO_4^{2-} has been recognized the chief immediate precursor to SO_4^{2-} in precipitation, the two networks confine the study to precipitation only (Pack, 1980), thus leaving a gap in our knowledge on the link between precipitation and atmospheric chemistry of SO_4^{2-}. In this section, we discuss the relationship between SO_4^{2-} in aerosols and precipitation at Whiteface Mountain.

12.1 Temporal Variation of Sulfate in Atmospheric Aerosols and Precipitation

The distribution patterns of SO_4^{2-} concentration reported by Pack (1978) in precipitation events from several eastern United States sites for 1976-77 are reproduced in Fig. 24a. In this plot monthly weighted ion concentration (WIC), defined below, of SO_4^{2-} are plotted against corresponding months.

Weighted ion concentration for any given month is calculated as

$$WIC = \frac{\Sigma \text{ ion concentration x individual sample volume}}{\text{Total monthly sample volume}}$$

WIC was found to be highly correlated between the sites studied (max. distance between any two sites $\sim$ 750 km) from which Pack (1978) concluded that SO_2 and SO_4^{2-} are well mixed over the eastern U.S. It is interesting to note the temporal distribution of SO_4^{2-} concentration in atmospheric particulates (Fig. 20) and atmospheric precipitation (Fig. 24a) more or less exhibit the same trend. It may be argued that this could be an artifact from considering events of two different years. To remove this uncertainty

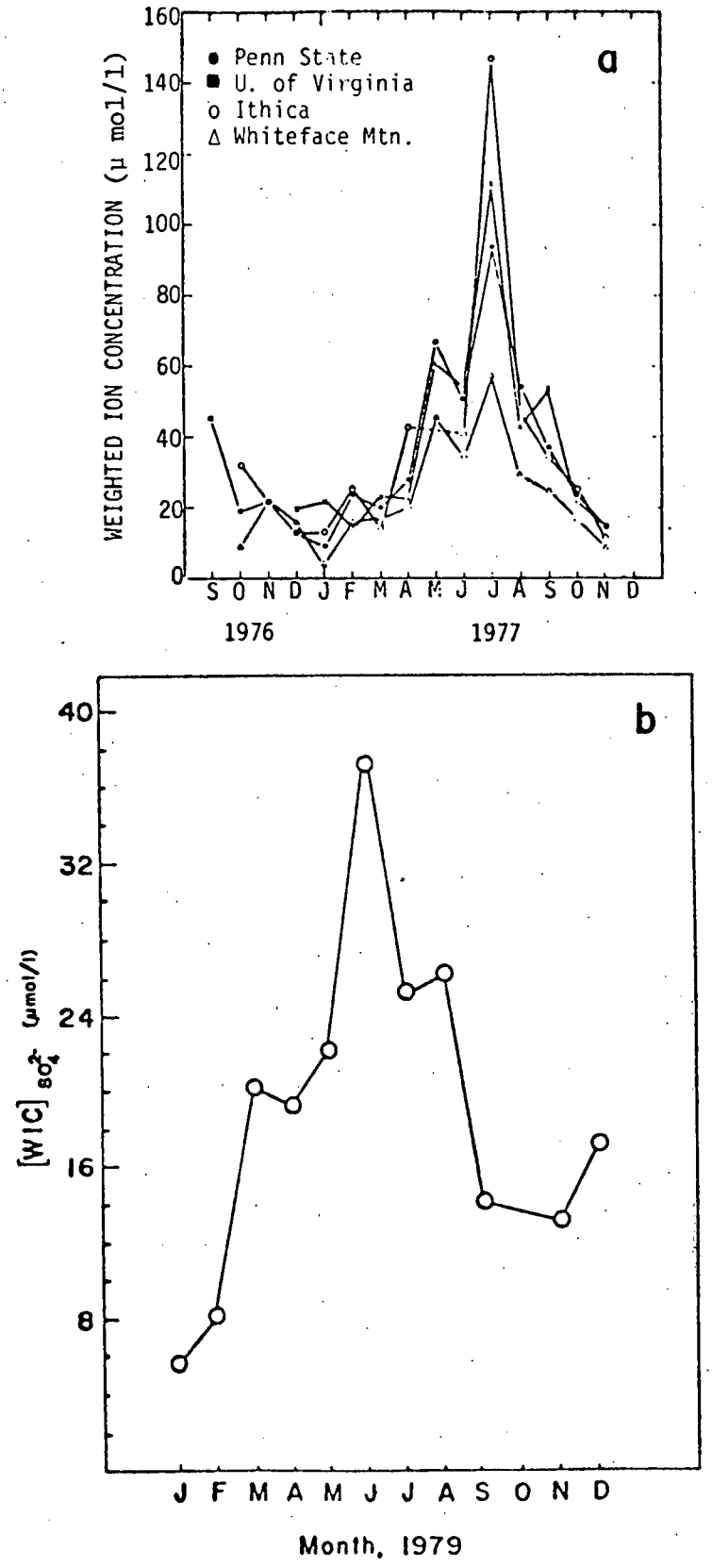

Fig. 24: (a) Sulfate monthly weighted ion concentration (WIC) in 1976-77 at 4 eastern U.S. sites (Ref. Pack, 1978). (b) Monthly weighted ion concentration (WIC) of SO_4^{2-} in atmospheric precipitation events of 1979 at Whiteface Mountain.

we calculated the WIC for SO_4^{2-} in precipitation events of 1979 at Whiteface Mountain (Fig. 24b). The data was made available by courtesy of Carmen Benkovitz (1980) from the MAP3S data bank. The MAP3S sample collection site and our sampling site are situated at two different heights, the former at an altitude of 0.64 km while latter at 1.5 km above mean sea level. We are aware of the fact that the WIC values at 0.64 km and 1.5 km for any given period could be different. Nonetheless, we do not expect drastic differences in the trends of temporal variations in WIC. In any case the WIC values used in this preliminary report will be corrected as and when the precipitation data at our sampling site become available. We once again find broad similarities in the WIC pattern (Fig. 24b) and air particulate SO_4^{2-} pattern (Fig. 20) of 1979.

In Fig. 25 the monthly WIC for SO_4^{2-} in the precipitation (ppt) events recorded at Whiteface Mountain (MAP3S data) were plotted against corresponding monthly averages of SO_4^{2-} in the air particulates at our sampling site. Good correlation can be seen between the quantities $(SO_4)^{2-}_{ppt}$ and $(SO_4)^{2-}_{air}$ with correlation coefficient (r) of 0.75. The data point for the month of October deviates substantially from the other points and was not included in the regression analysis. The reason for this is not clear at this point. The washout ratio for SO_4^{2-} (defined as the ratio of the concentration per unit mass of rain to the concentration per unit mass of air) calculated from the regression coefficients (Fig. 25) turns out to be 450, using an air density of 1.2 g/l. The air volumes in our sampling set up are normalized to STP. Garland (1978) obtained washout ratios of 1320 and 920 at two sites in U.K. Our value is half as much and suggest less efficient condensation and scavenging. However, we refrain from making any

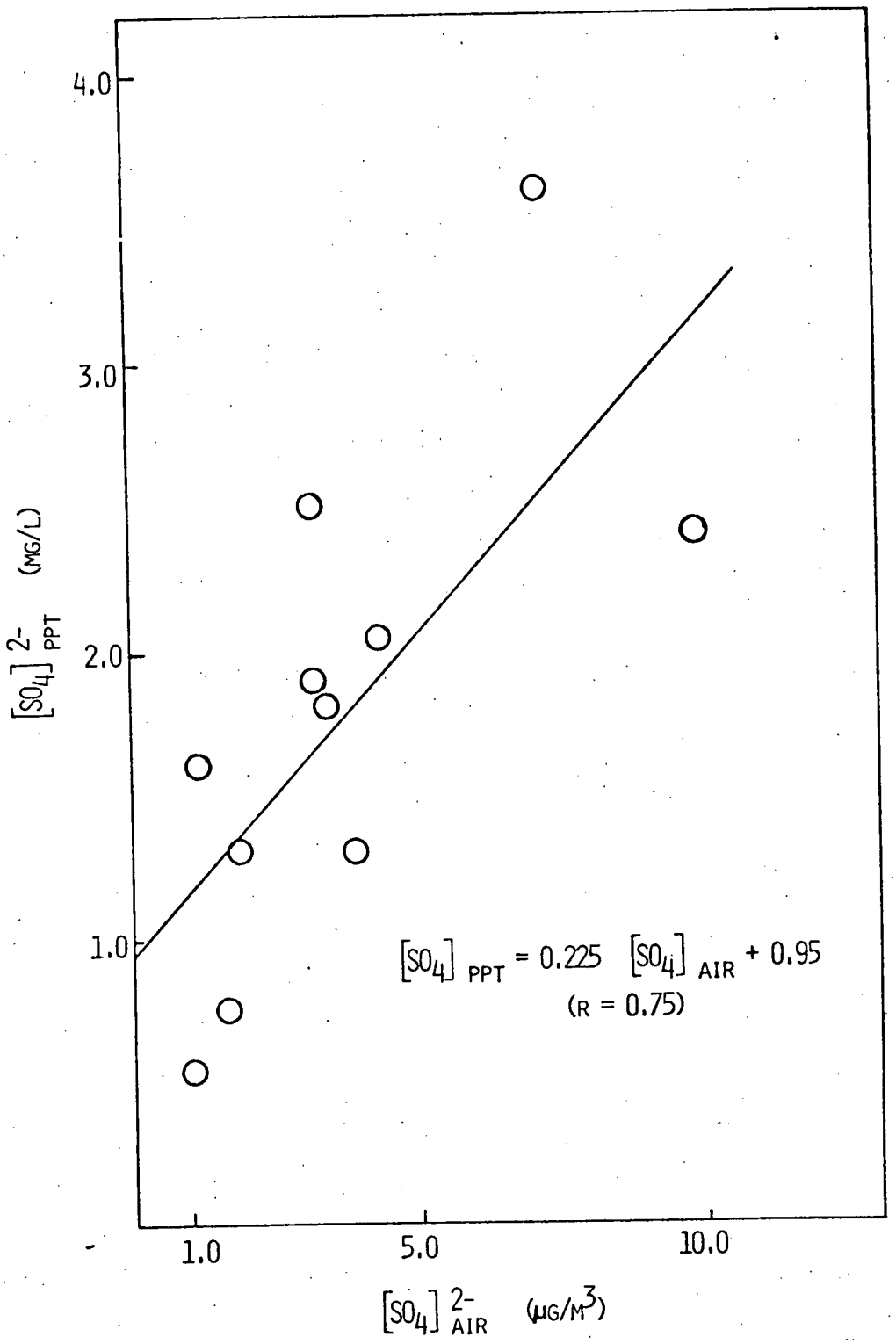

Fig. 25. Relationship of atmospheric particulate SO_4^{2-} - $[SO_4]^{2-}_{air}$ - and atmospheric precipitation SO_4^{2-} - $[SO_4]^{2-}_{PPT}$ - concentration at Whiteface Mountain (1979).

conclusions on the low washout ratio since the value may have to be revised as and when precipitation data at Whiteface Mountain are made available. The relationship between SO_4^{2-} in aerosols and precipitation (Fig. 25) can be readily explained by considering the fate of S compounds during transportation-atmospheric deposition.

12.2 Transportation-Deposition of Anthropogenic Sulfur

In the long-range transport of S compounds from emission sources to remote sites like Whiteface Mountain, the reduced forms of S compounds like H_2S, dimethyl sulfide, methyl mercaptans are oxidized to SO_2 and SO_4^{2-} so that in the ambient air at this site one expects essentially SO_2 and SO_4^{2-} as the most likely species. The total particulate S (TPS) at this site could best be correlated to water soluble S (WSS) by a linear regression (see Appendix V) [WSS] = 0.95 [TPS] - 0.16 ($r = 0.97$) where [WSS] and [TPS] are in $\mu g/m^3$ air.

The regression coefficients indicate that for TPS $\geq$ 1 $\mu g/m^3$, (which was the lowest monthly average recorded in 1979) $\geq$ 80% of the TPS is present as WSS. The next question is whether gaseous SO_2 or particulate SO_4^{2-} [SO_4^{2-} in air is mostly present as NH_4HSO_4 and $(NH_4)_2SO_4$] in ambient air or both relate to the SO_4^{2-} in rain.

Relationship between SO_2 and SO_4^{2-} in ambient air at this site has not been investigated. In plumes downwind of coal-fired sources, SO_2 to SO_4^{2-} ratios are usually 50-100 to 1 (Altshuller, 1976). At eastern non-urban sites this ratio drops down to about 1 indicating progressive oxidation of SO_2 to SO_4^{2-} during transport (Altshuller, 1976). In-situ SO_2 measurements have been made at Whiteface Mountain by EPRI under SURE project (Sulfate Regional Experiment) during 1979. However, the data is not

currently available to us. Hence, based on the ratio observed at eastern non-urban site (Altshuller, 1976), at Whiteface Mountain a ratio of 1:1 for SO_2 to SO_4^{2-} may be assumed. In his study on dry and wet removal of S from the atmosphere, Garland (1978) concluded that half of the SO_2 in the atmosphere is removed by 'dry deposition', the remainder is oxidized to SO_4^{2-} and removed in precipitation. This means that relative to particulate SO_4^{2-} gaseous SO_2 would contribute at most about 25% to the observed SO_4^{2-} in precipitations at Whiteface Mountain. Good correlation between $[SO_4]^{2-}_{rain}$ - $[SO_4]^{2-}_{air}$ ($r = 0.62$ and 0.68) and poor between $[SO_4]^{2-}_{rain}$ - $[SO_2]_{air}$ ($r = 0.19$ and 0.03) observed by Garland (1978) at two different stations in the U.S. suggests that S compounds in rain originate mainly from SO_4^{2-} aerosols. The good correlation between SO_4^{2-} concentrations in precipitation and aerosols shown in Fig. 25 is consistent with the results of Garland (1978).

13. DETERMINATION OF TOTAL PARTICULATE SULFUR BY PYROLYSIS MICROCOULOMETRY

Total particulate sulfur (TPS) in air samples can be determined by a new technique based on thermal volatilization at 1000°C, followed by controlled oxidation of sulfur compounds to SO_2 and coulometric titration of SO_2 with iodine. Calibration curves are linear within 5% from 0.1 to 10 µg S, the detection limit is 0.10 µg S (equivalent to 35 ng S/m^{-3} when 2000 m^3 of air are filtered), and the relative standard deviation (n = 10) are 48 and 5.1% at the 0.10 and 4.0 µg S levels. Recoveries for 20 organic and inorganic compounds, including refractory sulfates, elemental sulfur, sulfides, sulfites, sulfonates, and sulfones, vary from 79 to 88%. No interferences are observed for a number of non-sulfur-containing compounds, including nitrates, benzene, acetone, glucose, cellulose, silicates and carbonates. The technique has

been used to determine the presence of non-sulfates and of non-water-soluble sulfates in suspended particulates. Both TPS, using this technique, and water-soluble sulfate (WSS), using the methyl thymol blue method, were determined in daily air particulate samples collected at Whiteface Mountain, N.Y. during both winter and summer. Comparison of TPS and WSS values showed that WSS could usually account for all of the sulfur present in the samples. Occassionally during the summer months, however, elevated TPS values indicated the presence of sulfur in excess of the WSS value. The TPS concentrations ranged from 0.1 to 9.7 μg S/m^{-3} and the contribution from acid-soluble sulfites and sulfides, elemental sulfur and volatile S-containing organic compounds was negligible (< 0.5 μg S/m^{-3}).

A paper on this subject has been submitted for publication to Atmospheric Environment. A preprint is attached as Appendix V.

14. PRESENTATIONS AT SCIENTIFIC MEETINGS

1. L. Husain, K. Williams and L. Keenan, Sources of Trace Metals in New York State, ACS/CSF Chemical Congress, Honolulu, HI, April 1-6, 1979.

2. V.A. Dutkiewicz and L. Husain, The Determination of Stratospheric Subsidence Rates in Near Ground Level Air, ACS/CSL Chemical Congress Honolulu, HI, April 1-6, 1979.

3. L. Husain, A. Rusheed and V.A. Dutkiewicz, Determination of $^{7}Be/O_3$ Ratios in the Stratosphere, The Natural Radioactive Isotopes of Beryllium in the Environment, Meeting Sponsored by Yale University and the U.S. Department of Energy, New Haven, CT, October 1-2, 1979.

4. L. Husain, V.A. Dutkiewicz and A. Rusheed, Origin of Tropospheric Ozone, International Union of Geodesy and Geophysics, XVII General Assembly, Canberra, Australia, December 2-15, 1979.

5. L. Husain, V.A. Dutkiewicz and A. Rusheed, Asymmetry in the Stratospheric-Tropospheric Exchange in the Northern and Southern Hemispheres, Internatioanl Symposium on Middle Atmosphere Dynamics and Transport, University of Illinois, Urbana, IL, July 28-August 1, 1980.

6. V.A. Dutkiewicz, L. Husain and A. Rusheed, Stratospheric Ozone in the Planetary Boundary Layer, Quadrennial International Ozone Symposium, Boulder, Colorado, August 4-9, 1980.

7. E. Canelli and L. Husain, Determination of Sulfur Compounds in Atmospheric Aerosols in Pyrolysis-Microcoulometry. Accepted for presentation at the Second Chemical Congress of the North American Continent, San Francisco, CA, August 24-29, 1980

8. P. Parekh and L. Husain, Summertime Episodic Concentration of Trace Elements at Whiteface Mountain, N.Y. and Their Possible Sources. Accepted for presentation at the Second Chemical Congress of the North American Continent, San Francisco, CA, August 24-29, 1980.

15. PERSONNEL

Dr. Ali Rusheed, B.S. - University of Karachi, 1960
M.S. - University of Karachi, 1962
Ph.D. - University of London, 1968

Dr. Rusheed was a postdoctoral fellow (part-time) on this grant.

Dr. M. Jaffar, B.S. - Punjab University, 1964
M.S. - Punjab University, 1966
Ph.D. - Islamabad University, 1977

Dr. Jaffar was a postdoctoral fellow (part-time) on this grant.

Ms. Karen Williams, B.S. - State University of New York at Geneseo, 1975. Supported by NYS Department of Health.

Mr. A.R. Khan, B.S. - Aligarh University, 1975. Supported by this grant - part-time.

REFERENCES

Allen, S.E., A. Carlisle, E.J. White, and C.C. Evans, J. Ecol., 56, 497-504, 1968.

Altschuller, A.P., Environ. Sci. and Technol., 7, 709-712, 1973.

Altschuller, A.P., J. Air. Poll. Cont. Assoc., 26, 318-324, 1976.

Benkovitz, C.M., Private Comm., 1980.

Benkovitz, C.M. and J.L. Heffter, 'Users Guide to Heffter Interactive - Terminal Transport Model,' Internal Report, Atmospheric Sciences Division, BNL, Upton, N.Y., 1980.

Cawse, P.A., AERE Report R-7669, U.K., 1-80, 1974.

Coffey, P.E. and W.N. Stasiuk, Environ. Sci. Technol., 9, 59-62, 1975.

Dana, M.T., 'The MAP3S precipitation chemistry network': second periodic summary report, Battelle Pacific Northwest Laboratories, Richland, WA, 1979.

Danielsen, E.F. and V.A. Mohnen, J. Geophys. Res., 82, 5867-5877, 1977.

Dams, R., K.A. Rahn, and J.W. Winchester, Environ. Sci. and Technol., 6, 441-448, 1972.

Dutkiewicz, V.A. and L. Husain, Geophys. Res. Lett., 6, 171-174, 1979.

Ember, L.R., Chem. and Eng. News, 57 #49, 15-17, 1979.

Environmental Measurements Laboratory report, EML-353, U.S. Department of Energy, 1979.

Feely, H., J.P. Friend, H. Seitz, J.D. Martin, and W.E. Erleback, DASA-2166-3, Isotopes Inc., 1971.

Galvin, P.J., P.J. Samson, P.E. Coffey, and D. Romano, Environ. Sci. Technol., 12, 580-584, 1978.

Garland, J.A., Atmos. Environ., 12, 349-362, 1978.

Gidel, L.T., and M.A. Shapiro, J. Geophys. Res., 85, 4049-4058, 1980.

Harrison, R.M., in Handbook of Air Pollution Analysis, Chapter III, (ed., R. Perry and R. Young), John Wiley and Sons, N.Y., 1977.

Hartwig, S. and A. Sittkus, Nature, 241, 36-37, 1973.

Heffter, J.L., NOAA Tech. Memo, ERL-ARL-81, Boulder, CO, 1980.

Hornbeck, J.W., G.E. Likens, and J.S. Eaton, Water Air and Soil Pollution, 7, 355-365, 1977.

Husain, L., P.E. Coffey, R.E. Meyers, and R.T. Cederwall, Geophys. Res. Lett., 4, 363-365, 1977.

Husain, L., V.A. Dutkiewicz, P.E. Coffey, and V.A. Mohnen, 'Sources of Ozone and Sulfates in Northeastern United States,' Annual Report to US Department of Energy, number COO-4501-1, 1978.

Husain, L., A. Rusheed, and V.A. Dutkiewicz, in Proceedings of the Ozone/ Oxidants Interactions with the Total Environment Speciality Conf., (Houston, TX), Air Poll. Contr. Assoc., 247-259, 1979.

Husain, L and P.J. Samson, J. Geophys. Res., 84, 1237-1240, 1979.

Izard, H.H., and J.S. Jacobson, ed., Scientific papers from the public meeting on acid precipitation, Lake Placid, N.Y., Science and Technical Staff, N.Y. State Assembly, 1-161, Albany, NY, 1979.

Kellogg, W.W., R.D. Cadel, E.R. Allen, A.L. Lazrus, and E.A. Martell, Science, 175, 587-595, 1972.

King, R.R., J.S. Fordyce, A.C. Antonie, H.F. Leibecki, H.E. Neustadter, and S.M. Sidik, J. Air. Poll. Contr. Assoc., 26, 1073-1078.

Kleinman, M.T., T.J. Kneip and M. Eisenbud, in Proc. Trace Substances in Environmental Health-VIII, (ed., D.D. Hemphill), Univ. Missouri, Columbia, MO, 161-166, 1973.

Lal, D. and B. Peters, in Handbuch der Physik, 46, (ed., K. Sitte) Springer Verlag; Heidelberg, 551-612, 1967.

Likens, G.E., R.F. Wright, J.N. Galloway, and T.J. Butler, Scient. Amer., 241, 43-51, 1979.

Liv, S.C., D. Kley, M. McFarland, J. Mahlman, and H. Levy II,'On the Origin of Tropospheric Ozone' preprint, 1980.

Long, S.J., J.C. Suggs and J.F. Walling, J. Air. Poll. Contr. Assoc., 29, 28-31, 1979.

Ludwick, J.D., T.D. Fox, and L.L. Wendell, J. Air Poll. Contr. Assoc., 26, 565-569, 1976.

Machta, L., R.J. List, M.E. Smith, Jr., and H. Oeschger, in Precipitation Scavenging (1970), USAEC CONF-7000601, 465-474, 1970.

Mahlman, J.D., H. Levy II, and W.J. Moxin, J. Atmos. Sci., 37, 655-685, 1980.

Martell, E.A., in Radionuclides in the Environment, Advances in Chemistry Series 93, American Chemical Society, Washington, D.C., 138-157, 1970.

Martell, E.A. and H.E. Moore, J. Resch. Atmos., 8, 903-910, 1974.

Pack, D.W., Geophys. Res. Lett., 5, 673-674, 1978.

Pack, D.H., Science, 208, 1143-1145, 1980.

Perkins, P.J., and U.R.C. Gustafsson, in Int. Conf. on Environ. Sensing and Assessment, 2, IEEE Session No. 26-4, 1-10, 1976.

Rahn, K.A.,'The Chemical Composition of the Atmospheric Aerosol' Tech. Report, Univ. of Rhode Island, Providence, Rhode Island, 1976.

Reiter, E.R., Rev. Geophys. Space Phys., 13, 459-474, 1975.

Reiter, E.R., H. -J. Kanter, R. Reiter, and R. Sladkovic, Arch. Met. Geoph. Biokl., A 26, 179-186, 1977.

Reiter, R., H.-J. Kanter, R. Sladkovic and K. Potzl, US ERDA Document number NYO-3425-14, 1977.

Reiter, R., H.-J. Kanter, R. Sladkovic, W. Carnuth, and K. Potzl, US DOE Document Number NYO-3425-16, 1978.

Samson, P.J., Atmos. Environ., 12, 1889-1893, 1978.

Singh, H.B., F.L. Ludwig, and W.B. Johnson, Atmos. Environ., 12, 2185-2196, 1978.

Thompson, R.J., G.B. Morgan, and L.S. Purdue, Atomic Absorp. Newsletter, 9, 53-57, 1970.

Tiefermann, M.W., NASA Tech. Paper - 1451, NASA, Cleveland, OH, 1979.

Wolff, G.T., M.A. Ferman, and P.R. Monson, General Motors Research Publication GMR-2831, Env. #49, 1979A.

Wolff, G.T., P.J. Lioy, H. Golub, and J.S. Hawkins, Environ. Sci. and Technol., 13, 209-212, 1979B.

Young, J.A., N.A. Wogman, C.W. Thomas, and R.W. Perkins, in Radionuclides in the Environment, Advances in Chemistry Series 93, American Chemical Society, Washington, D.C., 1970.

Table 1. Daily Ozone, ^{7}Be, ^{32}P and ^{33}P Concentrations Measured at Whiteface Mountain, NY

Date		Ozone (ppb)	^{7}Be[a] (fCi/m^3)	^{32}P[b] (fCi/m^3)	^{33}P[c] (fCi/m^3)	$\frac{^{7}Be}{^{32}P}$	$\frac{^{7}Be}{O_3}$ ($fCi/m^3/ppbv$)
June	1	40	30				0.9
(1978)	2	74	150	2.9	4.5	51	2.0
	3	45					
	4	40	205	3.1	1.6	65	5.1
	5	43	205	<1.8			4.7
	6	48	295	3.6	3.4	82	6.2
	7		75	1.0[d]		75	
	8	62	45	0.5[e]		90	0.7
	9	50					
	10	43	260	1.8[d]		140	6.0
	11	84	230	4.0[d]		58	2.8
	12	77	230				3.0
	13	39	20	<0.4			0.5
	14	34	110	<0.4			3.2
	15	45	190	1.1[e]		170	4.2
	16	44	185	1.9	2.3	98	4.2
	17	80	150	3.9	1.3	38	1.8
	18	74	110	2.9	1.3	38	1.5
	19	58	60				1.1
	20	42	180	2.3	1.7	77	4.2
	21	67	230	5.2	4.2	44	3.4
	22	55					
	23	37	110	2.7		41	3.0
	24	40	235	1.0[e]		230	5.8
	25	45	180	4.1		43	3.9
	26	83	150	2.8	4.9	53	1.8
	27	68	150	3.0	1.8	51	2.2
	28	51	120	1.3[d]	2.0	91	2.3
	29	41	105	0.5[e]		130	2.6
July	1						
	2						
	3	59	225	3.0[d]		117	3.8
	4						
	5						
	6	75	200	3.0[d]		67	2.7
	7	88	185	2.5	1.5	74	2.1
	8	88	215	3.1		70	2.4
	9	56	45	1.6[d]		27	0.8
	10	49	95	1.1[d]		85	1.9
	11	26	50	<0.7			1.8
	12	35	195	2.4	1.5	82	5.6
	13	59	235	4.0	3.2	59	4.0
	14	71	160	3.6	2.7	45	2.3
	15	71	145	3.0	3.1	49	2.0
	16	77	170	3.4		50	2.2
	17	50	125	2.1[d]	2.9	59	2.5

Table Con't

July (1978)	18	45	220	3.7[d]	4.1	59	4.9
	19	73	230	2.3[d]	9.3	73	3.1
	20	102	300	5.1[d]	4.0	59	2.9
	21	104	210	4.1[d]		51	2.0
	22	70	90	1.8[d]		49	1.2
	23	63	100	2.5		39	1.5
	24	28	150	<0.8			5.3
	25	50	155	2.5[d]		61	3.1
	26	63	175	4.0[d]		44	2.8
	27	64	115	2.8[d]		41	1.8
	28	35	55	<0.6			1.5
	29	37					
	30	26	65	1.1[d]		57	2.4
	31	39	105	0.9[e]		110	2.6
August	1	51	100	1.7	1.2	58	1.9
	2	54	120	2.2[e]		54	2.2
	3	67	70	2.4[e]		29	1.0
	4	40	100	2.8[e]	0.5	35	2.4
	5	45	130	2.5[d]	2.5	52	2.9
	6	63	140	1.2[d]		120	2.2
	7	56	170	2.6		65	3.0
	8	57	65	1.3[e]	0.9	50	1.1
	9	65	95	1.6[e]	1.0	61	1.5
	10	30	55	1.5[d]		38	1.9
	11	44	155	2.7[d]	2.5	58	3.6
	12	66	70	1.7[e]		40	1.0
	13	71	145	5.8		25	2.0
	14	55	135	2.8[d]	5.5	48	2.5
	15	52	170	3.1[d]		54	3.2
	16	73	145	2.8[d]	3.6	51	2.0
	17	42	25	0.9[e]		31	0.6
	18	33	145	2.2[d]		66	4.4
	19	51	150	2.9	3.6	52	3.0
	20	30	350	4.9	2.7	72	11.6
	21	35	165				4.7
	22	45	240				5.3
	23	60	165	3.3	2.7	51	2.8
	24	53	50	1.4[d]	0.7	34	0.9
	25	31	35	<0.4			1.1
	26	32	105	1.8[d]		57	3.3
	27	30	125	1.4[e]		90	4.2
	28	59	95	1.5[d]		62	1.6
	29	44					
	30	30					
	31	40	120	2.7[d]	3.3	45	3.0
September	1	41	115	1.9[d]		60	2.8
	2	51	170	3.4[d]		50	3.3
	3	65	130	5.4[d]	4.9	24	2.0
	4	29	105	1.3[d]		78	3.6
	5	34	145	0.9[d]	2.7	160	4.3
	6	56	145	2.7		54	2.6
	7	25	30	0.8[d]		39	1.2
	8	26	130	<1.4			5.0
	9	23	60	0.9[d]	0.5	65	2.5

Table Con't

September	10	34	90	1.5[d]	1.0	60	2.6
(1978)	11	63					
	12	27	40	<0.4			1.4
	13	31	140	1.8		80	4.6
	14	44	160	1.8	2.1	89	3.7
	15	36	170	0.9[d]		190	4.7
	16	32	215	1.4[d]	1.1	160	6.8
	17	29	160	0.6[e]		260	5.4
	18	48	340	2.5	0.40	140	7.1
	19	47	370	5.2	6.7	71	7.8
	20	49	165	2.8		59	3.4
	21	60	60	0.8[e]		74	1.0
	22	25	40	0.4[e]		88	1.5
	23	35	280	1.1[d]		250	8.0
	24	48	170	1.7		99	3.5
	25	40					
	26	40	270	3.3		82	6.8
	27	56	205	3.8[e]		54	3.7
	28	33	40	0.6[e]		63	1.2
	29	35	65	1.5		45	1.9
	30	41	100	3.4		30	2.5
October	1	34	55	1.1[d]		53	1.6
	2	33	75	1.3[d]		59	2.2
	3	36	70	0.9[d]		76	2.0
	4	34	45	0.7[e]		63	1.3
	5	34	40	0.5[e]		84	1.2
	6	37	60	1.8		32	1.6
	7	21	<7	<0.5			0.3
	8	25	<16	<0.4			0.6
	9	29	55	0.8[d]		69	1.9
	10	36	70	1.9		37	1.9
	11	61	30	1.2[d]		25	0.5
	12	52	165	5.1		32	3.2
	13	42	50	2.1[d]		24	1.2
	14	24	<9	<0.4			0.4
	15	27	45	1.3		35	1.7
	16	29	110	1.5		75	3.9
	17	30	60	0.74		81	2.0
	18	35	85	2.12		40	2.4
	19	27	85	1.50		56	3.1
	20	31	115	2.13		55	3.7
	21	47	120				2.6
	22	61	175				2.9
	23	35	50				1.4
	24	29	15				0.5
	25	34	130				3.8
	26	33	50				1.5
	27	29					
	28	31	25				0.8
	29	30	70				2.3
	30	42					
	31	38					
November	1	32					
	2	37	180				4.9

Table Con't

November	3	47	190	4.0
(1978)	4	70	215	3.1
	5	78		
	6	66		
	7	31	110	3.5
	8	33	95	2.9
	9	36	160	4.4
	10	44		
	11	40	175	4.4
	12	34		
	13	39		
	14		25	
	15		90	
	16			
	17		220	
	18		20	
	19		80	
	20		185	
	21	37	150	4.0
	22		155	
	23		95	
	24	22		
	25	29		
	26	32		
	27	40		
	28	23		
	29	30	120	4.0
	20			
December	1	29		
	2	30		
	3	38		
	4	28		
	5	26		
	6	22	110	5.0
	7	35	215	6.1
	8	13	40	3.1
	9	32		
	10	32	70	2.2
	11	31	25	0.8
	12	23		
	13	24	100	4.2
	14	26	45	1.7
	15	21	85	4.0
	16	30		
	17	25	55	2.2
	18	33	80	2.4
	19	31		
	20	37		
	21	22		
	22	32		
	23	28		
	24	39		
	25	33		
	26	20		

Table Con't

December (1978)	27	22				
	28	32				
	29	38				
	30	43				
	31	36				
January (1979)	1	24				
	2	23				
	3	23				
	4	22	40	<0.5		1.8
	5	24	190	0.8[e]	240	7.9
	6	27				
	7	20				
	8	32				
	9	27	40			
	10	33	35	<0.4		1.1
	11	34	55	<0.5		1.6
	12	33	75	1.1[d]	69	2.4
	13	38	10	0.60[e]	20	0.3
	14	30	45	<0.4		1.4
	15	27	110	<0.5		4.1
	16	33	100	0.6[e]	160	3.0
	17	21	85	<0.4		4.0
	18	36	80	0.6[e]	130	2.2
	19	43	175	2.8	62	4.0
	20	42				
	21	34	7	<0.6		0.2
	22	35	35	<0.7		0.9
	23	41	140	0.6[e]	230	3.4
	24	41	80	0.6[e]	130	1.9
	25	35	15	<0.5		0.4
	26	31	<5	<0.7		
	27	36	15	<0.8		0.4
	28	25	<5	<0.5		
	29	32	10	<0.5		0.4
	30	35	10	<0.5		0.3
	31	33	15	<0.5		0.4
February	1	36	30	<0.5		0.9
	2	39	20	<0.4		0.7
	3	42	125	1.0[d]	120	2.9
	4	41	65	1.0[d]	65	1.6
	5	43	75	<0.5		1.7
	6	37	135	<0.6[d]		3.7
	7	44	120	0.8[d]	150	2.7
	8	22	50	<0.6		2.3
	9	13	60	0.4[e]	140	4.5
	10	39	100	0.7[d]	140	2.6
	11	40	125	0.8[d]	160	3.2
	12	42	95	<0.7		2.2
	13	40	135	1.3[d]	100	3.3
	14	40	215	1.4[d]	155	5.4
	15	43	290	2.6[d]	110	6.7
	16	46	140	0.8[d]	180	3.0
	17	40	140	0.8[d]	180	3.5

Table Con't

February	18	41	185	2.4		78	4.6
(1979)	19	46	190	4.0		47	4.1
	20	50	160	3.5		45	3.2
	21	55	75	1.0[d]		75	1.4
	22	48	185	2.8		65	3.8
	23	52	65	1.2[d]		54	1.3
	24	46	40	0.8[d]		52	0.9
	25	48	45	0.8[d]		56	0.9
	26	47	<5	<0.5			
	27	41					
	28	40	130	2.4		54	3.2
March	1	60					
	2	49	50	1.1[d]		46	1.0
	3	54	245	2.8		87	4.5
	4	57	40	<0.8			0.7
	5	45	8	<0.4			0.2
	6	38	110	1.5[d]		72	2.8
	7	42	50	1.3[d]		39	1.2
	8	42	40	1.0[e]		40	1.0
	9	41	60	0.9[e]		65	1.4
	10	46	55	1.0[d]		53	1.2
	11	42	55	0.8[e]		66	1.3
	12	33	160	2.8		56	4.8
	13	41	85	1.4		62	2.1
	14	46	75	1.4[d]		55	1.7
	15	39	90	1.2[d]		73	2.3
	16	38	80	2.5	3.0	31	2.1
	17		110	1.8[d]	2.6	60	
	18		135	1.5[d]	1.9	89	
	19		120	0.90[d]	1.6	140	
	20		65	0.9[d]		73	
	21		70	1.0[d]		70	
	22		90	3.5		25	
	23		115	2.2	1.8	53	
	24		115	3.7	4.7	30	
	25		35	0.9	1.6	35	
	26		75	2.3	4.6	33	
	27		245	3.7	3.8	66	
	28	46	205	6.7	5.9	30	4.4
	29	49	40		2.9		0.8
	30	47	25				
	31	67	195	2.6[d]		75	2.9
April	1	35					
	2	46	<6	<0.4			
	3	40	105	1.6[e]		66	2.6
	4	47	85	1.5[d]	2.3	55	1.8
	5	46	50	1.1[e]		46	1.1
	6	47	20	0.6[e]		33	0.4
	7	41	25	<1.3			0.6
	8	42	215				5.1
	9	55					
	10	45	110	1.8	2.4	60	2.4
	11	48	95	1.9	2.6	50	2.0

Table Con't

April	12	58	60	1.1[d]		55	1.1
(1979)	13	52	105	1.6[d]	2.4	65	2.0
	14	62	35				0.6
	15	54	25	<1.0			0.5
	16	47	30	<0.4			0.6
	17	41	185	3.0	4.1	61	2.5
	18	52	180	3.1	3.6	59	3.5
	19	55	210	3.5	4.3	61	3.9
	20	58	270	4.0	5.5	68	4.7
	21	61	235	4.5	5.0	53	3.9
	22	70	110	2.5	3.6	44	1.6
	23	62	100	2.5	2.8	39	1.6
	24	59	180	4.1	4.3	44	3.1
	25	78	170	3.2	4.4	53	2.2
	26	80	90	2.3	1.9	40	1.2
	27	66	15	<0.4			0.2
	28	54	70				1.3
	29	50	95	2.3	2.3	41	1.9
	30	58	125	2.1	2.2	59	2.2
May	1	44	40	0.9[d]		47	1.0
	2	44	145	3.3	3.6	44	3.3
	3	63	65	1.0[d]		65	1.0
	4	45	55	0.9[d]	1.6	61	1.2
	5	46	140	2.1	4.3	67	3.0
	6	52	175	2.8	3.6	63	3.4
	7	88	160	2.8	3.4	57	1.8
	8	88	<9	<0.4			
	9	73	150	2.9	3.8	51	2.0
	10	66	25	0.6[d]		40	0.4
	11	78	145	2.9	3.5	49	1.8
	12	46	45	0.9[d]		49	1.0
	13	47	90	2.0	2.1	45	1.9
	14	63	165	3.2	3.5	52	2.6
	15	63	120	2.0	1.9	46	1.9
	16	40	75	1.3[d]	1.7	58	1.9
	17	57	220	4.1	5.4	53	3.8
	18	45	90	1.5	5.6	61	2.0
	19	28	30	0.6		52	1.1
	20	39	85	2.2	3.1	39	2.2
	21	44	105	2.1	3.0	53	2.4
	22	48	200	3.7	3.9	54	4.1
	23	59	180	4.2		43	3.1
	24	53	50	0.9[d]	2.5	57	1.0
	25	34	70				2.1
	26	47	10				0.2
	27	49	80	1.7	1.3	39	1.6
	28	56	110	1.8	2.6	61	2.0
	29	52	95	2.1	2.1	46	1.9
	30	51	60	1.6	1.4	39	1.2
	31		85	1.8[d]	2.8	48	
June	1	53	105	2.2		48	1.7
	2	67	155	3.4		46	2.3
	3	75	185	4.1	3.2	45	2.5

Table Con't

June	4	79	235	5.4	3.1	43	3.0
(1979)	5	46	175	3.7	2.0	47	3.8
	6	47					
	7	100	55	1.7		33	0.6
	8	66	150	3.0		49	2.3
	9	61	135	2.9	3.7	46	2.2
	10	58	66	1.4[d]		47	1.1
	11	27	<50	<0.7			
	12	33	70	<0.4			2.1
	13	42	175	2.6	2.7	68	4.2
	14	60	185	3.7	2.9	50	3.1
	15	87	175	3.0	4.9	60	2.0
	16	113	180	2.4	4.8	75	1.6
	17	80	200	3.9	6.0	52	2.5
	18	38	95	2.2	1.9	43	2.5
	19	52	195	2.9	1.6	67	3.8
	20	58	160	3.2	4.9	50	2.8
	21	84	195	3.8	5.9	51	2.3
	22	52	175	3.6	0.8	48	3.4
	23	17	<50	<0.4			
	24	29	<65	<0.5			
	25	39	155	3.3	2.4	46	4.0
	26	60	155				2.6
	27	82	215	3.4	4.3	64	2.7
	28	73	180	3.7	2.7	49	2.5
	29	71	160	3.0	3.8	53	2.2
	30		100	2.0	8.7	50	
July	1	58					
	2	42	75	1.4[d]	0.8	54	1.8
	3	39	160	2.6[d]	2.5	62	4.1
	4	31	70	0.9[d]	0.9	80	2.3
	5	26					
	6	37	130	2.4	1.8	54	3.5
	7	42	150	2.2	4.8	68	3.6
	8	64	170	3.1	4.8	55	2.7
	9	73	170	2.6	4.7	65	2.7
	10	75	190	3.7	4.0	51	2.5
	11	69	90	2.0	2.7	45	1.3
	12	56	130	2.8	4.6	46	2.3
	13	52	190	3.1	4.3	61	3.7
	14	77	160	3.6	4.6	44	2.1
	15	57	85	2.0	3.2	42	1.5
	16	36	120	2.7	2.4	44	3.3
	17	44	100	2.2	1.9	45	2.3
	18	44	150	2.6	2.8	58	3.4
	19	68	200	4.1	6.3	49	2.9
	20	84	230	4.1	5.6	56	2.7
	21	90	250	4.7	8.0	53	2.8
	22	89	210	3.4	7.2	62	2.4
	23	81	230	4.1	4.8	56	2.8
	24	74	180	4.4	5.2	41	2.4
	25	52	25				0.5
	26	50	80	1.8	2.1	44	1.6
	27	43	90	1.8	4.1	49	2.1

Table Con't

July	28	58	190	2.5	2.5	73	4.4
(1979)	29	60	150	3.1	3.6	48	2.5
	30	63	110	3.5	4.7	31	1.8
	31		95	2.4	2.0	39	
August	1	58	140	3.1	3.4	45	2.4
	2	57	60				1.0
	3	63	160	4.0	5.2	40	2.5
	4	79	180	3.2	3.9	56	2.3
	5	52	100	2.5	3.1	40	1.9
	6	26	85	1.6[d]	1.6	54	3.3
	7	43	130	3.1	5.9	42	3.0
	8	39	110	2.2	2.1	50	2.8
	9	40	120	2.9	6.3	41	3.0
	10	45	20	0.5[e]		38	0.4
	11	27	65	1.8	1.1	37	2.5
	12	35	150	2.0	1.6	75	4.3
	13	36	130	2.4	2.1	54	3.6
	14	27	20	0.5[e]		44	0.8
	15	22	35	0.6[e]	<0.9	58	1.6
	16		130	0.8[d]	2.2	160	
	17		150	3.6	1.4	42	
	18		20	0.6[e]	<0.8	33	
	19		50	2.0	3.3	25	
	20		55	1.3[d]	<0.8	43	
	21	37	80	1.4[d]	2.1	57	2.2
	22	54	170	3.9	5.0	44	3.1
	23	57	70	1.9	1.8	37	1.2
	24	51	40	0.6	<1.0	63	0.7
	25	52	<6	<0.4			
	26	57	55	1.6	<1.0	36	1.0
	27	54	90	2.9	<0.9	32	1.7
	28	57	80	2.2	1.8	37	1.4
	29	56	45	1.3[d]	1.3	35	0.8
	30	40	90	2.4[d]	4.5	43	2.3
	31	36	100	1.6[d]	1.7	63	2.8
September	1	70	130	3.4[d]	1.8	38	1.9
	2	52	75	1.5[d]	<0.8	49	1.4
	3	31	55				1.7
	4	44	80	2.2	3.5	36	1.8
	5	41	105	3.0	<1.1	35	2.6
	6	30	<11	<0.4[d]			
	7	26	90	1.3[d]	1.8	70	3.5
	8	24	45	0.5[e]	2.3	86	1.8
	9	37	105	1.8[d]	2.6	58	2.8
	10	34	50	1.1[d]	1.1	47	1.5
	11	29	25	<0.4			0.9
	12	47	115	3.5	1.8	33	2.5
	13	59	100	2.0	2.2	49	1.7
	14	25	<13	<0.4[e]			
	15	26	40	0.7[d]	1.3	59	1.6
	16	39	95	1.5[d]	2.4	64	2.4
	17	60	100	2.1	1.3	49	1.7
	18	51	75	1.8	3.3	41	1.5

Table Con't

September	19	30	95	2.5	<0.9	38	3.2
(1979)	20	42	135	3.4	1.4	40	3.2
	21	42					
	22	26	70	1.1[d]	<1.7	64	2.7
	23	31	120	2.2	2.8	55	3.9
	24	42	125	2.8	1.7	44	2.9
	25	55					
	26	38	140	3.3	1.1	42	3.7
	27	58	115	2.1	2.4	54	2.0
	28	57	110	2.4	1.9	47	2.0
	29	77	95	2.2	1.4	43	1.2
	30						
October	1	50	120	2.9	1.5	41	2.4
	2	54	130	2.9	<1.3	41	2.4
	3	45	60				1.3
	4	54	100	2.5	1.7	40	1.8
	5	44	40	0.9[d]	1.1	45	0.9
	6	37	70	1.6[d]	2.0	43	1.9
	7	25	<11	<0.4			
	8	30	20	<0.4			0.7
	9	28	20	<0.4			0.7
	10	30	60	1.0[d]	1.8	59	2.0
	11	23	45	1.0[d]	<0.9	43	2.0
	12	22	<11	<0.4			
	13	20	<10	<0.4			
	14	25	<25	<0.4			
	15	24	<10	<0.4			
	16	33	60	1.4[d]	<1.1	44	1.8
	17	39	55	1.2[d]	<0.9	44	1.4
	18	41	110	1.8[d]	4.7	61	2.7
	19	55	85	1.2[d]	1.3	71	1.5
	20	53	110	2.0	2.0	55	2.1
	21	46	140	2.5[d]	2.7	56	3.0
	22	50	95	1.6[d]	1.0	59	1.9
	23	34	70	1.4[d]	2.1	49	2.0
	24	21	<7	<0.4			
	25	27	<11	<0.5			
	26	27	<10	<1.0			
	27	34	60	<0.5			1.8
	28	21	<10	<0.4[e]			
	29	26	20	0.6[e]	<1.0	37	0.8
	30	39	85	1.1[d]	<1.3	79	2.2
	31	45	140	2.9	<1.3	48	3.1
November	1	40	80	1.5[d]	<1.6	55	2.0
	2	32	60	<0.6[d]			1.9
	3	27	55	1.1[d]	<1.7	50	2.0
	4	27	55	1.3[d]	1.8	41	2.0
	5	37	120	2.9	2.5	41	3.2
	6	28	45	0.9[d]	<1.3	52	1.6
	7	23	55	1.4[d]	<1.6	38	2.4
	8	25	110	3.0	<1.0	37	4.0
	9	31	<11	<0.5	<1.3		
	10	31	55	1.0[d]	2.5	57	1.8

Table Con't

November	11	25	110	2.5[d]	<1.1	44	4.4
(1979)	12	29	120	1.3[d]	2.1	92	4.1
	13	23	40	1.0[d]	<2.0	39	1.7
	14	23	30	1.0[d]	<1.5	30	1.3
	15	22	30	1.2[d]	<1.3	23	1.4
	16	21	<13	<0.4[e]			
	17	20	25	0.5[e]	<1.0	50	1.3
	18	44	120	2.7	1.2	44	2.7
	19	59	140	3.3	4.2	42	2.4
	20	34	80	2.0	<1.1	39	2.4
	21	39	140	3.3[e]	1.3	42	3.6
	22	41	30	0.5[e]	<1.0	62	0.7
	23	40	140	2.2[d]	3.0	64	3.5
	24	32	70	1.1[d]	1.3	64	2.2
	25	40	40	0.8[d]	<1.1	53	1.0
	26	33	<10	<0.04			
	27	34	110	2.1	3.9	52	3.2
	28	27	25	0.7	1.7	39	0.9
	29	19	<10	<0.4[d]			
	30		40	1.0[d]	2.4	41	
December	1	27	50	1.3[d]	<1.3	40	1.8
	2	30	40	0.8[d]	1.5	49	1.3
	3	24	100	1.8[e]	1.2	57	4.2
	4	21	35	0.7[e]	1.4	49	1.7
	5	30	125	2.8	1.8	44	4.2
	6	31	80	1.8[e]	<0.9	43	2.6
	7	16	25	0.6[d]	1.3	45	1.6
	8	23	50	1.2[d]	<1.1	40	2.2
	9	21	55	1.5[d]	<0.9	38	2.6
	10	28	135	3.5	<0.9	39	4.8
	11	29	150	3.6	<1.1	42	5.2
	12	12	55	2.0[d]	<1.7	27	4.6
	13	26	55	1.5[d]	3.4	35	2.1
	14	26	60	1.9	<1.4	32	2.3
	15	27	120	3.4	2.6	35	4.4
	16	29	50	1.0	<0.9	49	1.7
	17	28	40	1.9	<1.4	22	1.4
	18	31	115	2.3	5.0	49	3.7
	19	32	165	4.0	<2.4	41	5.2
	20	34	120	2.4	<1.9	49	3.5
	21	42	85	2.2	<1.7	39	2.0
	22	49	125	2.6	4.1	48	2.6
	23	14	25	<0.5[d]			1.8
	24	29	35	0.9[d]	1.9	37	1.2
	25	19	<12	<0.4			
	26	14	<8	<0.4			
	27	13	<9	<0.5			
	28	21	25	1.1[e]	<1.1	23	1.2
	29	23	15	0.6[e]	<1.2	23	0.6
	30	28	60	1.5[e]	<1.2	39	2.1
	31						

Table Con't

a ^{7}Be as well as ^{32}P and ^{33}P concentrations were measured midnight to midnight during 1978 and noon to noon during 1979. ^{7}Be uncertainties at the 95% confidence level (3 sigma) are generally < ± 10% (see figure).

b Improved data reduction techniques have changed some of the ^{32}P and ^{33}P concentrations reported for June 1 - August 15, 1978 in the previous report. The data reported here should supercede any previously reported results. Uncertainties at the 95% conficence level (2 sigma) are < ± 15% unless otherwise shown.

c Due to low specific activity and counting efficiency for the ^{33}P soft betas (Emax = 248 Kev) the uncertainties are often > ± 30% (see figure). Therefore, it is advised that this data be used with appropriate care.

d Uncertainty, ± 15 to ± 30%.

e Uncertainty, > ± 30%.

Table 2. Summary of ^{7}Be and ^{90}Sr Concentrations Measured on GASP Filters

Exposure date		Altitude (km)	Latitude (^{o}N)	O_3 (ppbv)	^{7}Be (fCi/m^3)	^{90}Sr (fCi/m^3)
October	6	10.1	48-45		≤380	
(1977)	9	11.9	26-35		920±300	
	12	11.3	28-18		≤420	
	15	10.1	11-18		≤350	
	18	10.1	42-50		4800±480	
	21	10.7	34-27	136	2300±270	32±5
	24	10.9*	41-48	259	6400±750	
November	11	11.3	39-42	50	1300±200	
	14	11.3*	33-28	87	1700±200	
January	6	11.1	37-34	59	≤590	
(1978)	9	10.1	52-55	276	7300±580	270±15
	9	10.1	36-35	368	5300±800	275±30
	15	11.3	42-41	189	3700±400	90±17
	18	12.2	22-25	57	≤1000	
	21	11.3	35-40	157**	4000±200	150±9
	24	10.8*	23-31	135	990±120	
February	17	10.8	42-43	384**	5400±250	290±15
March	7	11.0	37-32	29	≤360	≤14
	10	11.0	37-35	29**	980±250	≤28
	12	10.5*	24-27	35**	≤470	40±26
	16	10.8*	22-29	71**	710±200	15±10
	16	10.4	54-56		6900±350	320±16
	19	10.0	36-35	89	≤1300	≤85
	20	10.7*	25-22	97**	≤590	≤60
April	18	11.7*	41-38	526	5300±300	290±30
	22	11.0	37-32	61	≤360	13±9
	23	11.3	38-42	236	2300±250	100±10
	25	11.3	23-31	91	180±100	19±10
	28	11.0	37-32	79	260±150	11±8
	29	11.0*	34-38	142**	2000±200	125±25
May	18	10.4*	36-25	32	580±170	40±7
	18	11.6	21-28	104	520±150	45±10
	24	11.3	38-42	341	4300±430	135±9
	27	11.4*	38-42	277	2600±300	85±7
	30	11.3	23-31	63	340±100	30±14
June	8	11.3	22-29	43	≤240	12±6
	11	11.9	40-41	70	630±190	10±7
	14	11.3*	41	130	1100±130	26±4
	17	10.1	22-32	82	≤300	
	17	10.7	38-35	432	5000±350	165±17
	20	11.3*	40-41	140	980±500	≤27

Table 2 (Con't)

July (1978)	29	10.1	52	255	4500±280	
August	1	11.0*	40-32	91	750±160	≤24
	4	9.8	34-29	58	≤150	
September	15	10.0	11-16	28	≤180	13±6
	21	11.3	38-42	82	1100±230	≤15
	27	11.3	22-29	31	≤120	≤15
	30	11.3	44-40	94	840±240	12±9
October	3	10.3	51-54	79	460±120	≤12
	3	11.3	22-28	51	500±300	≤30
	6	9.8	52	105	1300±130	13±5
	6	11.3	25-32	56	320±180	≤17
	6	11.3	32-35	54	≤340	≤30
	6	11.3	35-36	55	≤1600	≤60
	9	10.1	50-53	55	360±160	≤26
	9	11.8*	34-36	104	1100±170	23±12
	12	11.2	34-37	48	≤670	≤35
	12	10.1	52-54	76	1100±270	19±16
	15	10.7	34-28	39	≤280	≤13
	21	10.1	49-60	95	1600±200	22±6
	27	11.9	41-42	103	1400±480	20±18
	27	11.9	42-41	82	1600±550	≤25
	27	11.9	41-39	97	930±600	≤25
	27	11.9	39-39	44	≤460	≤29
	30	11.2	25-29	28	≤300	
	30	11.2	29-33	67	≤480	
November	8	11.0	37-30	36	400±200	≤15
	11	11.6*	40-39	30	≤180	≤18
December	5	11.3	36-40	40	≤240	
	5	11.3	40-42	50	220±110	
	17	11.0	37-32	151	1900±150	23±7
	23	11.3	33-36	100	1000±190	30±24
	23	11.6	25-30	61	840±230	≤40
	29	11.3	34-38	208	3100±320	≤35
	29	11.3	38-40	178	2400±240	≤40
	29	11.3	40-41	200	2300±340	≤40
January (1979)	9	11.1	42-41	517	6400±1300	≤240
	18	11.3	25-29	72	590±210	18±11
	18	11.6*	29-32	99	1100±290	32±21
	18	11.9	32-35	130	2200±260	33±10
	18	11.9	35-36	214	3600±1400	110±70
	21	11.3	40-42	60	650±65	≤35
February	8	11.3	37-40	154	1600±160	40±16
	27	11.8*	37-35	666	4800±720	110±75

Table 2 (Con't)

June	4	11.9	41-39	40***	≤400	
	4	11.9	38-36	60***	520±100	
	4	11.9	36-33	65***	170±60	
	5	11.9	32-28	122***	800±180	12±9
	5	11.9	28-24	62***	300±100	≤13
	10	11.6	24-28	44***	≤200	
	10	11.6	29-31	37***	200±170	
	10	11.6	31-33	39***	150±90	
	13	11.3	42-41	520	5100±570	80±60
	15	11.3	34-31	72	200±60	≤13
	15	11.3	31-27	69	150±70	
	24	11.3	37-41	114	510±140	≤15
	24	11.3	41-42	127	850±200	10±8
	24	11.3	42	375	2500±470	57±14
	29	11.3	37-39	42	≤300	≤18

*Average altitude.

**O_3 estimated from measurements in passenger cabin with corrections for O_3 destruction in the cabin and during compression, uncertainty ±20%.

***Pressurization pump inoperative O_3 corrected for low pressure uncertainty ±12 ppbv.

Table 3. Analysis of 5 Samples of Air Filters from High Point, N.J. by i) LTA/AAS, ii) WND/AAS and iii) INAA

Ser. No.	Collection Date		Concentration (ng/m^3 air) Na	K	Fe	Zn	Pb	Al
1	7/20/76	i)	127	190	697 (?)	327	124	932
		ii)	106	148	359	412	124	---
		iii)	203	254 (187)	464	297	---	---
2	7/21/76	i)	85	148	359	412	83	414
		ii)	211	148	169	539	124	124
		iii)	101	144	429	382	---	---
3	7/22/76	i)	232	190	330	61	104	414
		ii)	211	148	232	74	166	103
		iii)	258	187	342	62	---	---
4	7/23/76	i)	444	106	192	55	145	248
		ii)	401	106	120	120	186	<103
		iii)	295	101 (113)	163	27 (51)	---	---
5	7/24/76	i)	29	85	192	23	62	228
		ii)	127	108	114	42	124	<103
		iii)	40	79 (127)	194	24 (30)	---	---

*The values in parenthesis by Rahn using INAA (private communication).
LTA - Low Temperature Ashing
WND Wet Nitric acid Digestion
INAA - Instrumental Neutron Activation Analysis

Table 4. Elemental Concentrations in System Blanks[@] (Whatman 41 Filter Paper)

Ser. No.	Concentration (ng/cm^2)							
	Na	Mg	Al	K	Ca	Fe	Zn	Pb
1	250	30	50	30	100	50	20	5
2	320	40	80	60	130	60	30	5
3	330	40	80	62	250	60	ND	10
4	330	30	60	110	290	90	ND	10
5	ND	36	50	270?	450?	50	20	10
6	ND	<5	640?	90	370	70	20	10
7	300	20	50	60	240	50	10	10
8	390	180?	140	220?	190	70	180?	10
9	540?	40	160	130	230	80	30	10
10	370	100?	420?	90	450?	170?	20	10
11	310	30	60	70	100	60	20	10
12	360	40	90	90	180	70	20	20
13	ND	5	750?	150	100	70	30	10
14	420	80	290?	610?	330	280?	50	100?
15	780?	40	90	660?	240	50	60	20
16	740?	8	280?	110	150	50	20	230?
17	410	31	50	87	100	70	20	10
18	360	8	130	60	ND	50	ND	10
19	ND	ND	50	ND	ND	50	ND	10
20	ND	ND	60	ND	ND	50	30	10
21	310	30	50	110	130	<50	20	10
22	390	30	50	150	100	<50	20	10
23	340	20	60	130	100	50	ND	10
mean ng/cm^2 (this work)	346	31	76	94	185	61	26	11
($\pm 1\sigma$)	44	16	34	33	85	12	12	3
(reported)*	150	<80	12	15	140	40	<25	—

[@]For definition of system blank see text
*Dams et al. (1972).
ND Not determined
? Suspect values omitted in mean calculations

Table 5. Daily Concentrations of TSP, Na, Mg, Al, K, Ca, Fe, Zn, Pb and SO_4^{2-} in Air Particulates at Whiteface Mountain, New York

Date		TSP ($\times 10^3$)	Concentration (ng/m^3)								
			Na	Mg	Al	K	Ca	Fe	Zn	Pb	SO_4^{2-}
January*	1										
(1979)	2	NS									
	3	NS									
	4	ND	<70	<40	196	54	<80	38	≤14	11	1000
	5	ND	140	<40	132	112	<80	59	~8	17	1650
	6	NS									
	7	NS									
	8	NS									
	9	NS									
	10	9.1	<90	<40	104	37	<80	41	≤16	26	1650
	11	16.5	<80	<40	41	32	<80	16	≤16	<3	300
	12	27.4	<82	<40	40	<17	<80	13	≤16	13	5700
	13	19.3	<80	<40	68	<16	<80	10	≤16	<3	1650
	14	22.4									
	15	26.6	<75	<40	222	58	<80	105	18	29	3000
	16	12.5	<75	<40	90	<15	<80	18	≤15	9	<200
	17	6.9	90	<40	78	<15	<80	17	≤15		300
	18	18.8	<53	<40	293	27	<80	40	8	53	3400
	19	26.9	<71	<40	74	<14	<80	~6	<14	<3	<200
	20	NS									
	21	21.8	<60	<40	39	98	<80	<12	<12	<3	<200
	22	18.7	<60	<40	57	25	<80	<12	<12	5	300
	23	33.5	<86	<40	51	<17	<80	21	<17	7	1500
	24	39.2	<62	<40	126	<12	<80	<12	<12	7	1000
	25	29.6	<64	<40	41	26	<80	<12	<12	<3	<200
	26	26.3	<64	<40	17	<17	<80	≤12	<12	<3	400
	27	20.4	<68	<40	19	<14	<80	≤12	<12	<3	300
	28	21.0	ND	ND	ND	ND	<80	ND	ND	<3	<200
	29	19.4	<64	<40	15	<13	<80	<13	<13	<3	<200
	30	7.8	70	<40	17	<17	<80	<17	<17		<200
	31	7.3	<123	<40	25	<25	<80	<25	<25		<200

Table 5 (Con't)

		TSP	Na	Mg	Al	K	Ca	Fe	Zn	Pb	SO_4^{2-}
February* (1979)	1	5.4	104	<40	≤105	<11	<80	<10	19	<21	<200
	2	30.3	≤41	<40	≤102	<10	<80	<12	18	<20	<200
	3	34.5	≤41	<40	≤127	25	<80	<13	<13	<25	<200
	4	31.8	≤39	<40	<98	20	<80	<12	<12	<20	3350
	5	29.6	154	<40	≤128	51	<80	<10	<13	<26	400
	6	10.7	136	<40	16	<12	<80	<14	<12	≤23	700
	7	16.4	214	<40	<152	31	<80	<21	<15	≤30	450
	8	13.2	54	<40	<135	<14	<80	<16	<14	≤27	<200
	9	12.0	54	<40	<135	≤14	<80	16	16	≤3	<200
	10	14.4	86	<40	21	≤11	<80	24	41	≈2	<200
	11	15.4	280	<40	32	<20	<80	<20	<10	<2	<200
	12	15.5	136	<40	20	23	<80	14	<6	9	1300
	13	7.0	191	<40	24	24	<80	31	<6	3	350
	14	7.4	335	<40	24	19	<80	13	<5	<2	350
	15	6.7	178	<40	31	<13	<80	10	<7	<3	850
	16	10.2	301	<40	46	23	<80	33	<6	5	1350
	17	9.3	131	<40	35	22	<80	15	<5	7	1000
	18	8.9	86	<40	26	21	<80	17	<5	≈2	950
	19	13.1	251	<40	60	<25	<80	15	<12	5	2200
	20	10.3	102	<40	27	20	<80	14	<6	12	4600
	21	16.3	110	<40	86	44	155	38	9	22	6300
	22	16.1	103	<40	44	26	<80	75	<7	18	7300
	23	28.9	223	<40	60	25	223	27	≈5	15	3250
	24	22.5	149	<40	45	43	149	26	<5	9	3650
	25	24.6	<76	<40	49	<15	<80	<7	<7	19	3600
	26	18.2	<67	<40	45	27	267	<7	<7	4	350
	27	30.7	<60	<40	95	30	387	21	<8	36	ND
	28	24.3	<59	<40	62	29	352	29	<7	37	2000
March	1	NS									
	2	55.1	100	3	20	14	163	<6	11	67	7350
	3	67.8	161	43	102	56	351	35	11	32	4650
	4	42.6	123	18	49	38	206	13	3	9	1650
	5	50.2	94	3	19	19	200	<7	3	11	350
	6	29.6	53	11	41	24	96	14	10	34	8200
	7	23.0	68	7	41	35	114	14	8	37	8250

Table 5 (Con't)

		TSP	Na	Mg	Al	K	Ca	Fe	Zn	Pb	SO_4^{2-}
March	8	25.5	43	10	23	31	47	16	8	48	9700
(1979)	9	16.0	82	11	47	17	68	9	11	34	6900
	10	7.3	167	6	24	19	70	11	7	29	4550
	11	4.6	149	17	34	17	58	8	8	15	1800
	12	1.4	136	32	21	25	126	11	5	6	850
	13	ND	100	25	51	49	99	12	12	57	2500
	14	2.8	46	14	54	36	ND	19	18	20	1450
	15	3.5	94	21	24	42	81	-6	1	6	1000
	16	ND	96	20	30	49	63	15	10	21	2850
	17	ND	211	23	33	35	80	16	11	41	2800
	19	ND	146	27	32	41	118	13	9	10	850
	19	7.6	139	25	99	101	154	12	7	11	800
	20	4.4	ND	28	76	41	149	36	4	9	ND
	21	6.8	123	24	20	20	57	-5	<2	4	ND
	22	2.2	114	43	157	102	152	77	4	13	1300
	23	24.7	326	106	282	134	272	195	19	71	2450
	24	24.4	468	89	189	128	183	86	5	12	1700
	25	22.0	60	28	36	72	ND	7	2	13	2000
	26	58.3	114	20	89	56	93	11	11	8	850
	27	22.6	75	23	63	51	187	9	12	7	650
	28	25.5	45	29	126	46	135	64	12	29	1450
	29	31.2	72	12	31	59	37	<6	13	36	3250
	30	ND	29	~2	32	<7	<16	<6	<2	8	2100
	31	13.8	<46	<18	20	<9	<46	<5	7	67	4700
April	1	NS									
	2	9.3	115	<2	43	72	<16	<5	4	6	550
	3	4.1	67	31	80	64	67	17	8	7	1550
	4	7.6	94	26	212	84	118	46	21	16	1400
	5	5.7	89	17	129	79	39	30	10	7	1150
	6	10.7	34	10	171	32	48	26	95	5	300
	7	3.9	41	16	ND	16	57	36	4	4	900
	8	6.0	58	36	109	38	95	36	16	9	1150
	9	NS									
	10	7.8	111	24	132	37	75	25	9	14	1250
	11	6.3	137	25	98	45	128	44	17	17	650

Table 5 (Con't)

		TSP	Na	Mg	Al	K	Ca	Fe	Zn	Pb	SO_4^{2-}
April	12	7.0	50	24	86	49	149	88	12	10	850
(1979)	13	21.8	94	28	217	40	116	36	25	8	950
	14	21.3	55	28	129	53	191	42	19	13	4050
	15	14.0	19	10	79	22	52	11	16	14	2800
	16	11.1	45	13	92	24	48	<6	26	9	900
	17	4.5	64	29	100	37	117	36	11	7	1850
	18	6.6	59	52	134	68	302	50	12	16	1550
	19	7.9	106	85	191	130	487	134	33	34	1450
	20	12.7	84	97	200	117	528	124	13	10	1200
	21	20.2	54	124	412	201	394	161	33	44	2650
	22	23.0	78	54	180	118	148	110	32	64	9450
	23	15.5	91	87	210	99	504	111	9	14	2090
	24	37.8	157	289	745	417	725	353	34	77	8300
	25	45.8	202	<2	442	299	189	258	91	136	19200
	26	23.0	91	95	296	130	242	144	36	22	6350
	27	19.2	31	4	46	20	<16	<6	7	3	<200
	28	27.0	42	28	104	65	45	44	8	15	3750
	29	34.0	42	43	139	88	120	89	82	55	9100
	30	36.5	42	61	168	86	233	83	5	36	6550
May	1	18.1	77	29	96	66	94	23	27	11	1950
	2	20.4	71	66	206	115	142	101	6	5	2600
	3	28.3	66	59	244	110	141	137	16	69	4550
	4	3.9	20	22	81	28	68	15	3	7	1900
	5	21.4	71	68	209	107	165	123	9	12	2000
	6	18.9	97	86	291	161	259	116	16	12	2050
	7	32.9	92	80	218	115	752	109	8	69	8000
	8	26.4	45	8	65	20	~18	12	<2	4	650
	9	63.8	118	143	532	360	401	276	24	62	14500
	10	26.7	24	9	63	29	<16	122	<2	93	1500
	11	68.4	210	69	629	568	411	303	76	51	16200
	12	37.8	178	20	283	203	144	111	22	10	5850
	13	32.0	58	26	71	69	107	37	4	41	1450
	14	40.1	45	61	153	103	227	122	7	77	6750
	15	35.8	56	42	129	92	103	85	13	8	8300

Table 5 (Con't)

		TSP	Na	Mg	Al	K	Ca	Fe	Zn	Pb	SO_4^{2-}
May	16	20.3	33	16	52	26	<77	12	4	19	1600
(1979)	17	26.7	62	59	159	96	193	101	7	17	3200
	18	15.6	113	34	72	51	59	26	5	7	900
	19	24.6	90	75	264	106	235	152	6	6	600
	20	37.7	93	39	112	88	56	63	20	17	4400
	21	19.0	<20	6	23	9	<16	8	<2	6	3200
	22	27.0	~18	35	117	52	131	68	<2	6	2400
	23	38.3	43	40	124	77	106	85	15	41	11300
	24	21.8	<20	<2	12	<7	<16	~5	<2	4	300
	25	36.2	~22	10	32	16	33	~4	<2	5	300
	26	39.9	85	20	80	47	37	26	3	12	2050
	27	41.8	<20	17	73	26	<16	37	4	10	1450
	28	40.6	20	9	52	23	<16	21	5	9	5000
	29	41.1	53	12	67	32	26	17	3	16	11000
	30	30.3	ND	ND	ND	ND	ND	ND	ND	ND	2950
	31	39.3	ND	ND	ND	ND	ND	ND	ND	ND	6700
June**	1	27.0	105	53	182	98	141	73	10	17	5550
	2	37.0	92	133	13	183	480	202	20	28	12800
	3	37.1	132	218	716	277	578	331	24	32	7000
	4	44.1	58	313	1069	853	520	261	41	38	9000
	5	78.5	179	94	525	267	209	244	57	124	31600
	7	27.8	31	17	99	46	53	24	<2	3	900
	8	35.5	58	59	333	129	130	133	15	18	8700
	8	54.3	112	54	266	234	77	123	86	56	9700
	9	81.6	58	145	145	260	260	304	304	185	26100
	10	56.1	<71	63	77	176	71	159	60	63	11400
	11/1	ND	<16	~5	27	33	<16	<5	<2	2	<200
	11/2	ND	298	25	86	58	107	<27	6	11	<200
	11/3	ND	481	32	163	52	193	<31	7	9	<200
	12/1	ND	240	25	110	44	103	<21	12	4	<200
	12/2	ND	277	26	146	61	104	<26	16	6	<200
	12/3	ND	277	22	93	97	125	<23	4	5	<200
	12/4	ND	255	32	133	89	179	<28	17	10	<200
	13/1	ND	270	43	163	76	131	<26	26	28	<200
	13/2	ND	364	38	160	126	68	<25	25	11	<200
	13/3	ND	291	73	236	125	204	<35	23	14	<200
	13/4	ND	314	80	160	70	238	<30	25	20	<200

Table 5 (Con't)

		TSP	Na	Mg	Al	K	Ca	Fe	Zn	Pb	SO_4^{2-}
June (1979)	14/1	ND	223	49	134	56	129	<22	47	8	<200
	14/2	ND	221	37	125	102	173	<22	22	9	<200
	14/3	ND	356	47	113	123	218	<31	20	10	<200
	14/4	ND	465	120	333	244	427	94	16	25	1200
	15/1	ND	255	136	717	231	383	368	33	43	19100
	15/2	ND	281	180	935	345	555	435	60	78	22200
	15/3	ND	395	154	842	352	505	317	44	42	29600
	15/4	ND	903	214	938	424	593	521	37	59	19900
	16/1	ND	365	254	1072	504	772	589	40	70	24400
	16/2	ND	313	320	1625	661	818	800	75	111	18600
	16/3	ND	300	173	720	282	375	322	58	64	4800
	16/4	ND	363	204	907	381	480	361	18	72	24100
	17/1	ND	366	206	911	364	512	411	28	84	29200
	17/2	ND	456	281	940	438	932	393	56	93	26400
	17/3	ND	428	183	657	361	437	203	42	49	31300
	17/4	ND	225	81	417	153	239	136	16	43	34100
	18/1	ND	298	130	709	246	374	281	26	53	32600
	18/2	ND	248	43	261	106	98	76	6	30	4650
	18/3	ND	364	47	239	84	332	23	6	34	<200
	18/4	ND	311	65	357	98	254	82	5	22	<200
	19/1	ND	444	49	232	98	224	37	7	17	<200
	19/2	ND	322	55	244	35	358	<37	7	10	<200
	19/3	ND	409	72	292	90	552	63	16	18	<200
	19/4	ND	337	102	116	227	504	170	13	18	<200
	20/1	ND	406	158	616	188	459	260	5	11	<200
	20/2	ND	355	103	467	241	201	167	17	7	<200
	20/3	ND	340	91	469	194	218	146	16	17	<200
	20/4	ND	230	65	322	165	147	48	7	21	<200
	21/1	ND	244	131	500	213	359	209	22	13	<200
	21/2	ND	371	117	525	230	346	183	79	63	2350
	21/3	ND	369	119	500	236	231	188	45	71	2400
	21/4	ND	290	101	385	188	286	173	43	86	5700
	22/1	ND	540	144	628	243	319	330	64	97	9000
	22/2	ND	505	68	403	389	212	61	19	39	4700
	22/3	ND	286	60	317	169	151	122	7	39	14300
	22/4	ND	253	27	167	129	87	<30	19	30	5800

Table 5 (Con't)

		TSP	Na	Mg	Al	K	Ca	Fe	Zn	Pb	SO_4^{2-}
June	23/1	ND	205	21	148	59	82	<28	6	6	<200
(1979)	23/2	ND	221	23	138	114	149	<27	6	5	<200
	23/3	ND	254	23	190	77	138	<25	15	7	<200
	23/4	ND	<245	<2	1274?	496	203	<29	89	8	<200
	24/1	ND	236	12	113	608	118	<24	4	8	<200
	24/2	ND	131	13	63	55	44	<17	<2	8	<200
	24/3	ND	239	22	170	100	82	<28	6	7	<200
	24/4	ND	169	33	147	51	66	167	5	8	<200
	25/1	ND	219	30	194	98	111	<26	5	28	<200
	25/2	ND	236	35	179	99	62	<24	4	27	<200
	25/3	ND	44	25	179	58	162	67	5	11	300
	26	ND	60	63	283	128	180	196	17	54	860
	27	ND	161	58	357	241	376	268	71	49	1940
	28	ND	64	32	148	93	66	70	16	33	10200
	29	55.3	89	46	157	73	87	107	34	54	16800
	30	47.0	72	197	43	27	<16	14	<2	33	5560
July	1	NS									
	2	33.5	57	19	68	40	27	28	2	14	4060
	3	27.1	74	57	105	33	65	54	<2	9	300
	4	24.0	36	24	52	32	89	19	<2	8	300
	5	NS									
	6	31.4	69	43	120	40	95	50	2	24	900
	7	33.0	67	65	161	75	160	86	2	17	1150
	8	47.8	90	145	309	165	530	206	13	40	5000
	9	57.7	87	114	655	220	389	269	28	48	12700
	10	70.6	142	72	388	152	100	196	54	59	20100
	11	59.5	50	32	133	62	66	94	29	42	23800
	12	63.1	68	80	205	127	156	139	21	41	16300
	13	51.1	83	104	347	182	315	159	37	36	5900
	14	57.5	120	99	471	214	241	228	57	54	16000
	15	41.8	64	40	109	49	47	81	6	33	11100
	16	30.0	90	34	89	48	48	55	4	19	3200
	17	33.7	74	57	119	122	241	102	27	37	3250
	18	29.8	162	94	155	135	315	120	32	19	1750

Table 5 (Con't)

		TSP	Na	Mg	Al	K	Ca	Fe	Zn	Pb	SO_4^{2-}
July (1979)	19	42.2	104	148	438	141	526	202	19	63	6200
	20	63.4	134	137	527	238	472	332	195	64	34500
	21	53.7	160	228	602	312	778	364	239	52	14500
	22	54.8	142	198	629	276	653	375	230	61	18700
	23	67.5	158	246	556	350	944	448	327	67	23000
	24	27.6	ND	ND	ND	ND	ND	ND	ND	ND	9850
	25	70.5	111	76	406	158	207	29	132	52	8520
	26	46.6	119	37	180	67	75	138	<6	32	10000
	27	32.9	36	17	78	35	48	37	<17	15	1450
	28	50.0	47	29	108	67	311	306	61	42	9150
	29	48.8	109	35	172	140	157	128	28	40	7850
	30	58.5	112	64	432	193	173	227	24	61	11900
	31	32.4	64	28	187	73	60	128	<8	32	6500
August	1	41.6	103	43	204	81	104	102	34	39	3550
	2	28.8	28	19	69	55	24	28	<6	23	3800
	3	55.3	49	44	129	86	134	127	10	45	16500
	4	52.1	91	68	162	135	297	172	15	56	2900
	5	38.1	18	20	67	50	88	117	<6	21	1400
	6	28.4	60	23	70	44	110	37	<6	9	600
	7	44.5	48	26	122	66	92	106	7	21	900
	8	32.1	36	33	87	54	121	56	<6	9	1750
	9	39.1	42	45	98	50	92	72	6	12	850
	10	31.7	34	6	20	34	26	10	6	13	300
	11	31.0	59	17	33	88	83	21	3	15	600
	12	30.8	74	112	41	72	43	24	<2	14	300
	13	39.4	74	23	83	104	124	69	2	ND	2050
	14	24.7	74	11	44	111	134	36	3	5	300
	15	26.9	~17	6	21	16	34	9	<2	5	<200
	16	28.3	135	41	62	64	164	<6	<2	9	300
	17	43.4	57	63	185	<7	401	<6	7	ND	5400
	18	31.2	947	<26	ND	<7	<16	31	8	ND	2950
	19	42.4	2147	<2	ND	101	36	34	11	32	8400
	20	48.1	40	10	56	37	49	31	3	23	7600
	21	35.8	63	20	46	82	100	31	3	15	850
	22	41.9	55	31	134	105	138	103	5	67	5950

Table 5 (Con't)

		TSP	Na	Mg	Al	K	Ca	Fe	Zn	Pb	SO_4^{2-}
August (1979)	23	42.3	63	24	86	58	99	65	5	ND	6950
	24	36.8	65	7	22	55	97	10	7	20	7250
	25	25.6	14	~2	11	<7	23	~6	2	2	800
	26	43.8	33	19	50	34	86	36	7	5	8100
	27	40.3	61	30	59	60	168	40	3	24	4200
	28	54.4	35	22	58	49	118	89	23	5	5450
	29	40.4	30	5	28	30	21	21	4	19	3550
	30	39.1	40	18	59	44	66	40	7	14	3300
	31	33.9	30	14	44	30	68	21	2	10	1700
September	1	52.5	80	47	12	118	100	<6	35	2	6050
	2	41.2	52	13	41	27	21	37	7	5	9550
	3	33.7	22	11	37	20	39	16	20	9	3850
	4	26.0	78	32	116	49	84	70	23	20	5700
	5	44.1	210	153	1025	429	173	396	21	37	10100
	6	15.8	65	8	36	78	41	12	7	5	1100
	7	32.5	187	27	61	73	46	37	~2	10	ND
	8	28.8	250	3	123	61	56	41	<2	11	300
	9	33.8	106	31	110	50	75	69	~2	19	1900
	10	32.9	118	11	103	47	27	45	<2	9	2200
	11	30.4	56	5	35	14	<16	14	<2	5	300
	12	38.4	85	35	150	87	100	83	14	18	1900
	13	42.5	148	61	230	96	177	153	21	23	3050
	14	23.4	91	6	67	12	<16	14	2	5	300
	15	26.4	62	4	34	9	<16	11	<2	5	1900
	16	36.5	120	50	103	86	114	98	10	25	4350
	17	44.8	111	65	174	125	89	139	32	23	11900
	18	36.8	175	47	219	62	145	133	10	12	5900
	19	25.3	139	52	179	36	168	70	<2	7	300
	20	42.8	99	95	100	175	345	200	25	44	5750
	21	ND	224	40	206	126	108	125	17	59	ND
	22	31.5	1859	<2	ND	62	53	54	4	13	800
	23	21.6	348	<2	181	30	42	26	~2	9	300
	24	29.1	91	34	147	71	115	96	11	46	1100
	25	30.0	96	59	234	129	159	201	21	48	3850

Table 5 (Con't)

		TSP	Na	Mg	Al	K	Ca	Fe	Zn	Pb	SO_4^{2-}
September	26	45.6	850	6	ND	93	116	115	~2	13	1150
(1979)	27	35.7	122	22	ND	199	324	152	18	25	3000
	28	46.2	521	124	269	178	218	154	53	63	10700
	29	51.0	53	47	210	79	173	137	8	<26	12600
	30	NS									
October	1	54.9	124	51	159	137	62	116	15	<27	13100
	2	39.7	87	69	205	117	91	166	21	51	24800
	3	21.9	34	19	65	45	43	53	7	<21	5350
	4	40.2	90	52	219	123	130	185	27	68	14700
	5	20.2	57	14	62	60	19	37	17	16	1450
	6	22.3	39	26	97	76	98	78	13	<12	3850
	7	16.1	160	27	104	210	83	35	48	8	300
	8	12.9	67	8	88	89	<16	18	17	8	ND
	9	19.3	24	3	20	13	<16	10	<2	8	600
	10	21.0	21	5	25	9	<16	10	7	13	1800
	11	24.2	2015	<2	38	45	<16	39	4	<11	3000
	12	28.2	292	<2	211	18	<16	17	2	17	850
	13	25.5	28	3	16	<7	<16	<7	<2	5	300
	14	22.9	39	3	24	34	<16	<6	2	4	300
	15	23.0	19	2	14	18	16	21	2	2	1650
	16	18.8	413	<2	209	47	<16	10	5	2	2870
	17	29.4	141	13	172	193	100	193	25	71	3000
	18	19.0	36	16	103	81	45	58	6	25	3050
	19	49.1	89	34	175	141	49	135	24	74	1170
	20	45.0	38	15	69	101	<16	44	3	42	8050
	21	41.9	201	51	190	158	57	138	10	22	6850
	22	38.8	409	88	225	183	145	152	22	45	7150
	23	25.4	163	51	172	219	152	121	10	23	3400
	24	16.7	38	11	47	53	107	27	7	10	ND
	25	18.0	97	9	31	66	48	7	11	3	ND
	26	10.5	92	3	112	44	131	32	17	7	ND
	27	12.8	212	<2	137	36	20	9	4	11	300
	28	13.7	774	<2	309	39	30	7	4	15	550
	29	13.2	14	3	15	8	<16	<6	~2	15	800
	30	21.1	31	8	33	23	~18	13	4	2	300
	31	20.5	2519	5	745	74	40	66	6	14	600

Table 5 (Con't)

		TSP	Na	Mg	Al	K	Ca	Fe	Zn	Pb	SO_4^{2-}
November (1979)	1	30.3	1226	<2	323	57	48	86	21	2	3550
	2	26.7	115	<2	113	23	<16	21	7	10	550
	3	25.8	55	12	46	46	35	39	7	33	1150
	4	21.6	26	6	13	15	<16	<6	<2	5	1100
	5	22.9	50	7	75	65	78	44	19	31	1100
	6	29.2	87	74	111	104	138	150	79	70	ND
	7	20.0	52	4	21	38	<16	11	5	28	1900
	8	21.0	157	<2	79	29	~17	41	10	34	4350
	9	43.4	303	251	466	358	583	396	321	168	300
	10	21.0	18	6	29	10	<16	10	9	15	2300
	11	26.1	70	<2	75	42	<16	46	11	31	4900
	12	26.4	346	<2	106	245	41	48	62	32	5500
	13	27.3	229	<2	99	18	46	21	4	15	1400
	14	26.2	1351	<2	504	27	46	9	~2	10	300
	15	26.1	306	<2	195	33	<16	9	~2	11	550
	16	22.8	151	<2	73	57	<16	<8	10	13	ND
	17	24.6	87	4	12	29	<16	10	4	19	600
	18	27.3	54	15	52	54	24	29	4	20	1100
	19	46.8	111	63	315	202	184	205	33	56	7700
	20	45.2	57	9	53	50	<16	49	9	29	1150
	21	44.0	76	26	89	99	~17	56	12	26	600
	22	38.9	357	<2	42	231	<16	18	12	22	1400
	23	39.4	281	86	105	108	80	124	49	45	6200
	24	26.7	77	22	29	24	41	4	16	15	ND
	25	29.3	54	34	75	22	75	22	117	13	ND
	26	22.6	34	10	11	~7	<16	<6	6	2	ND
	27	17.2	53	21	144	92	36	78	18	35	2800
	28	9.7	798	<2	319	32	<16	~7	6	14	850
	29	8.5	142	<2	97	34	<16	25	16	21	600
	30	17.1	<68	<24	100	54	<68	51	16	29	1950
	31										
December	1	14.7	<55	≤18	53	44	<55	40	9	34	2650
	2	11.4	<62	≤22	141	25	<62	35	10	10	250
	3	14.9	<70	≈26	165	93	<58	96	12	30	300
	4	12.9	<60	≤17	120	48	<60	36	<6	10	600
	5	29.8	151	≈45	216	130	43	145	13	32	2950

Table 5 (Con't)

		TSP	Na	Mg	Al	K	Ca	Fe	Zn	Pb	SO_4^{2-}
December (1979)	6	27.2	173	61	281	151	130	50	19	50	2350
	7	23.8	<60	≤71	142	48	<60	43	<7	21	900
	8	23.0	<63	≈30	134	25	<63	25	<6	9	300
	9	19.7	40	≤20	162	79	<50	36	10	10	500
	10	24.8	<54	43	15	87	<65	137	11	35	2300
	11	31.2	146	84	112	170	97	170	22	51	3550
	12	11.2	<58	<9	12	23	<58	~7	<6	12	300
	13	11.3	<51	≤14	25	20	<51	14	<5	15	1050
	14	10.3	<57	≈25		23	<57	48	<6	13	600
	15	18.2	70	19	78	46	13	80	35	38	2150
	16	12.8	71	9	37	37	<16	74	30	13	500
	17	16.3	66	14	110	24	<16	36	24	8	600
	18	3.8	299	55	35	40	23	<6	3	4	300
	19	4.0	58	14	61	38	<16	43	14	26	1700
	20	6.8	44	11	46	37	19	85	10	24	4550
	21	12.1	54	8	32	48	26	23	7	10	1170
	22	19.5	114	21	75	84	29	37	17	32	2950
	23	12.3	44	3	19	17	<16	~7	<2	7	1550
	24	18.2	59	6	304	51	<16	~9	8	10	600
	25	16.7	41	31	187	78	36	61	5	15	300
	26	17.3	37	4	26	12	<16	<6	~2	10	300
	27	13.9	39	8	113	36	22	11	15	28	300
	28	10.5	65	10	97	54	<61	5	14	5	<200
	29	10.5	65	6	74	31	<16	<6	9	9	<200
	30	9.6	48	9	67	37	<16	<6	6	36	<200
	31	≈3.3	40	<2	2	<7	428?	<6	<7	<1	<200

TSP - Total suspended particulates.

NS - No sample (see text).

ND - Not determined.

* - Na, Mg, K, Ca and Zn measured under non-optimal conditions for samples of January and February.

** - June 11: 3 samples, 1100h-1200h, 1200h-1800h, 1800-00h. June 12-24: 6-h sampling, 00h-600h, 600h-1200h, 1200h-1800h and 1800h-00h. June 25: 3 samples, 00h-600h, 600h-1200h and 1200h (6/25)-800h (6/26).

Table 6. Monthly Averages for TSP, Na, Mg, Al, K, Ca, Fe, Zn, Pb and SO_4^{2-} in air particulates Collected in 1979 at Whiteface Mountain, New York

		concentration (ng/m^3)											
	Month (n) (nEp)	J (22) (1)	F (28) (3)	M (25) (8)	A (27) (5)	M (29) (13)	J (30) (18)	J (28) (19)	A (27) (9)	S (23) (3)	O (31) (7)	N (29) (3)	D (29) (1)
TSP (x10^3)	Mean	20	16	22	17	31	48*	47	38	34	25	27	16
	SE	±2	±2	±4	±2	±3	±5	±3	±2	±2	±2	±2	±1
	Range	7-39	5-35	1-68	4-46	4-68	27-82	24-71	25-55	16-53	11-55	9-47	4-31
Na	Mean	<77	≤134	120	77	66	259	92	260	221	266	232	75
	SE	±5	±16	±16	±8	±12	±17	±7	±124	±65	±99	±61	±10
	Range	<53-140	<39-335	29-468	19-202	<18-210	<16-903	36-162	17-2147	22-1859	14-2015	26-1351	37-299
Mg	Mean	--	--	25	44	40	87	80	28	40	21	26	23
	SE	--	--	±4	±10	±6	±9	±12	±4	±7	±4	±9	±4
	Range			<2-106	<2-289	<2-143	<2-320	17-246	<2-112	<2-153	<2-88	<2-251	<2-84
Al	Mean	81	65	62	183	156	377	270	74	154	132	116	98
	SE	±16	±8	±11	±28	±27	±40	±36	±9	±37	±25	±23	±14
	Range	15-293	16-95	19-282	43-442	12-629	13-1625	52-655	11-204	12-1025	14-745	11-504	2-304
K	Mean	≤32	≤23	46	90	97	191	129	59	90	80	73	53
	SE	±6	±2	±6	±16	±21	±19	±17	±6	±15	±11	±15	±7
	Range	<12-112	<10-51	<7-134	16-417	<7-568	27-853	32-350	<7-135	9-429	<7-219	7-358	<7-170
Ca	Mean	--	≤117	120	183	136	256	251	102	111	50	56	52
	SE	--	±16	±13	±34	±30	±23	±44	±14	±16	±8	±19	±13
	Range		<80-387	<16-351	<16-725	<16-752	<16-932	27-944	<16-401	<16-345	<16-152	<16-583	<16-428
Fe	Mean	≤24	<20	25	76	80	218	159	50	96	59	55	45
	SE	±5	±3	±7	±15	±14	±24	±22	±7	±15	±11	±14	±8
	Range	<6-105	<7-75	<5-195	<5-353	<4-303	<5-800	19-448	<6-172	<6-396	<6-185	<6-396	<6-170
Zn	Mean	<14	<11	8	25	8	30	54	7	13	12	27	11
	SE	±1	±1	±1	±5	±1	±5	±16	±1	±2	±2	±11	±11
	Range	<8-18	<5-41	<2-19	4-95	<2-76	<2-304	<2-327	<2-34	<2-53	<2-48	<2-321	<2-35
Pb	Mean	<11	≤15	26	24	24	34	37	17	21	20	24	18
	SE	±3	±2	±4	±5	±6	±4	±3	±3	±3	±4	±4	±2
	Range	<3-53	<2-37	4-67	3-136	4-93	2-185	8-67	2-67	2-63	2-74	2-168	<1-51
SO_4^{2-}	Mean	1000	1600	3200	3400	4300	8300	10000	3100	3900	1900	1900	1200
	SE	±220	±500	±550	±800	±800	±1700	±1600	±700	±800	±380	±380	±220
	Range	<200-5700	<200-7300	350-9700	<200-19200	300-16200	<200-34000	300-34500	<200-16500	300-12600	300-24800	300-7700	<200-4550

*Mean of 12 determinations

SE - Standard error of the mean = $\frac{\sigma}{\sqrt{n}}$, where σ is the standard deviation and n is the number of samples analyzed

nEp is the number of episodic cases with SO_4^{2-} concentrations $\geq$ 5000 ng/m^3

Table 7. Seasonal Variation in TSP, Elemental and SO_4^{2-} Concentration Levels in Aerosols at Whiteface Mountain, New York

Elements		Concentration (ng/m^3) Dec.-Feb.	Mar.-May	June-Aug.	Sep.-Nov.	Annual Mean
TSP ($x10^3$)		17	23	44	29	28
	R	0.61	0.82	1.57	1.04	
Mean Na		95	88	204	240	157
	R	0.61	0.56	1.30	1.53	
Mean Mg		48	36	65	29	45
	R	1.07	0.82	1.46	0.65	
Mean Al		81	134	240	134	147
	R	0.55	1.10	1.61	0.91	
Mean K		36	78	126	81	80
	R	0.45	0.97	1.57	1.01	
Mean Ca		83	146	203	72	126
	R	0.66	1.16	1.61	0.57	
Mean Fe		30	60	142	70	76
	R	0.39	0.80	1.88	0.93	
Mean Zn		12	14	30	17	18
	R	0.65	0.75	1.65	0.95	
Mean Pb		15	25	29	22	23
	R	0.65	1.09	1.30	0.96	
Mean SO_4^{2-}		1250	3600	7150	3150	3800
	R	0.33	0.95	1.88	0.83	

R = Ratio of quarterly concentrations to annual average concentrations in aerosols.

Table 8. Comparison of Background Concentration of Trace Elements in Aerosols at Whiteface Mountain with Reported Values

Element	Background Concentration (ng/m^3)					
	WMFS	Lerwick† U.K.	N.W.† Canada	Norway†	Empirical@	MPR†† (ng/m^3)
Mg	9	—	—	—	∿20	2-16
Al	42	56	70	46	——	30-60
K	37	—	—	—	∿50	20-60
Ca	41	—	—	—	∿40	20-60
Sc	0.025*	0.013	0.05	0.008	∿ 0.02	——
Cr	1.1*	1.2	0.62	0.65	∿ 0.6	——
Mn	7*	3.0	1.6	2.7	∿ 1.3	——
Fe	22	59	75	55	∿25	10-40
Zn	7	33	4.0	9.5	∿ 5	2-10
As	2.6*	1.4	0.33	2.0	∿ 0.3	——
Se	0.5*	0.36	0.05	0.27	∿ 0.04	——
Br	17*	18	0.6	4.9	∿ 0.6	——
Cs	0.024*	0.04	—	0.02	∿ 0.03	——
Pb	8	30	—	—	∿ 0.2	4-12

* Mean of 2 observations (July 5, 1975 and July 27, 1977).

†† Most probable range for trace element concentration in background aerosols at WMFS.

† From Cawse (1974)

@ From Rahn (1976)

APPENDIX I

DETERMINATION OF STRATOSPHERIC OZONE AT GROUND LEVEL USING ^{7}BE/OZONE RATIOS

Vincent A. Dutkiewicz and Liaquat Husain

New York State Department of Health, Division of Laboratories and Research

Empire State Plaza, Albany, New York 12201

Abstract. The ^{7}Be and O_3 concentrations were measured and the ^{7}Be/O_3 ratios calculated for air particulates collected on several flights of two specially equipped commercial B747 jetliners between altitudes of 10 and 12 km and latitudes of 21° to 55° N. Upper tropospheric ^{7}Be concentrations averaged about 520 pCi/10^3m^3, whereas the stratospheric average was about 4,700 pCi/10^3m^3. The ^{7}Be/O_3 ratio at 35° – 42° N was determined to be 10.78 pCi/10^3m^3/ppbv for April–June 1978. Concentrations of ^{7}Be and O_3 were also measured daily during June and July 1977 at Whiteface Mountain, New York. Daily variations in ^{7}Be data indicated the arrival of a stratospheric air mass on June 15–16. Comparison of ^{7}Be concentrations show approximately a tenfold dilution of the stratospheric air during tropospheric descent. The ^{7}Be/O_3 ratio on June 15–16 was 9.8 pCi/10^3m^3/ppbv within experimental error of the stratospheric value. This suggests that at least at times, stratospheric air, although diluted, reaches ground level without significant relative fractionation of ^{7}Be and O_3. Assuming this to be true on days when ^{7}Be concentration is > 200 pCi/10^3m^3 (or ≥ 5% of the stratospheric value), we have determined the stratospheric ozone concentration at Whiteface Mountain to vary between 19 and 47 ppbv for summer months. Thus at a remote location such as Whiteface Mountain both stratospheric and the tropospheric sources play an important role.

Introduction

The bulk of the earth's ozone is produced in the stratosphere, where it plays an important role shielding the earth's surface from solar untraviolet radiation. The stratosphere is characterized by a temperature increase with altitude, making it vertically stable compared to the troposphere below. The lower limit of the stratosphere is the tropopause, which varies in altitude from 8–10 km at the poles to approximately 16–20 km at the equator. The height of the tropopause is seasonal and variable, responding to the annual cycle of mean tropospheric temperature. Generally the temperature gradient between the stratosphere and the troposphere is considered sufficient to isolate the two regions, so that large-scale exchange through mixing is assumed to be negligibly small. Intermittent transfer of stratospheric ozone to the troposphere occurs during tropopause folding events (Danielsen, 1968). The descending stratospheric air could significantly add to the ground-level ozone concentrations. The time from intrusion through tropopause to the arrival at the ground level, as well as dilution through mixing during transport, varies from event to event. Therefore for ground-level stratospheric studies it is essential to determine concentrations of at least two conservative tracers.

Several studies (Husain et al., 1977; Ludwick et al., 1976; Reiter et al, 1976) have demonstrated the viability of using ^{7}Be ($t_{1/2}$ = 53.28 days) as a natural radioactive tracer to identify upper atmospheric air at ground level. Elevated ozone concentrations are observed to correlate with periods of high ^{7}Be activity. Although correlations between ^{7}Be and O_3 identify the presence of stratospheric air, such data are not sufficient to quantify the stratospheric contributions, as ozone is also produced at ground level. To accurately determine the stratospheric contributions from ^{7}Be and O_3 studies it is essential to know (1) the ^{7}Be/O_3 concentration ratios in the stratosphere and (2) the behavior of ^{7}Be aerosol and O_3 during the descent through the troposphere. Until now neither (1) nor (2) was accurately known. We are now able to present the first direct measurements of ^{7}Be/O_3 ratios in the stratosphere and upper troposphere.

Sampling and Analysis

The ^{7}Be concentrations were determined in air particulate samples collected between 10 and 12 km altitude on two commercial B747 jetliners by NASA's Global Atmospheric Sampling Program (GASP). The sampling equipment and procedures have been discussed elsewhere (Perkins and Gustafsson, 1976), so only certain highlights are presented here.

Outside air is drawn through the filter via a tube connected near the nose of the aircraft. Eight IPC 1478 filters are automatically positioned for sequential sampling at preprogrammed intervals. Each filter is exposed for about two hours, corresponding to a sampling distance of approximately 1100 miles and the filtering of approximately 150 kg of air. At least one filter from each eight-filter set is left unexposed as a blank. To insure that the sampling system is not contaminated by ground-level air, the inlet probe is capped when the plane descends below 6.1 km. Aircraft location and altitude during sampling are recorded from the aircraft's navigational instruments.

After exposure, the filters are placed in ultraclean polyethylene bags. The whole filter is analyzed γ-spectrometrically on a 7.5 x 7.5–cm NaI(Tl) detector connected to a 256-channel pulse-height analyzer and/or on a 45-cc Ge(Li) detector connected to a 8192-channel pulse-height analyzer. Absolute ^{7}Be activity level is determined by comparing the intensity of 478-keV γ-ray in the sample with that of a ^{7}Be standard counted under the same geometry. Uncertainty in the ^{7}Be activity determined by either of the two counting methods averages about ±15%.

Ozone was measured in situ using a continuous UV absorption photometer (Bowman and Horak, 1972; Reck et al., 1974). The errors in

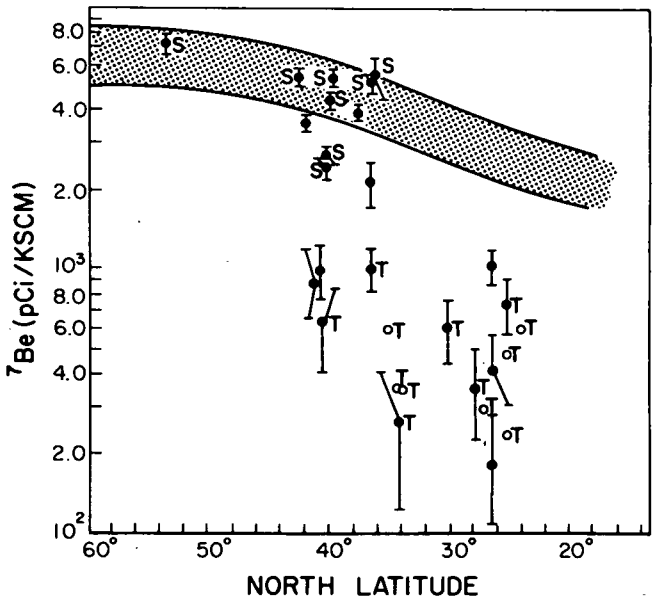

Figure 1. ^{7}Be concentrations at 10 to 12 km altitude versus average latitude. Uncertainities are shown as vertical bars; open circles correspond to upper-limit measurements. The designations S and T indicate stratospheric and tropospheric samples respectively, as explained in the text. The shaded curve is the theoretical ^{7}Be saturation activity for a stable atmosphere at 10- to 12 km altitude (Lal and Peters, 1967).

Paper number 9L0232.
0094-8276/79/039L-0232$01.00

TABLE 1. Measured Concentrations of O_3 and ^7Be and $^7Be/O_3$ Ratios in the Stratosphere and the Troposphere

Sampling Date (1978)		Latitude (°N)	O_3 (ppbv)	^7Be (pCi/KSCM)	$^7Be/O_3$ (pCi/KSCM /ppbv)
Stratosphere					
Jan.	9	36.8 – 35.0	368	5,330	14.48 ± 3.55
	9	51.6 – 55.1	276	7,280	26.38 ± 3.55
Feb.	17	41.8 – 42.7	384[a]	5,410	14.09 ± 3.55
April	18	41.0 – 38.3	526	5,290	10.06 ± 0.95
	23	38.3 – 42.0	236	2,330	9.87 ± 1.18
May	24	38.4 – 42.0	341	4,330	12.70 ± 0.83
	27	38.5 – 42.1	277	2,610	9.42 ± 0.71
June	17	37.9 – 35.0	432	5,020	11.62 ± 1.18
Average April–June					10.78
Troposphere					
Jan.	6	37.0 – 33.5	59	$\leq$590	$\leq$10.0
March	7	36.8 – 31.9	29	$\leq$360	$\leq$12.4
	10	37.0 – 34.6	29[a]	983	33.9 ± 11.8
	12	23.9 – 27.0	35[a]	$\leq$470	$\leq$13.4
	16	22.0 – 28.7	71	710	10.0 ± 3.5
	20	25.3 – 21.9	97[a]	$\leq$590	$\leq$ 6.1
April	22	37.0 – 31.2	61	$\leq$360	$\leq$ 5.9
	25	22.6 – 30.6	91	180	2.0 ± 1.2
	28	36.9 – 32.0	79	260	3.3 ± 2.0
May	18	36.0 – 25.0	32	580	18.1 ± 5.9
	30	23.0 – 31.0	63	340	5.4 ± 2.1
June	8	21.8 – 29.1	43	$\leq$240	$\leq$ 5.6
	11	40.0 – 41.0	70	628	9.0 ± 3.6
	17	22.2 – 32.3	82	$\leq$300	$\leq$ 3.6
Mixed Stratosphere + Troposphere					
Jan.	15	42.1 – 41.2	189[a]	3,670	19.42 ± 4.73
	21	34.8 – 40.1	157[a]	3,990	25.42 ± 5.92
	24	23.0 – 31.4	135	990	7.4 ± 1.4
April	29	34.1 – 38.4	142	2,050	14.43 ± 3.55
May	18	21.2 – 28.2	104	403	3.9 ± 1.6
June	14	41.1 – 41.2	130	860	5.4 ± 1.8
	20	40.5 – 41.0	140	970	6.9 ± 2.4

[a]Ozone concentrations estimated using ozone measured in the B747 jetliner's passenger cabin. Ozone destruction within the passenger cabin and during compression has been corrected. (Leżberg et al., 1977). Uncertainty, ± 20%.

ozone measurements are estimated to be approximately ± 5%. The data presented here cover flights from January through June 1978 and the latitude range from 21° to 55° N. Most samples were collected in the Western Hemisphere between 40° and 160° W, although several Eastern Hemisphere samples have also been analyzed. The ozone value used here is the average value measured during the particulate sampling. Concentrations are corrected to standard temperature and pressure (25° C, 760 mm Hg).

Results and Discussions

The measured ^7Be concentrations are shown in Fig. 1 as a function of latitude. Our ^7Be measurements, at 11-12 km, are in reasonable agreement with those obtained by Feely et al. (1971) at 12.2 km. From the monthly mean 1975–1976 tropopause heights (Falconer, 1978), samples collected below 30° latitude are expected to be purely tropospheric, while those between 43° and 30° may be stratospheric, tropospheric, or mixed. The sampling height relative to the tropopause is not known, but a reasonable designation of stratospheric and tropospheric air can be made from the average ozone concentrations. On the basis of GASP observations (Nastrom, 1977 and 1978), where the mean tropopause altitude has been independently determined, we have assigned samples with observed ozone $\geq$ 230 ppbv as stratospheric (S), those with ozone concentrations < 100 ppbv as tropospheric (T), and those with ozone concentrations between 100 and 229 ppbv as mixed stratospheric and tropospheric.

^7Be is naturally produced in the upper atmosphere by the interactions of cosmic ray protons and neutrons with oxygen and nitrogen. Atmospheric production rates computed by Lal and Peters (1967) indicate that the average stratospheric production rate of ^7Be is twice that of the troposphere. Because stratospheric aerosols, to which ^7Be becomes attached, remain suspended much longer than do those in the troposphere, the average specific activity ratio between stratospheric and tropospheric ^7Be has been estimated to be 28:1 (Lal and Suess, 1968).

Assuming secular equilibrium between ^7Be production and radioactive decay, the expected saturation activity at 10-12 km is shown as the shaded curve in Fig. 1 (interpolated from Lal and Peters, 1967). The data designated as stratospheric in this figure are in excellent agreement with the theoretical saturation concentrations, supporting the assumed designations. As expected, the data designated as tropospheric lie considerably below the saturation concentrations. Due to vertical mixing and scavenging processes in the troposphere, aerosol lifetimes are expected

to be rather short (see Fig. 21 in Reiter, 1975), so that equilibrium concentrations are not likely to be reached.

Table 1 gives the O_3 and ^7Be concentrations and $^7Be/O_3$ ratios for samples collected between January and June 1978. The samples have been classified as stratospheric, tropospheric, or mixed, as discussed above. The stratospheric ^7Be concentrations ranged between 2,330 and 7,280 pCi/KSCM with an average of 4,700 pCi/KSCM (KSCM = 1,000 m^3 air). Tropospheric ^7Be concentrations are much smaller, as would be expected, the average being 520 pCi/KSCM (excluding upper-limit measurements).

The $^7Be/O_3$ ratios are also listed in Table 1. Because of seasonal changes in stratospheric circulation patterns (e.g., Reiter, 1975), seasonal as well as latitudinal variations in ^7Be and O_3 concentrations and hence in $^7Be/O_3$ ratios are possible. However, data given in Table 1 are insufficient by themselves for any conclusions regarding seasonal variations. The stratospheric data between April and June at ~40° N appear to be constant within experimental uncertainties, with an average value of 10.78 ± 1.42 pCi/KSCM/ppbv. Uncertainties given for average values represent 1 standard deviation. The data for January-February at ~40° are slightly higher, with an average value of 17.8 ± 5.9 pCi/KSCM/ppbv. The tropospheric $^7Be/O_3$ ratios are highly variable, reflecting the vertical mixing and scavenging processes so prevalent in the troposphere.

We will now consider applying the stratospheric $^7Be/O_3$ ratios to ground-level measurements. In Fig. 2 we show daily ^7Be and O_3 concentrations determined at Whiteface Mountain from June 15 to July 14, 1977. Peak ^7Be concentrations were observed on June 15–16, 24–25, and 28 and July 1 and 3. Comparison of peak ^7Be concentrations with those measured in the upper troposphere at 10–12 km (Table 1) shows that ground-level concentrations are as high as, or even higher than, those observed in the upper troposphere. Ground-level peak ^7Be concentrations are approximately 5–10% of the stratospheric values. Therefore peak ^7Be concentrations cannot be attributed to transport from the upper troposphere. The dilution of the upper tropospheric air during descent to ground level would yield ^7Be values comparable to the observed background concentrations, which are much smaller than peak ^7Be concentrations (Fig. 2).

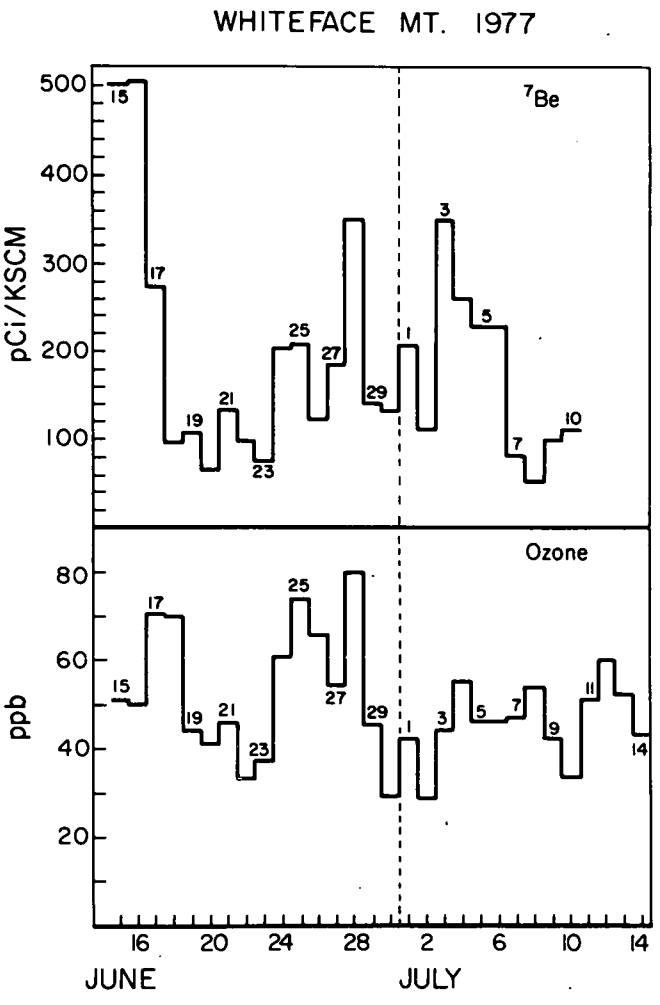

Figure 2. Daily ^7Be and 24-hr average ozone concentrations for June and July 1977 at the 1.5-km summit of Whiteface Mountain, New York. Stars represent lower-limit estimates. Selected days are shown in the figure to aid in intercomparisons. KSCM = kilo standard cubic meter (25°C, 760 mm Hg).

TABLE 2. Calculated Stratospheric Ozone during June and July 1977 at Whiteface Mountain, New York

Date (1977)		24-Hour Average Ozone (ppbv)	
		Total	Stratospheric[a]
June	15	51	46
	16	50	47
	17	71	25
	24	61	19
	25	74	19
	28	80	33
July	1	42	19
	3	44	32
	4	55	24
	5	46	21
	6	46	19

[a]Using $^7Be/O_3$ = 10.78 pCi/KSCM/ppbv; see text.

Since there are no ground-based ^7Be sources, the "peak" ^7Be must originate in the stratosphere. The observed relationship between ^7Be and potential vorticities support this hypothesis (Husain et al., 1977). The ^7Be peaks are accompanied by increase in ozone concentrations. Both ^7Be and ozone peak on June 24–25 and 28 and July 1. The ^7Be peaks of June 15–16 and July 3 are also accompanied by high ozone, but ozone concentrations peaked a day later. This 1-day delay has been observed before and explained by increased tropospheric contributions (Husain et al., 1977).

The stratospheric $^7Be/O_3$ ratios combined with the ground-level ^7Be can yield the ground-level ozone of stratospheric origin, assuming $^7Be/O_3$ ratios remain constant during transport. There is evidence that in cases of stratospheric intrusion the transport from stratosphere to troposphere is rapid (Reiter et al., 1975). The $^7Be/O_3$ ratio measured at Whiteface Mountain on June 15 and 16 is 9.8 pCi/KSCM/ppbv, almost identical to the stratospheric measurements for April–June. Thus, at least at times, the $^7Be/O_3$ ratio remains unchanged during the descent through the troposphere. Application of the $^7Be/O_3$ ratios to determine the ozone of stratospheric origin on days when peak ^7Be concentration is observed appears to be justified.

The calculated stratospheric ozone contributions given in Table 2 vary from 19 to 47 ppbv. These are 24-hour averages, and substantially higher contributions for a given hour are possible. The stratospheric ozone contributions range between 25 and 95% of the total ozone. Thus at a remote location such as Whiteface Mountain both tropospheric and stratospheric ozone sources play important roles. Neither the photochemical theory (Crutzen, 1973; Chameides and Walker, 1973, 1976; Fishman and Crutzen, 1978) nor models coupling photochemistry with transport (Chameides and Stedman, 1977) nor the stratospheric sources alone (Fabian, 1974; Fabian and Pruchniewicz, 1977) can explain our observations in entirety.

Acknowledgments. The authors are grateful to NASA Lewis Research Center and Porter Perkins, Jr., Erwin Lezberg, and Francis Humenik for their excellent cooperation in supplying the filters and the ozone data. Discussions with John M. Matuszek are gratefully acknowledged. The Whiteface Mountain Observatory is operated by the Atmospheric Sciences

Research Center of the State University of New York. Ozone measurements at Whiteface Mountain were carried out by the surveillance network of the Division of Air Resources, New York State Department of Environmental Conservation. B. Lance was largely responsible for γ-spectral analyses. This work was partially supported by U.S. Department of Energy Contract No. EE-77-S-02-4501.

References

Bowman, L.D. and R. F. Horak, Continuous Ultra-Violet Absorption Ozone Photometer, Anal. Instru., 10, 103–108, 1972.

Chameides, W. L. and D. H. Stedman, Tropospheric Ozone: Coupling Transport and Photochemistry, J. Geophys. Res., 82, 1787–1794, 1977.

Chameides, W. and J. C. G. Walker, A Photochemical Theory of Tropospheric Ozone, J. Geophys. Res., 78, 8751–8760, 1973.

Chameides, W. and J. C. G. Walker, A Time Dependent Photochemical Model for Ozone Near the Ground, J. Geophys. Res., 81, 413–420, 1976.

Crutzen, P.J., A Discussion of the Chemistry of Some Minor Constituents in the Stratosphere and Troposphere, Rep. AP–12, Institute of Meteorology, University of Stockholm, Stockholm, 1973.

Danielsen, E.F., Stratospheric-tropospheric Exchange Based on Radioactivity, Ozone and Potential Vorticity, J. Atmos. Sci., 25, 502–518, 1968.

Fabian, P., Comment on a Photochemical Theory of Tropospheric Ozone by Chameides, J. Geophys. Res., 79, 4124–4125, 1974.

Fabian, P. and P. G. Pruchniewicz, Meridional Distribution of Ozone in the Troposphere and Its Seasonal Variation, J. Geophys. Res., 82, 2063–2073, 1977.

Falconer, P. D., Global Atmospheric Sampling Program: Prospects for Establishing a Tropospheric Ozone Budget from Commercial Aircraft Data, in Air Quality Meteorology and Atmospheric Ozone, (ed. A. L. Morris and R. C. Barras), ASTM, Philadelphia, PA, pp 479–490, 1978.

Feely, H., J. P. Friend, H. Seitz, J. D. Martin and W. E. Erlebach, Final Report of Project Stardust, DASA-2166-3, Isotopes, Inc., 1971.

Fishman, J. and P. Crutzen, The Origin of Ozone in the Troposphere, Nature, 274, 855–858, 1978.

Husain, L., P. E. Coffey, R. E. Meyers and R. T. Cederwall, Ozone Transport from Stratosphere to Troposphere, Geophys. Res. Lett., 4, 363–365, 1977.

Lal, D. and B. Peters, Cosmic Ray Produced Radioactivity on Earth, in Handbuch der Physik, 46, (ed. K. Sitte), Springer Verlag, Heidelberg, 551–612, 1967.

Lal, D. and H. E. Suess, The Radioactivity of the Atmosphere and Hydrosphere, Ann. Rev. Nuclear Sci., 18, 407–434, 1968.

Lezberg, E. A., P. J. Perkins, D. R. Englund, D. J. Gauntner and J. D. Holdeman, Global Atmospheric Sampling Program, Aircraft Engine Emissions, NASA Conf. Publ. 2021, 323–355, 1977.

Ludwick, J. D., T. D. Fox and L. L. Wendall, Ozone and Radionuclide Correlations in Air of Marine Trajectories at Quillayute, Washington, J. Air Poll. Contr. Assoc., 26, 565–569, 1976.

Nastrom, G. D., Variability and Transport of Ozone at the Tropopause from the First Year of GASP Data, National Aeronautics and Space Administration Technical Report, NASA-CR-135176, 1977.

Nastrom, G. D., Variability of Ozone Near the Tropopause from GASP Data, National Aeronautics and Space Administration Technical Report, NASA-CR-135405, 1978.

Perkins, P. J. and U. R. C. Gustafsson, An Automated Atmospheric Sampling System Operating on 747 Airliners, in Int. Conf. on Env. Sensing and Assessment, 2, IEEE Session No. 26-4, 1–10, 1976.

Reck, G. M., D. Briehl and P. J. Perkins, Flight Test of a Pressurization System Used to Measure Minor Atmospheric Constituents from an Aircraft, NASA-TN-D-7576, 1974.

Reiter, E. R., Stratospheric-Tropospheric Exchange Processes, Rev. Geophys. Space Phys., 13, 459–474, 1975.

Reiter, E. R., W. Carnuth, H. -J. Kanter, K. Potzl, R. Reiter and R. Sladkovic, Measurements of Stratospheric Residence Times, Arch. Met. Geoph. Biokl., Ser. A, 24, 41–51, 1975.

Reiter, R., H. -J. Kanter, R. Sladkovic and K. Potzl, Measurements of Airborne Radioactivity and Its Meterological Application Part V, USERDA Document No. NYO-3425-12, 1976.

(Received October 16, 1978;
revised January 26, 1979;
accepted February 2, 1979.)

APPENDIX II

Long-Range Transport of Trace Elements

LIAQUAT HUSAIN

Division of Laboratories and Research, New York State Department of Health, Albany, New York 12201

PERRY J. SAMSON

Division of Air Resources, New York State Department of Environmental Conservation, Albany, New York 12233

Concentrations of 13 trace elements and total suspended particulates were measured for 24 consecutive days in July 1975 at Whiteface Mountain, a remote site in the Adirondack Mountains of New York. High episodic concentrations were observed during a five-day period, July 16 through 20. Air trajectory calculations showed that stagnant air masses originating southwest of Whiteface Mountain were the primary sources of these high concentrations. During July 1976 the sampling network was extended to four stations separated by hundreds of kilometers in New York State plus a site in New Jersey. Air trajectory calculations for July 19 and 20, when peak concentrations of particulates and trace metals were observed at all five stations, strongly suggest that the particulates and trace metals were transported from sources southwest of New York State.

Evidence exists of long-range transport of pollutants, including total suspended particulates (TSP), to distances as far as 2,000 km [*Elliot et al.*, 1974]. *Prospero* [1977] showed that the dust particles can be transported for several days before being removed from the air. This long-range transport of TSP may enhance the concentrations of TSP and associated trace metals, including toxic ones, in otherwise remote areas. Measurements at Whiteface Mountain, a rural site in the Adirondack Mountains in upstate New York, have shown high ozone [*Coffey and Stasiuk*, 1975; *Husain et al.*, 1977] and sulfate [*Galvin et al.*, 1978] levels comparable to those at many urban centers.

To investigate the possibility of long-range transport of TSP and trace metals into New York State from the industrial Midwest we have used a new approach. In this work we have collected daily samples for up to 24 consecutive days and from as many as five locations separated by hundreds of kilometers. Elemental concentrations were determined by instrumental neutron-activation analysis. To identify the regions through which the air had passed before reaching the sampling site, we analyzed air trajectories using the model developed by *Heffter et al.* [1975]. Episodic high elemental concentrations and air trajectories were then compared to deduce information regarding the transport of TSP and trace elements.

Air particulates were collected on July 1–24, 1975, at the Atmospheric Sciences Research Center's Observatory at the summit of Whiteface Mountain, New York, approximately 1.5 km above sea level. This location is approximately 450 km northeast of Buffalo, New York, and 450 km north of New York City. The nearest urban center is Syracuse, about 250 km to the southeast.

During July 1976 particulate samples were also collected at Albany, Schoharie, and Holland, all in New York State, and at High Point, New Jersey. The Albany sampling site was located 75 m above ground in an office tower at the State University of New York at Albany. Schoharie is northeast of the Catskill Mountains on a relatively isolated agricultural region. Holland is downwind about 60 km southeast from Buffalo. High Point is in the Kittatinny Mountains of northwest New Jersey about 500 m above sea level.

Particulates were collected with four high-volume samplers, operated sequentially for 24-hour periods. The particulates were collected on preweighed 25 × 20-cm Whatman 41 filter paper. Approximately 2000 m³ of air was filtered during each 24-hour collection. The collected samples were stored in a

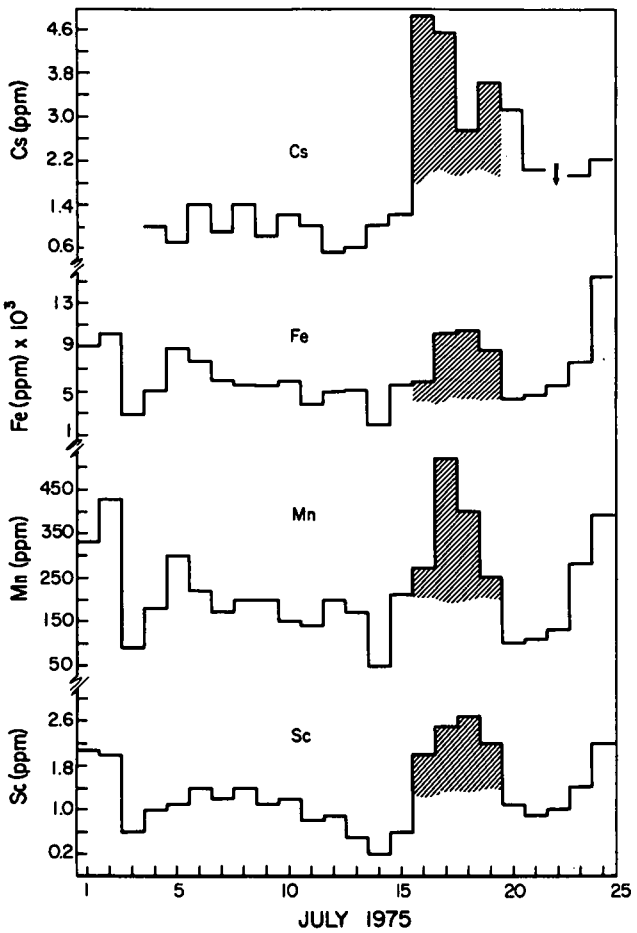

Fig. 1. Concentrations of four trace metals at Whiteface Mountain, New York, in July 1975. Shading designates the episode of peak concentrations (July 16–19). An arrow indicates elemental concentration is below the detection limit.

Paper number 8C1158.
0148-0227/79/008C-1158$01.00

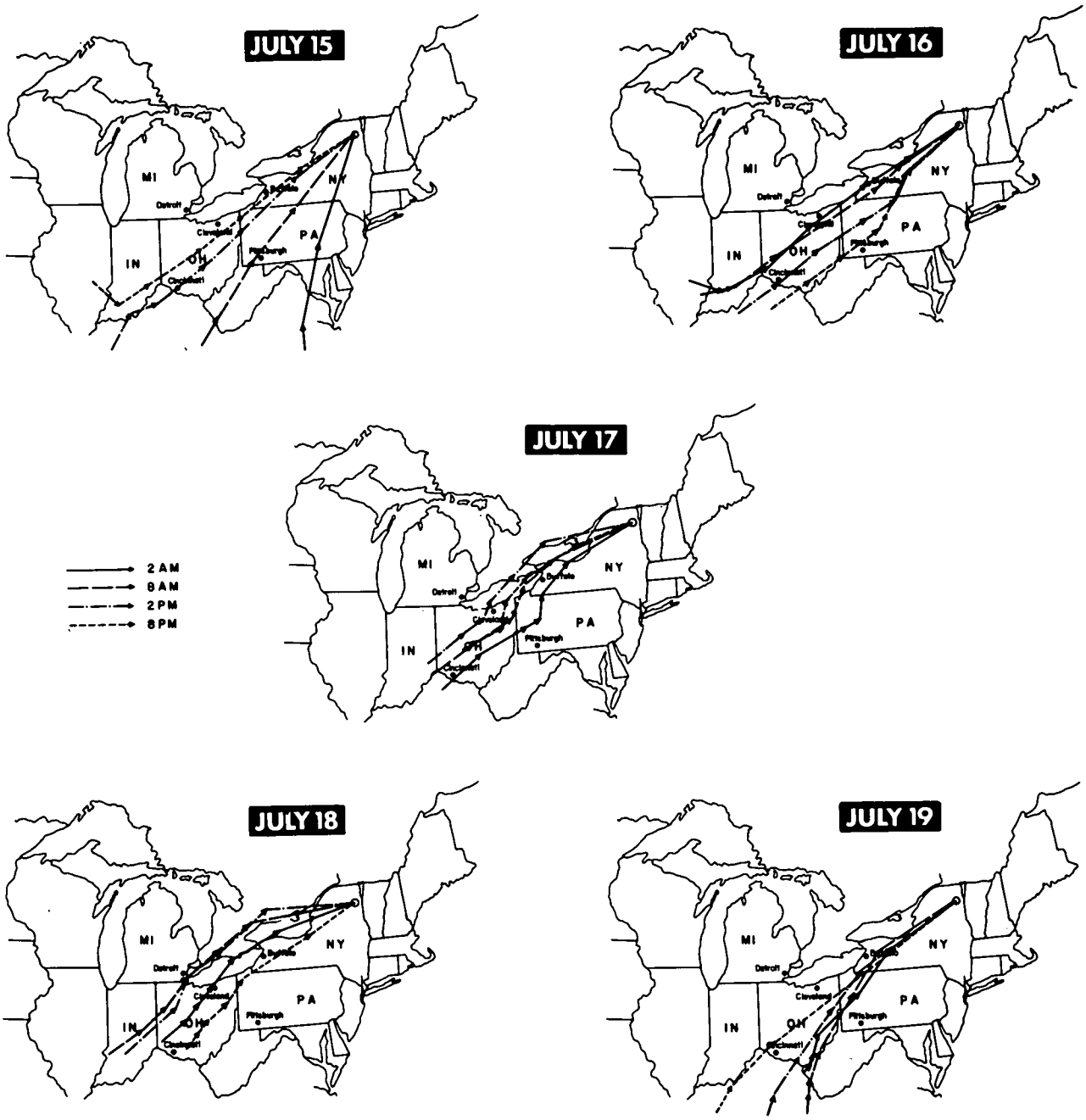

Fig. 2. Trajectories of air masses reaching Whiteface Mountain on July 15–19, 1975. Each arrow indicates a 12-hour movement of the air mass.

humidity- and temperature-controlled room (50% relative humidity, 21°C) before weighing. Trace element concentrations were measured by instrumental neutron-activation analysis. Details of the procedure will be published elsewhere.

Daily concentrations of Sc, Mn, Fe, and Cs are shown in Figure 1. A striking feature of these data are the high concentrations observed on July 16 through 19. Three other elements—Zn, As, and Se—and TSP also showed peak concentrations during this period. (For brevity the data are not given in Figure 1.) However, Br, Sb and Hg did not peak at this time.

The sources of these high episodic concentrations are not obvious, but an insight may be obtained by comparing the elemental data with measurements of sulfates at Whiteface Mountain during July 1–24, 1975 [*Lioy et al.*, 1977]. The variations of daily sulfate concentrations are quite similar to those of Sc, peaking on July 16–19. (For the six days July 14–19 the sulfate values were 1.1, 5.5, 7.0, 23.2, 23.4 and 4.4 μg SO_4/m^3 air, respectively.)

The primary source of atmospheric sulfate (combustion of fossil fuels) occurs infrequently in the vicinity of Whiteface Mountain. *Galvin et al.* [1978] have shown that the high sulfate levels there result from air-mass transport from the west and southwest. It appears reasonable to assume that sulfate and trace elements, which have simultaneous high concentrations, have also the same origin i.e., in air-mass transport.

To identify the areas from which the air masses containing high concentrations of metals, TSP, and sulfates originated, trajectories for July 15–19 were computed for each day during the study period (Figure 2), using the technique developed by

TABLE 1. Estimated 12-Hour Average Wind Speeds (m/s) Along Trajectories of Air Arriving at Whiteface Mountain, New York, on July 15–20, 1975

Date (1975)	Hours Prior to Arrival at Whiteface Mountain					
	60–72	48–60	36–48	24–36	12–24	0–12
July 15	16.5	16.7	22.9	28.4	27.7	32.2
July 16	18.2	20.1	22.0	17.8	15.8	24.8
July 17	18.4	12.4	7.0	11.2	18.7	28.5
July 18	11.6	9.9	11.5	14.8	22.5	29.7
July 19	9.8	13.6	17.2	24.9	28.1	39.1
July 20	29.3	38.3	44.8	45.2	44.0	43.2

Heffter et al. [1975]. Such trajectories are computed by time and space interpolation of measured wind velocities, averaged over a specific layer of the atmosphere, using 6-hour intervals corresponding to 2 a.m., 8 a.m., 2 p.m., and 8 p.m. EDT.

The trajectories were computed for the layer between 400 and 1400 m above the terrain. The lower limit was imposed to eliminate the wind field in the nocturnal surface inversion. This layer of light and variable winds is of little importance in the transport of atmospheric mixtures over more than a few tens of kilometers.

The weather on July 15 was characterized by high pressure building along the east coast, with a remnant stationary front running from Vermont to Georgia. Areas of precipitation formed along that front and produced moderate rainfall over much of the east coast, including most of eastern New York State. The pattern persisted on July 16, with precipitation over all but extreme northern New York. On July 17 the stationary front had dissipated, and strong high pressure had become established. There was no measurable precipitation in upstate New York. This warm, hazy weather continued until the evening of July 18, when an area of precipitation began to move through the state from west to east. Precipitation developed on July 19 as an upper-level trough moved over the state from the west.

The wind reaching Whiteface Mountain on July 17 and 18 arrived from the west. This westerly wind resulted when high pressure over western Pennsylvania caused the wind to flow from the eastern Midwest and western Pennsylvania northeastward into western New York and then in a more easterly direction toward Whiteface Mountain. Such conditions are often associated with stagnation in the Ohio region [*Samson*, 1978]; note the lengths of the 12-hour trajectory vectors.

As the trajectories computed for this period pass over the same general region, it is worthwhile to note the trajectories for each day studied. Table 1 lists the average 12-hour wind speed estimates for those trajectories computed to arrive at Whiteface Mountain at 1400 EST each day. The highest concentrations of trace elements and TSP (on July 17 and 18) were associated with low wind speeds occuring 36–72 hours prior to arrival at Whiteface. Increased wind speed on July 19 and 20 in the Midwest was associated with lower concentrations at Whiteface Mountain.

It is reasonable to suppose that during a stagnation episode in the Ohio region the air mass collects particulates produced in that area, where industrial sources release large amounts of pollutants such as sulfates and trace metals. Subsequent transport to New York State, as shown by the trajectories, would then explain the high elemental and sulfate concentrations observed at Whiteface Mountain.

High concentrations of Br, Hg, and Sb, however, do not appear to be associated with the July 16–20 episode. Automobiles are the most likely sources of the particulate Br, which would explain their poor correlation with the TSP and air mass trajectory. The source of Hg is not so clear. It appears to be associated with the air masses originating northwest of Whiteface Mountain, but no known major source of Hg, natural or anthropogenic, exists in upstate New York. Coal burning is a possible source, but its contribution to the observed Hg level cannot be determined at this time.

In order to test the hypothesis that much of the metals seen in New York State are transported from distant source, we extended our sampling region to include Holland, Schoharie, Albany, and Whiteface Mountain, New York, and High Point, New Jersey, during July 1976 If stagnant air masses in the Ohio region were the cause of high elemental and TSP concentrations at Whiteface Mountain, they would also affect other areas in the Northeast. All of the new sites, except Albany, are rural, although Holland is only about 60 km southeast of Buffalo. On July 20 an unmistakable peak in TSP concentrations was observed at all five stations (Figure 3), simultaneous with peaks of Na, K, Sc, Mn, Fe, Zn, and As. The same behavior was reported for sulfates [*Galvin et al.*, 1978].

Simultaneous occurrence of peak TSP, metals, and sulfate concentrations at locations hundreds of km apart strongly suggests a distant common source. Trajectory analyses show that air masses reached New York State on July 17, 1976, from the north and on July 18 from a more westerly direction. On July 20 the winds arriving in New York State originated in a stagnant air mass in the Midwest; the trajectories were similar to those for July 17, 1975 (Figure 2). The estimated trajectory wind speeds for this period show a distinct minimum for the air mass arriving on July 20, occurring 36–48 hours prior to its arrival [*Galvin et al.*, 1978]. These results again suggest that the high metal concentrations observed in upstate New York and New Jersey resulted from the transport of stagnant air masses in the Ohio region.

Although we have not used unique tracers to study the long-range transport of pollutants, a correlation was established between high episodic concentrations and air trajectories dur-

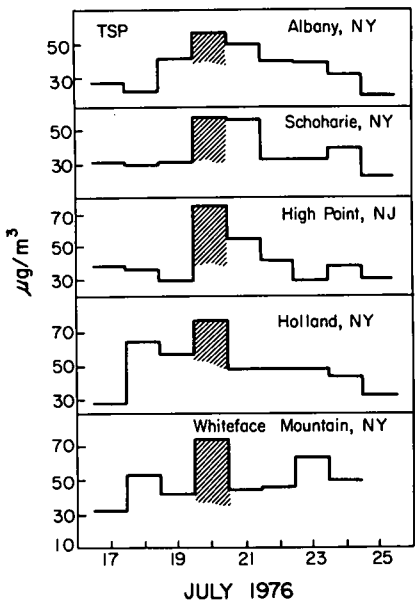

Fig. 3. Total solid particulate measurements during July 1976 in upstate New York and New Jersey. Shading designates the day of peak concentrations (July 20).

ing the summers of 1975 and 1976. This correlation indicates that high trace metal concentrations in much of New York State are due at times to the air flowing from stagnant conditions in the Midwest.

Acknowledgments. The authors express their appreciation to Volker Mohnen for providing sampling facilities at the Atmospheric Sciences Research Center's Whiteface Mountain Observatory; to J. M. Matuszek for many stimulating discussions; to S. House, R. McDermott, and D. Romano for assistance in sampling; to P. Lioy for providing the High Point samples; to J. B. Cumming for his hospitality and providing counting facilities at Brookhaven National Laboratory; and to B. Lance, L. Keenan, and K. Williams for assistance in counting and data reduction. This study was funded in part by Department of Energy contract EE-77-S-02-4501.A000.

REFERENCES

Coffey, P. E., and W. N. Stasiuk, Jr., Evidence of atmospheric transport of ozone into urban areas, *Environ. Sci. Technol., 9,* 59–62, 1975.

Elliot, W. P., F. L. Ramsey, and R. Johnston, Particle concentrations over the oceans, *J. Rech. Atmos., 8,* 939–945, 1974.

Galvin, P. J., P. J. Samson, P. E. Coffey, and D. Romano, Transport of sulfate to New York State, *Environ. Sci. Technol., 12,* 580–584, 1978.

Heffter, J. L., A. D. Taylor, and G. J. Ferber, A regional-continenta scale transport, diffusion, and deposition model, *NOAA Tech. Memo. ERL-ARL-50,* Air Resour. Lab., Silver Spring, Md., 1975.

Husain, L., P. E. Coffey, R. E. Meyers, and R. T. Cederwall, Ozone transport from stratosphere to troposphere, *Geophys. Res. Lett., 4,* 363–365, 1977.

Lioy, P. J., G. T. Wolff, J. S. Czachor, P. E. Coffey, W. N. Stasiuk, and D. Romano, Evidence of high atmospheric concentrations of sulfates detected at rural sites in the northeast, *J. Environ. Sci. Health, A12,* 1–14, 1977.

Prospero, J. M., Atmospheric dust studies in Barbados, *Bull. Amer. Meteorol. Soc.,* 645–652, 1977.

Samson, P. J., Ensemble trajectory analysis of summer sulfate concentrations in New York State, *Atmos. Environ., 12,* 1889–1893, 1978.

(Received March 15, 1978;
revised October 11, 1978;
accepted October 19, 1978.)

APPENDIX III

On the origin of tropospheric ozone

Liaquat Husain, Vincent A. Dutkiewicz & A. Rusheed*

Division of Laboratories and Research, New York State Department of Health, Albany, New York 12201

*On leave of absence from Pakistan Institute of Nuclear Science and Technology, Rawalpindi, Pakistan

The phenomenon of stratosphere-troposphere exchange for ozone has been studied using cosmic ray produced ^{7}Be as a tracer. It is demonstrated that the stratosphere-troposphere exchange is approximately two times higher in the northern hemisphere compared to that in the southern hemisphere. New determinations of $^{7}Be/O_3$ ratios at 10-12 km using commercial 747 jetliners are presented. A tropospheric ozone budget originating from the stratosphere is calculated from $^{7}Be/O_3$ ratios and ground level ^{7}Be concentrations. The results show that at least half of the annual average ground level ozone concentrations in the 20^{o}-$50^{o}N$ and essentially all of the ozone in the 60^{o}-$90^{o}N$ latitudinal bands originates in the stratosphere. In the southern hemisphere our calculations are hampered by the lack of $^{7}Be/O_3$ ratios measurements in the stratosphere as well as relatively less abundant ^{7}Be measurements especially 60^{o}-$90^{o}N$ latitudes. In the 10^{o}-$40^{o}S$ band our calculations suggest that at least half of the ozone in the middle latitudes of the southern hemisphere originates in the stratosphere.

THE ozone budget plays an important role in atmospheric chemistry, air quality criteria, and in the understanding of stratosphere-troposphere exchange mechanisms. The most generally accepted theory describing the ozone budget postulates that, except in polluted areas, ozone observed at ground level is transported from the stratosphere. Beginning with Crutzen,[1,2] several authors[3-7] have argued that photochemistry in the troposphere plays a dominant role in the tropospheric ozone budget. More recently, Fishman and Crutzen[7] have challenged the classical theory on the basis of: (1) the greater area of land relative to oceans in the northern hemisphere (NH) compared to that for the southern hemisphere (SH), and (2) the greater ozone destruction rate over land compared to that over ocean. They argue that the approximately equal ozone concentrations in the middle latitudes of the two hemispheres can only be accounted for by a stratospheric ozone flux in the NH which is three times that in the SH. Since their meteorological analyses do not yield such large hemispheric differences in stratosphere-troposphere exchange, Fishman and Crutzen[7] concluded that tropospheric ozone in the middle latitudes of the NH is not primarily of stratospheric origin. They proposed instead that oxidation of CO is the major source of tropospheric ozone. It appears necessary to develop a clearer understanding of tropospheric ozone sources.

In this paper, we demonstrate that the stratospheric-tropospheric exchange is indeed approximately 2 times higher in the NH than in the SH, describe a new concept to quantify the contribution of stratospheric ozone at ground level.

^{7}Be as a tracer of stratospheric ozone

The interactions of cosmic ray protons and neutrons with atmospheric oxygen, nitrogen, and argon produce a myriad of radionuclides,[8] including ^{7}Be (half-life, 53.3 d). Because of cosmic ray attenuation within the

the atmosphere and atmospheric circulation, the average ^{7}Be concentration in the stratosphere is estimated to be approximately 30 times that in the troposphere.[9] Rapid circulation and precipitation scavenging in the lower 5 km of the atmosphere, results in a mean residence time for aerosols of the order of a few days.[10-12] Thus, ^{7}Be production in the lower 5 km is very small accounting for only a few percent of the observed ground level ^{7}Be concentrations. Therefore, high ground level ^{7}Be concentration is a good indicator of subsidence of air from aloft.[13-15] Although the specific mechanisms are still debated,[12,16-18] stratospheric-tropospheric exchange appears well established. We have at times measured $^{7}Be/O_3$ ratios at altitudes just below the tropopause which were very similar to those measured in the stratosphere.[14] Subsidence of the stratospheric air will transport ozone and ^{7}Be to ground level. Concentrations of ^{7}Be and ozone so transported can be written as:

$$\frac{d}{dt}\,(^{7}Be)_T = \frac{(^{7}Be)_s}{\tau} + Q - (\lambda + k_1)\,(^{7}Be)_T \qquad (1)$$

$$\frac{d}{dt}\,(O_3)_T = \frac{(O_3)_s}{\tau} - k_2\,(O_3)_T \qquad (2)$$

where $(^{7}Be)_T$ = concentrations of ^{7}Be ($fCi/m^3 = 10^{-15}$ Ci/m^3) in the troposphere

$(O_3)_T$ = concentration of ozone (ppbv) in the troposphere

$(^{7}Be)_s$ and $(O_3)_s$ = concentrations of ^{7}Be (fCi/m^3) and ozone (ppbv), respectively, in the stratosphere

τ = stratospheric mean residence time (days)

Q = average tropospheric ^{7}Be production rate ($fCi/m^3/d$)

λ = decay constant of ^{7}Be ($0.0130\ d^{-1}$)

k_1 and k_2 = reciprocals of tropospheric mean residence times (days) of ^{7}Be and O_3, respectively.

Since there is no significant net annual change in ^{7}Be and ozone concentrations, the left hand side of equations (1) and (2) can be taken as zero. Rearranging and dividing equation (2) by (1) we obtain

$$(O_3)_T = \frac{1}{(^{7}Be/O_3)_s} \cdot \frac{(\lambda + k_1)}{k_2} \cdot \left[(^{7}Be)_T - \overline{Be_T}\right] \qquad (3)$$

where $\overline{Be_T} = Q/(\lambda + k_1)$ = the net average ^{7}Be concentration produced in the troposphere

Thus, ground level ^{7}Be concentrations can be used to determine the amount of stratospheric ozone if the stratospheric $^{7}Be/O_3$ ratio and the mean tropospheric residence times of ^{7}Be and ozone are known.

In an earlier paper,[14] we reported the first measurements of $^{7}Be/O_3$ ratios in the statosphere at 35°-42°N for January-June 1978. Here we report additional $^{7}Be/O_3$ ratio measurements at 10-12 km altitude, 20°-50°N for the October 1977-March 1979 period. Experimental details of these measurements are similar to those described by Dutkiewicz and Husain.[14] The ratios are shown in Figure 1, with vertical bars representing estimated uncertainties. The average stratospheric $^{7}Be/O_3$ ratios for each of the four seasons are shown by solid lines. Also shown in Figure 1 for comparison are $^{7}Be/O_3$ ratios (dashed lines) estimated from other ozone[19,20] and ^{7}Be measurements[21] between 12 and 21 km. Although these ^{7}Be and ozone measurements were carried out in separate experiments, sometimes years apart, they provide $^{7}Be/O_3$ ratios which agree well with our results obtained from the simultaneous measurements of ^{7}Be and ozone. The agreement between our $^{7}Be/O_3$ measurement at 11.5 km and the calculated value integrated over 12-21 km suggests that $^{7}Be/O_3$ ratios remain relatively constant throughout the lower stratosphere.

From out measurements, we deduce an annual average $^{7}Be/O_3$ ratio in the stratosphere of 10.9 ($fCi/m^3/ppbv$) for 30^{o}-$60^{o}N$ latitude band. Because of the excellent agreement between the stratospheric $^{7}Be/O_3$ ratio deduced from ozone measurements of Dutsch[20] and Hering and Borden[19] and ^{7}Be (Feely et al[21]), we have used their measurements to deduce the stratospheric $^{7}Be/O_3$ ratio for the 0^{o}-30^{o} (15.3 $fCi/m^3/ppbv$) and 60^{o}-90^{o} (8.7 $fCi/m^3/ppbv$) latitude bands. A correction factor of 1.09 determined by normalizing the calculated $^{7}Be/O_3$ ratio with our accurately determined ratio for 30^{o}-$60^{o}N$ band was applied to the calculated $^{7}Be/O_3$ ratio for 0^{o}-30^{o} and 60^{o}-90^{o}.

Stratospheric-tropospheric exchange

Because ^{7}Be appears to accurately trace stratospheric air masses, global ^{7}Be measurements can provide a basis for studying stratospheric-tropospheric exchange. In Figure 2 we have constructed the latitudinal profile of ^{7}Be using annual average concentrations measured below 2 km altitude. The individual sites which are included in Figure 2 are summarized in Table 1. Many of the sites in the Environmental Measurement Laboratory (EML) network[22] have had monthly ^{7}Be determined on a continuous basis since 1970. Thus, 8 years of ^{7}Be data are available for averaging at these sites. To account for random occurences of incomplete data at some EML sites, monthly data for each site were averaged and the grand average (Shown as ⊙ in Figure 2) was computed by averaging the yearly averages inversely weighted by the number of months of data available each year. Since most of the data points in Figure 2 represent ^{7}Be averaged for more than one year, with many representing 8 years of ^{7}Be measurements, these data should be representative of the ^{7}Be concentration in

surface air. Although the average ^{7}Be concentration in the lower stratosphere is approximately 30 times that in the surface air, the magnitude of stratospheric ^{7}Be present in the troposphere depends upon the intensity of stratospheric-tropospheric exchange, transport process and the mean residence time. Therefore, before ^{7}Be concentrations from Figure 2 can be compared in the two hemispheres, the tropospheric ^{7}Be contribution should be subtracted. Since the ^{7}Be production in the troposphere depends on the flux of cosmic ray protons and neutrons, air density, and irradiation times, the tropospheric component can be safely assumed to be the same in the two hemispheres. It is also apparent that the tropospheric ^{7}Be component can be directly measured only in the region where the stratospheric influences are trivial. It is widely recognized that at the equator the stratospheric influences are vanishingly small. The global circulation patterns[12] also imply a minimal stratospheric ^{7}Be contribution at $60^{o}N$. Figure 2 provides a testimony to these suggestions, the observed ^{7}Be levels at $60^{o}N$ and at the equator are very low and about equal. Lal and Peters[8] calculations show some variation with latitude in the tropospheric ^{7}Be production rates. We have normalized the observed ^{7}Be concentration at the equator with Lal and Peters[8] latitudinal profile to deduce the tropospheric ^{7}Be contribution at all latitudes in both hemispheres (dashed lines in Figure 2). For 20^{o}-$40^{o}N$ the average tropospheric ^{7}Be contribution is approximately 25% of the observed ^{7}Be values, whereas for 10^{o}-$40^{o}S$ this contribution is about 45%.

An examination of the most comprehensive collection of worldwide ^{7}Be data (Figure 2) unmistakably shows significant hemispheric asymmetries. In the NH, a prominent peak is observed at about 30^{o}-$35^{o}N$, with minima at the equator and $\sim 60^{o}$. At latitudes above $60^{o}N$, the ^{7}Be concentration rapidly increases up to $80^{o}N$. No data exists at $\sim 90^{o}N$ hence we have carried out an extrapolation. In the SH the ^{7}Be data are understandably less abundant. However, a peak at $\sim 25^{o}$

is indicated. No ground level ^{7}Be measurements above 60°S are known to us. However, a ^{7}Be measurement at 2.8 km at the South Pole show a high ^{7}Be concentration of 111 fCi/m^3.[22] We have not included this datum as we have excluded all other high altitude measurements. For completeness we have carried out an extrapolation from 60°S to the South Pole, assuming the variation is similar to that for 60°-90°N. Integration of the ^{7}Be concentration profiles, weighting by the cosine of the latitudes to account for the area in a latitude band, and subtracting the tropospheric ^{7}Be component (as depicted by the lower dash curve, Figure 2) we obtain a stratospheric ^{7}Be flux ratio in the NH/SH of 1.8. The greatest asymmetry occurs between 20° and 40° where we calculate a NH/SH of 2.1. Even if the solid curve in Figure 2 is biased to pass through the three points of highest concentration in the SH, for 20°-40° the ratio of the stratospheric ^{7}Be in the NH/SH reduces only slightly, to 1.8. Additional measurements in the SH and especially between 10° and 40° will facilitate hemispheric comparisons. In spite of this, we feel that the ^{7}Be data in the SH are sufficient to define a fairly accurate profile of stratospheric ^{7}Be flux. From the above discussion we conclude that the stratospheric ^{7}Be flux in the NH is approximately twice that in the SH. Our conclusion finds substantial support from the global circulation model (GCM) calculation of Mahlman *et al*[26] and Gidel and Shapiro[27] who have determined a NH/SH ratio of 1.85 and 1.96, respectively, for stratospheric ozone.

The major features of the ^{7}Be profile in Figure 2 can be qualitatively explained by the Hadley cell circulation patterns[12] in the troposphere. The descending branches of the Hadley cell are also situated nearly at the same latitudes as the ^{7}Be peaks, namely, poles, ~30°N and ~20°S. The ascending branches of the Hadley cells are located near the equator and 60° in both

hemispheres. Minima in the ^{7}Be concentrations are also observed at the equator, $\sim 60^{o}N$ and $\sim 60^{o}S$. Therefore, the peaks and valleys in the ^{7}Be concentration profile may be associated, respectively, with the descending and the ascending branches of the Hadley cell. Mass transfer processes including Hadley cell circulation introduce large amounts of stratospheric air mass in the upper troposphere at mid latitudes both in the NH and the SH. The descending branch of the Hadley cell, whether penetrating from the stratosphere or residing entirely in the troposphere, may subsequently transfer the intruded stratospheric air mass to the lower troposphere. In the lower troposphere the descending branch of the Hadley cell undergoes meridional transport.[12] The sharpness of the ^{7}Be peak, particularly in the NH, is however inconsistent with significant meridional transport in the lower troposphere. Since the aerosol residence time in the lowest 5 km is relatively short, of the order of a few days,[10-12] stratospheric ^{7}Be is not likely to undergo significant meridional transport. However, stratospheric species with longer residence times in the lower troposphere may undergo significantly meridional transport. Such species will exhibit a broader meridional profile than that indicated for ^{7}Be in Figure 2.

Mean tropospheric residence times

The mean tropospheric aerosol residence time in the NH has been estimated by several authors to be about 30 days using fission products.[28] We are not aware of any estimates of mean tropospheric residence time in the SH, but there are no a priori reasons to believe that the mean aerosol residence time in the SH will be significantly different from that in the NH. Concentration of ^{89}Sr and ^{90}Sr in aerosols collected monthly have been reported for the SH.[22] Using ^{89}Sr and ^{90}Sr concentrations obtained for samples collected at Puerto Montt, Chile (41^{o} 27' S, 72^{o} 57' W) immediately after the French nuclear explosion at

Mururoa Atoll (21° S, 135° W) on August 14, 1971 and a calculational procedure developed by Kuroda,[29] we obtain a mean tropospheric aerosol residence time of 40 ± 19 days at 41°S. This value is in reasonable agreement with a mean residence time of 30 days obtained by Beck and Kuroda[28] at 36° N, 97° W. Since the residence time for the NH obtained by Beck and Kuroda[28] are based on superior data (individual rain samples vs. monthly air particulates composite), we use a value for k_1 of 0.033 d^{-1} for both the NH and SH.

For the observed upper tropospheric ozone concentrations and destruction rates of ozone at the earth's surface, Fabian and Pruchniewicz[30] have calculated the mean tropospheric residence time of ozone varying from 42 days at the pole to 88 days at the equator. These calculations assume ozone is an inert specie in the troposphere. In view of the photochemical reactivity of ozone this assumption probably is not valid. In a recent one-dimensional model calculations, which involve both chemistry and transport, Hameed[31] has estimated ozone mean residence times at all latitudes in both the NH and the SH. For 20°-40°N, and 60°-90°N latitudinal belts, average mean residence times of 30 and 148 days respectively, were obtained.[31]

Ozone budget

Using the mean residence time for ^7Be and ozone, $^7Be/O_3$ ratios measured in this work, and the average ^7Be concentration from Figure 2 (corrected for tropospheric ^7Be component), we can calculate the ground level ozone contribution from the stratosphere using equation (3). For 20°-50°N our calculations yeild a value of 14 ppbv for stratospheric ozone contributions in the surface air. Fishman and Crutzen (1978) have calculated a value of 25 ppbv for the total tropospheric ozone concentration at 20°-60°N. Thus, our calculations suggest that in the 20°-40°N latitudinal band approximately 56% of the ozone is trans-

ported from the stratosphere. This estimate finds excellent support from recent calculations by Gidel and Shapiro[27] who have used GCM to estimate that in 20°-40° N band approximately 60% ozone originates from the stratosphere. In the 60°-90° N latitudinal band our technique yields 34 ppbv for the stratospheric ozone contribution, which is higher than the ozonesonde value of ∿ 25 ppbv for this latitude band[7]. Most likely explanation for the higher ozone value is probably that the 148 days mean residence[31] time for ozone is too high. Fabian and Pruehniewicz[30] on the basis of surface destruction rate alone estimated an ozone mean residence time of 42 days for 60-90° N. Hameed's[31] calculation includes both surface destruction and chemistry in the troposphere. At the same times serious discrepancy occurs in the ozone mean residence time in 20°-40° N calculated by the above authors. For example, we have used Hameed's[30] calculated value of 30 days, which is substantially smaller than 47 days estimated by Fabian and Pruehniewicz[30]. Therefore, our estimates of stratospheric ozone component in 20°-40° band should be considered as a minimum. An upward revision of the 30 day mean residence time would linearly increase our estimated ozone concentration. More work on the ozone mean residence time is essentially to our improving the understanding of the origin of ozone.

We have not determined the $^{7}Be/O_3$ ratios in the southern hamisphere stratosphere. Application of our NH measurement in the SH presumes that the ^{7}Be and ozone vertical profiles vary in the same way as they do in the NH. There is evidence that the ozone vertical profile are different in the NH and the SH[27]. Therefore, the validity of the NH measurements of $^{7}Be/O_3$ in the SH requires that the ^{7}Be also show a variation similar to that of ozone. Assuming this to be the case, we estimate a stratospheric ozone contribution of 10 ppbv for 10°-40° S, which compares rather favorably with the observed ozone levels of 13 ppbv for 15°-30° S and is half of the 20 ppbv concentration estimated for 30°-40° S.

Conclusion

The use of ^{7}Be concentrations measured at ground level with stratospheric $^{7}Be/O_3$ ratios provides a technique for determining the stratospheric ozone contribution to the troposphere. Our calculations suggest that the stratosphere at least provides half the tropospheric ozone. Furthermore, the stratospheric-tropospheric exchange rate in the NH is $\sim$ 2 times that in the SH.

The authors are grateful to NASA Lewis Research Center and Porter Perkins, Jr., Erwin Lezberg, and Francis Humenik for their excellent cooperation in supplying the filters and the ozone data. Discussions with Dr. J. M. Matuszek, Jr. are gratefully acknowledged.

This work has been partially supported by the U.S. Department of Energy under contract No. EE-77-4501 and the U.S. Environmental Protection Agency Grant S-8059/3-01 (project director, Dr. B. Dimitriades).

References

1. Crutzen, P.J., Rep. AP-12, Institute of Meteorology, University of Stockholm, Stockholm, 1973.

2. Crutzen, P.J., Tellus 26, 47-57, 1974.

3. Chameides, W. & Walker, J.C.G. J. Geophys. Res 78, 8751-8760, 1973.

4. Chameides, W.L. & Stedman, D.H. J. Geophys. Res. 82, 1787-1794, 1977.

5. Chameides, W.L. & Walker, J.C.G. J. Geophys. Res. 81, 413-420, 1976.

6. Fishman, J. & Crutzen, P.J. J. Geophys. Res. 82, 5897-5906, 1977.

7. Fishman, J. & Crutzen, P.J. Nature 274, 855-858, 1978.

8. Lal, D. & Peters, B. in Handbuch der Physik 46 (ed Sitte, K) 551-612 (Springer Verlag; Heidelberg, 1767).

9. Lal, D. & Suess, H. Ann Rev. Nucl. Sci. 18, 407-434, 1968.

10. Machta, L., List, R.J., Smith, M.E. & Oeschger, H. in Precipitation Scavenging (ed Engelman, R.J. & Slinn, W.G.N.), 465-474 AEC Symposium Series 22, NITS, U.S. Department of Commerce, Springfield, Va.), 1970.

11. Martell, E.A. & Moore, H.E., J. Rech. Atmos. 8, 903-910, 1974.

12. Reiter, E.R. Rev. Geophys. Space Phys. 13, 459-474 (1975).

13. Husain, L., Coffey, P.E., Meyers, R.E. & Cederwall, R.T. Geophys. Res. Lett. 4, 363-365 (1977).

14. Dutkiewicz, V.A. & Husain, L. Geophys. Res. Lett. 6, 171-174 (1979).

15. Reiter, R., Kanter, H.-J., Sladkovic, R. & Potzl, K. USERDA Document No. NYO-3425-14 (1977).

16. Reiter, E.R. in Air Quality Meteorology and Atmospheric Ozone, STP653 (ed. Morris, B.L. & Barras, R.C.), 506-519, (American Soc. Testing & Materials, Philadelphia, PA), 1978.

17. Danielsen, E.F. J. Atmos. Sci. 25, 502-518 (1968).

18. Danielsen, E.F. & Mohnen, V.A. J. Geophys. Res. 82, 5867-5877 (1977).

19. Hering, W.S. & Borden, T.R., Jr. U.S. Air Force Cambridge Research Laboratories Report No. AFCRL-64-30 (IV) (1967).

20. Dutsch, H.U. Adv. Geophys. 15, 219-322 (1971).

21. Feely, H., Friend, J.P., Seitz, H., Martin, J.D. & Erlebach, W.E. Final Report of Project Stardust, DASA-2166-3, Isotopes, Inc. (1971).

22. U.S. Department of Energy, Environmental Measurements Laboratory Report EML-342 (1978).

23. Hartwig, S. & Sittkus, A. Nature 241, 36-37, 1973.

24. Shapiro, M. & Forbes, Resha. J. Geophys. Res.

25. Bleichrodt, J.F. J. Geophys. Res. 83, 3058-3062 (1978).

26. Mahlman, J.D., Levy II, H. & Moxim, W.J. J. Atmos. Sci., in press.

27. Gidel, L.T. & Shapiro, M.A., preprint.

28. Beck, J.N. & Kuroda, P.K. J. Geophys. Res. 71, 2451-2556 (1966).

29. Kuroda, P.K. Argonne National Laboratory Report ANL-5920 (1958).

30. Fabian, P. & Pruchniewicz, P.G. J. Geophys. Res. 82, 2063-2072 (1977).

31. Hameed, S., in preparation.

Table 1. Site Locations and Sampling Times for Global ^{7}Be Measurements

Site	Location		Years Sampled	Reference
Nord, Greenland	82°N	17°W	1970-1975	22
Thule, Greenland	77°N	69°W	1970-1972	22
Barrow, Alaska	71°N	156°W	1975-1977	22
Kap Tobin, Greenland	70°N	22°W	1973-1977	22
Tromso, Norway	70°N	19°E	1978	**
Lerwick, U.K.	60°N	1°W	1978	**
Eskdalemuir, U.K.	55°N	3°W	1978	**
Orfordness, U.K.	52°N	2°E	1978	**
Milford Haven, U.K.	52°N	5°W	1978	**
Chilton, U.K.	52°N	1°W	1978	**
Braunshweig	52°N	10°E	1966-1968	23
Moosonee, Canada	51°N	80°W	1970-1977	22
Freiburg-Schavinsland	48°N	8°E	1966-1968	23
Moosonee, Canada	51°N	80°W	1970-1977	22
Helena, Montana	47°N	112°W	1973-1977	22
Whiteface Mounatin, New York	44°N	74°W	1978-1979	This work
Salt Lake City, Utah	41°N	111°W	1971-1975	22
New York, New York	41°N	74°W	1970-1977	22
BNL, Upton, New York	41°N	73°W	1971-1978	***
Rocky Flats, Colorado	40°N	105°W	1972-1977	22
Sterling, Virginia	39°N	77°W	1970-1974	22
Richmond, California	38°N	122°W	1973-1977	22
Gibraltar	36°N	6°W	1978	22
Fullerton, California	34°N	118°W	1973-1975	24
Miami, Florida	26°N	80°W	1970-1977	22
Bimini, Bahamas	26°N	79°W	1970-1972	22
Hong Kong	22°N	114°E	1978	**
San Juan, Puerto Rico	18°N	66°W	1970-1974	22
Balboa, Panama Canal Zone	9°N	80°W	1970-1976	22
Merida, Venezuela	9°N	71°W	1972-1974	22
Singapore	1°N	104°E	1978	**
Guayaquil, Equador	2°S	80°W	1970-1977	**
Lima, Peru	12°S	77°W	1970-1977	22
Darwin, Australia	12°S	131°E	1978	**
Tutuila, Samoa	14°S	171°W	1976-1977	22
Antofagasta, Chile	24°S	70°W	1970-1977	22
Pretoria, South Africa	26°S	28°E	1978	**
Easter Island	27°S	109°W	1971-1977	22
Santiago, Chile	33°S	71°W	1970-1977	22
Aspendale, Australia	38°S	145°E	1978	**
Ohakea, New Zealand	40°S	175°E	1978	**
Puerto Montt, Chile	41°S	73°W	1970-1977	22
Punta Arenas, Chile	53°S	61°W	1973-1977	22
Antarctica	63°S	61°W	1973-1977	22

*Sites given in Bliechrodt[25] for 68°-42°N are not duplicated here.
**Peirson Personal Communication.
***Naidu Personal Communication.

Figure Captions

Fig. 1. $^{7}Be/O_3$ ratios calculate from measurements of simultaneous sampling of particulates and in situ determination of ozone during October 1977 and Febraury 1979. Vertical bars represent 1 σ uncertainties. Solid horizontal lines represent average of $^{7}Be/O_3$ ratios observed during the four seasons. Dashed lines represent calculated $^{7}Be/O_3$ ratios from ozone measurements of Dutsch[11] and Hering and Borden,[10] and ^{7}Be measurements of Feely et al.[12] In their experiments, O_3 and ^{7}Be sampling was not carried simultaneously, nor at the same locations.

Fig. 2. Meridional profile of annual average ^{7}Be concentration in ground level air (< 2 km). The solid line is a freehand curve through the data. The short dashed extensions to the poles are extrapolations. The long dashed curve is estimated tropospheric ^{7}Be concentration as explained in the text.

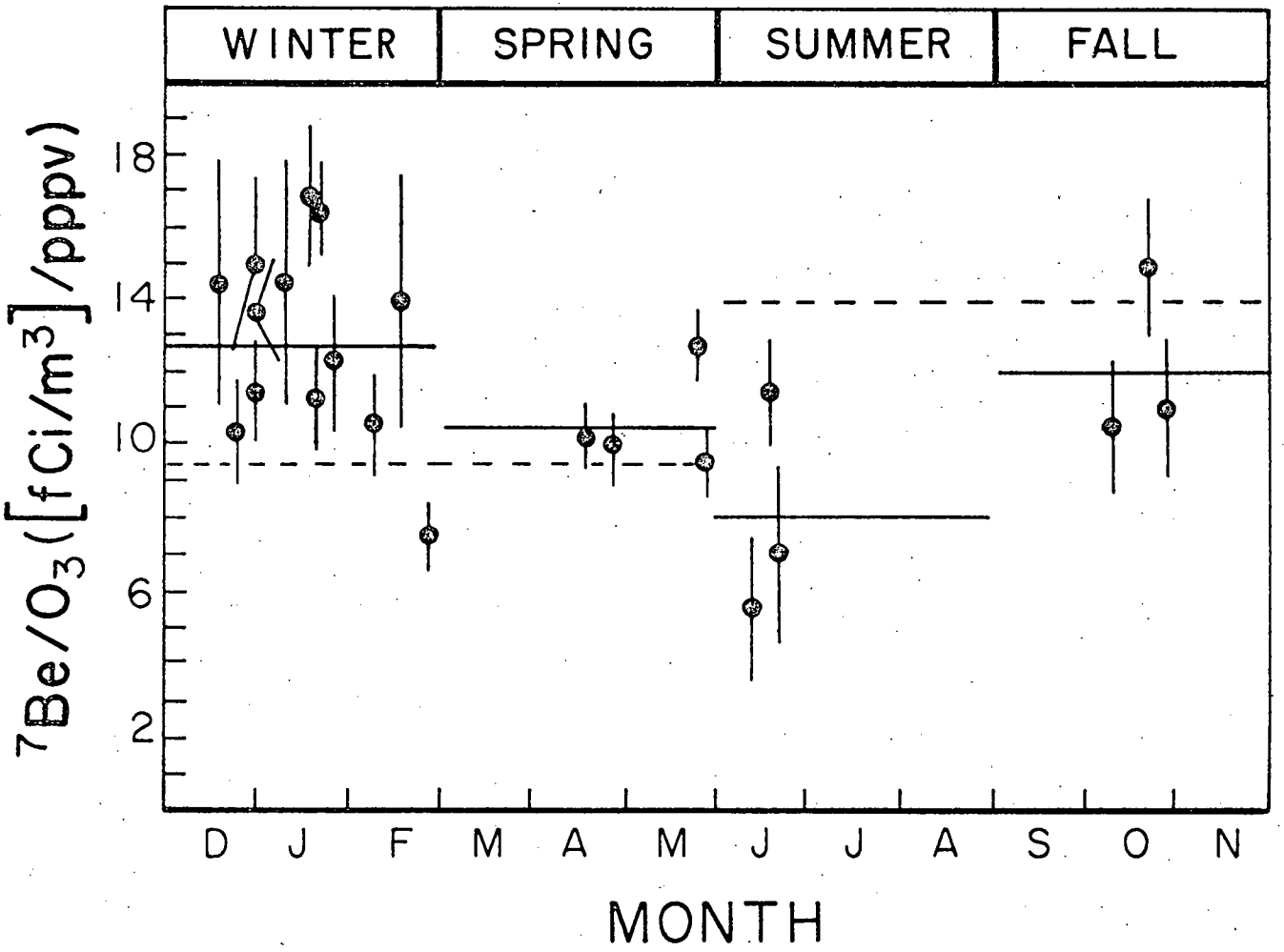
WINTER
SPRING
SUMMER
FALL
$^7Be/O_3$ ([fCi/m^3]/pppv)
18
14
10
6
2
D
J
F
M
A
M
J
J
A
S
O
N
MONTH

Fig. 1

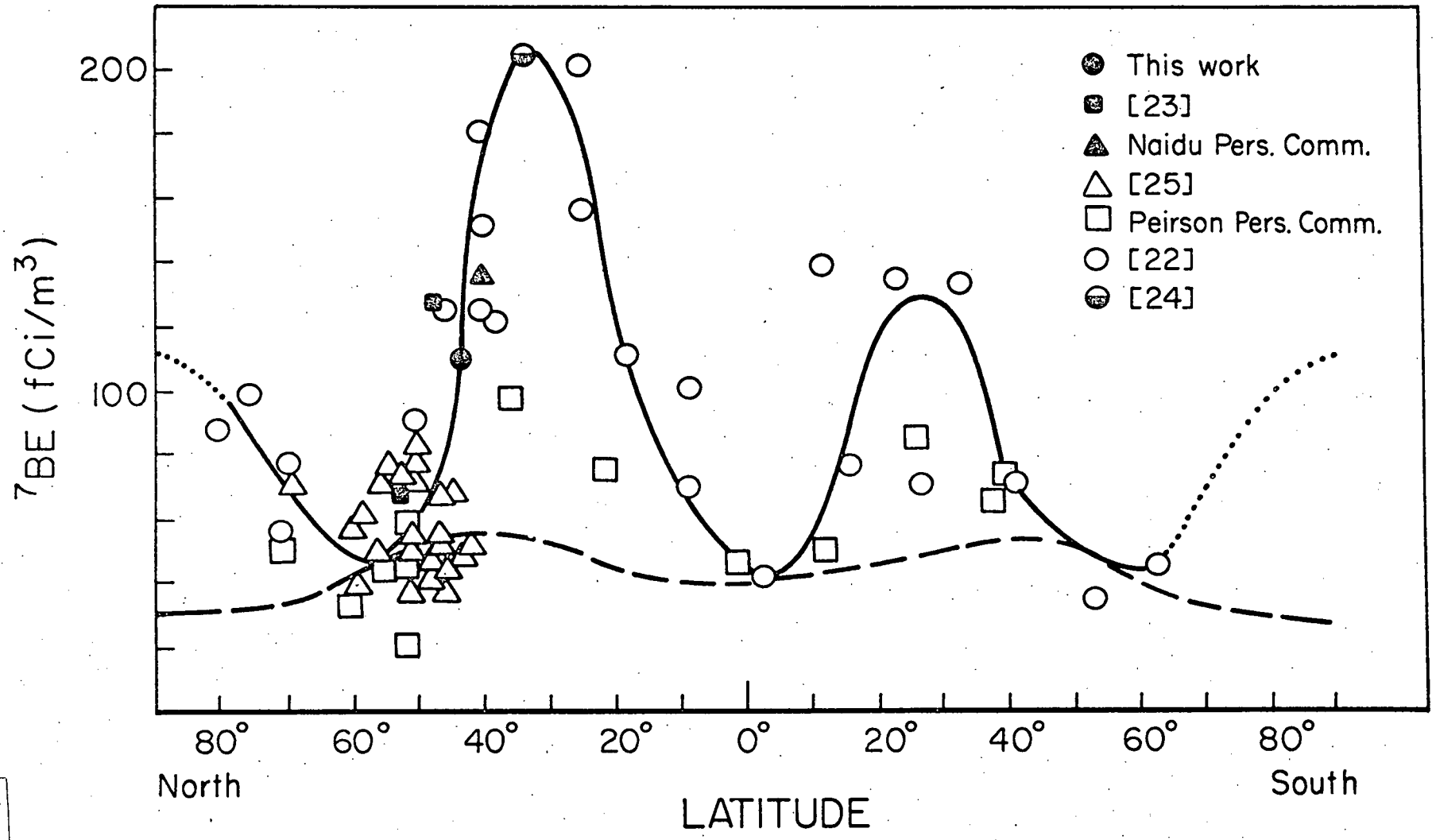
200
100
^{7}BE (fCi/m^{3})
This work
[23]
Naidu Pers. Comm.
[25]
Peirson Pers. Comm.
[22]
[24]
80°
60°
40°
20°
0°
20°
40°
60°
80°
North
South
LATITUDE

Fig. 2

APPENDIX IV

Transport Time of Stratospheric Air from Tropopause to Ground Level

V.A. Dutkiewicz, A. Rusheed* and L. Husain

Division of Laboratories and Research, New York State Department of Health
Albany, New York 12201

*Present address: Pakistan Institute of Nuclear Science and Technology, Rawalpindi, Pakistan.

Abstract

The transport time of stratospheric air reaching Whiteface Mountain, New York, was studied using the activity ratios of cosmic ray-produced $^{7}Be/^{32}P$. The observed ratios can be expressed as a function of the fraction of observed ^{7}Be which originated in the stratosphere and the time spent by the stratospheric air parcel in the troposphere prior to sampling. Thus, for cases where the stratospheric and tropospheric ^{7}Be components can be inferred and the stratospheric component dominates, the transport time can be determined from $^{7}Be/^{32}P$ activity ratios. For the summers of 1977 and 1978 and the spring and the summer of 1979, 44 occasions when stratospheric air reached this site were studied. The mean transport time was 7 days, but on most occasions the time was $\leq$ 5 days. For the fall of 1978 and the winter and fall of 1979, 12 cases were studied. The mean transport time was 16 days, but many occasions suggesting longer transport times were not included due to large uncertainties in the $^{7}Be/^{32}P$ ratios. The transport times determined in this work are much shorter than those estimated for stratospheric-tropospheric exchange occurring via mean meridional circulation but comparable to travel times associated with tropopause folding events. These results provide compeling evidence in support of tropopause folding as the predominant mechanism for stratospheric-tropospheric exchange.

Introduction

Transport of stratospheric air into troposphere is accompanied by a transfer of large amounts of stratospheric trace constituents, such as ozone, bomb-produced fission products, and cosmic ray-produced radionuclides. Since the stratospheric ozone concentration is of the order of parts per million, it has been suggested [Danielsen and Mohnen, 1977] that transport of stratospheric air during the relatively rapid tropopause folding could significantly increase ground-level ozone concentrations. We have demonstrated [Husain et al., 1977, 1979, 1980; Dutkiewicz and Husain, 1979] the usefulness of the cosmogenic isotope ^{7}Be as a tracer of stratospheric ozone in ground-level air.

To accurately determine the stratospheric ozone contribution from ^{7}Be and ^{32}P concentrations, it is essential to know (a)the $^{7}Be/O_3$ (and/or $^{32}P/O_3$) concentration ratios in the stratosphere, (b)the transport time from the tropopause to ground level, and (c) the removal of ^{7}Be (and/or ^{32}P) aerosols and ozone during the descent through the troposphere. We have recently reported [Dutkiewicz and Husain, 1979; Husain et al., 1980] on the determination of $^{7}Be/O_3$ concentration ratios in the stratosphere. The transport time from intrusion through the tropopause to arrival at ground level is likely to vary from event to event and season to season. No direct measurements of transport time are available, although Reiter and Mahlmen [1965] reported an incident of transport of radioactive fallout from the tropopause to the ground in approximately 2 days. Recently, Danielsen [1980] has used isentropic trajectories to trace back in time aircraft observations of high ozone concentrations at 5.4 km to the boundaries of the stratosphere. Danielsen [1980] determined a travel time of 3 days for high ozone episode observed on a flight from San Francisco, Calif., to Hilo, Hawaii.

The magnitude of the transport time bears directly on the mechanisms of stratosphere-troposphere exchange. Mean meridional circulation and large-

scale eddy transport in the vicinity of the jet streams (tropopause folding) are considered primarily responsible for most of the stratospheric-tropospheric exchange [Reiter, 1975, 1978; Danielsen, 1968, 1980; Danielsen and Mohnen, 1977]. However, the relative importance of the two mechanisms is still being debated. Danielsen [1980] has estimated the transport time via tropopause folding to be $\sim$ 100 times faster than that by the zonal-seasonal mean circulation. Hence a determination of transport time is not only important for accurate determination of concentrations of stratospheric species at ground-level but it bears directly on the exchange mechanisms as well.

In this paper we show that it is possible to determine transport time by using two cosmogenic radionuclides of different half-lives if their concentration ratios in the stratosphere and the aerosol mean residence time are known. We have used our measurements of daily ^{7}Be and ^{32}P concentrations at Whiteface Mountain, New York, to determine transport times. Since our technique uses ground level measurements it can conveniently provide data on a continuous year-round basis.

Experimental

The Whiteface Mountain field station is a weather observatory at the remote summit of Whiteface Mountain ($44^{o}N$, 1.5 km), operated by the Atmospheric Sciences Research Center of the State University of New York at Albany. At the upper floor of this observatory, total suspended particulate samples were collected daily with high-volume air samplers. Air was drawn in at the roof through a 20-cm-diameter aluminum pipe, which was warmed with heating coils during winter months to remove ice crystals. Four samplers were mounted horizontally in a sealed, stainless-steel sampling chamber, shown schematically in Fig. 1. Air entered the chamber through the inlet pipe in the roof and was drawn through 20 x 25-cm Whatman 41 filters by one of the high-volume blowers, which were run sequentially 24 h each (midnight to midnight in 1977 and 1978, and noon to noon in 1979). Sample inter-

ference was tested by operating a single sampler for 7 days, while the rest had blank filters. The blank filters had no detectable ^{7}Be activity (<30 pCi); the sampled filter had 1600 pCi ^{7}Be. To assure accurate air volumes, each sampler was equipped with a Sierra model 310 mass-flow controller, set at a flow rate of 1.3 m^3 (STP)/min. Controller calibration was checked periodically by measuring the pressure drop across a standard orifice and the manufacturer's calibration tables, with appropriate corrections for ambient temperature and pressure. Absolute uncertainty in the air volume was estimated to be ± 3%.

^{7}Be concentrations were determined by γ-ray spectroscopy of the whole filter [Husain et al., 1977]. The uncertainty in ^{7}Be concentrations is generally within ± 10%, except for samples with very low concentrations ($\leq$ 50 fCi/m^3; 1 fCi = 10^{-15} Ci). After γ-counting, 75% of each filter was used to determine ^{32}P and ^{33}P activity by low-level β-counting, after the phosphorus was radiochemically separated from the sample [unpublished procedure]. Uncertainties in ^{32}P counts are within ± 10% for concentrations > 3 fCi/m^3, approach ± 20% at 1 fCi/m^3, and rapidly increase for lower concentrations. The detection limit for ^{32}P was generally 0.4 fCi/m^3.

Transport Time for Air Descending from Tropopause to Ground Level

The interaction of cosmic ray protons and neutrons with oxygen, nitrogen, and argon atoms in the atmosphere produces ^{7}Be and ^{32}P. Their activity ratio is expressed as

$$\frac{^{7}Be}{^{32}P} = {}^{7}R_{32} = \frac{Q_7}{Q_{32}} \cdot \frac{(1-e^{-\lambda_7 t})}{(1-e^{-\lambda_{32} t})} \qquad (1)$$

where Q_7 and Q_{32} are the production rates of ^{7}Be and ^{32}P, λ_7 and λ_{32} are their

decay constants, and t is the length of time the air mass has been irradiated by cosmic rays.

In the stratosphere t is long compared to the ^{7}Be and ^{32}P half-lives, since the mean residence time of aerosols is ~1 year [Reiter, 1975]. Hence the ^{7}Be and ^{32}P activities can be safely considered to be in equilibrium, and (1) reduces to

$$^{7}R_{32}(\text{equil}) = \frac{Q_7}{Q_{32}} \tag{2}$$

Approximately 90 measurements in the stratosphere by Feely et al. [1971] yielded an average $^{7}R_{32}$ ratio of 80. Theoretical calculations by Lal and Peters [1967], using estimated reaction cross-sections and particle energy spectra, yielded $^{7}R_{32}(\text{equil}) = 100$. Considering the uncertainties involved in the theoretical calculations, as well as in experimental measurements, the agreement is excellent. Since the experimental measurements involve fewer assumptions, we shall use the measured $^{7}R_{32}(\text{equil})$ of 80 throughout this paper.

Mixing is far more rapid in the troposphere than in the stratosphere. Hence t is expected to be comparable to the ^{32}P half-life, and equilibrium $^{7}R_{32}$ ratio as expressed by (2) will not be achieved. In addition to the tropospheric production, the observed ^{7}Be and ^{32}P concentrations include a transported stratospheric component. In the absence of stratospheric air the observed ^{7}Be and ^{32}P ratios in the troposphere can be expressed as

$$^{7}R_{32} = \frac{\lambda_7}{\lambda_{32}} \cdot {}^{7}R_{32}(\text{equil}) \cdot \frac{\lambda_{32} + \frac{1}{\tau}}{\lambda_7 + \frac{1}{\tau}} \tag{3}$$

where τ is the mean tropospheric aerosol residence time.

The mean tropospheric residence time has been measured using radon daughters, fissiogenic ^{89}Sr and ^{90}Sr, or the cosmogenic ^{7}Be and ^{32}P [see, for example, Martell and Moore, 1974]. The results tend to group according to the radionuclides used: of the order of 6 days for radon daughters [Martell and Moore, 1974], but about 30 days for fissiogenic ^{89}Sr and ^{90}Sr and cosmogenic ^{7}Be and ^{32}P [Beck and Kuroda, 1966; Bleichrodt, 1978]. Efforts have been made to reconcile mean residence times obtained by different techniques. For example, Kuroda et al. [1978] obtained roughly concordant residence times from the $^{89}Sr/^{90}Sr$ and $^{210}Po/^{210}Pb$ ratios in rain samples collected at Fayetteville, Arkansas. Gavini et al. [1974] showed that their data for radon daughters in sequential samples in rainstorms are consistent with a 30-day mean aerosol residence time. Since this work uses ^{7}Be and ^{32}P as tracers, the above arguments are quite compelling in favor of a 30-day mean residence time. Inserting in (3) the values τ = 30 days, $^{7}R_{32}(equil)$ = 80, and the well-known decay constants, we obtain a tropospheric $^{7}R_{32}$ ratio of 38. The variation of $^{7}R_{32}$ ratio with τ is not linear. For example, τ = 15 days will reduce $^{7}R_{32}$ only to 31, but at $^{7}R_{32}$ = 50, τ will be 74 days, unrealistically long for tropospheric aerosols. As will be seen later, the observed $^{7}R_{32}$ data are, in general, only slightly affected by relatively large variations of τ.

A stratospheric air mass entering the troposphere will mix with tropospheric air during subsidence. The mixing of two air masses with mean $^{7}R_{32}$ ratios of 38 and 80 will produce an observed $^{7}R_{32}$ ratio between 38 and 80, depending on the proportions of the stratospheric and tropospheric components. In addition, when stratospheric air resides in the troposphere for more than a few days, $^{7}R_{32}$ ratio in the stratospheric component will increase by a factor $e^{\alpha T}$, where $\alpha = (\lambda_{32} - \lambda_{7}) = 0.035$ and T is the time the stratospheric

air has resided in the troposphere. The larger the value of T, the larger $^{7}R_{32}$ ratio becomes. Thus observed $^{7}R_{32}$ ratios depend, not only on the relative amounts of stratospheric and tropospheric air present, but also on the transport time of the stratospheric air parcel within the troposphere:

$$^{7}R_{32} = \frac{(A_7)_{obs}}{(A_{32})_{obs}} = \frac{(A_7)_{obs}}{(A_{32})_{strat} + (A_{32})_{trop}} \tag{4}$$

where A represents radionuclide concentration in fCi/m^3. Expressing A_{32} in terms of the respective ^{7}Be concentrations and using $^{7}R_{32} = 80$ for stratosphere and 38 for troposphere, (4) becomes

$$^{7}R_{32} = \frac{(A_7)_{obs}}{\frac{(A_7)_{strat}}{80 \exp(\alpha T)} + \frac{(A_7)_{obs} - (A_7)_{strat}}{38}} \tag{5}$$

If f is the fraction of the observed ^{7}Be concentration which originated in the stratosphere, we can write

$$f = \frac{(A_7)_{strat}}{(A_7)_{obs}} = \frac{(A_7)_{obs} - (A_7)_{trop}}{(A_7)_{obs}} \tag{6}$$

From (5) and (6) we obtain

$$^{7}R_{32} = \frac{1}{\frac{f}{80 \exp(\alpha T)} + \frac{1-f}{38}} \tag{7}$$

From (7) T could be determined from the measured values of $^{7}R_{32}$ ratios if f is known.

Since f is the net fraction of stratospheric ^{7}Be reaching ground level, dilution need not be in one step but is permitted throughout subsidence in the troposphere. The influence of transport time on $^{7}R_{32}$ ratios for selected

Values of f, is shown in Fig. 2. For example, for a stratospheric air parcel subsiding without dilution, $^{7}R_{32}$ ratio would be $\geq$ 80. On the other hand, for a 50% stratospheric and 50% tropospheric air parcel, $^{7}R_{32}$ ratio will not exceed 68 even after 70 days in the troposphere. For cases where f $\leq$ 50%, meaningful estimates of T can not be made.

To describe an air parcel as, say 90% stratospheric does not mean that 90% of the air is of stratospheric origin; rather, 90% of its ^{7}Be content is of stratospheric origin. To illustrate this point, Dutkiewicz and Husain [1979] found an average lower stratospheric ^{7}Be concentration at 34°-42°N to be 4,200 fCi/m^{3}. Let a stratospheric air mass be represented by this concentration and $^{7}R_{32}$ = 80. A 20-fold dilution of such an air parcel with tropospheric air containing 50 fCi/m^{3} ^{7}Be (see discussion later) and $^{7}R_{32}$ ratio of 80, would yield a ^{7}Be concentration of (0.05 x 4,200 + 0.95 x 50) = 258 fCi/m^{3}. Although stratospheric air contribution was only 5%, the stratospheric ^{7}Be component (f) amounts to 81% of the resultant air mass. For such an air parcel $^{7}R_{32}$ ratio will be 258/(2.63 + 1.25) or 66.

It is obvious that even very small amounts of stratospheric air can seriously alter the tropospheric ^{7}Be and ^{32}P content. Therein lies the basis of the usefulness of cosmogenic nuclides as tracers of stratospheric air. As pointed out earlier, to determine the transport time, T, from (7) it is necessary to know f. This can be determined for individual cases from the measured ^{7}Be concentrations if $(A_7)_{trop}$ in (6) is known. Based on rather extensive ^{7}Be data for both the northern and southern hemispheres, we have previously shown [Husain et al., 1980] the average tropospheric ^{7}Be concentration to be about 50 fCi/m^{3} at ~44°N. The average tropospheric ^{7}Be component at Whiteface Mountain can also be determined from daily ^{7}Be and ^{32}P measurements at this site. Assuming that days when $^{7}R_{32} \leq 40$ correspond to purely tropo-

spheric air, we obtain an average ^{7}Be concentration of 60 fCi/m^3. This data set corresponds to 90 of the 420 days sampled. The two averages are in excellent agreement. Since the lower value (50 fCi/m^3) is based on data obtained globally over about 8 years, we will use it in this paper. However, if we were to use ^{7}Be tropospheric component of 60 fCi/m^3 the transport times will increase by about 1-3 days for $\underline{T} < 15$. In isolated cases, when f ~0.5 the effect may be larger. These differences are not critical to the main conclusions of the paper.

Results and Discussion

Daily ^{7}Be and ^{32}P concentrations and $^{7}R_{32}$ ratios measured at Whiteface Mountain in June-August 1977 and from June 1978 through December 1979 are given by month in a supplementary table.[1] In this total of 420 days $^{7}R_{32}$ ratio varied from ~20 to 250. The frequency distribution of $^{7}R_{32}$ ratios for 1977-79 is shown in Fig. 3.

In 1979 the $^{7}R_{32}$ ratio distribution peaked at a lower value (40-45) than in 1977 and 1978. This suggests either a smaller stratospheric ^{7}Be component or shorter transport times for the stratospheric air during 1979. The average ^{7}Be concentration was 100 fCi/m^3 in 1979, as against 140 fCi/m^3 in 1977-78. However, the 1977 and 1978 data covered only the summer and fall, so this comparison may be biased. Daily $^{7}R_{32}$ ratios for June-October 1978 at San Antonio Texas [Rusheed et al., unpublished data], were generally lower than at Whiteface Mountain. In 60% of the samples at San Antonio $^{7}R_{32}$ ratio was ≤ 45, in comparison with 21% for 1977 and 1978 and 35% for 1979 at Whiteface Mountain. Yet the maximum $^{7}R_{32}$ ratio at San Antonio was 87, while at Whiteface Mountain ~10% of the $^{7}R_{32}$ values were ≥ 100, suggesting a smaller stratospheric flux of ^{7}Be at San Antonio during this period.

[1]The supplementary table is available with the entire article on microfiche. Order from the American Geophysical Union.

Daily ^{7}Be, ^{32}P, and $^{7}R_{32}$ values can be used to deduce transport times from (6) and (7), as discussed earlier. Due to large variations in ^{7}Be and ^{32}P concentrations and the resultant large variations in $^{7}R_{32}$ ratios, not all data will yield meaningful values of $\underline{T}$. We shall therefore consider only the 56 days when $^{7}R_{32} \geq 60$ and the uncertainty in $^{7}R_{32}$ ratio was $\leq \pm 20\%$. Using $\underline{f}$ determined from (6) and $^{7}R_{32}$ as given in Table 1, we used (7) to deduce the transport times, which varied from 1 to 36 days (Table 1, Fig. 4). For 50% of the cases $\underline{T}$ was ≤ 5 days; for 85% of the cases it was ≤ 15 days. These results suggest that relatively short transport times from tropopause to the ground are relatively common occurrences. It should be emphasized that no realistic modification of any of the parameters in our formulation (7) will qualitatively change our results (Table 1). For example, if we were to increase the tropospheric ^{7}Be component from 50 to 100 fCi/m^3 (which we think to be gross overestimation) the data in Table 1 will yield an average transport time of < 20 days.

This observation could have a profound effect in determining whether the stratosphere-troposphere exchange occurs primarily via tropopause folding [Danielsen, 1968] or mean meridional motion [Reiter, 1975]. The tropopause folding events proceed rapidly, and air parcels may reach ground level in a few days. The stratospheric air parcel transported into the troposphere via mean meridional circulation will take longer to reach ground level. Reiter [1978] has estimated transport time via mean meridional motion in winter at ~50 days. Danielsen's [1980] estimate transport times of the order of 100 to 300 days. Our results are clearly incompatible with such long transport times.

Assuming that the tropopause folding events are associated with $\underline{T} \leq 15$ days, such events occur at Whiteface Mountain about 11% of the time, i.e., 40 events/year. If only 1979 data are considered (to minimize seasonal bias), there

were 26 such events on 284 days sampled, or 33 events/year. This is significantly higher than the 22 and 23 events given by Reiter [1975] for the whole North American longitude sector during 1963 and 1964, particularly since the meridional profile of ^{7}Be suggests that the maximum exchange of stratospheric air occurs at ~30°N [Husain et al., 1980].

The longest transport times were generally observed during September 1978 (Table 1). The averages were $\underline{T}$ = 16 days for fall plus winter and $\underline{T}$ = 7 days for spring plus summer. However, there were many cases, primarily during September 1978 and early 1979, where ^{32}P concentrations were very low resulting in high values of $^{7}R_{32}$ (> 80). Due to the low ^{32}P activity in these samples, uncertainties in $^{7}R_{32}$ are large (> ± 20%) so they have not been included in Table 1. Generally high $^{7}R_{32}$ ratios will yield larger values of $\underline{T}$. For example, of the 50 days sampled during January and February, 1979, 21 had $^{7}R_{32}$ > 80, and many were only lower limit results. A lower limit estimate of $\underline{T}$ can be made with these results by setting $\underline{f}$ = 1.0 in (7). A value of $\underline{T}$ > 20 days is obtained for these 21 days. Thus, the transport of stratospheric air to this site is slower by at least a factor of 3 during this period compared to spring and summer months.

For September-December 1979 $^{7}R_{32}$ and ^{7}Be concentrations were generally low, suggesting little stratospheric influx. However, during September 1978 there were episodes where both $^{7}R_{32}$ and ^{7}Be concentration were high. We will look at these episodes in detail.

The daily variations in ^{7}Be concentration and $^{7}R_{32}$ ratios for August-September 1978 are shown in Fig. 5. On August 20 an unusually high ^{7}Be concentration of 350 fCi/m^{3} was observed. The $^{7}R_{32}$ was also high (72), suggest-

ing the presence of stratospheric air. ^{7}Be concentrations exceeding 200 fCi/m^3, or about 5% of the stratospheric value [Dutkiewicz and Husain, 1979], were observed on August 22 and on September 16, 18, 19, 23, 26 and 27. The $^{7}R_{32}$ ratios were also high. From (7) we have determined the transport times for the peak ^{7}Be days in August-September, and from the transport times we have back-calculated the days on which the stratospheric air entered the troposphere, (Table 2).

Our calculations suggest that air parcels entered the troposphere between August 16 and 19. The August 20 sample yields a transport time of 1 day, pinpointing an intrusion on August 19. The samples collected on September 13, 14, 18 and 24 suggest intrusion during August 16-19, but the uncertainties in the determination of T are sufficiently large that from September samples we cannot pinpoint intrusion times a month before. If these samples originated from the same intrusion, the August 20 sample suggests August 19 as the date of entry of the stratospheric air.

The possibility that the September samples originated from the same intrusion finds support in the measured $^{7}R_{32}$ ratios. In Fig. 5 we show a decay curve for ^{7}Be half-life 53.4 days/^{32}P (14.3 days), assuming a stratospheric intrusion on August 19. This curve, which corresponds to the maximum $^{7}R_{32}$ ratio possible for stratospheric air entering the troposphere around August 19, fits the measured $^{7}R_{32}$ data fairly well, implying that a parcel of stratospheric air had remained relatively intact in the troposphere for about a month. Because the uncertainties in $^{7}R_{32}$ for September 5, 8, 15-17, and 23 exceed ± 20%, these days were not considered in Tables 1 and 2. However, data for these dates agree with the decay curve in Fig. 5.

On September 13-16 the ^{7}Be concentration and $^{7}R_{32}$ increased together (Fig. 5), with $^{7}R_{32}$ = 260 on September 17, when ^{7}Be was 160 fCi/m^{3}. On September 18 ^{7}Be increased to 330 fCi/m^{3}, while $^{7}R_{32}$ decreased to 140. On September 19 ^{7}Be peaked at 350 fCi/m^{3}, while $^{7}R_{32}$ ratio fell to 70. The high ^{7}Be concentration and falling $^{7}R_{32}$ on September 19 suggests the arrival of a fresh stratospheric air mass (Table 2), whereas on September 15-17 $^{7}R_{32}$ was consistent with stratospheric air which had been in the troposphere for 25-30 days. These changes in ^{7}Be and $^{7}R_{32}$ on September 13-20 give the impression of two separate layers of stratospheric air subsiding, with the bottom layer (the one arriving first) having spent considerable time in the troposphere prior to subsidence. A similar situation may have occurred on September 22-28. Analysis of meterologic data aloft during this period may help to varify whether a large, stable stratospheric subsidence had occurred, as suggested by the ^{7}Be and $^{7}R_{32}$ data (Table 2, Fig. 5).

Conclusion

We have developed a method to determine transport times of stratospheric air parcels from the tropopause to ground level. The method is based on measurements of ^{7}Be and ^{32}P concentrations in aerosols. The transport times are rapid (50% of the time, $\leq$ 5 days; 85% of the time, $\leq$ 15 days), although isolated transport times of about 30 days are observed, generally during fall or winter months. The transport times determined here are consistent with those determined by Danielsen [1980] for tropopause folding events, but inconsistent with times estimated for mean meridional motion. Our results suggest tropopause folding as the dominant mechanism for the mass exchange between stratosphere-troposphere, at least during the spring and summer months.

Acknowledgements. This work was partially supported by U.S. Department of Energy Contract DE-AC02-77EV04501. We are grateful to the Atmospheric Sciences Research Center, State University of New York at Albany for assistance in sample collection; to A. R. Khan for the radiochemical analyses of ^{7}Be and ^{32}P; and to J. M. Matuszek, Jr. and our Division's Radiological Sciences Laboratory for ^{7}Be counting.

References

Beck, J.N. and P.K. Kuroda, Radiostrontium fallout from the nuclear explosion of October 16, 1964, J. Geophys. Res., 71, 2451-2456, 1966.

Bleichrodt, J.F., Mean tropospheric residence time of cosmic-ray-produced Beryllium-7 at north temperate latitudes, J. Geophys. Res., 83, 3058-3062, 1978.

Danielson, E.F., Stratospheric-tropospheric exchange based on radioactivity, ozone and potential vorticity, J. Atmos. Sci., 25, 502-518, 1968.

Danielson, E.F., Stratospheric source for unexpectedly large values of ozone measured over the Pacific Ocean during Gametag, August 1977, J. Geophys. Res., 85, 401-412, 1980.

Danielson, E.F., and V.A. Mohnen, Project Duststorm report; Ozone transport, in situ measurements, and meteorological analysis of tropopause folding, J. Geophys. Res., 82, 5867-5877, 1977.

Dutkiewicz, V.A. and L. Husain, Determiantion of stratospheric ozone at ground level using ^{7}Be/Ozone ratios, Geophys. Res. Lett., 6, 171-174, 1979.

Feely, H., J.P. Friend, H. Seitz, J.D. Martin, and W.E. Erlebach, Final report of Project Stardust, DASA-2166-3, Isotopes, Inc., 1971.

Gavini, M.B., J.N. Beck and P.K. Kuroda, Mean residence times of the long-lived radon daughters in the atmosphere, J. Geophys. Res., 79, 4447-4452, 1974.

Husain, L., P.E. Coffey, R.E. Meyers, and R.T. Cederwall, Ozone transport from stratosphere to troposphere, Geophys. Res. Lett., 4, 363-365, 1977.

Husain, L., A. Rusheed, and V.A. Dutkiewicz, Sources of natural ozone: Statospheric intrusions in Texas, in Proceedings of the Ozone/Oxidants: Interactions with the Total Environment Speciality Conference, Air Pollution Control Association, 247-259, 1979.

Husain, L., V.A. Dutkiewicz, and A. Rusheed, On the origin of tropospheric ozone, submitted to Nature, 1980.

Kuroda, P.K., P.Y. Daniel, A. Nevissi, J.N. Beck and J.L. Meason, Atmospheric residence times of Sr-90 and Pb-210, J. Radioanal. Chem., 43, 443-450, 1978.

Lal, D., and B. Peters, Cosmic-ray produced radioactivity on the earth, Handbuch der Physik, 46, (ed. K. Sitte), Springer-Verlag, Heidelberg, 551-612, 1967.

Martell, E.A. and H.E. Moore, Tropospheric aerosol residence times: A critical review, J. Rech. Atomos., 8, 903-910, 1974.

Reiter, E.R., Stratospheric-tropospheric exchange processes, Rev. Geophys. and Space Phys., 13, 459-474, 1975.

Reiter, E.R., Impact of stratospheric ozone on tropospheric concentrations, Air Quality Meteorology and Atmospheric Ozone, ASTM STP 653, A.L. Morris and R.C. Barras, Eds., American Society for Testing and Materials, 506-519, 1978.

Reiter, E.R. and J.D. Mahlman, Atmospheric transport processes leading to radioactive fallout over the United States in November 1962, in Radioactive Fallout from Nuclear Weapons Tests, USAEC, CONF-765, 450-463, 1965.

TABLE 1. Estimated Transport Time of Air from the Tropopause to Whiteface Mountain for Selected Days during 1977-1979

Date		$^{7}R_{32}$	^{7}Be (fCi/m^3)	f	T* (days)
1977					
July	20	63	250	.80	~1
	21	70	270	.81	3
	22	80	140	.64	27
	24	65	210	.76	2
	25	68	175	.71	6
	28	61	325	.85	~1
	29	61	245	.80	~1
	31	67	195	.74	4
August	3	66	190	.74	3
	6	81	160	.69	20
	7	62	165	.70	2
1978					
June	4	65	205	.76	~1
	6	82	295	.83	8
	16	98	185	.73	31
	20	77	180	.72	13
July	6	67	200	.75	3
	7	74	185	.73	10
	8	70	215	.77	4
	12	82	200	.75	14
	19	99	230	.78	23
August	7	65	170	.71	4
	20	72	350	.86	~1
September	13	80	140	.64	27
	14	89	160	.69	29
	18	136	340	.86	30
	19	71	370	.86	~1
	24	99	170	.71	36
	26	82	270	.81	10
1979					
January	19	62	175	.71	~1
February	15	111	290	.83	23
	18	78	185	.73	13
	22	65	185	.73	3
March	3	87	245	.80	13
	17	60	110	.55	10
	27	66	245	.80	~1
April	10	60	110	.55	10
	17	61	185	.73	~1
	19	61	210	.77	~1
	20	68	270	.81	~1
May	5	67	140	.64	11
	6	63	175	.71	2
	28	61	110	.55	11
June	13	68	175	.71	6
	15	60	175	.71	~1
	16	75	180	.72	12
	19	67	195	.74	4
	27	64	215	.77	~1
July	3	62	160	.69	2
	7	68	150	.66	10
	9	65	170	.71	4
	13	61	190	.74	~1
	22	62	210	.77	~1
	28	76	190	.74	11
August	12	75	150	.66	18
September		NONE			
October	18	61	110	.55	11
November	23	64	140	.64	7
December		NONE			

*When the transport time is of the order of a few days, say 1 to 3 days, the change in $^{7}R_{32}$ ratio due to the decay of ^{32}P and ^{7}Be is relatively small. Consequently, the uncertainty in the determination of T is relatively large. We have indicated this by an approximate sign for all values of T = 1 day.

Table 2. $^{7}R_{32}$, ^{7}Be Concentration, Transport Time of Stratospheric Air, and Tropospheric Entry Date for Selected Days at Whiteface Mountain

Date (1978)	$^{7}R_{32}$	^{7}Be (fCi/m^3)	T (days)	Date entering the troposphere
August 20	72	350	1	August 19*
September 13	80	140	27	August 17*
14	89	160	29	August 16*
18	136	340	30	August 19*
19	71	370	1	September 18†
24	99	170	36	August 19*
26	82	270	10	September 16†

*Within the experimental uncertainties of the measurements we may be sampling one stratospheric intrusion around August 16-19, 1978.

†Within the experimental uncertainties there may only be one intrusion occurring around September 18.

FIGURE CAPTIONS

Fig. 1. Schematic of the high-volume air sampling unit. (1) Observatory roof. (2) Air inlet pipe. (3) Stainless-steel chamber. (4) High-volume blowers. (5) 20 x 25-cm filter holders. (6) Mass-flow controller probe. (7) Door gasket.

Fig. 2. Variation of $^{7}Be/^{32}P$ ratios with transport time for selected percentages of stratospheric ^{7}Be (f).

Fig. 3. Frequency distribution of $^{7}Be/^{32}P$ ratios for June-August 1977 and June-October 1978 (lower histogram) and for all of 1979 (upper histogram).

Fig. 4. Frequency distribution of transport times (T) for stratospheric air to Whiteface Mountain for selected days (Table 2).

Fig. 5. Daily ^{7}Be concentration and $^{7}Be/^{32}P$ ratios for August-September 1978. Periods of $^{7}Be > 200$ fCi/m^{3} are indicated by arrows. The shaded portions of the upper figure indicate periods when $^{7}R_{32} > 80$. The solid curve is the predicted change in $^{7}Be/^{32}P$ ratio for stratospheric air which entered the troposphere on August 19, as explained in the text.

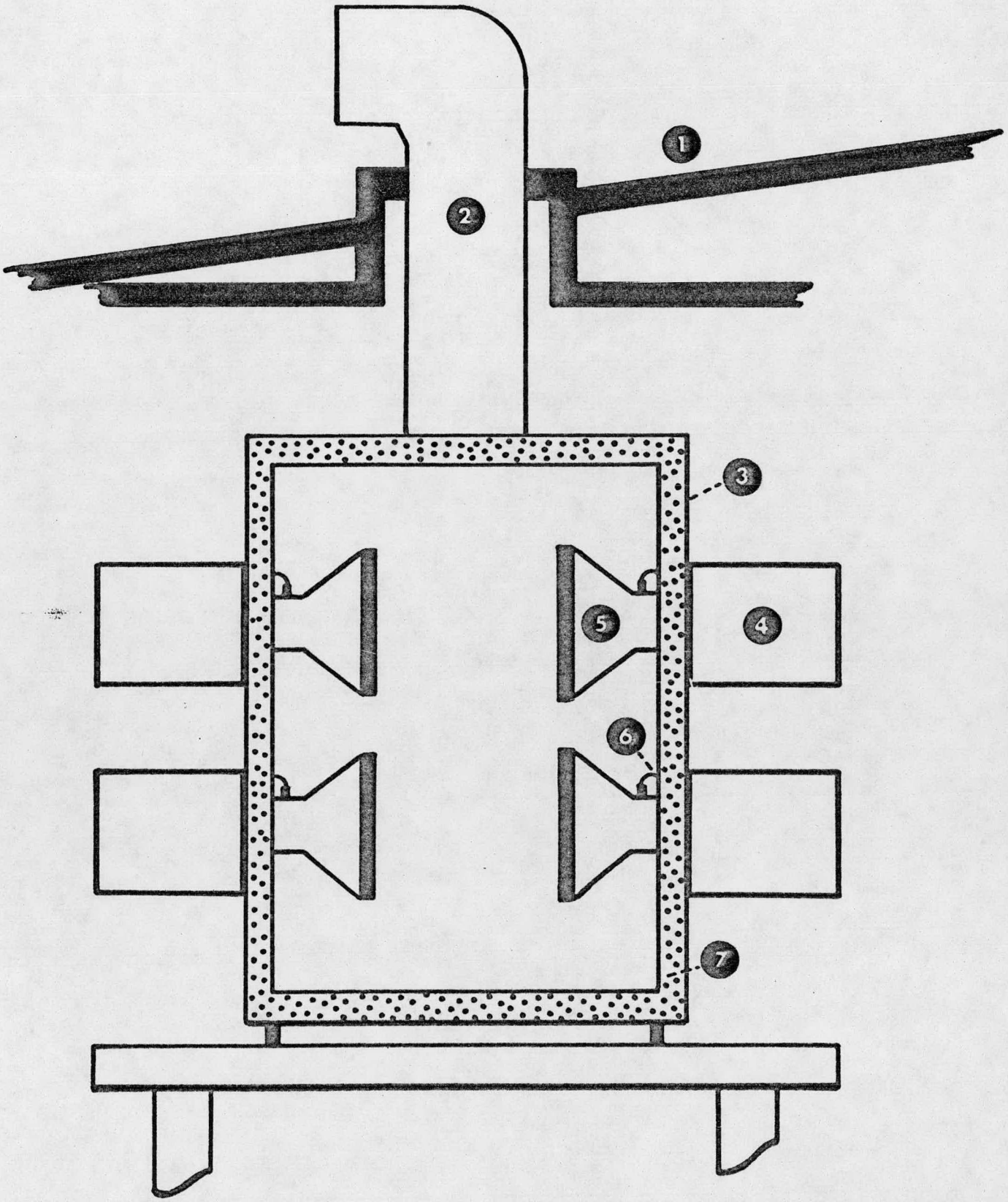

Fig. 1

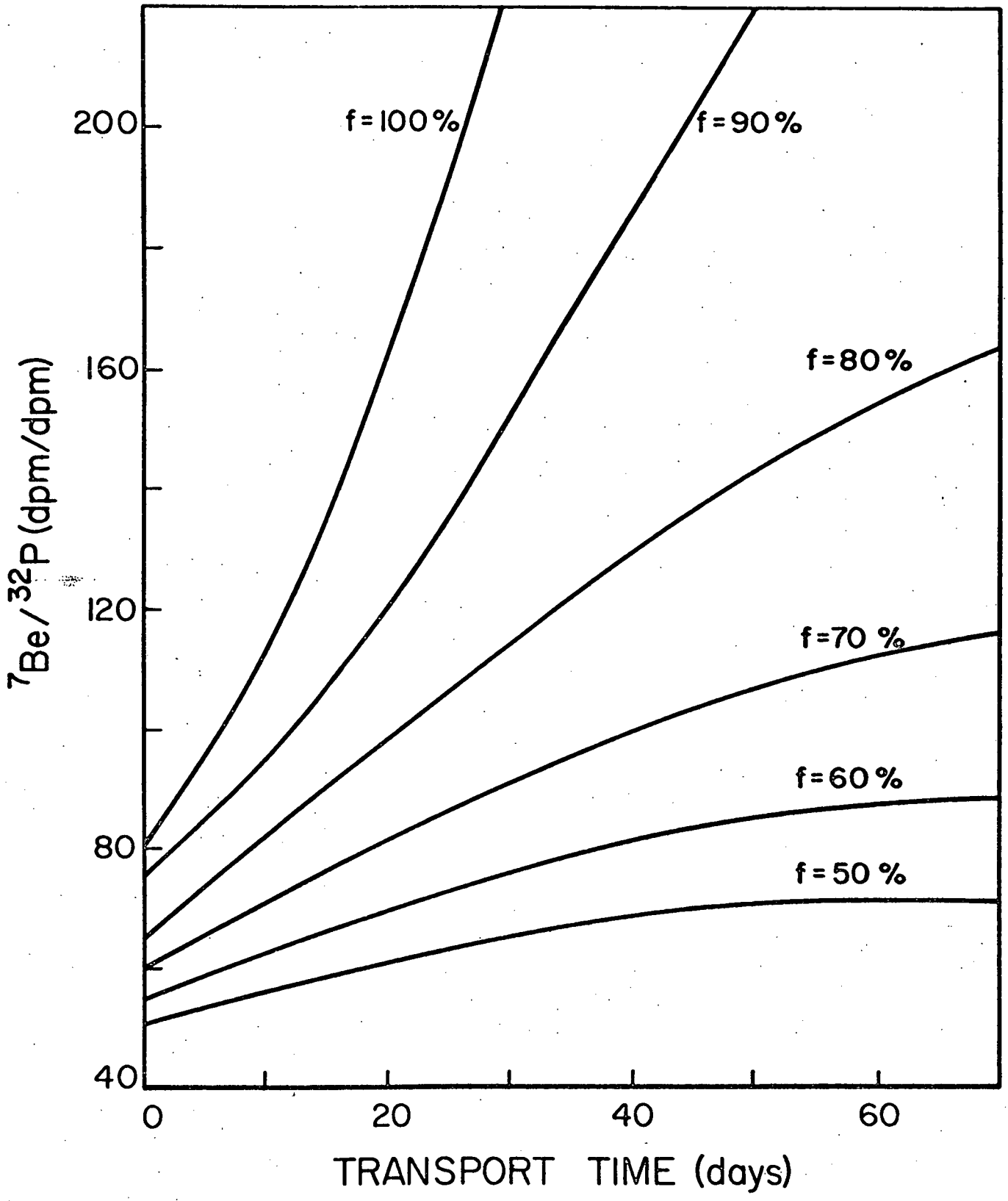
f=100%
f=90%
f=80%
f=70%
f=60%
f=50%
200
160
120
80
40
0
20
40
60
$^{7}Be/^{32}P$ (dpm/dpm)
TRANSPORT TIME (days)

Fig. 2

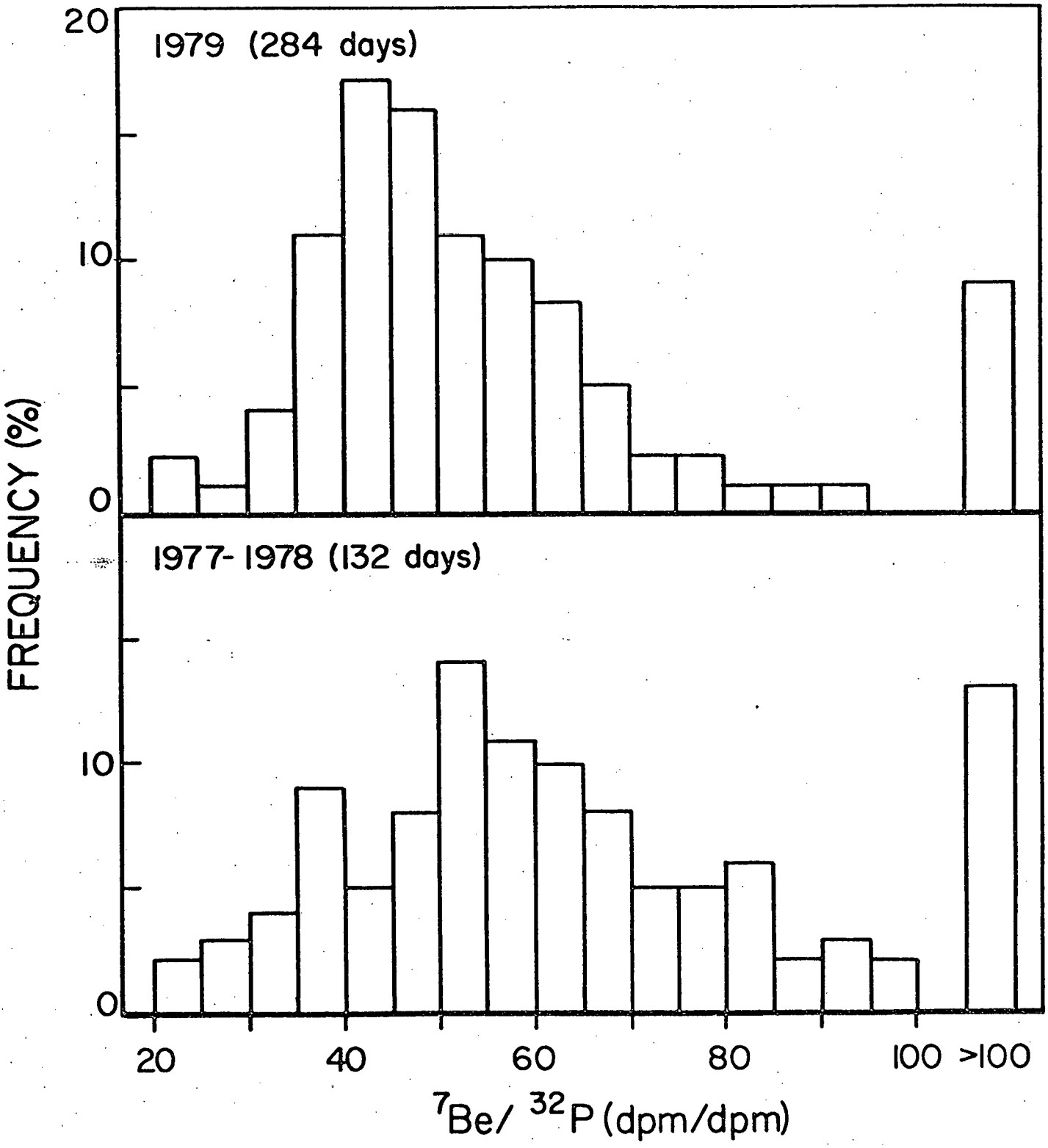
1979 (284 days)
1977-1978 (132 days)
FREQUENCY (%)
20
10
0
10
0
20
40
60
80
100
>100
$^{7}Be/^{32}P$ (dpm/dpm)

Fig. 3

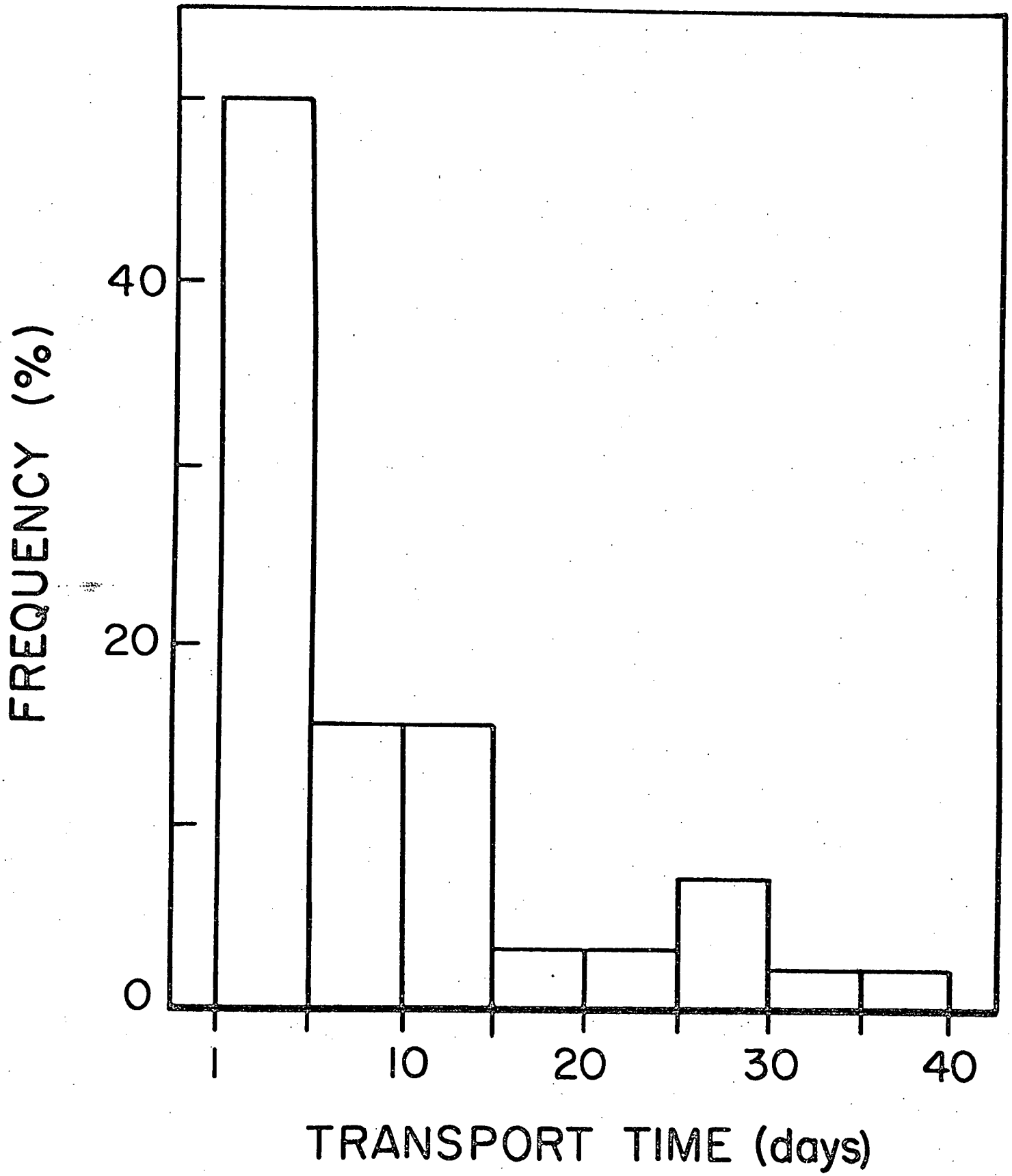

Fig. 4

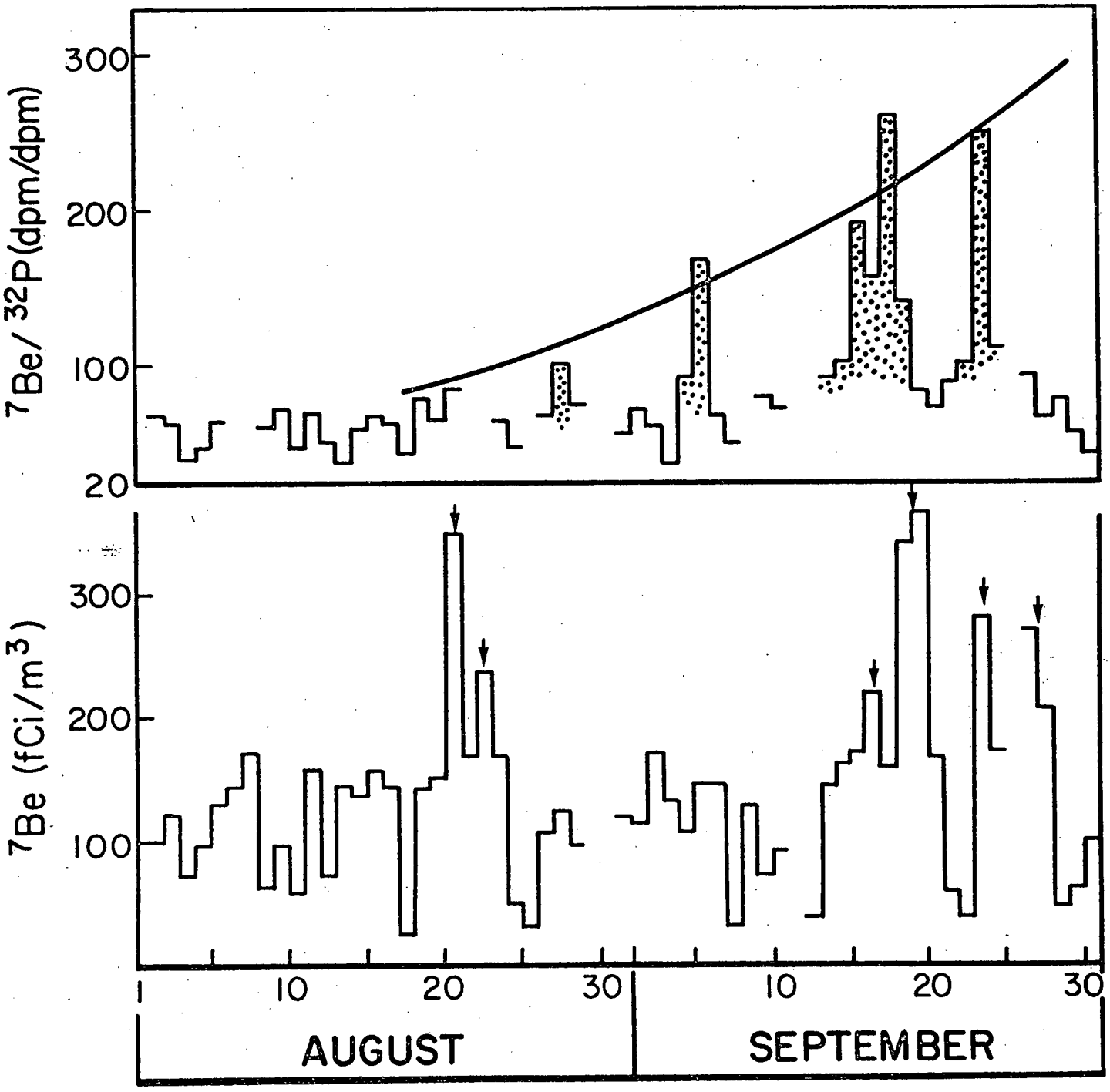
$^{7}Be/^{32}P$(dpm/dpm)
300
200
100
20
^{7}Be (fCi/m^{3})
300
200
100
1
10
20
30
10
20
30
AUGUST
SEPTEMBER

Fig. 5

Supplementary Table Daily ^{7}Be and ^{32}P Concentrations and $^{7}R_{32}$ ratios for 1977-79 at Whiteface Mountain

ay	^{7}Be (fCi/m^3)	$^{32}P^a$ (fCi/m^3)	$^{7}R_{32}$	^{7}Be (fCi/m^3)	$^{32}P^a$ (fCi/m^3)	$^{7}R_{32}$	^{7}Be (fCi/m^3)	$^{32}P^a$ (fCi/m^3)	$^{7}R_{32}$
		JUNE 1977			JULY 1977			AUGUST 1977	
1				205			240	4.8	49
2				110			170	3.8	45
3				350			190	2.9	66
4				260			175	4.9	36
5				225			95	2.4	39
6				200			160	2.0	81
7				80			165	2.6	62
8				45			105	2.9	36
9				100					
0				110					
11							135	2.8	49
2							170	2.9	59
13							235		
4							125	2.5	51
15	500						100	1.3[b]	76
6	505								
17	275								
18	100								
9	110			295	5.4	55			
20	70			250	4.0	63			
1	135			270	3.8	70			
22	105			140	1.8	80			
3	80			155	2.9	55			
24	205			210	3.2	65			
5	205			175	2.6	68			
26	120								
7	185			130	2.8	47			
28	355			325	5.3	61			
29	140			245	4.0	61			
0	130			80	1.3[b]	61			
3				195	2.9	67			

Supplementary
Table (con't)

Day	JUNE 1978			JULY 1978			AUGUST 1978		
1	35						100	1.7	58
2	150	2.9	51				120	2.2[c]	54
3				225	3.0[b]	117	70	2.4[c]	29
4	205	3.1	65				100	2.8[c]	35
5	205	≤1.8					130	2.5[b]	52
6	295	3.6	82	200	3.0[b]	67	140	1.2[b]	118
7	75	1.0[b]	75	185	2.5	74	170	2.6	65
8	45	0.5[c]	90	215	3.1	70	65	1.3[c]	50
9				45	1.6[b]	27	95	1.6[c]	61
0	260	1.8[b]	140	95	1.1[b]	85	55	1.5[b]	38
1	230	4.0[b]	58	50	≤0.7		155	2.7[b]	58
2	230			195	2.4	82	70	1.7[c]	40
3	20	≤0.4		235	4.0	59	145	5.8	25
4	110	≤0.4		160	3.6	45	135	2.8[b]	48
5	190	1.1[c]	172	145	3.0	49	170	3.1[b]	54
6	185	1.9	98	170	3.4	50	145	2.8[b]	51
7	150	3.9	38	125	2.1[b]	59	25	0.9[c]	31
8	110	2.9	38	220	3.7	59	145	2.2[b]	66
9	60			230	2.3[b]	99	150	2.9	52
0	180	2.3	77	300	5.1[b]	59	350	4.9	72
1	230	5.2	44	210	4.1[b]	51	165		
2				90	1.8[b]	49	240		
3	110	2.7	41	100	2.5	39	165	3.3	51
4	235	1.0[c]	234	150	≤0.8		50	1.4[b]	34
5	180	4.1	43	155	2.5[b]	61	35	≤0.4	
6	150	2.8	53	175	4.0[b]	44	105	1.8[b]	57
7	150	3.0	51	115	2.8[b]	41	125	1.4[C]	90
8	120	1.3[b]	91	55	≤0.6		95	1.5[b]	62
9	105	0.5[c]	130						
0				65	1.1[b]	57			
1				105	0.9[c]	114	120	2.7[b]	45

Supplementary
Table (con't)

D	SEPTEMBER 1978			OCTOBER 1978			NOVEMBER 1978
1	115	1.9[b]	60	55	1.1[b]	53	
2	170	3.4[b]	50	75	1.3[b]	59	180
3	130	5.4[b]	24	72	0.9[b]	76	190
4	105	1.3[b]	78	45	0.7[c]	63	215
5	145	0.9[b]	160	40	0.5[c]	84	
6	145	2.7	54	60	1.8	32	
7	30	0.8[b]	39	≤ 7	≤0.5		110
8	130	≤1.4		≤16	≤0.4		95
9	60	0.9[b]	65	55	0.8[b]	69	160
10	90	1.5[b]	60	70	1.9	37	
11				30	1.2[b]	25	175
12	40	≤0.4		165	5.1	32	
13	140	1.8	80	50	2.1[b]	24	
14	160	1.8	89	≤ 9	≤0.4		25
15	170	0.9[b]	190	45	1.3	35	90
16	215	1.4[b]	155	110	1.6[b]	70	
17	160	0.6[c]	260	60	0.7[b]	81	220
18	340	2.5	136	85	2.2	39	20
19	370	5.2	71	85	1.5	56	80
20	165	2.8	59	115	1.8[b]	64	185
21	60	0.8[c]	74	120	1.6[b]	75	150
22	40	0.4[c]	88	175	3.7[b]	47	155
23	280	1.1[b]	250	50			95
24	170	1.7	99	15			
25				130			
26	270	3.3	82	50			
27	205	3.8	54				
28	40	0.6[c]	63	25			
29	65	1.5	45	70			120
30	100	3.4	30				
31							

Supplementary Table (con't)

Day	DECEMBER 1978	JANUARY 1979			FEBRUARY 1979		
1					30	≤0.5	
2					30	≤0.4	
3					125	1.0[b]	123
4		40	≤0.5		65	1.0[b]	65
5		190	0.8[c]	236	75	≤0.5	
6	110				135	≤0.6	
7	215				120	0.8[b]	152
8	40				50	≤0.6	
9		40			60	0.4[c]	145
10	70	35	≤0.4		100	0.7[b]	144
11	25	55	≤0.5		125	0.8[b]	157
12		75	1.1[b]	69	95	≤0.7	
13	100	10	0.6[c]	20	135	1.3[b]	102
14	45	45	≤0.4		220	1.4[b]	155
15	85	110	≤0.5		290	2.6	111
16		100	0.6[c]	165	140	0.8[b]	175
17	55	85	≤0.4		140	0.8[b]	175
18	80	80	0.6[c]	132	185	2.4	78
19		175	2.8	62	190	4.0	47
20					160	3.5	45
21		7	≤0.6		75	1.0[b]	75
22		35	≤0.7		185	2.8	65
23		140	0.6[c]	230	65	1.2[b]	54
24		80	0.6[c]	130	40	0.8[b]	52
25		15	≤0.5		45	0.8[b]	56
26		≤5	≤0.7		≤5	≤0.5	
27		15	≤0.8				
28		≤5	≤0.5		130	2.4	54
29		10	≤0.5				
30		10	≤0.5				
31		15	≤0.5				

Supplementary
Table (con't)

Day	MARCH 1979			APRIL 1979			MAY 1979		
1							40	0.9[b]	47
2	50	1.1[b]	46	≤6	≤0.4		145	3.3	44
3	245	2.8	87	105	1.6[c]	66	65	1.0[b]	65
4	40	≤0.8		85	1.5[b]	55	55	0.9[b]	61
5	8	≤0.4		50	1.1[c]	46	140	2.1	67
6	110	1.5[b]	72	20	0.6[c]	33	175	2.8	63
7	50	1.3[b]	39	25	≤1.3		160	2.8	57
8	40	1.0[c]	40	215			≤9	≤0.4	
9	60	0.9[c]	65				150	2.9	51
10	55	1.0[b]	53	110	1.8	60	25	0.6[b]	40
11	55	0.8[c]	66	95	1.9	50	145	2.9	49
12	160	2.8	56	60	1.1[b]	55	45	0.9[b]	49
13	85	1.4[b]	62	105	1.6[b]	66	90	2.0	45
14	75	1.4[b]	55	35			165	3.2	52
15	90	1.2[b]	73	25	≤1.0		120	2.6	46
16	80	2.5	31	30	≤0.4		75	1.3[b]	58
17	110	1.8	60	185	3.0	61	220	4.1	53
18	135	1.5[b]	89	180	3.1	59	90	1.5[b]	61
19	120	0.9[b]	136	210	3.5	61	30	0.6[c]	52
20	65	0.9[b]	73	270	4.0	68	85	2.2	39
21	70	1.0[b]	70	240	4.5	53	105	2.1	53
22	90	3.5	25	110	2.5	44	200	3.7	54
23	115	2.2	53	95	2.5	39	180	4.2	43
24	115	3.7	30	180	4.1	44	50	0.9[b]	57
25	35	0.9[b]	35	170	3.2	53	70		
26	75	2.3	33	90	2.3	40	10		
27	245	3.7	66	14	≤0.4		80	1.7	39
28	205	6.7	30	70			110	1.8	61
29	40			95	2.3	41	95	2.1	46
30	25			125	2.1	59	60	1.6	39
31	195	2.6[b]	75				85	1.8[b]	48

Supplementary
Table (con't)

	JUNE 1979			JULY 1979			AUGUST 1979		
1	105	2.2	48				140	3.1	45
2	155	3.4	46	75	1.4[b]	54	60		
3	185	4.1	45	160	2.6	62	160	4.0	40
4	235	5.4[b]	43	70	0.9[b]	80	180	3.2	56
5	175	3.7	47				100	2.5	40
6				130	2.4	54	85	1.6[b]	54
7	55	1.7	33	150	2.2	68	130	3.1	42
8	150	3.0	49	170	3.1	55	110	2.2	50
9	135	2.9	46	170	2.6	65	120	2.9	41
10	65	1.4[c]	47	190	3.7	51	20	0.5[c]	38
11	≤50	≤0.7		90	2.0	45	65	1.8	37
12	70	≤0.4		130	2.8	46	150	2.0	75
13	175	2.6	68	190	3.1	61	130	2.4	54
14	185	3.7	50	160	3.6	44	20	0.5[c]	44
15	175	3.0	60	85	2.0	42	35	0.6[c]	58
16	180	2.4	75	120	2.7	44	130	0.8[b]	160
17	200	3.9	52	100	2.2	45	150	3.6	42
18	95	2.2	43	150	2.6	58	20	0.6[c]	33
19	195	2.9	67	200	4.1	49	50	2.0	25
20	160	3.2	50	230	4.1	56	55	1.3[b]	43
21	195	3.8	51	250	4.7	53	80	1.4[b]	57
22	175	3.6	48	210	3.4	62	170	3.9	44
23	≤55	≤0.4		230	4.1	56	70	1.9	37
24	≤65	≤0.5		180	4.4	41	40	0.6[c]	63
25	155	3.3	46	30			≤6	≤0.4	
26	155			80	1.8	44	55	1.6	36
27	215	3.4	64	90	1.8	49	90	2.9	32
28	180	2.7	49	190	2.5	76	80	2.2	37
29	160	3.0	53	150	3.1	48	45	1.3[b]	35
30	100	2.0	50	110	3.5	31	90	2.4	41
31				95	2.4	39	100	1.6[b]	63

Table 4 (con't)

	SEPTEMBER 1979			OCTOBER 1979			NOVEMBER 1979		
1	130	3.4	38	120	2.9	41	80	1.5[b]	55
2	75	1.5[b]	49	130	2.9	45	60	≤0.6	
3	55			60			55	1.1[b]	50
4	80	2.2	36	100	2.5	40	55	1.3[b]	41
5	105	3.0	35	40	0.9[b]	45	120	2.9	41
6	≤15	≤0.4		70	1.6[b]	43	45	0.9[b]	52
7	90	1.3[b]	70	≤15	≤0.4		55	1.4[b]	38
8	45	0.5[c]	86	20	≤0.4		110	3.0	37
9	105	1.8	58	20	≤0.4		≤11	≤0.5	
10	50	1.1[b]	47	60	1.0[b]	59	55	1.0[b]	57
11	25	≤0.4		45	1.0[b]	43	110	2.5	44
12	115	3.5	33	≤15	≤0.4		120	1.3[b]	92
13	100	2.0	49	≤ 9	≤0.4		40	1.0[b]	39
14	≤15	≤0.4		≤25	≤0.4		30	1.0[b]	30
15	40	0.7[c]	59	≤10	≤0.4		30	1.2[b]	23
16	95	1.5[b]	64	60	1.4[b]	44	≤13	≤0.4	
17	100	2.1	49	55	1.2[b]	44	25	0.5[c]	50
18	75	1.8	41	110	1.8	61	120	2.7	44
19	95	2.5	38	85	1.2[b]	71	140	3.3	42
20	135	3.4	40	110	2.0	55	80	2.0	39
21				140	2.5	56	140	3.3	42
22	70	1.1[b]	64	95	1.6[b]	59	30	0.5[c]	62
23	120	2.2	55	70	1.4[b]	49	140	2.2	64
24	125	2.8	44	≤ 7	≤0.4		70	1.1[b]	64
25				≤11	≤0.5		40	0.8[b]	53
26	140	3.3	42	≤10	≤1.0		≤10	≤0.4	
27	115	2.1	54	60	≤0.5		110	2.1	52
28	110	2.4	47	≤10	≤0.4		25	0.7[c]	39
29	95	2.2	43	20	0.6[c]	37	≤10	≤0.4	
30				85	1.1[b]	79	40	1.0[b]	41
31				140	2.9	48			

Supplementary
Table (con't)

Day	DECEMBER 1979		
1	50	1.3[b]	40
2	40	0.8[b]	49
3	100	1.8	57
4	35	0.7[c]	49
5	125	2.8	44
6	80	1.8	43
7	25	0.6[c]	45
8	50	1.2[b]	40
9	55	1.5[b]	38
10	135	3.5	39
11	150	3.6	42
12	55	2.0	27
13	55	1.5[b]	35
14	60	1.9	32
15	120	3.4	35
16	50	1.0[b]	49
17	40	1.9	22
18	115	2.3	49
19	165	4.0	41
20	120	2.4	49
21	85	2.2	39
22	125	2.6	48
23	25	≤0.5	
24	35	0.9[b]	37
25	≤12	≤0.4	
26	≤ 8	≤0.4	
27	≤ 9	≤0.5	
28	25	1.1[b]	23
29	15	0.6[c]	23
30	60	1.5[b]	39
31			

[a]Uncertainty <± 15% unless otherwise shown.

[b]Uncertainty, ± 15 to ± 30%.

[c]Uncertainty >± 30%.

APPENDIX V

DETERMINATION OF TOTAL PARTICULATE SULFUR AT WHITEFACE MOUNTAIN, N.Y., BY PYROLYSIS MICROCOULOMETRY

EDMONDO CANELLI and LIAQUAT HUSAIN

Division of Laboratories and Research, New York State Department of Health, Albany, New York 12201

Abstract - Total particulate sulfur (TPS) in air samples can be determined by a technique based on thermal volatilization at 1000°C, followed by controlled oxidation of sulfur compounds to SO_2 and coulometric titration of SO_2 with iodine. Calibration curves are linear within 5% from 0.1 to 10 µg S, the detection limit is 0.10 µg S (equivalent to 35 ng S m^{-3} when 2000 m^3 of air are filtered), and the relative standard deviations (n = 10) are 48 and 5.1% at the 0.10 and 4.0 µg S levels. Recoveries for 20 organic and inorganic compounds, including refractory sulfates, elemental sulfur, sulfides, sulfites, sulfonates, and sulfones, vary from 79 to 88%. No interferences are observed for a number of non-sulfur-containing compounds, including nitrates, benzene, acetone, glucose, cellulose, silicates and carbonates. The technique was also used to determine the presence of non-sulfates and of non-water-soluble sulfates. Both TPS, using this technique, and water-soluble sulfate (WSS), using the methyl thymol blue method, were determined in daily air particulate samples collected at Whiteface Mountain, N.Y. during both winter and summer. Comparison of TPS and WSS values showed that WSS could usually account for all of the sulfur present in the samples. Occasionally during the summer

---

months, however, elevated TPS values indicated the presence of sulfur in excess of the WSS value. The TPS concentrations ranged from 0.1 to 9.7 μg S m^{-3} and the contribution from acid-soluble sulfites and sulfides, elemental sulfur and volatile, S-containing organic compounds was negligible (<0.05 μg S m^{-3}).

INTRODUCTION

Sulfur is an important component of tropospheric aerosols occurring - primarily in the fine-particle fraction (Stevens and Dzubay, 1978) - as $(NH_4)_2SO_4$, NH_4HSO_4, and H_2SO_4, but sulfates of Na, Mg, Ca and Zn have also been identified (Charlson et al., 1978). Organic sulfur compounds such as alkyl hydrogen sulfates, sulfonates, thiosulfates and dithionate compounds may additionally be present (Charlson et al., 1978). Only concentrations of water-soluble sulfate (WSS), however, have been extensively studied (e.g. Brosset et al., 1975). Determination of WSS by an analytical technique such as the methyl thymol blue method (Lazrus et al., 1966), when combined with total particulate sulfur (TPS) determination, would yield the concentration of non-WSS fraction.

Sensitive instrumentation for determining TPS has been developed fairly recently. The most common instrumental methods are based on either energy-dispersive X-ray fluorescence spectrometry (Goulding and Jaklevic, 1973; Loo et al., 1978) or on thermal volatilization followed by flame photometric determination (Mudgett et al., 1974). The latter type of procedure, although particularly promising for in situ aerosol analysis, may suffer from incomplete recoveries (Newman, 1978). In the former technique sample matrices may cause errors due to X-ray attenuation, especially when high-volume samples are used to collect the aerosols.

Pyrolysis-microcoulometry has been successfully applied in the petroleum industry (Killer, 1974; White, 1977) to determine trace amounts of sulfur in organics. In this work we report a simple procedure utilizing pyrolysis-microcoulometry to determine the TPS concentrations in air particulates collected at Whiteface Mountain, New York. The procedure is rapid and suitable for small samples (30 mm^2), and it offers the potential of determining sulfide and sulfite fractions.

EXPERIMENTAL

Materials and Methods

Reagent-grade chemicals were used throughout. Deionized, distilled water was used to prepare reagents and test solutions. Compounds insoluble in water were dissolved in benzene. $NH_2(CH_2)_2SO_3H$ (taurine) and Na_2SO_4 were selected as calibration and control compounds because they can be obtained in very pure form and their aqueous solutions are stable over a long period of time. In addition Na_2SO_4 is a very refractory sulfur compound, and sulfonates and sulfates are probable components of atmospheric particulates. Calibration solutions containing 200 to 300 ng S/$\mu\ell$ were stored in closed glass vials at 4°C (Na_2SO_4) or -10°C (taurine) for up to 1 month without measurable changes in concentration. The remaining solutions were tested within 30 min of their preparation. Calcium carbonate, sodium silicate and cellulose were added directly to blanks or samples without prior dissolution in a solvent. An aqueous solution containing 40.0 mℓ of glacial acetic acid and 40.0 g of glucose per ℓ was used to acidify the sample and to obtain a source of excess C, which at 1000°C optimizes recovery of sulfates. The titration electrolyte was prepared by dissolving 5.0 mℓ of glacial acetic

acid, 5.0 g of KI, and 6.0 g of sodium azide in distilled water and diluting to 1 ℓ. Atmospheric particulates were collected on 20 cm x 25 cm Whatman 41 filter paper using high-volume samplers. Approximately 2000 m^3 of air were filtered in a 24-h collection period (Husain and Samson, 1979). For the WSS determination, a 4.0 cm x 4.0 cm section of the filter was extracted with 50 mℓ of distilled water at 85-95°C for 3 h. The aqueous extract was analyzed for sulfate by the automated methylthymol blue method (A.P.H.A., 1975).

Total Particulate Sulfur Determination

Sulfur compounds present in the total suspended particulates are pyrolyzed at high temperature and preferentially oxidized to SO_2 in presence of O_2. SO_2 is measured in a titration cell according to

$$H_2SO_3 + I_2 + H_2O \rightleftarrows 4H^+ + SO_4^{2-} + 2I^-.$$

The current required to produce the titrant I_2 is a direct measure of the amount of SO_2 present in the titration cell.

The Dohrman (Dohrman, Santa Clara, California) apparatus used in this work (Fig. 1) consists of a sample inlet, a furnace fitted with a quartz pyrolysis tube and providing three independently controlled heating zones, a titration cell and an integrating microcoulometer directly providing digital readout (in ng of S). The furnace is operated at 1000 ± 10°C in the inlet and center zones. High-purity He is passed through the inlet zone at 50 mℓ min^{-1}, and O_2 is injected into the center zone at 10 mℓ min^{-1}.

For TPS analysis filter discs approximately 29.7 mm^2 are placed on a platinum boat and inserted into the injection module. The system is closed, 20 µℓ of the acetic acid-glucose solution is added through the septum and the sample is heated to ∿ 30°C. At this stage H_2S and SO_2 are liberated from

the sulfides and sulfites and analyzed in the titration cell. After 2 min the sample is advanced into the drying zone (125 ± 5°C), where water, volatile organics, elemental sulfur and any remaining H_2S and SO_2 are volatilized. After 2 min the sample is moved into the pyrolysis zone, where all remaining sulfur compounds volatilize, including refractory sulfates (which probably undergo prior reduction to SO_2 in the presence of excess of C produced by the flash carbonization of the cellulose discs and the added glucose). Sulfur-containing vapors and gases are carried into the center oxidation zone. SO_3 yield is minimized by high C and low O_2 concentrations and high temperature. The SO_2 is then titrated with I_2. The sample is pyrolyzed for at least 5 min, or until the counting rate decreases to less than 5 ng min^{-1}.

After every 10 samples the electrolyte is replaced and blank and control samples are analyzed to monitor instrumental performance. Two- to 20-μℓ test solutions are injected onto blank or sample discs just prior to the addition of the acid-glucose solution. Benzene is allowed to evaporate at 30°C before addition of the acetic acid-glucose solution. The system is calibrated daily with duplicate analyses of sodium sulfate and taurine standards containing 2000 to 5000 ng S. Linearity within the analytical range is confirmed weekly by analyzing 100, 500, 1000, 3000, 6000 and 10,000 ng S of each standard compound. Sample controls (low and high S contents) and spiked samples are also periodically tested to monitor instrument performance.

Recovery Studies

The high pyrolysis temperature (1000 ± 10°C) and the relatively low oxygen flow rate (10 mℓ min^{-1}) were selected to optimize recovery of inorganic and organic sulfates. The low temperature (700-720°C) recommended by White

(1977) to obtain nearly 100% recovery for several organic sulfur compounds is unsatisfactory for refractory sulfates such as Na_2SO_4, $CaSO_4$ or $MgSO_4$. In preliminary experiments at 800°C and without cellulose and glucose, recoveries for sodium sulfate and methyl potassium sulfate were <1 and 32% respectively. Recovery increased to 72%, however, when Na_2SO_4 was pyrolyzed on cellulose discs after addition of the acetic acid-glucose solution. Similar low sulfate recoveries were obtained at 1000°C when the oxygen flow rate was increased or when O_2 was injected in the inlet zone. The omission of glucose also reduced recovery of Na_2SO_4 to 61% at 1000°C.

Twenty inorganic and organic sulfur compounds, including sulfuric acid and sulfates previously identified in tropospheric particulate samples (Charlson et al., 1978), sulfur, sulfides, sulfites, thiosulfates, sulfonates and sulfones were analyzed with or without suspended air particulates. When standard solutions of these compounds were added to blank cellulose discs, mean recoveries of duplicate determinations varied from 79 to 88%, with individual values within 3.0% of the mean (Table 1). Recoveries for spiked samples were within 3% of those listed in Table 1. Some of the compounds tested produced detectable signals at 30°C (acetic acid - glucose stage) or 125°C (drying stage). As expected, at 30°C, sodium sulfite and sodium sulfide were partially recovered in 2 min (16 and 23%). Recoveries of sulfite and sulfide increased to 38 and 48% after 6 min in the 30°C zone. Longer times in this zone (10-15 min) did not increase significantly recoveries, indicating that different conditions are necessary for optimum recoveries of acid-soluble sulfites and sulfides. The incomplete recoveries at 125°C (58 and 50%) probably resulted from partial oxidation to sulfate under these conditions. Diethyldithio sodium carbamate was also partially recovered at 30 and 125°C (17 and 68%).

To assess possible interferences by common inorganic or organic compounds, blanks, samples and standards were supplemented with various amounts of selected sompounds. Cellulose, acetic acid, glucose, stearic acid, sodium chloride, nitric acid, calcium carbonate, benzene and acetone did not interfere at the levels listed in Table 2.

Linearity within the analytical range (0.10 to 10.0 μg S) was confirmed by analyzing six sodium sulfate or taurine standards. The detection limit, defined as the amount of S detectable with a relative standard deviation of 50% (n = 10), is 0.10 μg S, which is equivalent to 35 ng S m^{-3} when 2000 m^3 of air are filtered. The relative standard deviations for two particulate samples containing 0.10 and 4.03 μg S (0.06 and 2.84 μg S m^{-3} air) were 48 and 5.1% respectively.

Sample Uniformity

Since the filter discs analyzed for TPS are a very small fraction of the total filter, are they quantitatively representative of the aerosol collected? To check this we measured TPS in 10 discs punched out at random from the particulate sample collected on 27 June, 1977. The measured concentrations were 2.88, 2.96, 2.63, 2.90, 2.54, 2.80, 2.94, 2.72 and 2.71 μg S m^{-3}. The average, 2.80, agrees with the WSS value determined on a 4.0 cm x 4.0 cm piece of the same filter. These data strongly suggest that the 29.7-mm^2 discs constitute representative samples for the TPS measurements.

RESULTS AND DISCUSSION

To check for the presence of non-WSS species, measurements of TPS and WSS were carried out on 125 particulate samples collected at Whiteface Mountain (Fig. 2). The sulfur concentrations ranged from 0.1 to 9.7 μg m^{-3}. Contribution from

acid-soluble sulfites and sulfides, elemental sulfur and volatile sulfur-containing organic compounds was below the maximum analytical background level of 80 ng S (signal at 125°C), indicating that this S fraction was lower than $\simeq 0.05$ μg S m^{-3}. Overall the TPS and WSS concentrations are in excellent agreement. A linear relationship between TPS and WSS is expressed by

$$WSS = 0.95\ TPS - 0.16\ \mu g\ S\ m^{-3} \qquad (1)$$

with a correlation coefficient of 0.972.

Stevens and Dzubey (1978) compared WSS and TPS (by EDXRF) values for fine- and coarse-particle samples. They also found excellent agreement between the two sets of values (correlation coefficient, 0.997) in the fine-particle fractions, but in the coarse fraction the TPS values were considerably greater than the corresponding WSS. The calculated linear regression (1) may suggest the presence of a small non-WSS sulfur fraction. It may also, however, simply reflect a slight negative bias of the water-extraction procedure, especially at low concentrations.

Several non-WSS sulfur species have been detected in atmospheric aerosols (Lee et al., 1976; Charlson et al., 1978). Water-insoluble sulfates such as $CaSO_4$ may be introduced into the atmosphere by wind erosion of gypsum deposits or by industrial pollution. Formation of sulfate esters, sulfonates and sulfones is also probable by reaction of H_2SO_4 and SO_2 with olefins, alcohols and other reactive organic compounds that coexist with sulfates in tropospheric aerosols (Charlson et al., 1978). Polycyclic, S-containing aromatic compounds such as dibenzothiophene, its methyl and ethyl derivatives and naphthobenzothiophene can also be introduced into ambient air from incomplete combustion processes or from coal, carbon black or automotive tire dust

(Lee and Hites, 1976; Kwan and Yem, 1979). The toxicity of these non-WSS compounds may be much greater than that of WSS species. In general, however, the contribution of this sulfur fraction to the TPS value is expected to be small since common oxidative pryolytic processes probably produce mainly WSS species, particularly ammonium sulfates (Charlson et al., 1978). Thus the situation TPS>>WSS would be expected only occasionally, associated with specific pollution episodes or emission sources.

During June 1979 we carried out particulate sampling for 6-h periods on several days. The TPS and WSS measurements are in excellent agreement overall (Table 3) suggesting that WSS can account for all of the sulfur present in aerosols. However, a marked disagreement is observed in a sample collected on 16 June between 1200 and 1800 (EDT), and another, smaller discrepency is observed in a sample collected on 18 June between 0600 and 1200. Repeated analyses on the 16 June sample by both techniques used in this work corroborated the measurements given in Table 3. Although this disagreement between the TPS and WSS concentrations suggests the presence of a relatively high non-WSS sulfur fraction in these samples, such exceptional TPS values cannot be satisfactorily explained on the basis of the available data. Additional chemical and perhaps microscopic analyses could have assisted in characterizing the non-WSS species, but our sample, unfortunately, was insufficient for these tests.

In summary, the data presented in this work suggest that even at a forested site such as Whiteface Mountain, WSS can account for essentially all of the sulfur observed. Occasionally, however, non-WSS may also be present. The new TPS method proposed here is rapid, simple and precise. When used in

combination with a WSS procedure it is also useful for determining non-WSS sulfur species, which may aid in the identification of pollution sources and in the assessment of toxicologic potentials.

Acknowledgments - We express our appreciation to Karen Williams, A.R. Khan and Robert Weinbloom for assistance in sulfur analysis, and to the Atmospheric Sciences Research Center of the State University of New York at Albany for particulate sampling at Whiteface Mountain. This work was partly supported by U.D. Department of Energy Contract DE-AC02-77EV04501.

REFERENCES

American Public Health Association (1975) Standard Methods for the Examination of Water and Wastewater, 14th Edn, APHA, Washington, D.C., pp. 628-630.

Brosset, C. B., Andreasson, K. and Ferm, M. (1975) The nature and possible origin of acid particles observed at the Swedish West Coast. Atmospheric Environment 9, 631-642.

Charlson R. J., Covert D. S., Larson T. V. and Waagoner, A. P. (1978) Chemical properties of tropospheric sulfur aerosols. Atmospheric Environment 12, 39-53.

Goulding F. S. and Jaklevic J. M. (1973) X-Ray fluorescence spectrometer for airborne particulate monitoring. EPA contract R2-73-182, U.S. Environmental Protection Agency, Washington, D.C.

Husain L. and Samson P. J. (1979) Long range transport of trace elements. J. Geophysical Research 84, 1237-1240.

Killer F. C. A. (1974) Sub-ppm sulfur analysis by microcoulometry. In Analytical Developments in the Petroleum Industry (Edited by D. H. Hodge), Applied Science Publishers Ltd., England.

Kwan C. L. and Yem T.F. (1979) Electron spin resonance study of coal by line width and line shape analysis. Analytical Chemistry 51, 1225-1229.

Lazrus A. L., Hill K. C. and Lodge J. P. (1966) A new colorimetric microdetermination of sulfate ion. Proceedings of 1965 Technicon symposia Automation in Analytical Chemistry, Mediad Inc., New York.

Lee M. L. and Hites R. A. (1976) Characterization of sulfur-containing polycyclic aromatic compounds in carbon blacks. Analytical Chemistry 48, 1890-1893.

Lee M. L., Novotmy M. and Bartle K. D. (1976) Gas chromatography, mass spectrometry and nuclear magnetic resonance determination of polynuclear aromatic hydrocarbons in airborne particulates. Analytical Chemistry 48, 1566-1572.

Loo B. W., French W. R., Gatti R. C., Goulding F. S., Jaklevic J. M., Llacer J. and Thomspon A. C. (1978) Large-scale measurement of airborne particulate sulfur. Atmospheric Environment 12, 759-771.

Mudgett P. S., Richards L. W. and Roehrig J. R. (1974) A new technique to measure sulfuric acid in the atmosphere. In Analytical Methods Applied to Air Pollution Measurement (Edited by R. Stevens and Henpet). Ann Arbor Science Publishers, Inc., Ann Arbor.

Newman L. (1978) Techniques for determining the chemical composition of aerosol sulfur compounds. Atmospheric Environment 12, 113-125.

Stevens R. K. and Dzubay T. G. (1978) Sampling and analysis of atmospheric sulfates and related species. Atmospheric Environment 12, 55-68.

White C. (1977) Determination of low levels of sulfur in organics by combustion microcoulometry. Analytical Chemistry 49, 1615-1618.

Table 1. Recovery of typical inorganic and organic sulfur compounds

Compound	µg S	Mean recovery (%)		
		30°C	125°C	1000°C
Ammonium sulfate	2.85	<1.0	<1.0	81
Calcium sulfate	2.00	<1.0	<1.0	84
Magnesium sulfate	2.73	<1.0	<1.0	86
Sodium sulfate	3.20	<1.0	<1.0	83
Sulfuric acid	1.60	<1.0	<1.0	84
Sodium sulfite	3.20	16	50	83
Sodium thiosulfate	4.40	<1.0	5.6	80
Sulfur	8.00	<1.0	69	81
Sodium Sulfide	2.20	23	58	82
Benzene sulfonamide	2.20	<1.0	7.0	84
Dibenzothiophene	3.30	<1.0	68	84
Diethyldithio sodium carbamate	3.50	17	68	80
Fenylsulfone	2.70	<1.0	54	81
Mercaptoethanol	1.86	<1.0	61	80
Methionine	1.90	<1.0	<1.0	79
Methyl potassium sulfate	2.80	<1.0	<1.0	79
Sulfanilic acid	1.34	<1.0	<1.0	87
Taurine	3.60	<1.0	<1.0	81
Thiophene	4.10	<1.0	86	88
Thiourea	5.04	<1.0	3.5	81

Table 2. Selected compounds which do not interfere with determination of total sulfur in air particulate samples

Compound	Amount added (µg)
Nitric Acid	16
Sodium Chloride	16
Calcium Carbonate	50
Cellulose	2500
Acetic Acid	800
Glucose	800
Stearic Acid	50
Sodium Silicate	150
Benzene	1800
Acetone	800

Table 3. Determination of sulfur concentrations in 6-h samples collected at Whiteface Mountain during June 1979

Date	Time, EDT	TPS ($\mu g\ S\ m^{-3}$)	WSS ($\mu g\ S\ m^{-3}$)
15 June	0000 - 0600	7.7	6.4
	0600 - 1200	8.0	7.4
	1200 - 1800	9.9	9.9
	1800 - 2400	6.7	6.6
16 June	0000 - 0600	8.5	8.1
	0600 - 1200	6.8	6.2
	1200 - 1800	9.0	1.6
	1800 - 2400	9.1	8.0
17 June	0000 - 0600	8.9	9.7
	0600 - 1200	8.4	8.8
	1200 - 1800	9.7	10.4
	1800 - 2400	7.6	8.0
18 June	0000 - 0600	9.6	10.8
	0600 - 1200	4.4	1.5
	1200 - 1800	0.6	<0.2
	1800 - 2400	0.3	<0.2
22 June	0000 - 0600	3.8	3.0
	0600 - 1200	2.2	1.6
	1200 - 1800	5.5	4.8
	1800 - 2400	2.9	1.9

FIGURE LEGENDS

Fig. 1. Analytical apparatus for the determination of total particulate sulfur.

Fig. 2. Comparison of water-soluble sulfate (WSS) and total particulate sulfur (TPS) concentrations in 125 samples collected at Whiteface Mountain, New York.

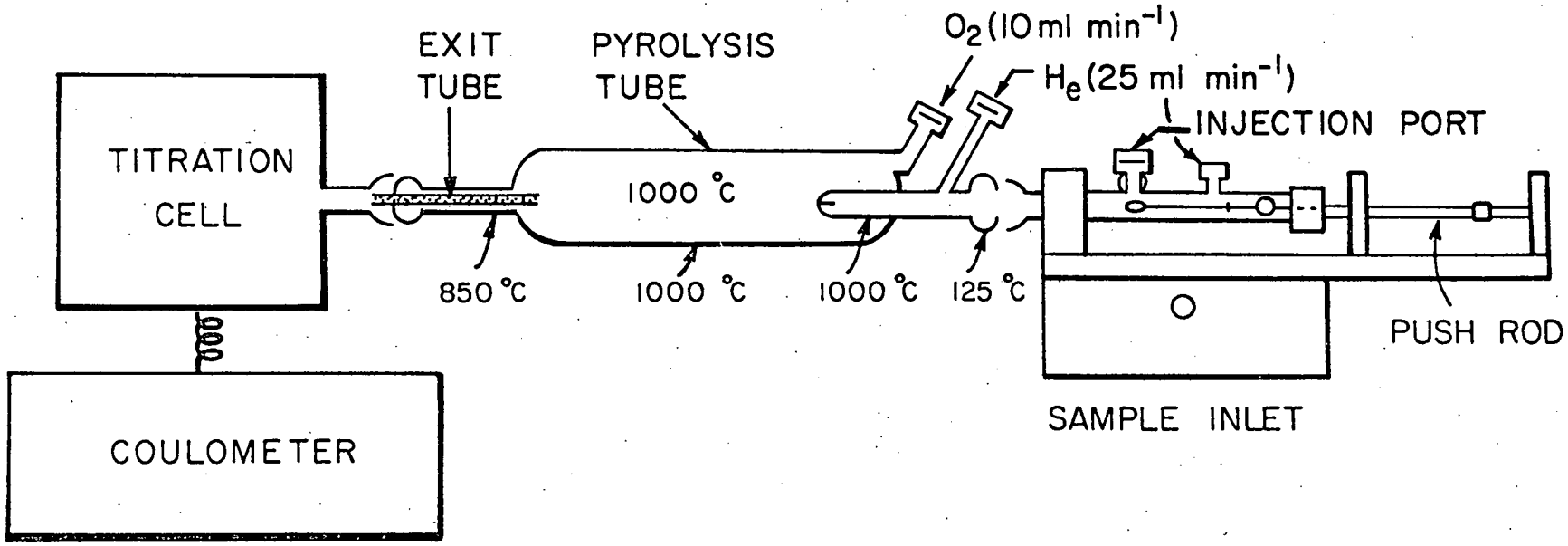
EXIT
TUBE
PYROLYSIS
TUBE
O_2 (10 ml min^{-1})
H_e (25 ml min^{-1})
INJECTION PORT
TITRATION
CELL
1000 °C
850 °C
1000 °C
1000 °C
125 °C
PUSH ROD
SAMPLE INLET
COULOMETER

Fig. 1

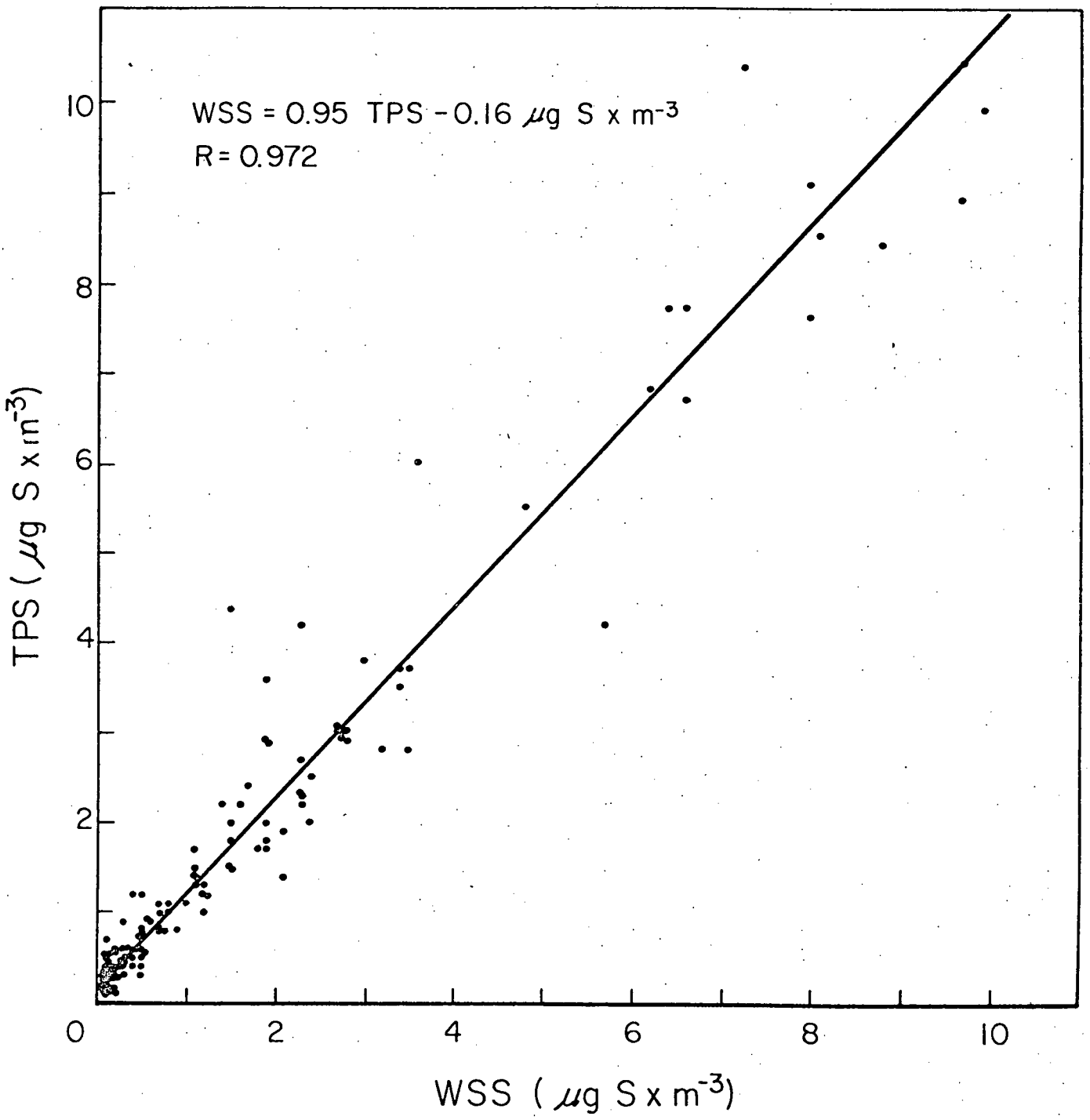

Fig. 2

APPENDIX VI

SUMMERTIME CONCENTRATION OF TRACE ELEMENTS IN ATMOSPHERIC AEROSOLS AT REMOTE SITES IN NEW YORK STATE

P. P. Parekh and Liaquat Husain

Division of Laboratories and Research
New York State Department of Health
Albany, New York 12201, U.S.A.

Abstract - Ninety-four samples of air particulates collected during the summers of 1975-1977 at one remote, two rural and one urban site in New York and one rural site in New Jersey were analyzed for up to 13 elements by instrumental neutron activation analysis. Eighteen samples showed high episodic concentrations of several trace elements and sulfate. SO_4^{2-}, Cr, Zn, As, Se, Br and Sb were distinctly enriched in these aerosols, relative to their crustal abundances. (Sc was used as the reference for the crustal component.) Episodic and nonepisodic events were statistically indistinguishable if only the means and ranges of elemental concentrations and the enrichment factors were considered. However, correlation matrix and factor analysis showed that while nonepisodic cases had inexplicably complex factor loading structures, the structure for episodic cases was simple. Episodic events therefore appear to be better indicators of the sources of remote aerosols. Four factors were sufficient to account for 81% of the total variance in the episodic system. When the dependence of the factors on the set of elements was correlated with the elemental emission patterns of probable sources and the air trajectory data, four probable sources of the trace elements in these aerosols were identified: distant coal-fired power plants and/or sulfide ore smelters (for SO_4^{2-}, As, Se), refuse incinerators (for Zn, Sb), iron and steel works (for Cr and possibly Fe, Mn) lying south-southwest and/or northwest of the site studied and local automobile exhaust (for Br).

INTRODUCTION

Few systematic studies have been made of trace elements in atmospheric aerosols at remote sites, as distinct from urban areas. Husain and Samson (1979) showed that trace elements, including such toxic ones as Se, As, Sb and Zn, could be transported by air masses from pollution sources over long distances to remote regions. Long-range transport of airborne particulates is well documented (Elliot et al., 1974; Prospero, 1977; Prodi and Fea, 1979). Such aerosols containing SO_4^{2-} (Lioy et al., 1977; Galvin et al., 1978) are primarily responsible for the acid rain that is devastating the ecologic system of remote regions of New York State.

As part of an investigation of the distribution and transport of toxic species by airborne particulates from source to site, we have studied the trace elements transported with SO_4^{2-} to learn whether they have common pollution sources and, if so, whether their distribution patterns could help to identify these sources.

The concentrations of several toxic elements (Pb, As, Se, Sb, Cd, Zn, S) in fly ash from coal-fired power plants increase markedly with decreasing particle size (Davison et al., 1974). Linton et al. (1976) showed that fly ash particulates with aerodynamic diameters of $\sim$1 μm or less contain as much as 80% of the total elemental mass. Since the smallest particles have the longest atmospheric residence times, the potential of long-range transport of micron- and submicron-size particulates, which are concentrated in toxic elements, is greater than for large-size components. Moreover, these small particulates are preferentially deposited in the human respiratory system (Natusch et al., 1974; Davison et al., 1974; Natusch and Wallace, 1974).

We have analyzed the distribution of trace elements in air particulates collected during three consecutive summers (1975-77) at various remote and rural sites of New York State and one site in New Jersey. To identify the sources we used two approaches: (a) comparison of the enrichment factors for several elements with the patterns of elemental emission from probable sources and (b) correlation matrix and factor analysis of the same data.

EXPERIMENTAL

Sample collection

Air particulate samples were collected with high-volume samplers for 24-h sampling periods by filtering about 2000 m^3 air through Whatman 41 filter paper (20 cm x 25 cm). At Whiteface Mountain Field Station in New York State sampling began on July 1 in 1975 and 1976 and on June 15 in 1977. A total of 56 samples from this station (24 for 1975, 8 for 1976, and 26 for 1977) were analyzed for trace elements.

In addition, air particulates were collected by the same procedure for 9 days (July 17-25) in 1976 at two rural sites (Schoharie and Holland) and one urban site (Albany) in New York and at a rural site (High Point) in New Jersey.

Total suspended particulates

The total suspended particulate (TSP) loading was determined by weighing the filter paper, before and after loading, at constant temperature and humidity (50% relative humidity, 21°C).

Determination of soluble SO_4^{2-}

Soluble SO_4^{2-} was determined by extracting from 16 cm^2 of the filter with 50 ml of double-distilled water at 80-90°C, reducing the volume to 20 ml and

determining SO_4^{2-} in the water extract by an automated colorimetric method using methyl thymol blue (Lazrus et al., 1966). By comparing the results so obtained with the total S determined by a microcoulometric method (Canelli and Husain, 1980) we found that essentially all the S trapped in the filter paper was present as soluble SO_4^{2-}.

Instrumental neutron activation analysis of trace elements

About 50 cm^2 of the aerosol-loaded filters were irradiated at the High-Flux Beam Reactor of Brookhaven National Laboratory, along with a multielement comparator and filter paper blanks, at a flux of 1-2 x 10^{14} $ncm^{-2}s^{-1}$ for 20-30 min.

The γ-activity of the irradiated samples and standards was counted with high-resolution Ge(Li) detector (full-width at half maximum ≈ 2.1 KeV at 1332 KeV) coupled to a 4096-channel analyzer. The concentrations of 9 to 13 elements (Na, K, Sc, Cr, Mn, Fe, Zn, As, Se, Br, Sb, Cs and He) were determined by judiciously selecting the characteristic γ-lines of the nuclides of interest and the delay intervals between irradiation and counting.

RESULTS AND DISCUSSION

Episodic and nonepisodic cases

The analytical results for TSP, trace elements and SO_4^{2-} in all samples are presented in Tables 1 and 2. On certain days (italicized in the tables) the concentrations of SO_4^{2-} and most of the trace elements were markedly elevated. Two such episodes are shown in Fig. 1. Distinct peaks of ozone concentrations, produced by photochemical reactions of oxygen with essentially anthropogenic sources (NO_x), were also observed invariably on all of these days.

Such simultaneous sporadic increases in SO_4^{2-} and trace metals at rural and remote sites, with no conceivable local causes, could only be considered episodic. We therefore grouped separately the episodic (Ep) data and the

nonepisodic (NEp) data for a comparative study of the distribution profiles of trace elements and made a statistical search for gross or subtle differences between the two cases. We also attempted to learn whether one could determine the much-debated background aerosol concentrations by studying the NEp trace element distribution and enrichment patterns. However, we do not intend to imply that events classified as NEp are brought about entirely by local or regional causes.

Range, mean and standard deviation

Except for Zn and Br, the average concentrations of all elements for all Ep events during the three summers were in remarkable agreement. Data for Whiteface Mountain in 1975 (four events) and 1977 (six events) are given in Table 3. For brevity the 1976 data from all stations are not tabulated, but they can be inferred from Tables 1 and 2.

This fairly uniform distribution pattern of trace elements during Ep events is consistent with Husain and Samson's inference (1979) of a common distant source(s) for the trace elements in question. The elements are then advected to widely scattered sites by polluted air masses that had been stagnant over the pollution centers. Husain and Samson's air trajectory analysis showed that the pollution centers were located south and southwest of these sites. The fluctuations in Br averages in the present data are not surprising, since Br concentrations can be considerably influenced by local Br immissions in automobile exhaust. This is obvious in the relatively high concentrations of Br in aerosols from urban Albany, as compared to rural Schoharie or remote Whiteface Mountain.

The high mean concentration of Zn in 1977, compared to 1975 (Table 3), appears to reflect primarily the high concentrations in the samples of 28 and 29 June 1977 (Table 1), although similar high concentrations had been observed on 2 and 13 July 1975. Lewis and Macias recently (1980) encountered a similar situation for Zn and attributed it to contamination from a malfunctioning sampler pump motor. If these unrealistically high Zn concentrations in June 1977 are disregarded, the mean for 1977 compares well with that for 1975 (Tables 3 and 4).

For the NEp data at Whiteface Mountain (Table 4) the mean concentrations in 1975 and 1977 of all elements except Br agreed within 1 standard deviation (σ). The mean Br concentrations were remarkably constant for 1975 and 1977 and probably suggest comparable auto traffic. The very high Br mean in 1976 NEp summer aerosols from the other sites is an artifact from the inclusion of data from the city of Albany (Table 2).

Although the Ep mean concentrations were significantly higher than NEp means, Ep and NEp events are not statistically distinguishable purely by their concentration levels or ranges. SO_4^{2-} concentrations appear to be in good agreement for Ep events of 1975 through 1977 and distinctly higher than those for the NEp events although at a 95% confidence level (2σ) this distinction also vanishes.

Enrichment factor

Of the various elements which can be used to evaluate crust-derived components in the aerosols, Al, Si and Sc are by far the most reliable. In the present work Sc was chosen as a reference material for the crustal component, since instrumental neutron activation analysis can determine Sc at <ppb

concentrations with high accuracy and precision. This method in any case is not convenient for analysis of Al and Si.

In an independent study Al concentrations were determined by atomic adsorption spectrophotometry for five samples collected at High Point, New Jersey, on 20-24 July 1976 (Table 2). The average enrichment factor (EF) was calculated for these five samples via Al and Sc based on crustal averages from Mason (1966). The EF calculated with Sc as reference was systematically higher by about 30-40% for all the elements analyzed, but since we have used the EF in the discussion only qualitatively, our conclusions are not likely to be affected. Because of the uncertainty in the true crustal precursors to our aerosols, we have not considered EF < 10 as true enrichment.

For Ep events Cr, Zn, As, Se, Br, Sb and SO_4^{2-} are undoubtedly enriched (Table 3), more so in 1977 than in 1975. While the EF for Zn, As, Se, Sb and SO_4^{2-} are about double, Br is enriched about fivefold.

The NEp aerosols are similarly enriched in Cr, Zn, As, Se, Sb, Br and SO_4^{2-} and show the same upward trend from 1975 to 1977 (Table 4). The high EF for Br in 1976 samples presumably arose from a localized source (automobile exhaust). Thus the difference in EF between Ep and NEp events is not statistically significant.

How can one explain the similarity in the distribution and enrichment patterns of trace elements studied for Ep and NEp events? Evidently, the trace element distribution profile during the summer is shaped predominantly by the Ep events. These outbursts manifest in the peak concentrations seen in Figure 1 and are followed by quiescent NEp periods. The ambient NEp aerosols are probably diluted aerosols from the episodic period mixed with aerosols of regional origin. Another episodic outburst may or may not disturb the profile, depending on whether the parent source for the Ep events is the same or not.

This model is of course oversimplified. Several physicochemical factors also influence the trace element distribution patterns.

NEp aerosols - natural or pollution-derived?

Are the aerosols at remote areas like Whiteface Mountain, especially in NEp periods, natural or anthropogenic?

Gordon et al. (1973) believe that the trace elements V, Fe, Cu, Zn, As, Se and Sb (EF 2.4 to 2400) in aerosols from two nonurban sites in Canada, Twin Gorges and Algonquin, are not necessarily anthropogenic. The more volatile As, Se and Sb could be derived from natural processes such as volcanic activities, supporting their statement by Weiss et al.'s (1971a) observation of constant Se concentrations in preindustrial and recent Greenland ice, in contrast to a twofold increase of S and a greater increase of Pb in recent times. Duce et al. (1975) found comparable enrichment factors for 12 elements in North Atlantic and South Pole aerosols. Since the latter were derived from natural sources, they concluded that even anomalously high EF for Zn, Cu, Cd, Pb, Sb and Se at remote sites of the Northern Hemisphere may be due to natural rather than anthropogenic sources.

Nevertheless, we do not ascribe to natural sources the high EF we observed for several elements in NEp aerosols at remote sites like Whiteface Mountain. One reason is that the trace element contents of NEp aerosols there vary considerably from day to day, which would not be expected for background aerosols of natural origin at a remote site. The increase in the mean trace element concentrations in NEp aerosols of 1977, as compared to those of 1975, resembles the pattern of the Ep aerosols, which undoubtedly are pollution-derived.

Secondly, the mean concentrations in NEp aerosols are much above Rahn's (1976) empirically estimated minimum concentration for background aerosols

(which at least allows one to make an educated guess on the order of magnitude for such hypothetical background aerosols) and 1 to 3 orders of magnitude higher than those at the South Pole (Zoller et al., 1974).

Finally, as shown below, there was a fair to good linear correlation between SO_4^{2-} and Se for NEp events (r = 0.50 for 1975 and 0.69 for 1977) and Ep events (r = 0.67). Se was specifically chosen for this comparison because it is one of the elements considered by Duce et al. (1975) and Gordon et al. (1973) to prove their point. The mean concentrations of SO_4^{2-} in these aerosols are much higher than the reported ambient concentrations (Kellogg et al., 1972). As a matter of fact, SO_4^{2-} in the summer aerosols at Whiteface Mountain is demonstrably of anthropogenic origin (Lioy et al., 1977; Galvin et al., 1978).

Correlation matrix and factor analysis of Ep events

To examine the interelement relationships within the Ep and the NEp events -- and to sort out the data more objectively in order to estimate the parent sources of these elements we performed both correlation matrix and factor analysis with the help of Bio-Medical Data (BMD) Program Package BMDP-77 (Dixon, 1977). Because Ep data for any one summer were statistically rather limited for such analysis, we pooled all the Ep data for all three summers and all five sites. In this approach we assumed, of course, the same parent population for all these events; but the means, ranges, EF for the trace elements and air trajectory analysis (Husain and Samson, 1979) seem to justify that assumption. Unfortunately, this approach excluded the data for Cr, Se and Cs, which were not determined in air samples of 1976.

The matrix for linear correlation coefficients for 18 Ep events is given in Table 5. For n = 18, correlation coefficient values greater than 0.60 in this matrix indicate a statistically significant (α = 0.01) relationship

(Pearson and Hartley, 1976). Good correlation can be seen between Fe, Mn, Sc and K, all of which are present in the aluminosilicate phase (e.g., crustal dust or rock); their EF are not significantly above crustal averages. The volatiles As, Se and S also show good correlation. (Linear regression analysis was performed manually for the pair Se-SO_4^{2-} and AS-SO_4^{2-}, based on the 10 Ep data points of 1975 and 1977. The analysis yielded r = 0.67 and 0.85 respectively.) However, these three volatiles were poorly correlated with Sb, which had a statistically significant correlation only with Zn. A Sb-Zn correlation has been reported by others (Dams et al., 1971; Rahn, 1971; Greenberg et al., 1974; Hopke et al., 1976), and we shall elaborate on it below.

The As-Se-SO_4^{2-} correlation suggest that these elements were carried together in the same air mass. SO_4^{2-} is principally associated with fossil-fuel combustion, and our observed high EF for As and Se are typical for fly ash from coal-fired power plants (Davison et al., 1974; Rahn, 1976). We therefore conclude that these three elements came from the same primary source -- fossil fuel. A moderately high correlation is also seen for As-Sc-Mn and, to a lesser extent, between As and Fe. The meaning of these correlations will become clear from the factor analysis below. As expected, Br shows either poor or negative correlation with the other elements studied.

In recent years factor analysis has been successfully applied for data reduction in aerosol studies (Hopke et al., 1976; Lewis and Macias, 1980). With the BMD program factor extraction using principal components orthogonal varimax rotation, retention of factors with eigenvalues > 1.00 and communality estimation from factors after one iteration were the defaults employed.

The results for factor loadings obtained by this method on combined Ep events of 1975-1977 are given in Table 6. The four factors account for 81% of the total variance of the measured variables.

Factor 1 shows high loading for Sc, Mn, Fe, As and SO_4^{2-} and medium loading for K. This factor accounts for approximately 40% of the total variance in the system. (In factor analysis of 10 Ep events in 1975 and 1977, Se also fell in Factor 1, with a loading of 0.96.) Solely on the basis of first three elements (Sc, Mn, Fe) and the last one (K) this factor would seem to represent a crustal component (dust, rock). However, the inclusion of As, SO_4^{2-} and Se shows that a significant quantity of the supposedly crustal dust is, in fact, material from coal combustion, including fly ash of the coal particulate itself. This is not surprising, since the concentration ratios of many elements (including Fe, Mn, Sc and K) in suspended particles from coal combustion, relative to the Al concentration, are similar to concentration ratios in crustal material (Hopke et al., 1976). The bulk of the aluminosilicate matrix in these Ep aerosols is thus being transported to the sites from a coal-fired plant(s) and does not represent pick-up of crustal material by air masses along their trajectories.

Factor 2 has a very high loading for Zn and Sb and accounts for about 19% of the total variance. Greenberg et al. (1974) report that suspended particles in the plant stack of a municipal incinerator in Alexandria, Virginia, are highly enriched in Zn and Sb. Hopke et al. (1976) ascribe the Zn-Sb correlation in Boston air particulates to a similar source. Factor 2 could therefore be attributed to refuse incineration.

Factor 3 shows a high loading for Na (and a relatively low loading for K), which is typical of sea-salt aerosols. This is a rather unlikely source because the sites studied are remote from the sea. External contamination with Na due to improper sample handling, especially in summer days, could show up as a secluded high loading. This seems a good educated guess. However, in the

absence of any proof, we describe Factor 3 as an unidentified source. Factor 4 is strongly dependent on Br content, as indicated by its high loading of 0.9, which implicates automotive exhaust as the source (King, et al., 1976; Lewis and Macias, 1980). As mentioned above, Cr, which shows distinct enrichment, was not included in this factor analysis; but in a separate factor analysis of 10 Ep events of 1975-77 for which Cr figures are available, the picture as a whole remains unchanged. As, Se, SO_4^{2-}, Sc and Mn exhibited high loading in Factor 1. Factor 2 showed high loading in Fe, Cr, and Mn, the group Zn-Sb adhered together but was shown under Factor 4.

The association of Fe, Cr and Mn in Factor 2 suggest that in addition to fossil fuel (coal, in particular) as a source of Fe and Mn, there could be a common source for all three elements -- iron and steel works (Neustadter et al., 1976). The mean weighted enrichment factors for Fe and Mn for 10 combined Ep events in 1975 and 1977 are 2.4 and 4.2 respectively. The enrichment may be real, though only marginally high. The crustal averages of Fe, Mn and Cr are 50,000, 950 and 100 ppm (Mason, 1966) respectively, so a contribution of the crustal component (in this case, fly ash from coal combustion) to the particulate loading could overwhelm the contribution from ferrous metal industry in the order Fe > Mn > Cr. Factor 3 showed high loading for Na, K and Br. The includion of Na and K with Br is not explicable.

Correlation matrix and factor analysis of NEp events

Correlation matrix and factor analysis was also performed for NEp events of 1975 and 1977. Since the factor analysis is derived from the correlation matrix, the matrix is reflected in factor analysis. For conciseness, only the factor analysis will be presented.

Preliminary to the factor analysis, we did a regression analysis of pairs of elements with the help of the BMD program to get a feeling for the inter-element relationships. In the Ep events the pair As-SO_4^{2-} had been well correlated, but in the NEp events of 1975 As was poorly correlated with SO_4^{2-} ($r = 0.23$; see Fig. 2, line a). Two outlying data points (question-marked) which seemed to distort the linear regression were excluded in a revised regression analysis (line b).

Four factors were sufficient to explain 88% of the total variance in NEp events in 1975 (Table 7). Factor 1 has medium to high loading for TSP, Na, K, Sc, Mn, Fe, Zn and suprisingly Br. It indicates the presence of crustal dust in the NEp aerosols. In Factor 2 As, Se and SO_4^{2-} show high loading, while TSP, Sc, Mn, Fe and Zn show medium loading. The link between TSP and the matrix elements (Factor 1) and volatiles, especially SO_4^{2-} is not surprising. As Lewis and Macias (1980) have shown, $(NH_4)_2SO_4$, which is the dominant form of SO_4^{2-} in the aerosols, forms about 42% of the fine fraction, while about 38% of the coarse fraction in the Charleston aerosols is the aluminosilicate matrix. The association of Sc, Mn and Fe with the volatiles As, Se and SO_4^{2-} in Factor 2 is similar to the Factor 1 structure of Ep events and could stem from a similar source. The association of Zn with Se (and other volatiles) in Factor 2 was also observed in a fine component of the Charleston aerosol by Lewis and Macias (1980), who suggest a complex combination of anthropogenic sources. In Factor 3, in contract to Ep events, Sb is related not to Zn but, strangely enough, to Cr. Only Factor 4 shows a strong dependence of Cs (loading = 0.92).

The loading structures of Factors 3 and 4 seem inexplicably complex. None of the factors is related to Hg. Presumably Hg belongs to the later factor, which has an eigenvalue < 1 and so was not extracted by the program. This

seems to indicate that Hg is associated with a unique factor unrelated to any of the four dominant ones. In unpolluted air Hg has been reported at < 1 to 10 ng/m^3 and results from degassing of the earth's crust (Weiss et al., 1971b). The major fraction of atmospheric Hg is gaseous, composed of several volatile species (Johnson and Braman, 1974). Fogg and Fitzgerald (1979) found no more than 5% of total Hg present as particulate matter. Thus about 0.5 ng/m^3 (upper limit of 10 ng Hg/m^3 taken) could be expected in the ambient aerosols. Our mean value of 0.54 ng/m^3 seems to suggest that the Hg in air particulates at Whiteface Mountain may be of natural origin. The unique factor suggested by factor analysis does not seem surprising.

Factor analysis of NEp events in 1977 also revealed four factors accounting for about 83% of the variance (Table 7). Sb and Cs were omitted in this analysis because of incomplete data for the two elements. Factor 1 showed high loadings for the volatiles As, Se, SO_4^{2-} and Br and a medium loading for Zn. Although the loading structure of this factor resembled that of Factor 2 of the 1975 NEp cases, the volatiles are not associated with the crustal component. The remaining three factors are inconsistent. The high loadings for Fe and Sc in Factor 2 indicate a crustal source but surprisingly little or no dependence for the crustal components Mn and K. On the other hand, high loadings for these two elements can be seen in Factor 3 along with a medium loading for Zn. The association of Cr with Fe in Factor 2 had also been seen in Ep events in 1975-77. Factor 4 shows a high loading for Na and a medium loading for As and Cr. No reasonable explanation can be given for these three factors, nor can their identity be interpreted.

In their multivariate analysis of Boston air particulates Hopke et al. (1976) encountered a similar distribution of Mn. They attributed it to size

fractionation of Mn, the larger particle Mn as dust factor and the finer component with the Se factor. Such a size differentiation might partially explain some of the distributions in Factors 2-4; but many observations, such as the association of K with Mn in Factor 3, are difficult to reconcile on this basis.

In contrast to Ep events, the NEp events are not clear-cut, and source identification from NEp data cannot be as straightforward. What, then, brings about the observed elemental differentiation if, as explained earlier, the NEp aerosols are diluted aerosols of the preceding Ep events?

The physicochemical factors that control the distribution of aerosolborne trace elements are highly complex. The depths of the mixing columns, the stability of the atmosphere, wind speed and wind direction are by far the most important physical meteorological factors that govern atmospheric dispersion of airborne trace metals and suspended particulates. Superimposed on these factors are such chemical processes as phase change, coagulation, chemical reactions and fractionation, all of which occur simultaneously during dispersion and sedimentation.

Using dispersion factor (DF), i.e. mixing depth times wind speed, as an index of atmospheric dispersion, Kleinman et al. (1973) observed a significant correlation between DF, TSP and most trace metal concentrations. They attributed high concentrations of TSP and several trace metals during summer months in New York City to changes in DF. We believe that a similar change in DF brought about the Ep high concentrations of trace metals and TSP observed in our study. In long-range transport to remote sites like Whiteface Mountain changes in DF at the sources play a more dominant role in shaping the Ep profiles in question than changes at the site (Husain and Samson, 1979). Presum-

ably low DF at emission sources lead to Ep patterns characterized by higher trace metal and particulate loadings per unit volume of air from those sources. The Ep events therefore seem to be good signatures of the parent sources.

NEp events do not retain the source identity as well. An example is the trace element distribution profile observed on 20 July 1975. From the linear correlation between As-SO_4^{2-} and Se-SO_4^{2-} generally seen in Ep events (Fig. 3) we deduce that for about 13.5 $\mu g/m^3$ of SO_4^{2-} observed on this day (which is a typical Ep concentration), approximately 2.2 ng Se/m^3 and 2.7 ng As/m^3 should be present in the sample. Such concentrations of As and Se should have been detected by instrumental neutron activation analysis, especially because this sample had low concentrations of other elements (Fe, Cr, Zn, Br) and hence a low γ-spectral background. Yet neither element was detected in this sample. Was it the precipitation front moving from west to east from the evening of July 18 (Husain and Samson, 1979) that caused such a differentiation between Se-SO_4^{2-} or As-SO_4^{2-}? Although physicochemical factors responsible for the fractionation are too complex, the case in point certainly serves to illustrate how the memory effects of Ep precursors could be distorted in a NEp observation.

CONCLUSION

Ep and NEp events cannot be distinguished statistically on the basis of mean trace element concentrations and EF in summer aerosols. However, correlation matrix and factor analysis reveal that unlike NEp events, the Ep events have simple, easily interpretable loading structures. Such analysis of the distribution and enrichment patterns of trace elements in Ep aerosols, when compared with emission patterns of probable sources, suggest that these aerosols at Whiteface Mountain derived from four pollution sources: coal-fired

power plants (S, K, Sc, Mn, Fe, As and Se), municipal refuse incinerators (Zn and Sb), iron and steel works (Cr and possibly Fe, Mn) and automobile exhaust (Br). The available air trajectory data indicate that the main pollution sources lie south and southwest of Whiteface Mountain (for Ep events of 16-19 July 1975, 20 July 1976 and 17 June 1977); or northwest, i.e. north of the Finger Lakes (for Ep events of 24,28 June and 24,29 July 1977); or west (for Ep events of 21 July 1977).

It would be reasonable to infer that the Cleveland, Ohio, and Pittsburgh, Pennsylvania, regions in the south-southwest (with their several coal-fired power plants and heavy iron and steel industries) and the Sudbury, Ontario, region in the northwest (with its massive sulfide ore smelters) may be the pollution sources for SO_4^{2-} and several trace elements found in the summer aerosols at remote and rural sites of New York State.

Acknowledgments

The Whiteface Mountain Field Station is operated by the Atmospheric Sciences Research Center, State University of New York at Albany. The filter samples were supplied by the Division of Air, New York State Department of Environmental Conservation. We are grateful to M. M. Reddy for advice and assistance in statistical analysis, J. B. Cummings and the Chemistry Department of Brookhaven National Laboratory for providing γ-counting facilities of the short-lived nuclides, and K. Williams and A. R. Khan for their assistance in experimental work. This study was partially supported by U.S. Department of Energy Contract DE-AC02-77EV04501.

REFERENCES

Canelli E. and Husain L., Determination of total particulate sulfur in air samples at Whiteface Mountain, N.Y. by pyrolysis microcoulometry. Atmos. Envir. (to be submitted).

Dams R., Robbins J. A., Rahn, K. A. and Winchester J. W. (1971) Quantitative relationships among trace elements over industrialized NW Indiana, In Proc. Symp. Nuclear Techniques in Environmental Pollution, IAEA, Vienna, pp. 139-157.

Davison R.L., Natusch D.F.S. and Wallace J.R. (1974) Trace elements in fly ash: dependence of concentration on particle size. Environ. Sci. Technol. 8, 1107-1113.

Dixon W.J. ed. (1977) Biomedical Computer Programs Univ. of Cal. Press, Los Angeles.

Duce R.A., Hoffman G.L. and Zoller W.H. (1975) Atmospheric trace metals at remote northern and southern hemisphere sites: Pollution or natural?, Science 187, 59-61.

Elliot W.P., Ramsey F. :. and Johnston R. (1974) Particle concentrations over the oceans, J. Rech. Atmos. 8, 939-945.

Fogg T.R. and Fitzgerald W.F. (1979). Mercury in southern New England coastal rains, J. Geophys Res. 84, 6987-6989.

Galvin P.J., Samson P.J., Coffey P.E. and Romano D. (1978) Transport of sulfate to New York State, Environ. Sci. Technol. 12, 580-584.

Gordon G.E., Zoller W.H. and Gladney E.S. (1973) Abnormally enriched trace elements in the atmosphere, Proc. 'Trace Substances in Environmental Health-VII'ed. D. D. Hemphill, Univ. Missouri-Columbia, Missouri, pp. 167-174.

Greenberg R.R., Zoller W.H. and Gordon G.E. (1974) Trace elements emitted from municipal incinerators. Proc. August 1974 National meeting of the American Chemical Society, Atlantic City, New Jersey (abstract only).

Hopke P. K., Gladney E. S., Gordon G. E., Zoller W. H. and Jones A. G. (1976). The use of multivariate analysis to identify sources of selected elements in the Boston urban aerosol, Atmos. Environ. 10, 1015-1025.

Husain L. and Samson P. J. (1979). Long-range transport of trace elements, J. Geophys. Res. 84, 1237-1240.

Johnson D. L. and Braman R. S. (1974). Distribution of atmospheric mercury species near ground, Environ. Sci. Technol. 8, 1003-1009.

Kellogg W. W., Cadle R.D., Allen E. R., Lazrus A. L. and Martell E. A. (1972). The sulfur cycle, Science 175, 587-595.

King R. R., Fordyce J. S., Antoine A. C., Leibecki H. F., Neustadter H. E., and Sidik S. M. (1976). Elemental composition of airborne particulates and source identification: An extensive one year survey, J. Air Poll. Contr. Assoc. 26, 1073-1978.

Kleinman M. T., Kneip T. J., and Eisenbud M. (1973). Meteorological influences on airborne trace metals and suspended particulates, Proc. 'Trace Substances in Environmental Health-VII ed. D.D. Hemphill, Univ. Missouri - Columbia, Missouri, pp. 161-166.

Lazrus A. L., Hill K. C., and Lodge J. P. (1966). Proc. 1965 Technicon Symp. Automation in Anal. Chem., Mediad Inc., New York.

Lewis C. W., and Macias E. S. (1980). Composition of size-fractionated aerosol in Charleston, West Virginia, Atmos. Environ., 14, 185-194.

Linton R. W., Loh A., Natusch D. F. S., Evans Jr. C. A., and Williams P. (1976). Surface predominance of trace elements in airborne particles, Science 191, 852-854.

Lioy P. J., Wolff G. T., Czachor J. S., Coffey P. E., Stasiuk W. N., and Romano D. (1977). Evidence of high atmospheric concentrations of sulfates detected at rural sites in the northeast, J. Environ. Sci. Health, A12, 1-14.

Mason B., Principles of Geochemistry (1966) Wiley, New York, N.Y.

Natusch D. F. S., Wallace J. R., and Evans Jr. C. A. (1974). Toxic trace elements: Preferential concentration in respirable particles, Science 183, 202-204.

Natusch D. F. S., and Wallace J. R. (1974) Urban aerosol toxicity: The influence of particle size, Science 186, 695-699.

Neustadter H. E., Fordyce J. S., and King R. B. (1976) Elemental composition of airborne particulates and source identification: Data analysis techniques, J. Air Poll. Cont. Assoc. 26, 1079-1084.

Pearson E. S., and Hartley H. O. Ed. (1976) Biometrika Tables for Statisticians, vol. 1, p. 149, Biometrika Trust.

Prodi F., and Fea G. (1979) A case of transport and deposition of Saharan dust over the Italian penninsula and Southern Europe, J. Geophys. Res. 84, 6951-6960.

Prospero J. M. (1977) Atmospheric dust studies in Barbados, Bull. Amer. Meteorol. Soc. 645-652.

Rahn K. A. (1971) Sources of trace elements in aerosols - An approach to clean air, U.S.A.E.C. Report COO-1705-9, Univ. Mich., Ann Arbor, Mich.

Rahn K. A. (1976) The chemical composition of the atmospheric aerosol, Tech. Report., Univ. of Rhode Island, Rhode Island.

Weiss H. V., Koide M., and Goldberg E. D. (1971a) Selenium and sulfur in Greenland ice sheet: Relation to fossil fuel combustion, Science 172, 261-263.

Weiss H. V., Koide M., and Goldberg E. D. (1971b) Mercury and lead in the Greenland ice sheet: Evidence of recent input by man, Science 174, 692-694.

Zoller W. H., Gladney E. S., and Duce R. A. (1974) Atmospheric concentrations and sources of trace metals at the South Pole, Science 183, 198-200.

Table 1. Elemental concentrations in air particulates at Whiteface Mountain, New York, July 1975 and June - July 1977

Date	Suspended particulates (μg/m³)	Concentration (ng/m³) Na	K	Sc	Cr	Mn	Fe	Zn	As	Se	Br	Sb	Cs	Hg	SO_4^{2-}*
1975															
July 1	34	144	168	0.070	2.5	11.1	310	12	ND	ND	6.9	ND	ND	1.25	—
2	51	154	293	0.113	5.8	22	526	100?	2.7	0.82	15.1	0.42	0.080	0.64	1200
3	38	39	114	0.030	2.9	3.6	111	18	0.9	0.24	7.8	0.17	0.033	0.62	3120
4	33	88	92	0.039	2.9	5.9	166	24	0.7	0.24	6.1	0.11	0.034	0.93	1170
5	36	102	123	0.039	1.7	10.9	356	16	4.1	0.70	14	0.41	0.024	0.79	470
6	41	100	151	0.059	2.8	8.9	314	25	2.3	0.92	26	0.63	0.059	0.39	2300
7	47	153	151	0.062	4.2	7.9	275	31	2.5	0.92	34	2.1	0.057	0.42	5790
8	54	188	148	0.090	3.4	10.6	295	61	3.8	1.84	21	1.6	0.095	0.34	11000
9	44	52	84	0.057	3.2	8.6	237	23	2.6	1.16	12	0.50	0.032	0.48	7800
10	34	53	90	0.039	2.4	5.2	200	14	0.6	0.24	8.8	0.12	0.038	1.46	740
11	44	85	116	0.038	2.8	6.2	162	18	1.3	0.70	12	0.27	0.044	0.64	4120
12	42	72	96	0.039	3.37	8.5	206	25	1.7	0.70	13	0.52	0.020	0.34	3100
13	33	27	38	0.015	5.47	5.6	164	209?	ND	0.20	7.2	0.30	0.020	ND	4270
14	24	15	24	0.0057	3.60	1.3	42	7	1.0	0.14	5.3	0.28	0.024	0.27	1130
15	34	37	62	0.021	4.9	7.0	187	20	1.1	0.79	13	ND	0.048	0.60	5530
16	40	53	111	0.071	2.6	10.6	229	24	1.4	1.28	14	1.45	0.139	0.48	7030
17	62	96	229	0.15	8.1	32	627	56	5.1	4.6	18	1.38	0.280	0.008	23210
18	81	123	253	0.22	12.9	32	841	59	4.1	5.0	15	2.14	0.220	ND	23350
19	69	155	250	0.15	19.2	17	591	42	3.0	1.86	12	ND	0.250	ND	4410
20	32	19	56	0.034	2.4	3.1	132	8	ND	ND	6.5	ND	0.098	0.075	13470
21	22	15	52	0.020	2.31	2.5	98	19	0.5	0.59	2.8	ND	0.040	0.79	1140
22	24	101	89	0.024	3.5	3.2	129	15	2.8	ND	6.5	ND	ND	ND	1910
23	35	71	151	0.049	5.4	9.7	261	20	1.6	0.42	13	3.88	0.068	0.17	5840
24	41	58	116	0.093	20.3	16.0	629	34	1.7	0.95	9	1.72	0.085	0.12	17890
1977															
June 16	—	80	143	0.034	1.67	8.1	237	33	1.15	ND	10.7	ND	ND	—	1530
17	—	88	192	0.059	6.9	19.8	450	93	3.36	3.40	35	2.94	0.13	—	19790
18	—	156	146	0.043	33	11.6	390	27	2.02	1.03	14	ND	0.077	—	3650
19	—	43	280	0.038	14.2	57	607	28	0.07	0.32	4.4	ND	ND	—	2810
20	—	21	68	0.010	7.0	77	117	21	0.55	ND	2.1	—	ND	—	2330
21	—	68	140	0.016	5.4	44	164	29	0.53	0.30	5.0	0.17	1.29	—	710
22	—	194	560	0.010	3.3	42	87	91	2.31	1.19	7.6	0.33	ND	—	1960
23	—	537	151	0.017	37	12.6	333	60	ND	0.30	7.2	0.27	0.03	—	1080
24	—	163	327	0.081	9.6	18.3	650	39	2.97	2.53	36	1.35	0.15	—	10210
25	—	32	73	0.006	1.88	3.5	70	25	0.97	0.79	8.5	ND	0.25	—	6980
26	—	36	85	0.005	3.3	13	105	27	1.18	0.75	0.7	ND	ND	—	940
27	—	94	180	0.018	7.9	18	395	175?	2.63	1.54	19	ND	ND	—	8430
28	—	106	238	0.067	6.6	12.6	515	313?	3.56	3.10	39	2.50	0.15	—	21480
29	—	34	115	0.025	7.1	10.5	298	44	0.98	0.69	13	2.12	0.05	—	5210
30	—	29	109	0.019	1.80	12.5	225	96	0.53	0.30	3.7	ND	0.30	—	1090
July 1	—	91	215	0.048	2.4	13.2	365	40	1.31	1.51	22	ND	0.04	—	5390
19	—	75	222	0.052	3.1	16	474	41	2.01	2.47	23	2.53	0.13	—	7070
20	—	84	137	0.042	1.90	9.7	335	37	ND	0.92	18	ND	ND	—	540
21	—	92	154	0.040	2.4	10.4	380	44	1.84	1.23	21	ND	0.07	—	17110
23	—	59	80	0.021	0.71	5.5	191	18	1.50	0.21	13	ND	ND	—	900
24	—	82	207	0.075	4.5	19	548	42	2.52	1.99	45	ND	0.21	—	10070
25	—	63	99	0.034	12.3	9.6	354	50	2.02	1.20	15	ND	0.15	—	6400
27	—	49	55	0.011	0.44	3.1	106	12	0.99	0.27	19	ND	ND	—	430
28	—	66	104	0.029	1.01	6.7	237	25	ND	0.42	24	ND	0.05	—	3220
29	—	171	213	0.062	9.2	22	674	348?	1.75	1.60	61	3.16	ND	—	10670
30	—	114	71	0.004	3.5	20	135	34	1.37	0.98	20	1.59	0.03	—	5720

ND = not detected.

? = contamination suspected.

*1975 SO_4^{2-} data: Lioy et al. (1977). *1977 SO_4^{2-} data: this work.

Table 2. Simultaneous measurements of certain trace elements in air particulates at five stations in New York State and New Jersey, July 1976

Site	Date	Suspended particulates ($\mu g/m^3$)	Concentration (ng/m^3) Na	K	Sc	Mn	Fe	Zn	As	Br	Sb	SO_4^{2-}*
White-face Mountain, New York	July 17	31	24	27	.008	3.87	191	12	1.04	2.8	.16	2900
	18	53	71	104	.028	10.5	315	58	2.67	41	.68	4600
	19	41	--	104	.032	27.1	352	30	2.07	31	.44	5100
	20	74	354	315	.090	26.4	802	87	3.23	41	1.26	24600
	21	43	470	709	.008	4.67	96	7	0.34	27	.09	2600
	22	45	59	70	.022	7.36	201	15	0.28	0.7	.16	900
	23	63	154	185	.030	6.80	284	38	0.49	16	.70	5400
	24	49	59	51	.025	3.1	169	11	0.55	15	.31	2300
High Point, New Jersey	July 17	37	56	70	.026	6.16	147	18	1.64	53	1.37	4380
	17	37	39	76	.022	3.8	156	18	1.80	74	1.20	--
	18	35	58	101	.047	8.4	247	12	0.98	68	.56	2210
	19	29	97	134	.065	13.7	355	52	1.64	62	.79	4370
	20	75	203	254	.157	27.2	464	297	4.17	128	2.44	19100
	21	55	126	144	.078	13.0	429	382	3.22	43	ND	--
	21	55	101	144	.081	14.0	524	376	3.50	64	1.30	11320
	22	41	258	187	.065	22.1	342	62	1.04	125	2.10	3650
	23	29	295	101	.026	5.2	163	27	0.90	130	2.50	3060
	24	38	40	79	.028	7.1	194	24	1.9	55	1.40	7654
	25	31	39	90	.031	4.4	170	7	0.70	77	0.14	1460
Schoharie, New York	July 17	30	77	113	.028	6.8	222	16	1.94	71	.53	6000
	18	28	69	138	.041	10.7	220	13	1.14	120	.39	3600
	19	30	71	127	.042	8.9	277	15	1.14	187	.67	3400
	20	57	87	229	.130	18.7	674	42	2.66	44	.96	20000
	21	56	81	163	.078	18.0	605	53	3.43	39	1.14	19000
	22	32	58	140	.035	16.3	202	18	0.52	33	.64	2500
	23	32	90	107	.034	5.5	202	24	0.85	82	1.50	6700
	24	39	47	105	.030	6.2	218	15	2.00	44	0.99	12900
	25	22	48	118	.036	4.4	213	10	0.40	81	ND	600
Holland, New York	July 17	26	70	118	.036	10.5	293	20	1.32	86	.28	1600
	18	64	--	207	.076	28.0	716	31	2.23	82	.71	7800
	19	55	123	197	.126	39.0	1079	31	2.30	75	1.56	7600
	20	76	155	339	.210	46.0	1773	80	5.11	74	1.74	24900
	21	46	88	185	.067	16.0	752	34	2.01	135	1.32	9500
	22	46	65	164	.072	13.0	628	20	0.99	189	.93	2400
	23	46	73	133	.052	13.0	514	51	2.50	82	.81	11900
	24	41	55	133	.052	17.0	632	32	1.00	222	.72	5300
	25	29	49	136	.044	9.9	404	17	1.80	365	.51	1800
Albany, New York	July 17	27	121	108	.026	6.6	239	22	1.66	146	1.80	7600
	18	22	--	229	.042	12.5	371	15	1.22	146	0.60	1300
	19	42	193	193	.085	15.0	633	17	1.52	143	2.0	5600
	20	57	134	372	.129	21.9	773	65	2.32	128	2.2	15000
	21	51	118	208	.073	14.9	479	72	2.58	231	2.2	15400
	22	41	152	235	.077	37.0	663	27	ND	292	1.4	1400
	23	40	430	237	.078	10.0	551	72	1.20	313	1.7	6000
	24	33	80	111	.029	6.3	248	20	1.30	295	1.0	8200
	25	20	69	87	.038	5.0	274	7	ND	182	0.14	500

ND = not detected

* SO_4^{2-} data for Whiteface Mountain, Schoharie, Holland and Albany from Galvin et al. (1978). SO_4^{2-} in High Point samples was determined by microcoulometry.

Table 3. Ranges, mean elemental concentrations and enrichment factors for Ep Aerosols of summer 1975 (N = 4) and 1977 (N = 6) at Whiteface Mountain

Element or ion	Range (ng/m^3)		Mean (ng/m^3)		Standard Deviation		Enrichment Factor	
	1975	1977	1975	1977	1975	1977	1975	1977
Na	58-188	82-171	116	117	55	40	0.5	1.1
K	116-253	154-327	187	222	65	59	0.9	2.4
Sc	0.09-0.22	0.04-0.08	0.14	0.06	0.06	0.014	≡1.0	≡1.0
Cr	3.4-20.3	2.4-9.6	11	7	7	3	14.3	18
Mn	11-32	10-22	23	17	11	5	3.1	4.9
Fe	295-841	380-674	598	536	226	113	1.5	3.0
Zn	34-61	39-348	53	147(55)*	13	144	96	580(217)*
As	1.7-5.1	1.8-3.6	4	3	1	0.77	268	420
Se	0.95-5.0	1.2-3.4	3	2	2	0.85	7500	12,030
Br	9-21	21-61	16	40	5	13	820	4400
Sb	1.4-1.2	0.1-3.2	2	2	0.32	1	1130	2400
Cs	0.09-0.28	0.02-0.21	0.17	0.12	0.09	0.067	7.2	11.2
SO_4^{2-}	11,000-23,350	10,100-21,500	18,862	14,900	5825	5200	3080	5240

*Values in parentheses calculated after excluding the suspect values in Table 1.

Table 4. Ranges, mean elemental concentrations and enrichment factors for NEp aerosols of summer 1975 (N = 14-19) and 1977 (N = 17-20) at Whiteface Mountain

Element or ion	Range (ng/m^3)		Mean (ng/m^3)		Standard Deviation		Enrichment Factor	
	1975	1977	1975	1977	1975	1977	1975	1977
Na	15-155	21-573	80	96	47	112	1.0	2.4
K	24-293	55-580	119	153	67	116	1.6	4.2
Sc	0.006-0.15	0.004-0.062	0.05	0.03	0.04	0.02	≡1.0	≡1.0
Cr	2-19	0.44-37.0	4	7	4	10	15.0	53
Mn	1-22	3.1-77	8	20	5	20	3.0	15
Fe	42-591	70-607	240	261	138	145	1.7	3.7
Zn	7-100	12-175	25(20)	46(39)*	20	37	126(101)*	460(390)*
As	0.5-4.1	0.07-2.63	2	1	1	0.71	360	520
Se	0.14-1.86	0.21-2.47	0.7	0.84	0.5	0.59	4670	11,200
Br	3-34	0.70-24.0	12	13	7	7	1710	3570
Sb	0.11-3.88	———	0.8	———	1	———	1450	———
Cs	0.02-0.25	———	0.06	———	0.06	———	7.1	———
SO_4^{2-}	470-7800	429-8425	3393	3319	2306	2590	1530	2990

*Values in parentheses calculated after excluding the suspect values in Table 2.

Table 5. Correlation matrix for combined Ep events of 1975-77 (N = 18)

	Na	K	Sc	Mn	Fe	Zn	As	Br	Sb	SO_4
Na	1.0									
K	0.48	1.0								
Sc	0.03	0.46	1.0							
Mn	0.22	0.57	0.82	1.0						
Fe	0.21	0.61	0.72	0.88	1.0					
Zn	0.14	0.03	-0.26	-0.08	-0.03	1.0				
As	0.13	0.30	0.64	0.65	0.46	-0.12	1.0			
Br	0.04	0.28	-0.06	-0.03	0.08	0.04	-0.18	1.0		
Sb	0.08	0.15	0.07	0.13	0.09	0.62	0.07	0.27	1.0	
SO_4^{2-}	0.11	0.20	0.54	0.57	0.48	-0.07	0.68	-0.17	0.07	1.0

Table 6. Factor analysis for combined Ep events of 1975-77

Element or ion	Factor 1	Factor 2	Factor 3	Factor 4	Communality
Na	0.05	0.09	0.94	-0.07	0.90
K	0.48	0.02	0.62	0.44	0.81
Sc	0.91	-0.12	-0.02	0.10	0.85
Mn	0.92	0.01	0.21	0.10	0.90
Fe	0.82	-0.003	0.25	0.24	0.79
Zn	-0.15	0.90	0.15	-0.07	0.86
As	0.79	0.01	0.04	-0.24	0.68
Br	-0.09	0.12	0.02	0.90	0.84
Sb	0.13	0.89	-0.04	0.23	0.86
SO_4^{2-}	0.74	0.07	0.001	-0.29	0.63

Table 7. Factor analysis for NEp events of summer 1975 and 1977 at Whiteface Mountain

Element or ion	Factor 1		Factor 2		Factor 3		Factor 4		Communality	
	1975	1977	1975	1977	1975	1977	1975	1977	1975	1977
TSP	0.62	——	0.65	——	0.01	——	0.06	——	0.81	—
Na	0.91	0.20	0.28	0.002	0.09	0.33	-0.06	0.90	0.91	0.95
K	0.81	0.09	0.23	0.05	0.21	0.82	0.31	0.41	0.85	0.86
Sc	0.56	0.31	0.59	0.87	-0.01	-0.01	0.56	0.02	0.98	0.85
Cr	0.29	-0.15	-0.05	0.66	0.93	-0.06	-0.01	0.51	0.96	0.73
Mn	0.50	-0.34	0.54	0.24	0.20	0.83	0.54	0.04	0.88	0.87
Fe	0.73	0.25	0.46	0.90	0.11	0.23	0.35	-0.16	0.88	0.95
Zn	0.59	0.57	0.61	-0.22	-0.04	0.55	0.16	-0.01	0.75	0.67
As	0.41	0.71	0.79	-0.08	0.37	0.02	-0.07	0.62	0.94	0.90
Se	0.12	0.84	0.87	0.27	-0.05	0.10	0.40	0.22	0.93	0.84
Br	0.77	0.72	0.45	0.21	0.20	-0.37	0.03	0.18	0.85	0.73
SO_4^{2-}	0.09	0.83	0.71	0.24	0.41	-0.06	0.43	-0.08	0.86	0.76
Sb	0.36	—	0.003	—	0.78	—	0.47	—	0.96	—
Cs	0.10	—	0.20	—	0.06	—	0.92	—	0.89	—
Hg	0.08	—	-0.44	—	-0.80	—	0.04	—	0.84	—

CAPTION

Fig. 1. Concentrations of S (as SO_4^{2-}), Sc, Fe, As, Se and Br for 20-30 June 1977, showing episodic peaks on 24 and 28 June.

Fig. 2. Regression lines for the pair As-SO_4^{2-} for NEp events of 1975 with (-) and without (-·-) the two suspect data points (question-marked):

For solid line, $[As] = 0.001\ [SO_4^{2-}] + 1.4$ ($r = 0.23$)

For broken line, $[As] = 0.0021\ [SO_4^{2-}] + 0.68$ ($r = 0.70$).

Fig. 3. Linear regression for As-SO_4^{2-} (o) and Se-SO_4^{2-} (Δ) for Ep events in 1975-1977:

$[As] = 0.00012\ [SO_4^{2-}] + 1.1$ ($r = 0.68$).

$[Se] = 0.00017\ [SO_4^{2-}] - 0.15$ ($r = 0.67$).

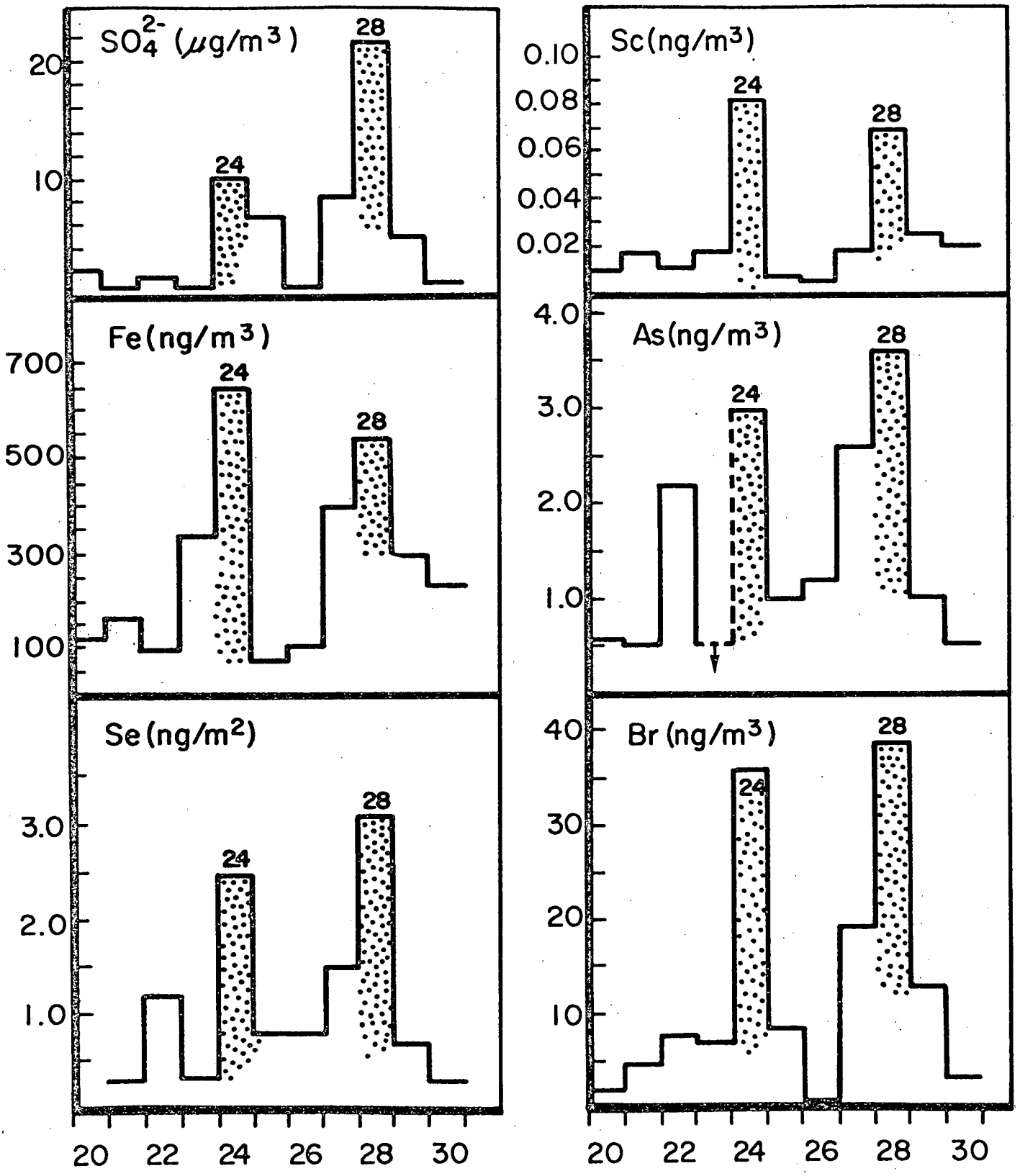
SO_4^{2-} ($\mu g/m^3$)
20
10
24
28
Sc(ng/m³)
0.10
0.08
0.06
0.04
0.02
Fe(ng/m³)
700
500
300
100
As(ng/m³)
4.0
3.0
2.0
1.0
Se(ng/m²)
3.0
2.0
1.0
Br(ng/m³)
40
30
20
10
20 22 24 26 28 30
DATE (June, 1977)

Fig. 1

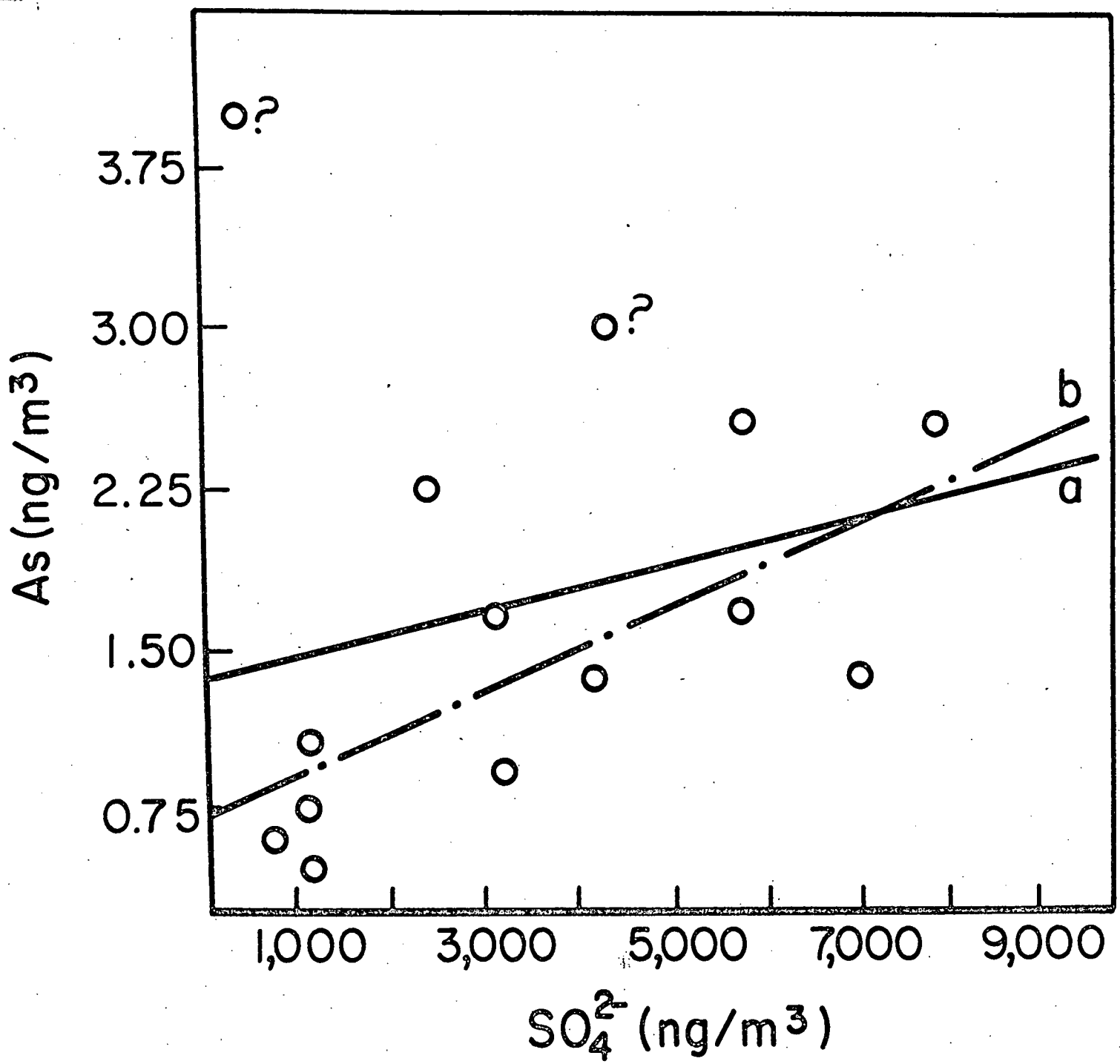
o?
o?
3.75
3.00
2.25
1.50
0.75
As (ng/m³)
b
a
1,000
3,000
5,000
7,000
9,000
SO4 2- (ng/m³)

Fig. 2

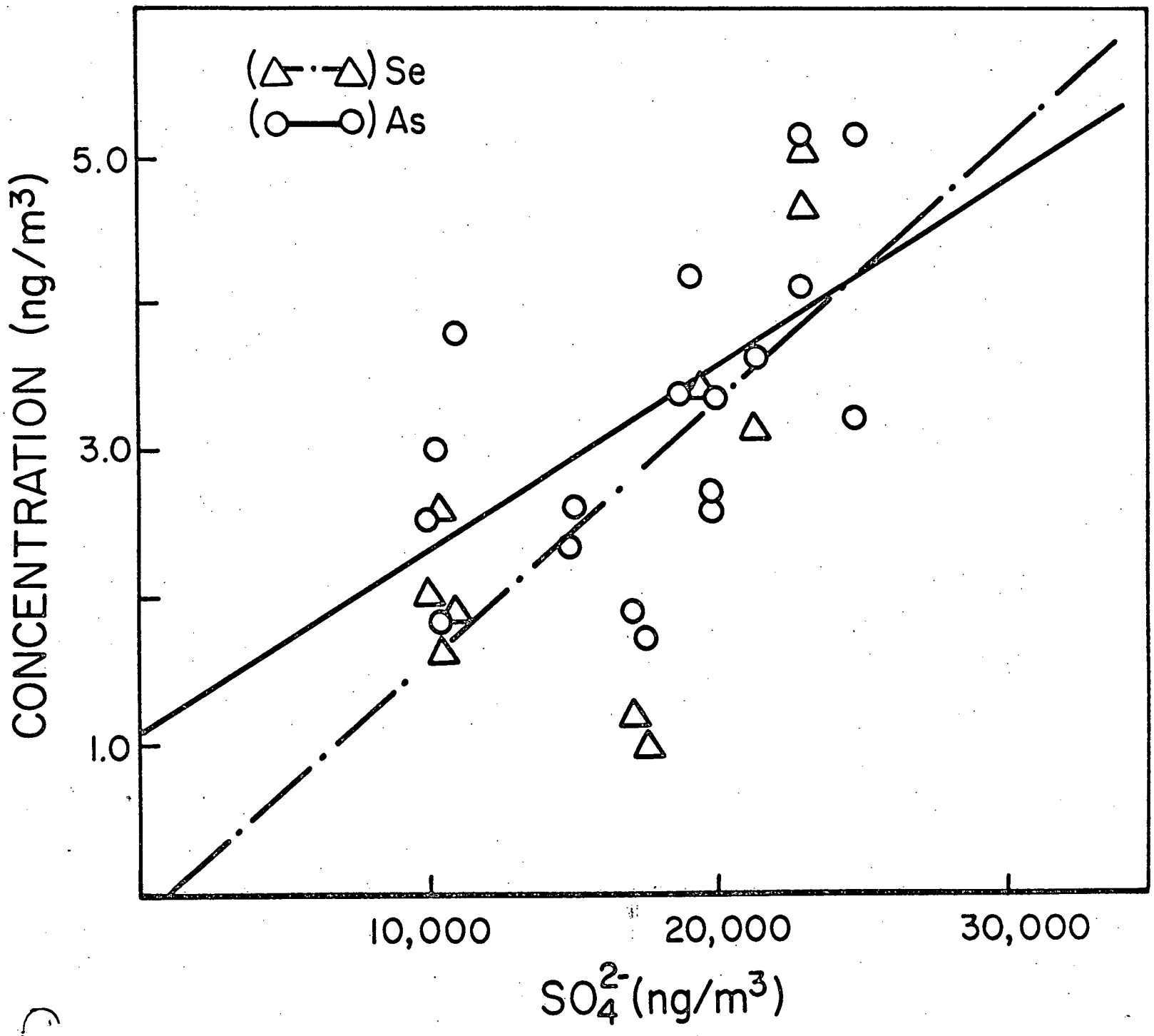
(△···△) Se
(○—○) As
CONCENTRATION (ng/m3)
5.0
3.0
1.0
10,000
20,000
30,000
SO4 2- (ng/m3)

Fig. 3